People's Democratic Republic of Algeria
Ministry of Higher Education and Scientific Research

University of Batna 2– Mostefa Ben Boulaïd
Faculty of Technology
Department of Mechanical Engineering

Thesis

Performed at
(Energic and Industrial Systems Studying Laboratory-**LESEI**)

Submitted to the Department of Mechanical Engineering in partial fulfilment of the requirements for the degree of:

LMD Doctor in Mechanical Engineering
Option: Energetics

Theme:

Numerical Study of Turbulent Mixing with or without Chemical Reactions in Various Geometrical Configurations

by:

LACHRAF Abdelbasset

Before the Jury Composed of:

Mr. DEMAGH Yassine	Professor	University of Batna 2	President
Mr. SI AMEUR Mohamed	Professor	University of Batna 2	Supervisor
Mr. BRIMA Abdelhafid	Professor	University of Batna 2	Examiner
Mr. KABAR Yassine	Professor	Nat. Poly. School of Constantine	Examiner
Mr. CHEHHAT Abdelmajid	Associate Professor	University of Khenchela	Examiner
Mr. BESSANANE Nabil	Associate Professor	University of Batna 2	Invited

10/03/2024

Title Page

Numerical Study of Turbulent Mixing with or without Chemical Reactions in Various Geometrical Configurations

Dedication

I dedicate this thesis to my family, whose unwavering support and encouragement have been the driving force behind my journey in the field of micro combustion. Their love, understanding, and sacrifices have fueled my passion and commitment to pursue knowledge and make a meaningful contribution to the scientific community. I am forever grateful for their belief in me and their constant encouragement throughout this academic endeavor. This achievement is as much theirs as it is mine.

Acknowledgement

In the vast tapestry of academia, where ideas intertwine and knowledge unfolds, I pause to express my deepest gratitude and appreciation to those who have journeyed alongside me. Their unwavering support and profound impact have enriched my path in ways that words can only begin to capture.

To my esteemed advisor, **Mohamed Si-Ameur**, a beacon of wisdom and guidance, your scholarly brilliance and unwavering dedication have illuminated my academic pursuits. Your belief in my abilities and unwavering encouragement have propelled me forward, instilling in me the values of perseverance, curiosity, and intellectual curiosity. Your mentorship has nurtured my intellectual growth and shaped the trajectory of this dissertation. I am forever indebted to your expertise, encouragement, and belief in my abilities.

I extend my heartfelt gratitude to the members of my dissertation committee,

Mr. DEMAGH Yassine	Professor	University of Batna 2	President
Mr. BRIMA Abdelhafid	Professor	University of Batna 2	Examiner
Mr. KABAR Yassine	Professor	Nat. Poly. School of Constantine	Examiner
Mr. CHEHHAT Abdelmajid	Associate Professor	University of Khenchela	Examiner
Mr. BESSANANE Nabil	Associate Professor	University of Batna 2	Invited

whose invaluable insights and critical feedback have fortified the foundation of this work. Their scholarly contributions and rigorous examination have elevated the quality of my research and broadened my perspectives.

To the countless researchers and scholars whose works have laid the groundwork for my exploration, your intellectual legacy has fueled my curiosity and inspired my quest for knowledge. The tapestry of ideas woven by your contributions has served as a guiding light in my academic journey.

To my colleagues and collaborators, whose camaraderie and shared passion have created a vibrant intellectual community, thank you for the stimulating discussions, collaborative endeavors, and the unwavering support during the challenges encountered along the way. Together, we have traversed the field of ideas, fostering an environment of growth and discovery.

Lastly, to all those mentioned and the countless others who have played a role, no matter how small, in shaping this dissertation, I offer my heartfelt thanks. Your contributions have been invaluable, and I am honored to have had the opportunity to embark on this academic endeavor alongside such remarkable individuals.

Abstract

In recent years, the trend towards miniaturization has driven the advancement of micro-combustion-based power generators, with the Micro-Thermophotovoltaic (MTPV) system emerging as a promising technology. This doctoral research aims to enhance micro-combustor performance through innovative solutions. It investigates a novel micro-combustor design featuring equidistant angled ribs on the inner wall of the downstream channel. The study explores flow dynamics, combustion behavior, and thermal performance, revealing significant improvements in wall temperature levels and thermal efficiency with the introduction of angled ribs. Increasing rib number and heights further with the micro-combustor cross section enhances thermal performance by facilitating ignition and sustaining stable flames. The proposed micro-combustor configuration demonstrates superior thermal characteristics, contributing to the development of more efficient and sustainable energy generation technologies. Addressing existing research gaps, particularly in rib geometries, the study emphasizes the importance of an integrative analysis approach. By bridging the gaps, it aims to advance the field of micro-combustion and provide valuable insights for future innovations in sustainable power generation.

ملخص

في السنوات الأخيرة، حفزت حركة التصغير على تطوير مولدات الطاقة القائمة على الاحتراق الدقيق. من بين هذه المولدات، ظهر نظام الخلايا الكهروضوئية الدقيقة (MTPV) كتقنية واعدة، لتحويل الحرارة الإشعاعية من مولدات الاحتراق الصغيرة إلى كهرباء باستخدام الخلايا الكهروضوئية. يعد تعزيز أداء مولدات الاحتراق الصغيرة أمر بالغ الأهمية لتحقيق كفاءة الاحتراق، الاستقرار وتقليل الهدر. تتناول أبحاث الدكتوراه الحالية الحاجة إلى حلول مبتكرة لتعزيز أداء مولدات الاحتراق الصغيرة. تركز أبحاث الدكتوراه الحالية على الدراسة العددية لتصميم جديد لمولد الاحتراق الصغير يتميز بوجود أربعة أزواج من الأضلاع المائلة المتباعدة بالتساوي على الجدار الداخلي للقناة الثانية للمولد. تستكشف الدراسة حَرَكِيَّات (ديناميكيات = dynamics) التدفق، وسلوك الاحتراق، والأداء الحراري لهذا التكوين الجديد. تكشف النتائج عن تحسينات كبيرة في مستويات درجة حرارة الجدار الخارجي عند إدخال الأضلاع المائلة. علاوة على ذلك، عزز كل من زيادة عدد وارتفاع الأضلاع وكذلك شكل القطع الجانبي للمولد من الأداء الحراري بشكل كبير. يبرز التكوين المقترح لمولد الاحتراق الصغير خصائص حرارية متفوقة، مما يسهم في تطوير تكنولوجيا توليد الطاقة الأكثر كفاءة واستدامة. تهدف الدراسة إلى سد الفجوات وتقديم رؤى قيمة للابتكارات المستقبلية في توليد الطاقة المستدامة.

Keywords

1. **Micro-Combustion**
2. **Micro-Thermophotovoltaic (MTPV)**
3. **Geometric Configuration**
4. **Heat Transfer Enhancement**
5. **Flow Dynamics**

Highlights

1. **Addressing Research Gaps:** The thesis addresses critical research gaps in micro-combustion, particularly regarding the impact of geometric configurations on flow dynamics, stability, and efficiency. By bridging these gaps, the study advances our understanding of micro-combustion processes and offers insights for future research and innovation in sustainable power generation.
2. **Hydrogen Application Potential:** The central aim of the current doctoral research is to comprehensively investigate the potentials of hydrogen applications within the micro-combustion domain, positioning hydrogen as the fuel of the future.
3. **Innovative Micro-Combustor Design:** The thesis introduces a novel micro-combustor configuration featuring angled ribs on the inner wall of the downstream channel. This innovative design aims to enhance the combustion process and thermal performance.
4. **Numerical Investigation:** The study employs advanced numerical simulations to investigate various aspects of micro-combustion, including, combustion behavior, thermal characteristics and non-reacting and reacting flow dynamics. This approach provides valuable insights into the complex phenomena occurring in micro-combustors.
5. **Improved Thermal Performance:** The research demonstrates that the introduction of angled ribs leads to a significant increase in wall temperature levels. Moreover, varying the heights of the ribs results in enhanced thermal performance, contributing to increased energy efficiency.
6. **3D Analysis and MTPV Efficiency:** The thesis extends its investigation into the realm of three-dimensional (3D) analysis, examining the impact of geometric configurations on micro-combustion in cylindrical and planar combustion chambers. Furthermore, the study includes a comprehensive calculation of Micro-Thermophotovoltaic (MTPV) system efficiency, shedding light on the potential improvements that can be achieved in energy conversion and harnessing the benefits of micro-combustion for power generation applications. This multi-dimensional approach contributes to a more holistic understanding of micro-combustion processes and their relevance to enhancing energy conversion technologies.

Contents

List of Figures

List of Tables

Nomenclature

Roman symbols

A	Surface Area
Bi	Biot number
C_p	Specific heat at constant pressure, (J/kg.K)
$\overline{C_p}$	Mean specific heat at constant pressure, (J/kg.K)
C_{ps}	Specific heat at constant pressure of solid phase, (J/kg.K)
d_0	Quenching diameter, (mm)
d_1	Inlet diameter, (mm)
d_2	Outlet diameter, (mm)
d_s	Micro combustor outer diameter, (mm)
Da	Damköhler number
$D_{i,m}$	Mass diffusion coefficient for species i, (m^2/s)
$D_{T,i}$	Thermal diffusion coefficient for species i, (m^2/s)
D_t	Turbulent diffusivity, (m^2/s)
$\overline{D}$	Normalized Diffusion Coefficient
E_f	Total energy of the fluid, (J/kg)
Fo	Fourier number
g	Gravitational acceleration constant, (m/s^2)
h_0	Natural convective heat transfer coefficient, ($W/m^2.K$)
h_i	Enthalpy of specie i, (J/kg)
H	Ribs height, (mm)
I	Unit tensor
J_i	Diffusion flux of specie i, ($kg/m^2.s$)
k_{eff}	Effective thermal conductivity, (W/m.K)
Kn	Knudsen number
k	Thermal conductivity, (W/m.K)
k_w	Thermal conductivity of solid phase, (W/m.K)
l	Rib length, (mm)
l_c	characteristic length of micro combustor
Le	Lewis number
L_1	Total micro-combustor length, (mm)
L_2	Inlet micro-combustor length, (mm)

L_3	Distance between ribs, (mm)
M_i	molecular mass for specie i,
M_j	molecular mass for specie j,
p	Static pressure, (Pa)
$\bar{p}$	Normalized pressure
p_c	Characteristic pressure
p_{abs}	Gas absolute pressure, (Pa)
Pe	Peclet number
Q	Heat rate
Re	Reynolds number
R_i	Net production rate of species i / energy source, ($kg/m^3.s$)
s	Step height, (mm)
S_h	Fluid enthalpy source, (W/m^3)
S_R	Radiation energy source, (W/m^3)
Sc_t	Turbulent Schmidt number
t	Time, (s)
$\bar{t}$	Normalized time
t_1	Micro combustor wall thickness, (mm)
t_2	Selective emitter thickness, (mm)
t_α	Diffusion time scale of gas phase, (s)
t_a	Time scale of acoustic wave, (s)
t_c	Characteristic combustion time, (s)
t_h	Time scale heat loss, (s)
t_{ig}	Ignition time scale, (s)
t_{res}	Flow residence time, (s)
t_s	Diffusion time scale of solid phase, (s)
T	Temperature, (K)
$\bar{T}$	Normalized temperature
T_{ave}	Average outer wall temperature, (K)
T_c	Characteristic temperature
T_f	Flame temperature, (K)
T_s	Solid phase temperature, (K)
T_w	Outer wall temperature, (K)

T_∞	Ambient temperature, (K)
ΔT	Temperature difference, (K)
u	Velocity, (m/s)
$\bar{u}$	Normalized velocity
V_{in}	Inlet velocity, (m/s)
W	Ribs width, (m)
$\dot{w}''$	Reaction rate
$\bar{\dot{w}}''$	Normalized reaction rate
$\dot{w}''$	Characteristic reaction rate
x	Axial spatial coordinate
$\bar{x}$	Normalized axial spatial coordinate
x_c	Characteristic axial spatial coordinate
Δx	Mesh cell size in the *x* direction, (mm)
Δy	Mesh cell size in the *y* direction, (mm)
y_i	Mass fraction of specie *i*
$\bar{y}_i$	Normalized mass fraction of specie *i*
y_{ic}	Characteristic mass fraction of specie *i*

Greek symbols

α	Thermal diffusivity
γ	Non uniformity index
δ_f	Flame thickness, (m)
δ_D	Mass diffusion length, (m)
δ_α	Thermal diffusion length, (m)
ε	Outer wall emissivity
θ	Angle, degree (°)
λ	Mean free path, (m)
μ	Molecular viscosity, (Pa·s)
μ_t	Turbulent viscosity, (Pa·s)
ρ	Density, (kg/m^3)
σ	Stephan Boltzmann constant, ($W/m^2.K^4$)
σ_{ij}	Lennard-Jones parameters for species i and j, ($W/m^2.K^4$)
φ	Equivalence ratio
Ω_D	Diffusion collision integral,

Abbreviations

CFD	Computational Fluid Dynamics
EDC	Eddy Dissipation Conception
IC	Internal Combustion
ISAT	Iterative Solution Assignment Table
LPG	Liquefied Petroleum Gas
MCRD	Micro Combustor Rib Design
MCSD	Micro Combustor Simple Design
MEMS	Micro Electro Mechanical Systems
MICE	Micro Internal Combustion Engine
MTPV	Micro Thermophotovoltaic
MTEG	Micro Thermoelectrical Generator
TEG	Thermoelectrical Generator
TPV	Thermophotovoltaic
UAV	Unmanned Air Vehicle

Chemical Compounds

CO	Monoxide of Carbon
CO_2	Dioxide of Carbon
H_2	Hydrogen
CH_4	Methane
C_3H_8	Propane
SiC	Silicon Carbide
SiO_2	Silicon Dioxide
Si_3N_4	Silicon Nitride

Chapter I: General Introduction

I.1. Study Context

I.1.1. Micro Combustion Solutions

Over the last decade, a significant shift has emerged within the scientific community's attention in direct response to the growing trends and dynamic landscape of energy supply for miniature devices. Motivated by the challenges posed by traditional energy supplies, predominantly dependent on electrochemical batteries, particularly as they have encountered their technological and physical limitations. These limitations manifest in terms of weight, duration of discharging and recharging, and the number of recharge cycles. Furthermore, the central challenge arises from the inadequate small energy density-to-size ratio offered by these conventional sources, which represent a fundamental objective of the miniaturization movement [1]. Taking into account the motivations, needs, goals and the promising opportunities outlined earlier, a pivotal trajectory has unfolded over the past three decades. This trajectory centers around the imperative exploration and harnessing of the latent chemical energy stored within conventional hydrocarbon and hydrogen fuels, including both gaseous and liquid states. This shift is ignited by the huge density of energy per unit of weight and volume offered by the usual hydrocarbon's fuels compared to the energy capacity of standard electrochemical primary and rechargeable batteries, which can be up to 100 times higher. This stark contrast in energy storage capabilities between hydrocarbon fuels and even cutting-edge batteries, such as lithium-ion, underscores the immense potential of micro combustion solutions. Hydrocarbon fuels possess a remarkable energy storage capacity, boasting an energy density of approximately 45 MJ kg−1. In stark contrast, even the most advanced lithium-ion batteries, which represent the pinnacle of contemporary battery technology, offer a mere fraction of this energy density, around 0.50 MJ kg−1 [2]. This striking difference in energy density clearly highlights the superiority of hydrocarbon fuels as energy carriers. Furthermore, it's worth emphasizing another key player in this discussion, which hydrogen. The incredible high-specific-energy of hydrogen (120 MJ/kg) makes it a formidable contender in the quest for efficient energy storage and conversion. Hydrogen, when used as a fuel, boasts an astonishingly high energy content relative to its weight. These characteristic positions hydrogen as a prime candidate for various energy applications, particularly when weight restrictions and high energy demands are crucial factors [3]. To put it into perspective, even if we consider a scenario where only 10% of the thermal energy in hydrocarbon fuels is efficiently converted into electrical energy, taking into account losses associated with power extraction from the fuel, hydrocarbon fuels still offer more than 10 times the energy storage density compared to batteries [2]. These remarkable advantages extends further when we acknowledge the ease of replacement associated with hydrocarbon fuels. Unlike batteries, which require time-consuming recharging or replacement, hydrocarbon fuels can be swiftly replenished, making them exceptionally convenient and practical sources of energy (**Figure I.1.1)**. In essence, the incredible energy density of hydrocarbon fuels, coupled with their replaceability, positions them as an indispensable energy source, especially in situations where high energy demands and consistent supply are paramount. However, the inherent advantage of hydrocarbon fuels should not be underestimated, as it remains a critical factor in various sectors, including transportation, heavy industry, and emergency power generation. Therefore, the recognition of these inherent characteristics enables the development of micro combustion-based systems to convert a significant amount of the fuels chemical energy within compact spaces, making them particularly well-suited for microscale applications. This strategic shift has given rise to the field of Micro Combustion Solutions—an innovative and dynamic domain that has attracted extensive attention due to its transformative potential and profound implications. Furthermore, this concerted focus reflects a persevering effort to address the increasingly urgent call to tackle emerging environmental challenges, while simultaneously meeting the escalating energy needs of miniature systems and devices. Through ingeniously designed systems and devices, the inherent energy in hydrocarbon and hydrogen fuels is unlocked and channeled into diverse applications. These micro combustion-based solutions aim is to generate power in the range of a few watts to

milliwatts (1 mW - 100 W), in turn, the systems which generate power in order of kilowatts are not considered “micro” in the current scaling conventions implicitly adopted among the micro combustion community [3].

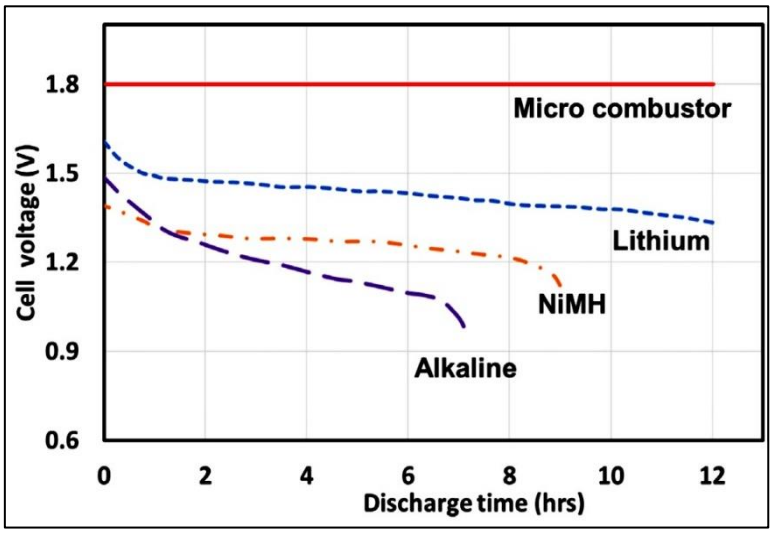

Figure I.1.1. *Discharge curve of different battery systems and the micro combustion-based solutions* [4].

This pioneering approach serves as a remarkable solution to the intricate challenge of powering miniature technologies efficiently and sustainably. The range of Micro Combustion Solutions encompasses an array of ingeniously engineered systems, each tailored to specific applications and industries. These systems harness combustion processes to yield remarkable advantages across a wide range of sectors. The development of such small-scale power /work generation solutions will allow overcoming the crucial problems faced today especially in terms of weight, duration of discharging and recharging, durability, and safety – issues that are particularly unavoidable in case of nuclear batteries. Moreover, the versatility of micro combustion-based systems is demonstrated by their capacity to deliver a broad spectrum of energy needs. These solutions go beyond powering MEMS devices, extending their influence to powering the conventional portable electronics and driving future explorations through micro propulsion systems. This adaptability knows no bounds, encompassing a wide range of applications. Notably, they serve as a dependable portable power source for MEMS devices, encompassing a variety of sensors and actuators, such as micropumps, micro-robots, micro rockets, microsatellites, micro communication devices, and micro drug delivery chips. Moreover, they present an enhanced alternative to current power sources for personal portable devices, spanning smartphones, personal computers, wireless communication equipment, and an array of industrial applications. This adaptability extends to military devices, eliminating the need for soldiers to transport heavy batteries for powering military communication equipment [5]. This addresses the immense energy requirements of battle arms like unmanned air or underwater vehicles, exoskeletons, and night scopes …etc. The unicity of these combustion-based systems emphasizes their potential to drive technological innovations across diverse sectors, empowering devices with the required energy while ensuring efficiency and reduced environmental impact. Furthermore, the controlled nature of combustion processes within these solutions allows for precise control over energy output and heat generation. This level of control is invaluable in applications where temperature regulation, localized heating, or energy conversion are critical. Micro Combustion Solutions contribute significantly to enhancing the overall operational efficiency and reliability of MEMS devices, further amplifying their applicability in real-world scenarios.

I.1.2. Micro Thermophotovoltaic System

In the recent two decades, MTPV systems shine as beacons of promise and innovation. Among the discussed spectrum of micro combustion solutions, MTPV systems are gaining substantial attention within the research community, standing out as a focal point in the exploration of micro combustion-based solutions. MTPVs distinguish themselves through their ability to seamlessly convert thermal energy into electricity through thermophotovoltaic cells. This unique attribute enables MTPVs to be remarkably efficient in transforming heat into a usable form of energy, setting them apart as a compelling candidate for sustainable power generation. MTPVs distinguish themselves from their counterparts not solely due to their ability to efficiently harness high-temperature heat, but also due to their adaptability and versatility across various applications. Beyond powering MEMS devices and commercial portable electronics, MTPVs provide also energy solutions for numerous applications in a wide range of environments, including aerospace, terrestrial, or maritime where microscale vehicles can navigate intricate environments and perform reconnaissance missions. However, the growing significance of MTPV systems stems from their multifaceted advantages:

- **System Design**

  MTPV systems are characterized by their meticulous compactness, primarily attributed to the minimized dimensions of components responsible for the direct conversion of thermal energy into electricity. These systems are known for their simplicity, featuring nonmoving parts, in stark contrast to micro engines such as Micro gas turbines and MICE, which often require intricate mechanical components. This simplicity not only contributes to their compactness but also reduces maintenance requirements and enhances their reliability, as there are fewer components that could potentially fail. On the other hand, the simplicity of these systems design allows for their versatility across a broad spectrum of applications [6].

- **Operational Characteristics**

  MTPVs exhibit quick start-up times, ideal for applications requiring instant power generation. In contrast, micro engines may have longer start-up times due to mechanical considerations. Furthermore, the absence of mechanical components subject to vibration in MTPVs makes them suitable for applications where vibration interference can be detrimental, unlike micro engines that can produce vibrations. Consequently, MTPVs operate silently, without the noise associated with micro engines. This is crucial for applications where noise pollution is a concern, such as in medical devices or microscale sensors.

- **Conversion Efficiency**

  MTPVs possess the remarkable ability to achieve high conversion efficiency, efficiently converting thermal energy into electricity. This advantage actually stems from the fact that the photovoltaic effect generally offers higher thermal-to-electric conversion efficiency compared to the Seebeck effect. The thermophotovoltaic cells (TPV) integrated into MTPV systems exhibit high conversion efficiency, especially when working with high-temperature heat sources like the micro combustion chambers under discussion [7]. TPV systems are particularly efficient when working with high-temperature heat sources, typically exceeding 1,000°C, while TEGs are more commonly employed in lower-temperature scenarios. In practical experiments, the highest efficiency achieved reached 35%. This was attained using an emitter temperature of 1,773 K in laboratory conditions with a custom-built measurement apparatus [8]. However, TPV cells can achieve relatively higher conversion efficiencies as they can be designed to match the spectral emission of the micro combustor's radiation to the bandgap of the thermophotovoltaic (TPV) cells **(Figure I.1.2)**. This spectral matching optimizes the conversion of photons into electrical energy [9].

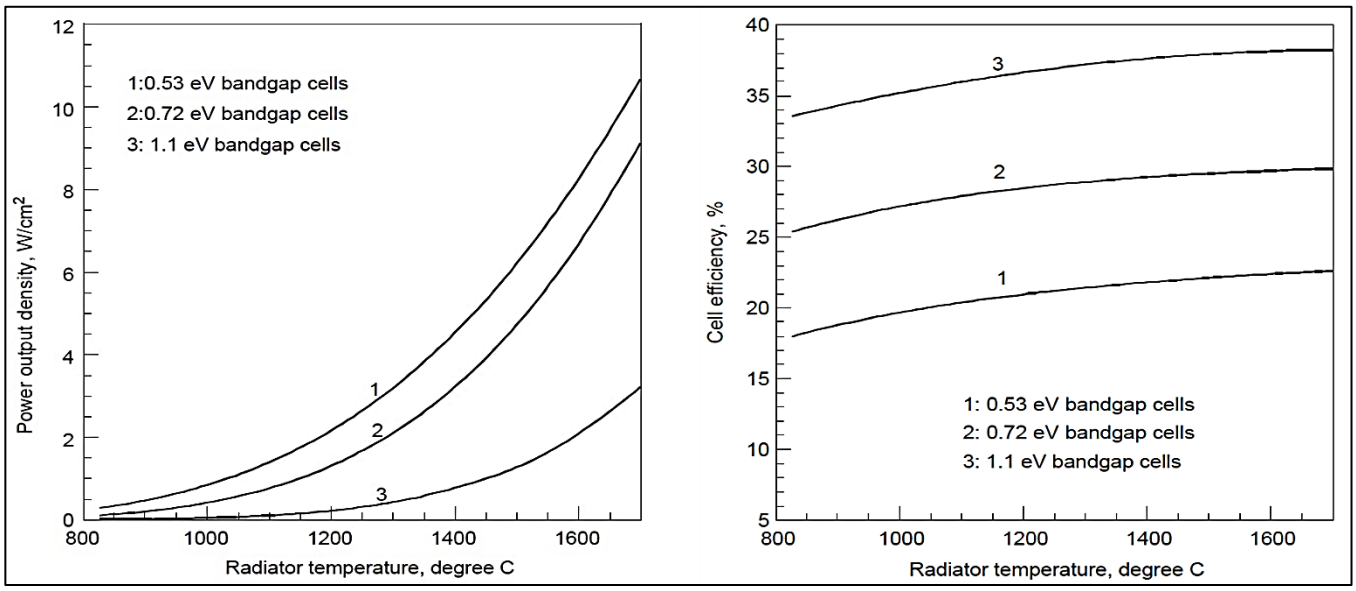

Figure I.1.2. *(a) Output electrical power density and (b) TPV cell efficiency in function of micro-combustor's wall temperature for different cell bandgap energies[9]*

Furthermore, MTPVs, as well as thermoelectric solutions in general, offer a unique advantage by directly converting thermal energy into electricity, bypassing the need for intermediate mechanical steps, as illustrated in **Figure I.1.3**. This inherent efficiency surpasses many other micro combustion solutions that involve mechanical work conversion, effectively reducing energy wastage caused by heat and friction losses. This distinctive characteristic positions MTPVs as leading candidates for sustainable power generation. The **Figure I.1.4** provides a visual representation of the thermal cycle of a 50W-class micro gas turbine system designed by Fu et al. [10]. This schematic diagram offers valuable insights into the system's design and efficiency. Within the micro gas turbine system, the compressor assumes a critical role in pressurizing incoming air. However, the compressor's efficiency is noted as 70%, indicating that approximately 30% of the energy supplied to the compressor is lost during the compression process, primarily as heat or other inefficiencies. Besides, the system's bearings, which are pivotal components, contribute to approximately 10% of power losses due mainly to friction and mechanical engineering inefficiencies. As we progress through the system, the micro gas turbine itself demonstrates an efficiency of 72%, implying that approximately 28% of the energy extracted from the combustion process is lost within the turbine, primarily as waste heat or other inefficiencies. Lastly, the generator's efficiency is reported as 70%, signifying that about 30% of the mechanical energy derived from the turbine is forfeited during the electricity generation phase. Consequently, only a mere 4.37% of the initial fuel energy remains as the final electrical output. In conclusion, when we summate these different power losses along the micro gas turbine system's various stages, we witness a substantial dissipation of energy at each step, underscoring the challenges in achieving high overall efficiency in micro gas turbine systems.

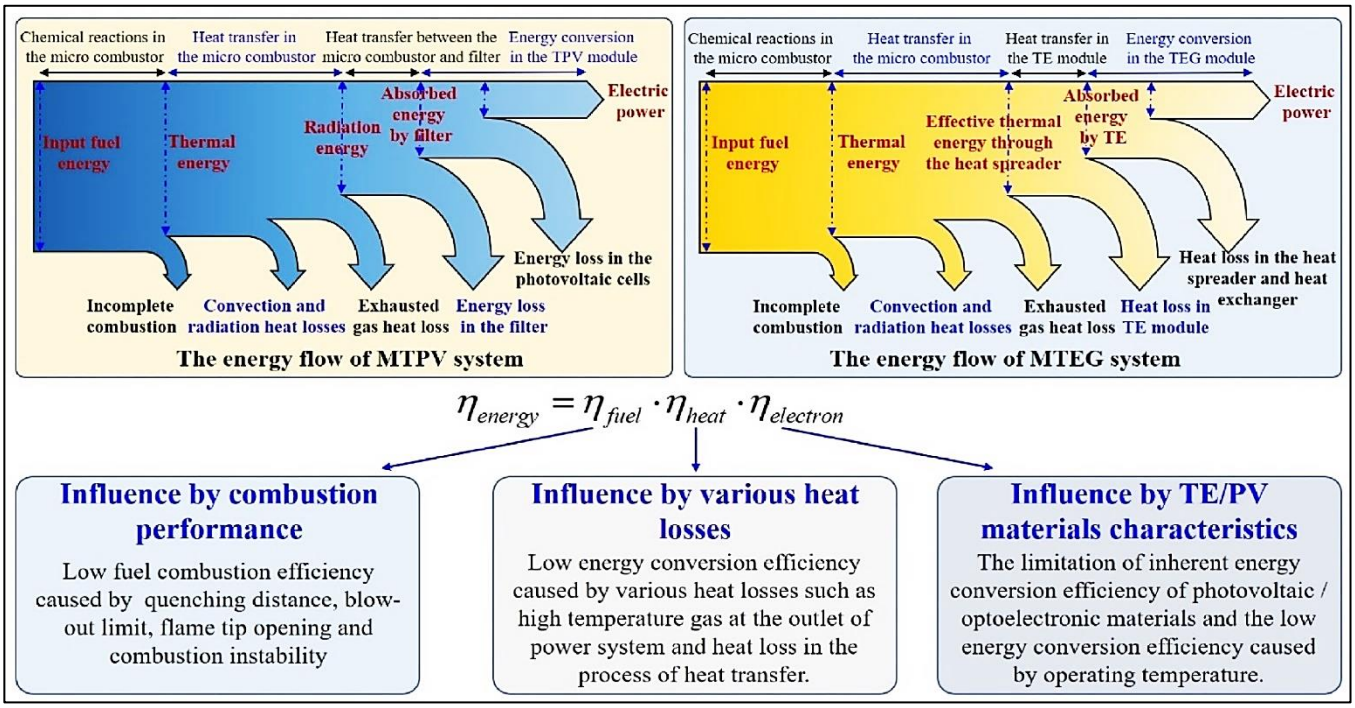

Figure I.1.3. *The energy flow of MTPV and MTEG system and the influence factors on the energy conversion efficiency of MTPV and MTEG system* [11].

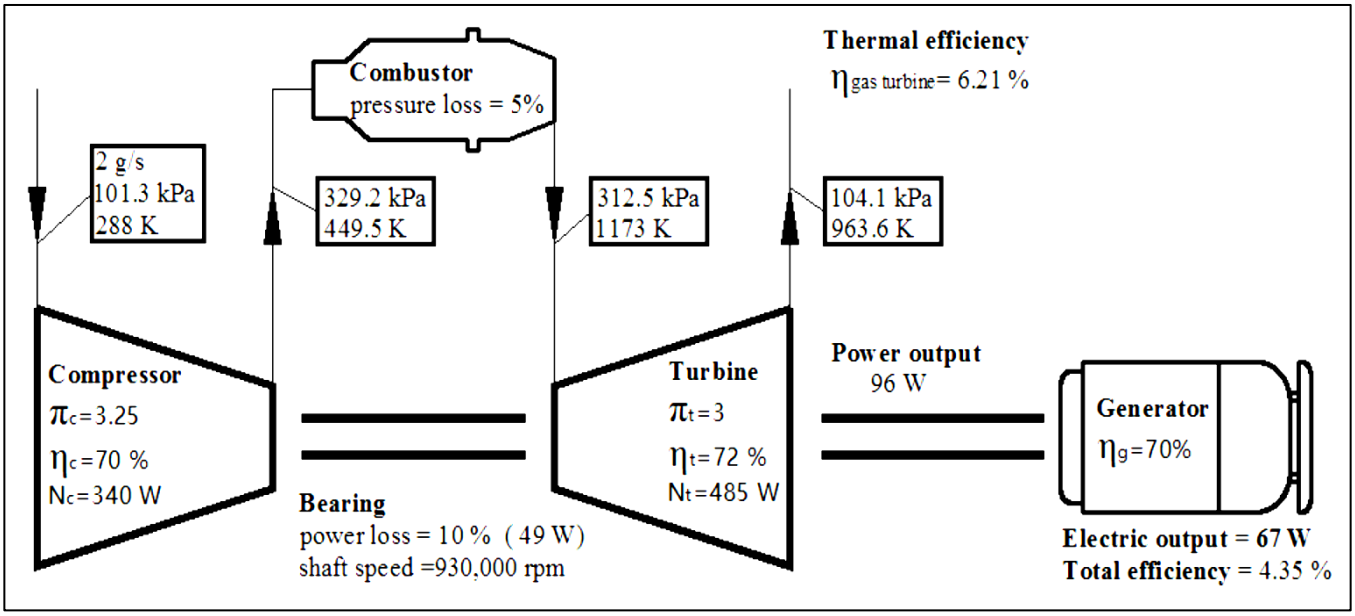

Figure I.1.4. *Schematic diagram of the thermal cycle of a 50W-class micro gas turbine system* [10].

- **Historical Background**

The historical development of Micro Thermophotovoltaic (MTPV) systems is deeply intertwined with the broader evolution of thermophotovoltaic (TPV) technology. Actually, the Micro Combustion-based MTPV Systems (MTPVs) are an evolution of TPV technology, specifically adapted for MEMS applications. The concept of harnessing thermal energy and converting it into electricity via photons remains the same. MTPVs inherit the principles and advancements of TPV but are tailored to meet the demands for micro-scale power generation solutions [2]. The review of historical background reveals that the origins of Thermophotovoltaic (TPV) concept are somewhat obscure. The early experimentation date back to the late 1950s where Dr. Henry H. Kolm at MIT's Lincoln Laboratory constructed an elementary TPV system in 1956, using a Coleman camping lantern as an emitter and a silicon solar cell for

photoconversion. This marked the initial exploration of TPV concepts, although further development was limited at that time. Substantial development in TPV began to take shape in the late 1960s, with Professor Pierre Aigrain, during his lectures at MIT, proposing the direct energy conversion concept of TPV. This ignited a wave of research activities. The MIT faculty authored conference papers and journal articles, while other academic institutions and the US Army at Fort Monmouth actively participated in advancing TPV technology. General Motors (GM) also played a pivotal role in industrial TPV development, focusing on TPV for portable power sources. The 1970s brought significant challenges to TPV development. The US Army and GM discontinued TPV efforts, primarily due to a preference for thermoelectric technology for covert power sources. TPV development experienced a resurgence during the 1980s, coinciding with a growing interest in renewable energy sources. Researchers like Horne at Boeing and Fraas in the US worked on TPV systems, and the efficiency of TPV improved to around 30%. Since the early 1990s, TPV development has continued, researchers at MIT, EDTEK Inc., JX Crystals Inc., and Quantum Group Inc. played crucial roles in advancing TPV technology. Research focused on narrow-bandgap cells, reflective surfaces to maximize photon capture, and multi-junction cells [12]. Efficiency improvements have been significant, culminating in an impressive 41.1% conversion efficiency by a TPV tandem system developed by MIT and the National Renewable Energy Laboratory in 2022 [13].

On the other hand, the review of the historical evolution of micro combustion-based MTPV systems reveals that the first attempts to use the TPV technology to harness the micro combustion released heat can be date back to the late 1990s. In 1997, Anthony C. Zuppero and his team introduced a pioneering miniature thermo-photovoltaic (TPV) device. This marked one of the earliest endeavors to leverage TPV technology for capturing the heat released from micro combustion. Their invention aimed at generating electrical power, primarily incorporated a heat source, represented in chemical reactor capable of utilizing various fuels, including liquid hydrocarbons like propane, LPG, butane, alcohols, oils, and diesel fuels, to produce a source of photons [14]. This inventive TPV device stands as an early example of the integration of TPV technology with micro combustion to harness heat for power generation, marking a notable milestone in the historical progression of micro combustion-based MTPV systems. The aforementioned shift toward miniaturization paved the way for the development of micro combustion solutions and the MTPV systems was tailored for micro-scale power generation needs. Therefore, the concept of micro combustion-based MTPV systems started to take shape in the 2000s. In 2002, Yang and his team at National University of Singapore by the collaboration of the California State Polytechnic University, they introduced the power microelectromechanical concept, which they termed the "micro thermophotovoltaic (MTPV) system" for the first time [15]. Researchers explored adapting TPV technology to microscale applications, aiming to harness the benefits of controlled micro combustion in powering MEMS-based systems. The system utilized micro combustion of hydrogen as fuel within a micro combustor with a volume of 0.1 cm^3. Fabrication and assembly of the system were relatively straightforward, and it was capable of generating 4.5 W of electrical power (**Figure I.1.5**). This marked the inception of MTPV as a distinct field within TPV. The experimental results obtained at the time, involving the micro flame tube, the selective emitter, and the GaSb cells, indicated the emergence of a simple solution for developing micropower generation without the need for any moving parts.

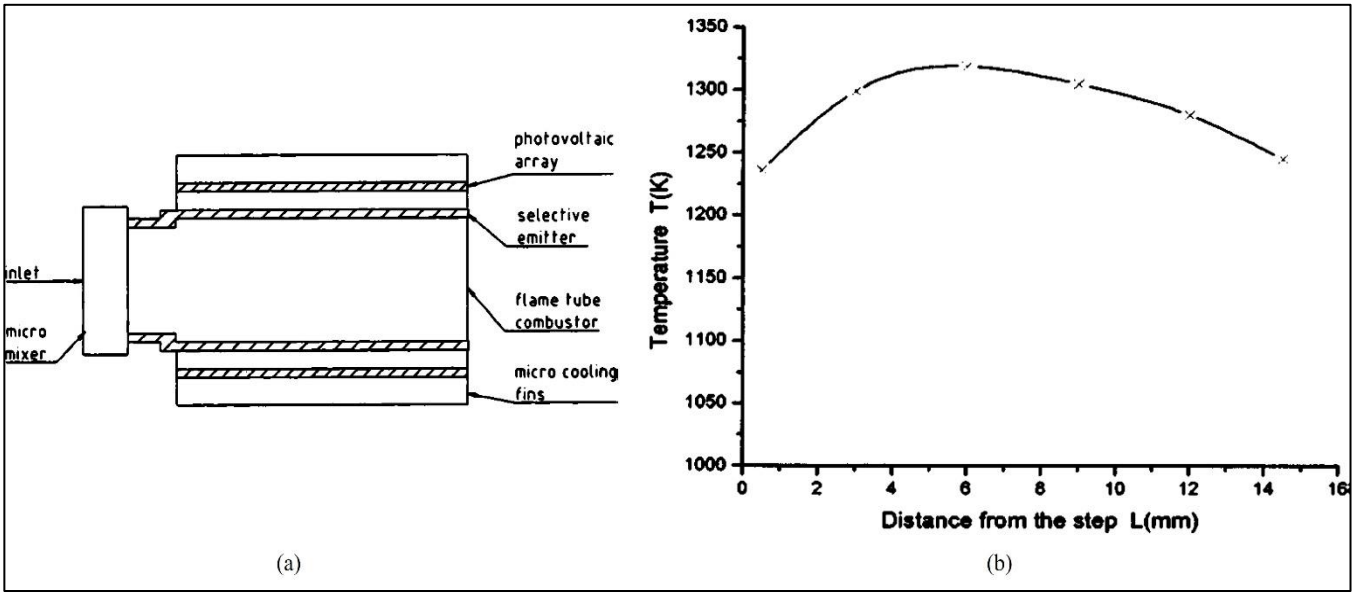

Figure I.1.5. *Schematic of Micro Thermophotovoltaic System developed by Yang et al.* [15]. *(b) Distribution of the temperature along the wall at V_{in}=12 m/s, φ=0.95.*

For a second time in 2002, Yang et al. [16] introduced a micro cylindrical combustion chamber with a backward-facing step (**Figure I.1.6**). The incorporation of this backward-facing step into the combustor design yielded several notable advantages. It enhanced the mixing of the fuel mixture, extended the residence time within the chamber, facilitated the convective transfer of combustion heat towards the outer wall of the micro combustor, and expanded the operational range in terms of flow rate and fuel-air ratio. Moreover, it was observed that the backward-facing step played a pivotal role in stabilizing the flame position, resulting in a uniform and high-temperature distribution along the combustor wall. Additionally, this design modification increased the local residence time of the fuel-air mixture, consequently leading to reduced CO emissions. Notably, the size of the backward-facing step was found to influence combustion stability, with larger step sizes corresponding to narrower flame stability limits. Consequently, micro combustor design and fuel flow rate, emerged as primary manipulative parameters governing combustion temperature and, by extension, the efficiency of MTPV systems.

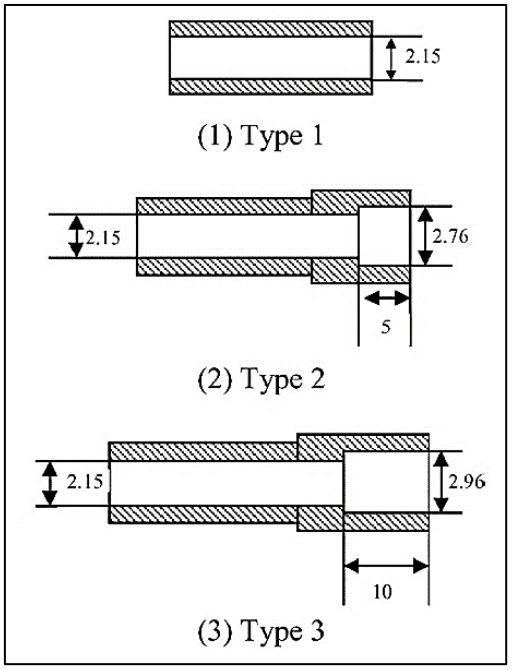

Figure I.1.6. *micro-cylindrical combustors with and without a backward facing step (in mm)* [16].

In 2005, Yang et al. [17] shifted their focus towards improving MTPV emitter materials to enhance system efficiency. Experimental results demonstrated that micro cylindrical combustors constructed from Silicon Carbide (SiC) and platinum exhibited distinct performance characteristics. The micro platinum combustor, owing to the catalytic effect of platinum, exhibited significantly higher temperatures along its wall compared to the SiC combustor, as shown in **Figure I.1.7**. Once again, the significance of the micro combustor configuration was emphasized as a crucial factor affecting the performance of MTPV systems. Increasing the height of the backward-facing step while reducing the combustion chamber diameter was shown to boost the short-circuit current and maximum output power of the system. Additionally, a novel wavelength-selective thermal emitter based on the resonator-pixel (RP) structure was proposed to enhance wavelength selectivity and power conversion efficiency within the system. These studies collectively contribute to the advancement of more efficient MTPV power generators, utilizing various emitting materials and exhibiting improved performance characteristics.

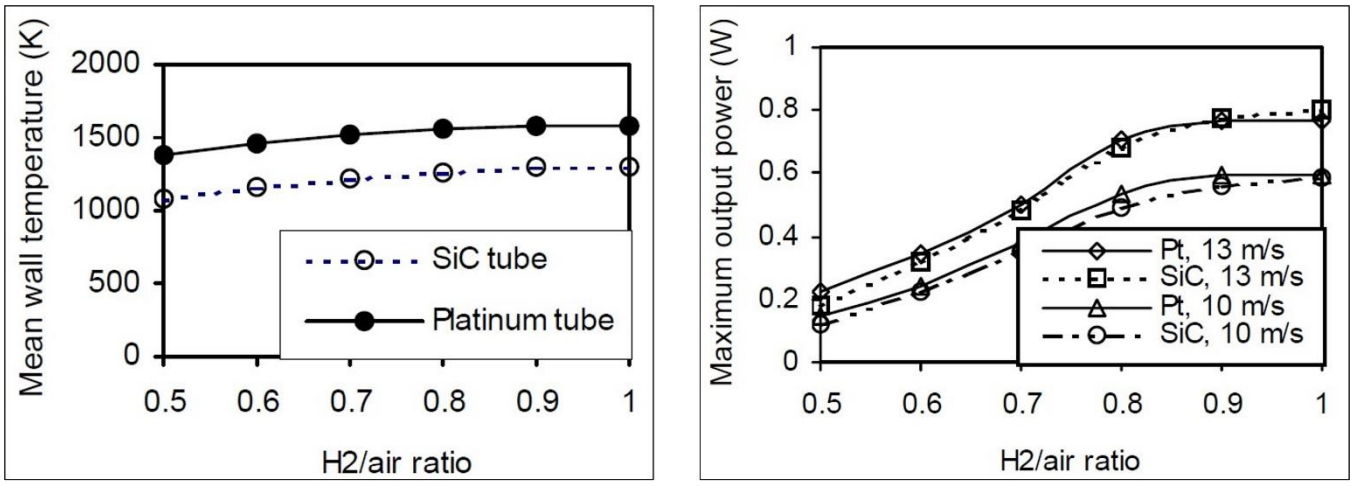

(a) (b)

Figure I.1.7. *MTPV system with different emitter materials. (a) Mean wall temperature at flow rate of 13 m/s. (b) Maximum output for different emitter materials at flow rate of 10 m/s and 13 m/s* [17].

In 2006, Pan et al. [18] conducted an experimental investigations into the effects of three primary parameters on micro-combustion. These parameters included the ratio of hydrogen to oxygen in the mixture, the ratio of nozzle diameter to combustor diameter, and the ratio of wall thickness to combustor diameter. The findings from their study revealed that achieving a high average wall temperature was possible with slightly oxygen-rich mixing ratios. The ratio of nozzle diameter to combustor diameter had an impact on both the magnitude and uniformity of the wall temperature distribution. Furthermore, the introduction of a newly designed thin-wall combustor, which reduced axial heat conduction loss, resulted in an increase in wall temperature of over 150 K. It is evident that optimizing these parameters can significantly enhance radiation heat output in MTPV energy conversion processes. However, Chia and Feng [2] conducted in 2007 a comprehensive examination of current micropower technologies, with a specific emphasis on a prototype micropower device utilizing thermophotovoltaic (TPV) principles for electricity generation. The primary focus of this review centers on identifying potential enhancements for the MTPV systems, particularly in terms of improving the efficiency of the micro-combustor, thermophotovoltaic (TPV) cells, and, consequently, the overall system efficiency. In their conclusions, the authors underscored the critical importance of material selection for the emitter (micro-combustor wall) in the design and construction of micro-TPV power devices. Opting for the most appropriate emitter material can lead to a substantial increase in electrical power output, thereby enhancing the overall efficiency of the device. As MTPV technology continued to advance, researchers delved also into materials science, micro combustor design and micro combustion techniques, to enhance the conversion efficiency and reliability of micro combustion-based MTPV systems. In 2010, a novel micro

thermophotovoltaic (MTPV) is presented by Pan et al. [19]. The MTPV system based on a sub-millimeter parallel planar micro combustor, in aim to achieve a higher radiation energy per unit volume and high electrical power density built on to the high surface to volume ratio of this shape of micro-combustor. It has been found that the combustion efficiency decreases with increasing hydrogen flow rate due to reduced residence time. The choice of nozzle shape also affects the average wall temperature, with rectangular nozzles resulting in higher temperatures compared to circular nozzles. Experimental results have shown good agreement with model predictions, with achieved electrical power matching the projected values. The overall efficiency and power density of the modular TPV power generator have been calculated to be 18.69% and 191.2 mW/cm² respectively.

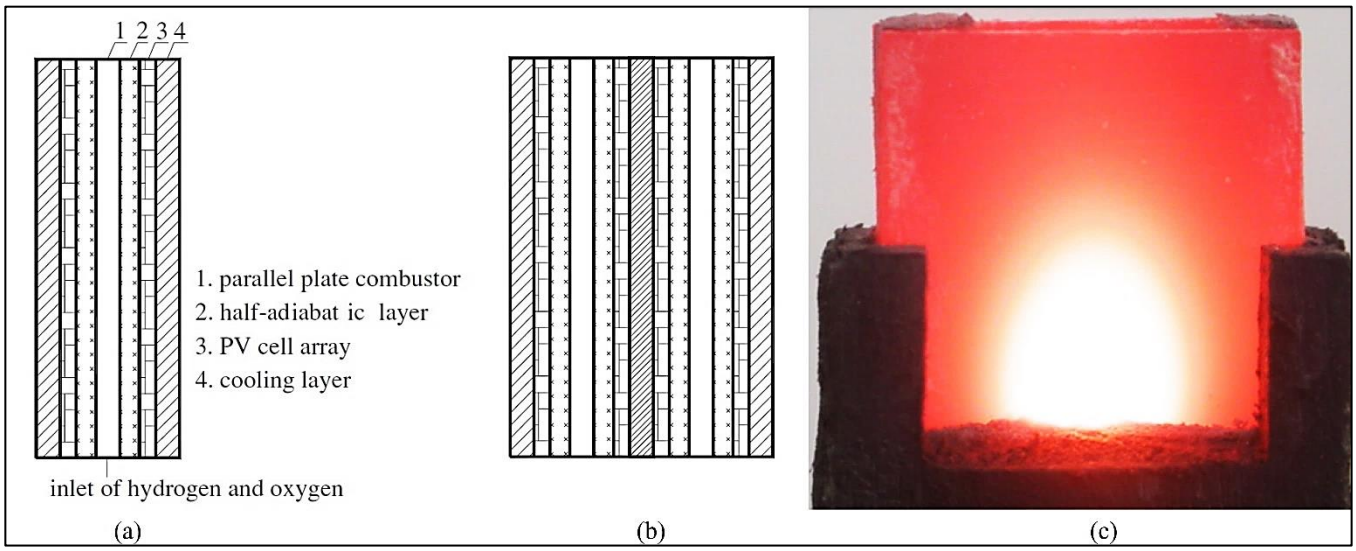

Figure I.1.8. *Schematic diagram of the modular TPV power generator: (a) sectional view of one MTPV; (b) Sectional view of the combination of two MTPV. (c) Photo of the micro combustor in operation* [19].

By this point, the micro combustion research community had begun to recognize the pivotal role of micro combustors in the development of MTPV systems. Subsequently, efforts in the field were predominantly directed towards comprehending the factors that influenced micro combustion. This research sought to optimize micro combustor designs while concurrently pursuing advancements in various systems, particularly MTEG. The central objective was to enhance the efficiency of micro combustion, a goal achieved by augmenting the efficacy of combustion processes under various operating conditions, including variations in flow rate and equivalence ratio of the reactive mixture. In 2017, Mustafa et al. [20] drove a comprehensive review of MTEG and MTPV systems, consolidating knowledge gathered from literature spanning the years 2000 to 2016. The authors note the emergence of MTPV systems as compelling areas of research and development. Along with MTEG systems, the review primarily focuses on summarizing the advancements made in combustion-driven MTEG and MTPV power generation solutions. In their review to the so far developed MTPV systems, the authors highlight the relatively recent but remarkable progress witnessed in the past first decade. Despite not yet fully realizing tangible benefits in emissions reduction, MTPV systems are increasingly gaining traction as a viable option in the energy market. This promising trajectory offers consumers an alternative, marking a significant stride in addressing the energy crisis. A significant exploration of the profound impacts of fuel-air mixtures and the fuel-air equivalence ratio on the thermal, combustion, and electrical characteristics of MTEG and MTPV systems. The authors shed light on the nuanced relationships between these variables, offering fresh perspectives on how fuel-air equivalence ratio intricately influences the performance of these power devices. However, they perceptively note the dearth of detailed mapping regarding combustion performance, highlighting a critical area for further exploration and advancement. They offer a separate perspective by inspecting the effects of power systems' operating conditions, compromising the aspiration for cleaner, greener systems with reduced emissions. However, in the last five years, a set of review

studies [21]–[26] recognized that various factors influenced micro-combustors within MTPV systems, affecting wall temperature level and uniformity and flame stability. These factors encompassed geometry configuration, thermal conductivity, operating conditions, fuel type, and cooling mechanisms. Existing studies proposed diverse designs, such as bluff-body shapes, backward-facing steps, and heat recirculation, to attain suitable wall temperatures and broad flame stability. The size and location of recirculation zones, notably those generated by a swirler, played crucial roles in stabilizing the flame and enhancing thermal performance. The incorporation of a backward-facing step into combustor design proved effective in maintaining flame stability. Furthermore, parameters like combustor diameter, combustor length, flow velocity, and fuel-air equivalence ratio influenced wall temperature distribution. Maintaining a high and uniform temperature along the wall was identified as crucial for optimizing the efficiency of micro-thermophotovoltaic systems.

I.2. Literature Review

I.2.1. Recent Progress in Micro Combustion

The miniaturization of technological systems has been the trend over the past few decades, resulting in the development of micro-electro-mechanical systems (MEMS) which are now widely used in various fields. However, traditional power sources such as electrochemical batteries are limited by their energy density to size ratio [2]. To address these limitations, a combustion-based micropower generator system such as the micro gas turbine, the micro thermoelectric generator (TEG), and the micro thermophotovoltaic (MTPV) systems having been developed since 1997 [27]. Micro-Thermophotovoltaic (MTPV) system technology is an increasingly prominent area of research in the field of micro combustion and particularly within MEMS electrical power generation market. MTPV systems utilize small-scale combustors and thermophotovoltaic cells to convert the chemical energy released from the combustion of hydrogen or hydrocarbon fuels into electrical energy. These systems hold great promise for small-scale power generation in portable electronics, as well as unmanned air and maritime vehicles, micro satellites, and MEMS remote sensors. However, in spite of its promising benefits, the micro combustion characteristics differ significantly from conventional combustion in terms of flow behavior, heat transfer mechanisms, flame structure, chemical kinetics, and combustion efficiency. The miniaturization of micro combustion chambers leads to the challenges of incomplete combustion risk, limited flame stability and narrow operating flow conditions. The excess heat loss through the micro-combustor's outer walls increases the issues of combustion instabilities and flame quenching. While, ensuring high level and uniform distribution of the outer wall temperature is an important factor for an advantageous thermal performance of micro combustors and the overall system (MTPV) efficiency. Furthermore, the significant challenge to bring under control the thermal performance of the MTPV micro combustor is not only based on the temperature exigencies but also on the hydrodynamic operating conditions such as the inlet velocity and mixing conditions such as equivalence ratio [28]. These challenges are due essentially to the surface-to-volume ratio which is extremely high and results in shorter flow residence time comparing to the reaction time of some elementary chemical reactions. Furthermore, the distinct and versatile nature of these challenges, includes flow, chemical and thermal aspects, make the control of the micro combustion process extremely challenging and interdisciplinary research.

For this purpose, the optimization of geometrical configurations and operating conditions have become promising approaches to bring into control the micro combustion and MTPV performance. Researchers are meticulously examining the cross-sections, shapes, and structures of micro combustors to optimize their thermal performance. This trend is underscored by the growing of numerical simulation studies, which delve into the intricacies of geometric design with the aim of achieving efficient and stable combustion. Simultaneously, due to its cost-effectiveness, scalability and flexibility, the enhancement of inner surface areas of micro combustors and management of reacting flows within it has gained

significant attention. Innovative enhancement strategies involving the manipulation of inner wall shapes, and the introduction of wall projections, flame holders, and turbulence inducers have all contributed to expanding the surface area available for heat transfer and widen the management of the micro combustion gases flow. The backward-facing step is a classic recirculation generator technique that combines the simplicity of geometry and provides at the same time a practical passive control technique to improve micro-combustion overall performance. In their early experimental study, Yang et al. [16] found that incorporating a backward-facing step enhances fuel-air mixing, prolongs residence time, and widens the operational range, resulting in a high and uniform temperature distribution. Furthermore, Sahota et al. [29] and Khandelwal et al. [30] conducted experimental investigations on cylindrical micro-combustors with two and three backward-facing steps, respectively. Both studies showed significant enhancements in flame stability limits for a wide range of mixtures and flow rates. Similarly, Akhtar et al. [31] extended the investigation of backward-facing step micro-combustors to different cross-sections. The numerical results indicated that both trapezoidal and triangular cross-sections have a favorable effect on the overall flow and thermal performance.

On the other hand, Jiaqiang et al. [32] investigated the effect of inlet pressure on H_2/air combustion in a backward-facing step micro-combustor. The study found that the hydrogen-to-air equivalence ratio and inlet flow rate have the largest and lowest effects on emitter thermal efficiency, respectively. Moreover, Jiaqiang et al. [33] analyzed the effects of step angle, wall materials, and inlet velocity on the premixed methane/air combustion of a two-step micro combustor. They found that using an angled step of 45° is very beneficial in terms of flame stability. The study demonstrated that the two-step micro combustor has good performance and higher synergy degree at inlet velocities of 2 m/s and 4 m/s, with more differences in combustion efficiency as inlet velocities increase. However, by comparing experimental and numerical results, Peng et al. [34] concluded that recirculation zones generated behind the backward-facing steps significantly affect flame location and stability. They observed that a properly stepped/flared inlet and heat recirculation zone contributed to ignition and improved efficiency. Zuo et al. [35] developed an improved micro-combustor with a rectangular rib. They obtained a higher and more uniform outer wall temperature distribution. Chen et al. [36] proposed an improved micro combustor with a rectangular rib. They found that the improved combustor had a larger recirculation zone, resulting in a higher wall temperature. However, the outer wall temperature decreased as the horizontal step length increased due to increased thermal resistance. Ni et al. [37] carried out a numerical investigation for three different cross-sectional ribs and found that the optimum design is U-shaped ribs. The numerical results revealed that the combustor with two ribs has a better overall performance. Besides, U-shaped ribs achieve to increase the mean temperature of the outer wall by 25.4 K compared to other designs. In addition, the temperature level of the micro-combustor with a double rib is relatively higher than that with a single rib combustor. On the other hand, the wall cavities have been commonly utilized to confine the micro-combustion products by creating recirculation zones within the cavities. Qamareen et al. [38] investigated a 2D micro combustor with a backward-facing step and triangular wall fin. They found that the wall fin blockage ratio significantly improves the combustor performance at lower inlet velocities (4-20 m/s).

The fin location and shape also influence the temperature distribution, and the combustion performance. The experimental and numerical investigations of Wan et al. [39] revealed that the employment of wall cavities led to a higher and uniform temperature level. Further investigations of the authors in subsequent years demonstrated that the variation of the cavities gap distance had a significant influence on the chemical and thermal performance [40]. Following that, Su et al. [41] proposed a double-cavity micro combustor for an MTPV system, which showed a higher and more uniform temperature distribution than a single-cavity combustor. Peng et al. [42] proposed a micro combustor with a front-cavity for micro-thermophotovoltaic systems, which improves flame stability, outer wall temperature, and energy conversion efficiency. Following that, Li et al. [43] investigated the effect of the aft ramp angle of the cavity on the lean hydrogen/air combustion efficiency in a micro-cavity combustor. They indicated that

the combustion efficiency is higher for θ = 90° compared to θ = 135° at low inlet velocities, owing to a shorter flame height and smaller stretch rate. Though, Zuo et al. [44] designed a micro-cylindrical combustor with a cavity for micro-thermophotovoltaic applications. They showed that the optimal cavity length and outlet diameter are 6 mm and 2 mm, respectively, with a mean outer wall temperature of 1306.88 K and low non-uniformity. Gao et al. [45] constructed a cavity combustor with guide vanes to improve combustion characteristics. The temperature is observed to be significantly higher, with better preheating and ignition effects, than the traditional cavity combustor.

Additional techniques have been utilized to control the flame in micro-combustors, including blockage inserts, bluff-bodies and wall shape. Tang et al. [46] proposed a micro-planar combustor with parallel separating plates and demonstrated that thermal performance improved compared to a straight combustor. Wenming et al. [47] found that using a block insert increased temperature levels and distribution uniformity. Tang et al. [48] also demonstrated the benefits of a cross-plate insert in increasing blow-off limit and outer wall temperature level. Wan et al. [49] proposed a diverging cylindrical micro-combustor with a central rod, which increased blow-off limits and flame stability [50], [51]. Wan et al. [52] confirmed that the introduction of bluff bodies greatly expands blow-off limits compared to traditional straight micro-combustors. The shape and dimensions of the bluff-body were found to significantly impact the flame blow-off limit, as highlighted by Fan et al. [53], [54]. Furthermore, Niu et al. [55] also demonstrated that trapezoidal bluff-bodies expanded the blow-off limits. While Yan et al. [56] confirmed that the triangular pyramid shape can extend the flame blow-off limits. Yang et al. [57] proposed a backward facing step micro-combustor with a converging-diverging downstream channel and demonstrated that thermal performance improved compared to the simple backward facing step combustor. Meanwhile, Han et al. [58] proposed a novel micro-combustor with a wavy inner wall and revealed that the wavy wall design significantly improved temperature uniformity, particularly for inlet velocities greater than 12 m/s.

I.2.2. Review of Research Gaps and Opportunities

In the context of our comprehensive exploration of various micro-combustion enhancement techniques, including backward-facing steps, ribs, pin fins, and wall cavities, it becomes evident that these techniques have shown promising improvements. They contribute to enhancing combustion performance by extending residence time and broadening the operational range. However, a closer examination reveals that the effectiveness of these techniques is influenced by a multitude of factors, such as fuel-to-air equivalence ratio, inlet flow rate, step angle, wall materials, cavity gap distance, and the height of ribs and pin fins. Despite the substantial research efforts devoted to individual enhancement techniques, the optimization of micro-combustor geometrical configurations remains an active and evolving area of study, particularly with regard to flow, combustion and thermal efficiency. There is a persistent need for further exploration and refinement of these configurations to achieve superior performance of MTPV. However, a comprehensive review reveals distinct gaps and unexplored opportunities within the current landscape of micro combustor optimization.

- **Preference of Singular Technique**

  The existing body of research primarily focuses on individual enhancement techniques, such as backward-facing steps, ribs, pin fins, and wall cavities. While this one-dimensional geometric approach of these studies has demonstrated improvements in combustion stability and temperature distribution, they often do not encompass the full spectrum of possibilities. The use of one technique may be valuable in isolating and understanding specific effects, it lacks an integrated approach that considers the combined effects of multiple techniques. The synergistic potential of employing a combination of these enhancements remains largely unexplored in the open literature.

- **Parameter Dependence and Variation**

Numerous investigations have shed light on the influence of key parameters—fuel-to-air equivalence ratio, inlet flow rate, step angle, wall materials, cavity gap distance, rib and pin fin height—on the efficacy of enhancement techniques. However, a systematic study that carefully explores the interplay and optimal ranges of these parameters, particularly concerning combined techniques, is visibly infrequent. Understanding the intricate dependencies and variations of these parameters is crucial for achieving a holistic optimization of micro-combustor performance.

- **Narrow Scope of Investigation**

  While studies have investigated geometrical configurations to enhance MTPV efficiency, the investigations scope has often been limited to specific challenges, such as flame stabilization. A notable research gap exists in the comprehensive optimization of micro-combustor geometries, considering flow efficiency as objective. The exploration of diverse geometrical configurations, potentially integrating various enhancement techniques, with a focus on flow, combustion, and thermal characteristics, and efficiency is an avenue suitable for further academic pursuit.

- **Missing of Comparative Analysis**

  An in-depth comparative analysis, systematically comparing the effectiveness of various enhancement techniques and their combinations, is conspicuously missing. Such an analysis could provide valuable insights into the relative merits and limitations of each technique and guide researchers towards the most efficient and effective approaches for micro-combustor enhancement.

In conclusion, while recent research has undoubtedly propelled the field of micro-combustion forward, a comprehensive and integrated approach encompassing various techniques, systematic parameter studies, and a focus on flow, combustion, and thermal efficiency is essential to bridge the identified research gaps. By addressing these gaps, the field can advance towards the goal of achieving highly efficient and stable micro combustors for Micro-Thermophotovoltaic (MTPV) systems. Future research endeavors should ambitiously strive to unlock the full potential of micro-scale combustion through innovative and comprehensive investigations.

I.3. Thesis Overview

I.3.1. Thesis Focus

The preceding reviews have shed light on the pivotal role played by the micro combustor in optimizing MTPV systems, emphasizing the need for innovative approaches to enhance their overall performance. Our extensive review of existing literature illuminated that the "wall projections" strategy, aimed at enhancing surface area, exhibited superior performance in enhancing heat transfer from the inner walls of micro-combustors to their external surfaces. Consequently, the key objective is to direct the flow towards the inner wall of the micro-combustor, recognizing it as a pivotal approach for optimizing the performance of Micro-Thermophotovoltaic (MTPV) systems. Our review of research gaps reveals the underexplored potential of ribs as a wall projection technique to enhance the micro combustor's inner surface area. The review reveals also that the integration of multiple enhancement techniques, such as combining backward-facing steps with ribs or wall cavities, presents a promising but underexplored area. Research to date has predominantly focused on individual techniques in isolation. Investigating the potential synergies when employing a combination of these enhancements could unveil new pathways for achieving enhanced combustion efficiency and thermal performance. Therefore, we have chosen to narrow our doctoral research focus in this direction, driven by a deliberate and strategic approach aimed at addressing critical gaps in existing research efforts while capitalizing on the promising findings of our contextual study. Our thesis focus can be summarized as follows:

1. **Effect of Geometry**

   The focus of this doctoral thesis centers on developing reliable micro combustor geometrical configurations that integrate a combination of a backward facing step and a novel-shaped rib as an enhancement technique. Thus, we carefully designed a micro combustor that incorporates a combination of a backward facing step and a rib with angled edges. The rib's shape, viewed perpendicularly to the axial direction of the micro combustor, is a trapezoid with equal sides, which we identify as the "trapezoidal rib." The aim is to minimize their impact on the flow and combustion stability. The trapezoidal shape of the ribs is not our sole novel contribution in the field of micro combustion and enhancement techniques. We also focus on defining the efficient number, and height of the introduced trapezoidal rib(s). The objective is to utilize these geometric parameters as passive control methods to enhance convective heat transfer, induce the generation of equitably distributed recirculation regions near the micro-combustor's inner wall, which can increase the residence time and provide a continuous ignition source. Furthermore, we focus on investigating the effect of the cross-section area of micro combustor on various aspects of micro combustion and MTPV system challenges. Thus, we propose a comparison between overall efficiency of cylindrical and planar micro combustor geometrical configurations that incorporate a combination of a backward facing step and multiple equidistant pairs of novel trapezoidal ribs.

2. **Effect of Operating Conditions**

   This doctoral thesis not only centers on advancing the field of micro-combustion by investigating the impact of geometric configuration approaches but also focuses on investigating the influence of operating conditions on various aspects of micro combustion and MTPV system challenges. The investigation focuses on defining the efficient operating range of inlet velocity and equivalence ratio for the turbulent mixture of micro combustion. Through a systematic numerical methodology and a deliberate analytical approach, we strive to advance our understanding of micro-combustion flow, chemical and thermal combined processes, and provide valuable insights to the field. Our ultimate goal is to enhance the overall performance and efficiency of micro combustors and MTPV systems.

I.3.2. Motivations

Micro-combustion, a fascinating field with applications ranging from power generation to propulsion systems, has witnessed remarkable advancements in recent years. However, as the quest for efficiency, sustainability, and miniaturization intensifies, so do the challenges encountered in harnessing the full potential of micro-scale combustion devices. The motivation behind this doctoral research lies in the pursuit of innovative solutions to these challenges and the drive to address critical gaps in our understanding of micro-combustion processes. Our motivations for embarking on this doctoral research journey in micro-combustion are multifaceted and are driven by the following key factors:

Central to our motivation is the imperative to empower sustainability and align our research efforts with the global momentum towards a 'green revolution.' The marriage of micro combustion and the Micro-Thermophotovoltaic (MTPV) system encapsulates a distinctive unicity, characterized by its simplicity and tangible real-world applicability. This distinctive trait amplifies the allure of this field, encouraging our resolve to delve deeper into its dynamics. Knowingly, the field of micro combustion is experiencing a dynamic surge, both in its research endeavors and the attention it garners from the scientific community. Its interdisciplinary nature and the diverse array of systems it encompasses serve as further catalysts for our scholarly engagement. The prevalence of numerical studies within this domain underscores its modern, data-centric character, amplifying its allure for our research pursuits. We are profoundly

motivated by the myriad challenges that micro combustion presents, ranging from fluid dynamics to combustion efficiency and thermal management. These challenges beckon us to explore and innovate, driving our determination to contribute to the development of novel enhancement techniques for both micro combustion and MTPV systems. Our motivation extends to the pervasive research gaps within this domain, which, instead of presenting hurdles, unfurl as vast opportunities for meaningful research and innovation. Specifically, we are propelled by the aspiration to bridge research gaps, focusing on the burgeoning trend of utilizing ribs as wall projections to influence flow dynamics and heat transfer within combustion. The immense potential for passive control and enhancement through the improvement of rib shape, number, and height captivates our research agenda. Moreover, the lack of a comprehensive integrative analysis approach addressing the multifaceted aspects of micro combustion - encompassing flow, combustion, and thermal challenges - fuels our motivation. We aim to delve into this uncharted territory, driven by the ambition to offer a more comprehensive understanding through meticulous comparison between flow characteristics under non-reacting and reacting conditions. This analytical approach is vital to unravel the effects of geometrical configuration on combustion characteristics and efficiency—an area that has garnered relatively less attention and is suitable for exploration.

I.3.3. Objectives

The primary objective of the present doctoral study is to assess numerically the flow-field, combustion and thermal performance and characterize the optimal operating conditions of a novel geometrical configuration designed specifically for MTPV applications. This novel system introduces the shape, number of ribs, and variable rib heights as passive control techniques aimed at facilitating the creation of equidistantly distributed recirculation zones along the inner wall of the micro combustor. Following the objective of our doctoral research subject in numerically study of turbulent mixing with or without chemical reactions in various geometrical configurations We outline the specific aims as follow:

- **Hydrogen Application Potentials**

  The primary objective of the current doctoral research is to harness the potential of hydrogen, a representative fuel of future, in order to advance the understanding and efficiency of its application in micro combustion-based systems.

- **Geometric Configuration Assessment**

  To comprehensively evaluate the impact of the new geometrical configuration on the performance of the micro combustor within MTPV systems.

- **Passive Control Enhancement**

  To investigate the effectiveness of the shape, number of ribs, and variable rib heights as a passive control technique for promoting the formation of equidistantly distributed recirculation zones within the micro combustor.

- **Micro Combustor Cross-section**

  To investigate the effectiveness of the micro combustor cross-section on the performance of the micro combustor within MTPV systems.

- **Operating Conditions Characterization**

  To systematically analyze the influence of both mixture inlet velocity and the hydrogen-to-air equivalence ratio on the thermal performance of the micro combustor.

By pursuing these objectives, we aim to advance our understanding of micro combustion within MTPV systems and contribute valuable insights into optimizing their performance, thus facilitating their application in various domains.

I.3.4. Strategy of Research

The research strategy employed in this thesis is meticulously designed to explore the effectiveness of a novel geometrical configuration for Micro Thermophotovoltaic (MTPV) micro combustors. The primary focus of this strategy is to assess the flow, combustion, and thermal efficiency of the proposed configuration, which includes a micro combustor with a single backward-facing step and multiple trapezoidal ribs. To systematically evaluate the impact of this configuration, the research proceeds through a sequence of meticulously crafted investigations:

2D – Two-dimensional Study

---

1. Impact of the Rib Shape

In the initial phase, the research employs 2D simulations to delve into the micro combustor's geometric features. This involves the investigation of the impact of introduction of the ribs and comparing the proposed trapezoidal angled edge ribs with other rib shapes, namely rectangular, curved, and triangular ribs.

2. Exploring the Influence of Rib Count

Building upon the initial findings, the research investigates the impact of the number of ribs within the micro combustor. This exploration spans a range from a single rib to six ribs, with careful consideration of equidistant spacing between the ribs. Each rib configuration is assessed to gauge its influence on flow field characteristics, combustion behavior, and thermal performance.

3. Assessing Rib Height Variations

The research strategy also encompasses an in-depth analysis of rib height. The rib height is systematically varied from 0.3 to 0.8, with 0.5 serving as the baseline. This exploration enables the assessment of how rib height affects critical aspects including flow field dynamics, combustion stability, and thermal behavior.

4. Effect of Operating Conditions

In the second part of the 2D study, we delve deeper into the chosen geometric configuration. This phase allows us to systematically evaluate how the mixture inlet velocity and hydrogen-to-air equivalence ratio influence the micro combustor's performance. Our objective is to determine the optimal operating conditions associated to the chosen geometrical configuration. These investigations shed light on their effects on flow, combustion, and thermal behavior.

3D Three-dimensional

---

4. Transition to Micro Combustor Cross Section

Building upon the insights gained from the rib-focused 2D investigations, the research extends its purview to the micro combustor's cross-sectional shape. Hence, two three-dimensional (3D) configurations, cylindrical and planar, are meticulously examined. This transition facilitates a comprehensive understanding of how the micro combustor's shape influences flow-field patterns, combustion performance, and thermal characteristics.

5. Impact on Overall MTPV System Performance

Finally, the research loops back to the core objective by investigating how the proposed geometrical configuration, along with its various parameters, affects the overall performance of the MTPV system. This holistic assessment provides invaluable insights into the real-world implications of the micro combustor's design on energy generation and MTPV system efficiency.

By systematically progressing through these research phases, the strategy ensures a comprehensive and nuanced evaluation of the proposed MTPV micro combustor configuration. Each step builds upon the previous one, concluding in a profound understanding of the configurations performance and its potential for enhancing power generation within the field of MTPV technology.

I.3.5. Thesis Structure

This thesis is structured to provide a comprehensive exploration of the micro combustion-based Micro Thermophotovoltaic (MTPV) systems, encompassing the fundamental principles, numerical modeling techniques, and extensive applications. The overall structure is designed to facilitate a systematic and progressive understanding of the research undertaken, allowing readers to delve into the subject matter with clarity and coherence.

Chapter I: General Introduction

I.1. Study Context: This chapter establishes the groundwork by presenting the technical and environmental background, current and emerging solutions in micro combustion, the significance of micro combustion solutions, and an introduction to the Micro Thermophotovoltaic (MTPV) system. It sets the stage for a comprehensive exploration of the subject.

I.2. Literature Review: Building upon the study context, this chapter conducts a thorough bibliographic analysis and literature review to discern the historical development, current challenges, and emerging solutions in the field of micro combustion-based power generation. It provides a solid foundation for the subsequent chapters.

I.3. Thesis Overview: This chapter introduces the readers to the primary focus, motivations, objectives, research strategy, and the structure of the thesis. It outlines the path of inquiry that will be followed in subsequent chapters.

Chapter II: Fundamentals

II.1. Micro Scale Combustion: Focusing on micro scale combustion, this chapter discusses its scalability, fundamental principles, challenges, and efficiency. It forms a vital foundation for the study of micro combustion within MTPV systems.

II.2. Micro Thermophotovoltaic Systems: This chapter delves into the fundamental principles of Micro Thermophotovoltaic (MTPV) systems, exploring their operating principle, structure, challenges and efficiency. It offers a comprehensive understanding of the core subject matter.

Chapter III: Methodology

III.1. Problem Formulation: This chapter formulates the research problem physically and mathematically, detailing the involved transport phenomena, as well as the mathematical assumptions, and governing equations employed in the mathematical modelling of the current doctoral numerical study.

III.2. Numerical Modeling: Providing a deeper insight into the research methodology, this chapter covers the numerical models, material properties, boundary conditions, discretization methods, solution control, and convergence criteria.

Chapter IV: Results

IV.1. 2D bidimensional: This chapter investigates the effect of geometry and operating conditions on the micro combustor in a bidimensional context, drawing significant conclusions from the findings.

IV.2. 3D Tridimensional: Expanding upon the previous 2D investigations, this section explores the effect of micro combustor cross section in a tridimensional context, offering evaluation of the proposed micro combustor configurations on the MTPV performance.

General Conclusion

This pivotal chapter summarizes our key findings, discusses significance, and highlights key contributions of our research objectives. Closing the thesis, this chapter outlines future research prospects within the field, mapping a course for continuous exploration and research.

Chapter II: Fundamentals

II.1. Micro Scale Combustion

The evolution of micro combustion represents a pivotal shift in the landscape of combustion science and engineering. In the pre-MEMS era, the study of combustion at small scales was largely confined to theoretical inquiries, with a primary focus on unraveling the enigma of quenching diameter. However, the advent of sophisticated microfabrication techniques and the ascent of microelectromechanical systems (MEMS) conducted in a new era. This era not only witnessed the flourishing of power MEMS but also gave birth to innovative micro combustion-based systems like MTPV (Micro Thermophotovoltaics), MTEG (Micro Thermoelectric Generators), and micro engines. Within these cutting-edge systems, the imperative for a dependable heat source has become increasingly apparent, a role frequently assumed by micro combustors. This need arises primarily from the remarkable energy density offered by traditional hydrocarbon fuels and, notably, by the revolutionary green energy fuel, hydrogen. Consequently, research dedicated to the application of combustion processes within micro-scale systems multiplied. These attempts engender a captivating confluence of physics, chemistry, and engineering—a synergy that characterizes the essence of micro combustion [59]. Despite the fundamental principles of combustion in conventional combustors, derived from established thermodynamics and chemistry, micro combustion within a confined scale resides in a unique niche within the combustion landscape. The miniaturization of combustion chambers give rise to a cascade of distinct behaviors and characteristics that demand careful exploration. It is towards this area that the boundaries of traditional combustion science are pushed, prompting researchers to delve into the complexities of flow dynamics, flame propagation, heat transfer, and chemical kinetics at scales previously unexplored. In the context of MTPV, the significance of micro combustion extends beyond the controlled and efficient combustion of fuels at the microscale, it becomes instrumental and finds a specific and compelling applications in micro power generation solutions. Given this recent evolutionary trajectory and the evolving nature of micro combustion field, ensuring clarity and precision in terminology is imperative, particularly to distinguish between theoretical and applied engineering studies. Therefore, it becomes essential to delve into the micro combustion scaling definitions and parameters. Hence, at the outset of this chapter, we embark on a discussion aimed at elucidating and refining the definitions and parameters pertaining to scaling. This clarification process is integral for harmonizing the practices employed within both sub-domains of micro combustion. However, understanding the fundamental principles of micro combustion is essential for harnessing the potential of micro combustor. Hence, in the following comprehensive exploration of micro combustion, we delve into the fundamental principles that govern micro combustion, focusing on the essential aspects of fluid dynamics, combustion behavior, and heat transfer. These principles provide the foundation for understanding how combustion processes operate within micro-scale environments, where factors like flow dynamics, combustion efficiency, and thermal characteristics take on new significance. This chapter serves as a foundational exploration to the current doctoral research and the subsequent analyses and investigations into the fascinating domain of micro-scale combustion.

II.1.1. Scaling Parameters

- **Primary Scales**

The scaling of micro combustion systems is a complex issue that encompasses various length and time scales, leading to nuanced definitions of what constitutes "micro-scale" combustion. The ambiguity arises from the arbitrary choices of reference length scales and the overlap with the concept of "mesoscale" combustion. To address this, researchers have employed three primary methods to define micro-scale combustion [60]:

1. **Micro Combustor Dimension**

   This approach uses the physical dimension of the combustor to classify combustion systems. If the combustor's physical length scale is below 1 mm, it's considered micro-combustion; otherwise, if it's larger than 1 mm but on the order of 1 cm, it's termed mesoscale combustion. This definition is common in the development of micro-engines. Within this method, two key length scales are considered: the size of the combustor's inner diameter (denoted as "d_1") and the structural dimensions of the micro combustor (denoted as "d_s").

2. **Flame Reference Length Scale**

   Another approach uses the quenching diameter as a reference length scale. Combustion is labeled micro-scale if the combustor size is smaller than the quenching diameter and mesoscale if larger. While this method aligns more with physical flame regimes, it is challenging to quantitatively define the micro/mesoscale boundary due to dependencies on mixture composition and wall properties.

3. **Micro Combustion System Dimension**

   This approach compares the length scale of the entire micro combustion-based system to that of conventional large-scale ones for similar purposes. For instance, a micro-combustor for a micro thermophotovoltaic systems doesn't necessarily imply the combustor is micro-scale; it simply indicates its application in a micro-satellite, UAVs which is relatively smaller compared to typical commercial satellites and air vehicles. This definition is used for our specific MTPV application.

- ## Theoretical Scales

Micro-combustion is tied to a multitude of physical and chemical processes, including but not limited to gas-phase reactions, surface reactions, molecular transport, thermal and mass diffusion, convection, and radiation. The combustion process in the context of micro-power generation encompasses a diverse range of length and time scales [60]. To comprehensively discuss the scaling parameters of micro combustion, we can categorize the information into the following:

Length Scales

The characterization of length scales is pivotal for understanding and modeling the behavior of these miniature systems:

- **Micro Combustor Lengths**

  This approach classifies combustion systems based on the physical dimensions of the micro combustor itself. Within this classification, two key length scales are considered: the size of the combustor's inner diameter (denoted as "d_1") and the structural dimensions of the micro combustor (denoted as "d_s").

- **Thermophysical and Flame Lengths**

  In the context of thermophysical and flame lengths, we encounter a range of parameters that shed light on the behavior of micro-scale combustion systems. These parameters offer insights into the complexities of combustion behavior at these miniature scales:

- **Flame thickness (δ_f)**

  The flame thickness, often denoted as δ_f, is a fundamental dimension in combustion physics. It characterizes the spatial extent over which combustion reactions occur within the flame front. In micro combustion, due to reduced length scales, flame thickness can have a substantial impact on

the overall combustion process. Understanding and controlling δ_f are critical for optimizing combustion efficiency.

- **Quenching diameter (d_0)**

  Another approach uses the flame as a reference length scales. Combustion is labeled micro-scale if the combustor size is smaller than the quenching diameter and mesoscale if larger. While this method aligns more with physical flame regimes, it is challenging to quantitatively define the micro/mesoscale boundary due to dependencies on mixture composition and wall properties. It's important to note that the quenching diameter is typically several times (denoted as ' d_0') the flame thickness, with the specific value of 'n' contingent upon the wall temperature. For instance, when the wall temperature is at room temperature, ' d_0' is approximately 15.

- **Mass diffusion length (δ_D)**

  The mass diffusion length, δ_D, plays a pivotal role in determining how chemical species mix within the combustion chamber. In micro-scale systems, where flow dynamics and diffusion processes are distinct, understanding δ_D is essential for achieving the desired fuel-air mixing and controlling combustion kinetics.

- **Thermal diffusion length (δ_α)**

  The thermal diffusion length, δ_α, governs the rate at which temperature variations propagate through the combustion medium. In micro combustion, where thermal gradients can be pronounced, δα influences the spatial distribution of temperature within the system. Managing δα is crucial for optimizing combustion stability and minimizing thermal gradients.

- **Mean free path (λ)**

  The mean free path (λ) of gas molecules in combination with δ_α plays a critical role in micro combustion. The mean free path represents the average distance a molecule travels before colliding with another molecule. In micro-scale systems, where gas molecules have shorter distances to travel, λ impacts the transport of heat and mass, affecting combustion behavior.

Time Scales

These time scales collectively influence the behavior of micro-scale combustion systems. They dictate the interplay between chemical reactions, heat transfer, and fluid dynamics, making them key parameters to consider when designing and optimizing micro combustion-based systems.

1. **Gas-Phase Time Scales**

- **Flow residence time (t_{res})**

  Flow residence time represents the average time a gas particle spends within the combustion chamber. In micro-scale systems, t_{res} becomes a critical factor as it determines the duration available for chemical reactions. When t_{res} approaches the characteristic combustion time (t_c), incomplete combustion can occur.

- **Characteristic combustion time (t_c)**

  Characteristic combustion time, t_c, signifies the time required for combustion reactions to progress significantly within the combustor. In micro combustion, t_c is vital for assessing whether combustion can proceed efficiently within the limited time available.

- **Diffusion time scale (t_α)**

  The diffusion time scale, t_α, reflects how quickly heat and mass are transported through the gas phase. In micro-scale systems, t_α influences the spatial distribution of temperature and species concentration, impacting combustion behavior.

- **Time scale of heat loss (t_h)**

  The time scale of heat loss, t_h, accounts for the rate at which heat is dissipated from the combustion chamber due to convective and radiative heat losses. Managing t_h is crucial to maintaining combustion stability, especially in micro-scale systems.

- **Time scale of acoustic wave (t_a)**

  In micro combustion, acoustic waves can have a profound effect due to the confined environment. t_a represents the time scale at which these acoustic waves propagate through the combustion chamber, influencing combustion dynamics.

- **Ignition time scale (t_{ig})**

  Ignition time scale, t_{ig}, characterizes the time required for the initiation of combustion once the reactants are introduced. In micro combustion, where ignition can be influenced by various factors, t_{ig} plays a crucial role in determining ignition success.

2. Solid Phase Time Scales

- **Diffusion time scale (t_s)**

  The diffusion time scale in the solid phase, t_s, represents the rate at which heat and mass are transported through solid materials within the micro combustion. Understanding t_s is essential for assessing how temperature gradients develop within the solid components.

II.1.2. Basic Concepts

In micro-scale combustion, the flow residence time becomes comparable to the characteristic combustion time, the large surface-to-volume (S/V) ratio results in severe heat loss effects. Flame extinction is governed by the ratio of heat loss to heat generation, emphasizing the importance of understanding flame extinction processes. The effects of the aforementioned length and time scales on combustion in microscale level can be understood through non-dimensional parameters. Parameters like the Peclet number (Pe), Knudsen number (Kn), and Biot number (Bi) which provide valuable insights into different aspects of micro combustion, allowing researchers to characterize and address various phenomena associated with these systems. This multidimensional approach is crucial for advancing our understanding of combustion processes at the micro-scale [3]. The 1D-dimensional normalized form of the governing equations for both the gas and solid phases, along with their respective boundary conditions, can be expressed as:

$$\frac{l_c}{t_c u_c}\frac{\partial \bar{u}}{\partial \bar{t}} + \bar{u}\frac{\partial \bar{u}}{\partial \bar{x}} = -\frac{p_c}{\rho_c u_c^2}\frac{1}{\bar{\rho}}\frac{\partial \bar{p}}{\partial \bar{x}} + \frac{1}{Re}\bar{v}\frac{\partial^2 \bar{u}}{\partial \bar{x}^2} + \frac{g l_c}{u_c^2} \qquad (II.1\text{-}1)$$

$$\frac{l_c}{t_c u_c}\frac{\partial \bar{T}}{\partial \bar{t}} + \bar{u}\frac{\partial \bar{T}}{\partial \bar{x}} = -\frac{1}{Pe}\bar{\alpha}\frac{\partial^2 \bar{T}}{\partial \bar{x}^2} + Da\frac{Q}{\bar{C}_p T_c}\bar{\dot{w}}'' \qquad (II.1\text{-}2)$$

$$\frac{l_c}{t_c u_c}\frac{\partial \bar{y}_i}{\partial \bar{t}} + \bar{u}\frac{\partial \bar{y}_i}{\partial \bar{x}} = \frac{1}{LePe}\bar{D}\frac{\partial^2 \bar{y}_i}{\partial \bar{x}^2} + Da\frac{1}{y_{ic}}\bar{\dot{w}}'' \qquad (II.1\text{-}3)$$

$$\frac{\partial \bar{T}_s}{\partial \bar{t}} = Fo\bar{\alpha}_s\frac{\partial \bar{T}_s}{\partial \bar{x}^2} \qquad (II.1\text{-}4)$$

The pertinent normalized boundary conditions for these equations are as follows:

$$\bar{u} = 0, \qquad \bar{\tau} = \frac{\mu_c u_c}{\tau_c l_c}\,\bar{\mu}\,\frac{\partial \bar{u}}{\partial \bar{y}}$$

$$\bar{T} = \bar{T}_w, \qquad \lambda_s \frac{\partial \bar{T}_s}{\partial \bar{x}} = \lambda \frac{\partial \bar{T}}{\partial \bar{x}} \frac{\partial \bar{T}_s}{\partial \bar{x}} = Bi(\bar{T}_s - 1)$$

$$\bar{y}_i = 0, \qquad \frac{\partial \bar{y}_i}{\partial \bar{x}} = (Le \cdot Pe)\bar{y}_i$$

The effects of these parameters on micro-scale combustion are described using non-dimensional parameters. For instance, when the size of the micro combustor approaches approximately ten times that of the flame thickness or nears the quenching diameter, phenomena such as flame extinction or instability begin to manifest due to factors such as wall heat dissipation and radical quenching, which are influenced by wall temperature conditions. Moreover, the mixing of fuel and oxidizer becomes constrained by molecular diffusion. This scenario can lead to the coalescence of wall heat loss and auto-ignition at localized hot spots, resulting in the observation of isolated flame cells, as well as the presence of steady or unsteady flame patterns within the system. As the size of the combustor diminishes, the time scale associated with thermal diffusion in the solid phase becomes comparable to the time scale of combustion itself. This convergence causes the flame temperature to synchronize with the temperature of the structure, giving rise to multiple flame regimes, including both typical flames and weaker flames. These phenomena have been substantiated through a series of experiments and theoretical analyses. The substantial coupling between the flame and the wall in this scenario can substantially expand the flammability limits of the flame, primarily due to the influence of excess enthalpy [3]. With increasing wall temperatures, the ignition time shortens, and it becomes possible to observe weak flames or even flameless combustion. When the ignition time approaches the flow residence time, and the combustor size is in close proximity to the quenching limit, flame instability arises in the form of flame extinction and reignition. The connection between wall temperature and the flame's characteristics is governed by the Biot number, which quantifies the ratio of the diffusion time scale to the convective and radiative heat loss time scales. When the Biot number is large, changes in wall temperature have minimal effects. However, when the Biot number is not large, changes in wall temperature can significantly impact combustion at small scales. Additionally, the Fourier number, reflecting the ratio of the combustion time scale to the diffusion time scale in the solid phase, affects the temperature distribution within the combustor's solid phase. If the Fourier number is exceptionally large, and there is adequate reactivity maintained during transient reactor response, the temperature distribution within the solid phase can be approximated as quasi-steady-state. Further reducing the scale of the combustor, for example, when the Knudsen number exceeds 0.01, introduces non-equilibrium transport effects, such as temperature and concentration variations at the wall surface, that begin to influence combustion. Numerous researchers have delved into these complexities and have identified the pronounced influence of non-equilibrium effects on ignition and extinction phenomena. In micro-scale combustion, when the flow residence time closely approaches the characteristic combustion time, incomplete combustion leading to extinction becomes a prominent occurrence. Additionally, the Lewis number effect (Le) becomes a factor affecting thermal-diffusional instability. However, distinct from conventional combustion at larger scales, the thermal transport within the solid phase significantly alters the effective Lewis number and the boundaries of flame instability. Notably, when mixture Lewis numbers approach or fall below unity, phenomena such as spinning combustion and pulsating combustion have been observed. Furthermore, due to the confinement imposed by the walls and the elevated wall temperatures, acoustic waves exert a substantial influence on microscale combustion. All these intricacies can be systematically characterized through the relative length and time scales, while also necessitating consideration of unsteady temperature distributions within the solid phase.

II.1.3. Challenges

- **Fluid**

a. Flow-field Characteristics

Micro combustors, due to their small size and intricate designs, introduce unique challenges to fluid dynamics. The constraining factor in these micro combustors is the diminutive diameter of channels responsible for the intake of reactants, exhaust of products, and the actual combustion process, which rises a fundamental alteration in fluid behavior. One critical parameter characterizing this change is the Reynolds number, which quantifies the dominance of viscous forces compared to inertial forces in a fluid flow. These small dimensions lead to a critical parameter of the Reynolds number. In the case of meso-scale systems designed to produce 100 watts of power and employing a stoichiometric mixture of octane and air with a system efficiency of 10%, the volumetric flow rate of the gaseous mixture is approximately 0.4 liters per second. This calculation assumes a 5 mm diameter intake tube. The resulting Reynolds number, a dimensionless number representing the ratio of inertial forces to viscous forces, falls within the range of 5000 or lower. The precise value depends on factors like gas temperature. In contrast, when dealing with microscale systems generating a mere 100 milliwatts of power and equipped with a 0.5 mm diameter intake, the Reynolds number is notably smaller, around 50. In both cases, the low Reynolds numbers indicates that flow within these micro combustors predominantly exhibits laminar characteristics. Laminar flow, characterized by smooth and predictable fluid motion, is the dominant mode in these small-scale systems. Consequently, mixing of different species within these micro combustors is primarily driven by diffusion, which relies on the natural tendency of molecules to spread out and equalize their concentrations. It's important to note that this laminar flow regime presents its own set of challenges and considerations, significantly different from the turbulent flow found in larger-scale systems [3]. On the other hand, viscosity, as fundamental property of fluids, plays a crucial role in micro-channels. Due to the small dimensions of these channels, viscous effects become more pronounced. Viscosity can be understood as a measure of a fluid's resistance to flow. In micro combustors, these effects lead to increased frictional losses, which means that more pumping energy is required to maintain the desired flow rates. This is particularly important because excessive energy consumption can affect the overall efficiency of micro combustor. However, it's worth noting that viscous forces can also have a beneficial aspect in micro combustors. These forces can help mitigate some of the challenges that are characteristic of small-scale systems. For example, they can reduce the potential for gas leakage through joints or moving surfaces. In applications like internal combustion engines (IC engines), where efficiency depends on factors such as the compression ratio, minimizing leakage at piston (or rotor)/housing interfaces is critical.

b. Challenges at Small Length Scales

At miniature length scales, which often characterize MEMS (Micro-Electro-Mechanical Systems) devices and their components, a host of intricate challenges and unconventional behaviors emerge. These challenges stem from the fact that fluid flow in such micro combustors operates within what is known as the near-Stokesian regime. In this regime, the Reynolds number, a dimensionless parameter governing flow behavior, is typically less than one. This has profound implications for fluid dynamics and heat transfer, introducing complexities not typically encountered in macroscopic contexts. One notable effect of operating at these extremely small scales is the heightened sensitivity of fluid flow to temperature variations. Even minor changes in temperature can exert significant influence on volumetric flow rates, a phenomenon that demands meticulous control and management in micro-combustor design and operation. Additionally, the small dimensions of micro-channels give rise to substantial velocity gradients within the fluid. These gradients result in elevated wall frictional losses, which, in turn, translate into high

convective heat transfer coefficients. Such characteristics introduce two major consequences: increased pressure losses within the micro combustors and enhanced diffusive mixing of species within the fluid. The heightened pressure losses are of practical significance as they affect overall system efficiency and performance. Furthermore, the intensified heat transfer between the fluid and the channel walls presents thermal management challenges that necessitate innovative solutions in the design of micro-scale combustors and thermal systems. However, it is worth noted that the characteristic length of currently developed micro-combustors, including those within MTPV systems, surpasses the molecular mean-free path (λ) of the flowing gases. This phenomenon maintains the fundamental physical-chemical behavior of fluids in these micro-combustors similar to their macro-scale counterparts. As an illustrative example, when air traverses a channel with a hydraulic diameter of 0.1 mm, the Knudsen number (Kn) assumes a value on the order of 10^{-3}, which is clearly smaller than that characterizing free molecule flow (Kn > 1). Consequently, established thermo-fluid hypotheses, such as the no-slip condition and the continuum medium assumption, remain valid. Furthermore, the small length scales in micro-combustors significantly affect the dynamics and energy requirements related to phase change and two-phase flows. Phase change from liquid to vapor in micro-scale channels occurs abruptly and unpredictably due to the high surface area to volume ratio, enhancing nucleation and wetting effects at the wall. Additionally, the behavior of bubbles in these small channels diverges significantly from macroscopic behavior, further complicating the phase change process. Moreover, smaller dimensions increase the pressure and energy demands for atomization due to the inverse relationship between droplet surface energy and radius of curvature. Developing micron-sized droplets that evaporate and mix within micro-scale residence times necessitates advanced techniques such as MEMS-based micro-electrospray atomizers.

- ## Combustion

Micro-scale combustion brings distinct challenges rooted in the juxtaposition of chemical reactions and thermos-physical constraints [61]. Unique fundamental, primarily related to timescales, material constraints, heat transfer, and fluid-structure thermal coupling, are illustrated as follow:

a. Timescales Constraints

A fundamental necessary for micro-combustion is that the residence time, which is the physical time it takes the different reactants and products gases to flow within the micro combustor, must surpass the time required for the chemical reaction, known as combustion time. In gas-phase combustion within flow systems like gas turbine combustors, the residence time hinges on the combustion chamber's size and the reactant stream's flow rate. Conversely, in closed systems like internal combustion engines, the rpm of the engine additionally influences the residence time. For catalytic combustion, species diffusion to the wall and species absorption/desorption at the wall become critical determinants of residence time. Given the typically diminutive residence times in micro-combustors, achieving short chemical times is pivotal to complete the combustion process within these chambers. Moreover, when reactants are not premixed and the fuel is in liquid form, additional time and volume are required for fuel evaporation and mixing. Liquid evaporation and mixing at the anticipated low Reynolds numbers in these systems are inherently slow, posing a significant temporal challenge. Innovative approaches like burning liquid fuel while forming a liquid film along the combustion chamber wall have been explored. This technique not only reduces heat losses but also inhibits wall quenching by keeping the combustor walls cooled. Moreover, it maintains large vaporization rates due to the micro-combustor's large surface-to-volume ratio. This fundamental time constraints can be quantified using the homogeneous Damköhler number (Da), which is the ratio of the residence time to the characteristic chemical reaction time. Ensuring a Damköhler number (Da) greater than unity is necessary for complete combustion. Achieving this requires either increasing the flow residence time or decreasing the chemical reaction time. Residence time can be extended by altering the size of the combustion chamber, reducing the mass flow rate, or increasing the operating pressure. On

the other hand, chemical reaction time primarily depends on fuel properties and mixture temperature. High power density requirements necessitate high mass flow rates through small chamber volumes, making it challenging to reduce the mass flow rate per unit volume without compromising power density. Thus, there's an inherent trade-off between power density and flow residence time. An additional timescale, in the case of catalytic combustors, diffusion time, becomes crucial. This parameter reflects the time required for fuel and oxidizer molecules to interact with the active catalytic surface, profoundly affecting micro combustor operation. Several non-dimensional parameters, including Damköhler numbers (Da), help determine which process governs performance, with diffusion time playing a pivotal role.

b. Thermal Fluid Structure Coupling

In micro combustors, heat transfer at the chamber walls becomes a significant factor, in stark contrast to large-scale combustors where it's often neglected. As the size of the micro combustor volume diminishes, the surface-to-volume ratio amplifies. This amplification leads to amplified combustor surface heat losses and an increased likelihood of radical species destruction near the wall. These mechanisms compound the chemical time, potentially stalling gas-phase combustion or extinguishing an ongoing reaction. This leads to two critical consequences. First, large thermal losses directly impact combustor efficiency, making it challenging to achieve efficiencies exceeding 99%, unlike large-scale combustors. Additionally, heat loss results in lower reaction temperatures, which can extend kinetic times and narrow flammability limits, further complicating the constraint of short residence time. Mitigating these challenges necessitates innovative thermo-chemical management techniques. Thus, to avert quenching, techniques like utilizing excess enthalpy combustors, establishing adiabatic walls through symmetrical stacking of planar micro combustors (insulated temperature boundary condition), employing high-temperature ceramic walls, and leveraging surface coatings have been instrumental. Pioneering work on excess enthalpy, recirculating burners demonstrated the optimization of combustion reactions by preheating fuel-air mixtures using product enthalpy, notably in the "Swiss roll" combustor. The recirculation of exhaust efficiently reduced heat losses and facilitated steady combustion with mixtures well below normal flammability limits. These advancements have been extended to thin tubes and micro-combustors.

c. Materials Constraints

Elevated combustor wall temperatures serve a dual purpose. Firstly, they prevent quenching, critical for the uninterrupted combustion process. Secondly, by diminishing chemical time, they counteract the limitation imposed by the small physical time inherent in micro-combustors. Ceramic materials like Silicon Dioxide (SiO_2), Silicon Carbide (SiC), and Silicon Nitride (Si_3N_4), capable of withstanding high temperatures, emerge as suitable candidates for micro combustors. Coating combustor walls with inert materials offers another viable approach to reduce radical recombination and chemical quenching at relatively low temperatures. Despite the surface-to-volume ratio presenting challenges for gas-phase combustion, it augments catalytic combustion. Catalytic reactions, although generally slower than gas-phase reactions, benefit from the increased surface area and lower reaction temperatures. Hence, implementing micro-scale combustors using catalytic reactions may be more viable than relying solely on gas-phase reactions. Catalytic surfaces, especially in micro-channels, have been investigated to stabilize flame structure, optimize combustion efficiencies, and reduce emissions.

• Thermal and Heat Transfer

a. Buoyancy and Heat Transfer

At the characteristic length scales of micro-combustion chambers, the role of heat transfer via natural convection diminishes due to the limited induced buoyant flow. However, other forms of heat transfer become significant. Conduction through the gas to surrounding surfaces and forced convection in the

intake and exhaust channels and the combustor wall are notable because temperature gradients intensify as the characteristic length decreases. Additionally, heat transfer by radiation becomes more prominent as the characteristic length decreases, primarily due to the increased view factor. Furthermore, as micro combustor size decreases, the surface-to-volume ratio grows, further amplifying heat transfer effects at the combustor's surface or boundary. While this can be advantageous in components relying on heat transfer, like MTPV and MTEG systems, it can pose challenges in systems where surface heat losses could reduce performance, such as in micro heaters and micro reactors due to wall quenching [62].

b. Heat Losses in Combustors Wall

It's worth noting that the small buoyant forces and the low thermal conductivity of air (λ_a~ 0.03 W/mK) result in relatively minor heat losses from a combustor when compared to its total heat generation. A rough estimate of the order of magnitude of heat losses from a combustor to the surrounding air can be obtained using a simple 1-D, steady-state calculation. The heat flux from the hot gases in the combustion chamber to the ambient air surrounding the combustor can be approximated as:

$$\frac{q}{A} = \frac{T_g - T_a}{\frac{1}{h_g} + \frac{1}{\lambda_s} + \frac{1}{\frac{\lambda_a}{l_c} + h_{ra}}} \qquad \textit{(II.1-5)}$$

In this equation, the subscript g represents the hot gases in the combustion chamber, and the subscript a represents the air surrounding the combustor. For instance, in the case of a meso-size combustor with a characteristic length of l_c = 20 mm, capable of providing around 50W power, combustion gas and ambient air temperatures of T_g =1,000°C and T_a = 20°C, a heat transfer coefficient of h_g = 100 W/m^{2}K (accounting for convection and radiation), a *SiC* combustor housing (λ_s = 500 W/mK), and a linearized radiative heat transfer coefficient from the housing to the ambient air of h_{ra} = 130 W/m^{2}K, Equation (II.1-5) yields a heat flux of approximately 0.05 W/mm^2. Assuming a combustion chamber area of 25 mm^2, the heat loss from the combustion gases amounts to roughly 1.3 W, approximately 3% of the combustor's output. Several insights can be drawn from Equation (II.1-5), including the negligible contribution of solid conduction and the relatively minor impact of heat convection through air compared to radiation at these small scales [62].

c. Forced Flow and Heat Transfer

When there is forced flow, as in an intake manifold or a gas turbine compressor, the heat transfer from the combustion chamber to the incoming air becomes considerably higher than the previously calculated scenario (λ_a and lc in Equation (II.1-5) would be replaced by a heat transfer coefficient, h_a >100 W/m^{2}K). Enhanced heat transfer to the incoming gas in the intake manifold is a significant concern in combustors using premixed reactants for combustion. While preheating the reactants aids in sustaining combustion at scales smaller than the quenching distance, it can lead to auto-ignition of the mixture in the inlet port. Therefore, insulation measures are required to control the amount of heat transferred to the incoming fuel/air mixture. Moreover, heating the reactants in the intake manifold results in a lower mass charge in the combustion chamber due to reduced density, leading to a reduction in the potential net power output of the system. Lower density also increases compression work per unit mass, ultimately lowering overall system efficiencies. This issue is particularly critical in gas turbines where compressor power requirements heavily influence overall efficiency. Consequently, effective thermal management is essential to minimize heat losses and optimize combustor performance.

d. Uniform Temperature and Thermal Gradients

Most micro combustion-based systems and especially the MTPV systems tend to operate at relatively uniform temperatures due to their small size. For example, a steel or silicon micro combustor with a

length scale of 10 mm, subjected to moderate convection and radiation, exhibits a Biot number (Bi) of approximately 0.002. This value is significantly smaller than what is typically considered sufficient for a heat transfer analysis (Bi < 0.1). Consequently, a uniform temperature approximation can adequately describe the internal temperature of the combustor (as a boundary condition for Equation (II.1-2)). Reduced thermal gradients in such cases alleviate thermal expansion stresses and associated misalignments in moving parts. However, challenges arise when large thermal gradients are required for high micro combustor performance, as seen in thermoelectric generators. This issue also affects gas-cycle type systems (heat engines) because their efficiency hinges on the temperature ratio between high and low temperature reservoirs. Achieving or maintaining a significant temperature ratio can be challenging, necessitating complicated thermal management solutions [62].

e. Transient Heat Transport

Effective thermal management extends beyond spatial temperature gradients and encompasses transient heat transport considerations. Significant disparities in characteristic time scales between the gas and solid phases or in periodic heat input from intermittent combustion can result in quasi-insulating conditions at the boundary. For instance, in a compression ignition engine where combustion time is much shorter than the heat transfer time through the engine housing, heat losses from the combustion reaction to the wall may be negligible due to the limited time available for heat transfer [62].

II.1.4. Micro Combustion Efficiency

Analyzing micro combustion efficiency is of paramount significance in enhancing the performance of micro combustion-based systems, especially for MTPV (Micro Thermophotovoltaic) systems. Understanding combustion efficiency provides crucial insights into the extent of fuel and oxidizer interaction and the effectiveness of fuel consumption and conversion into thermal energy. This understanding aids in evaluating the impact of micro combustor geometric configurations or operating conditions and enables the optimization of combustion processes for enhanced energy output. However, the micro combustion efficiency can be categorized into chemical efficiency and thermal efficiency, calculated as follow:

- **Chemical Efficiency**

The micro combustion's chemical efficiency η_{chem} is defined as the conversion rate of fuel and is calculated as follows:

$$\eta_{chem} = 1 - \frac{Y_{f,out}}{Y_{f,in}} \qquad \textit{(II.1-6)}$$

here, $Y_{f,in}$ represents the inlet fuel mass fraction, and $Y_{f,out}$ is the outlet fuel mass fraction.

- **Thermal Efficiency**

The thermal efficiency of micro combustion η_{therm} is calculated as follows:

$$\eta_{therm} = \frac{P_{\text{Comb}}}{P_{fuel}} \qquad \textit{(II.1-7)}$$

where, P_{fuel} represents the theoretical potential thermal power of the inputted fuel and is calculated as:

$$P_{\text{fuel}} = \dot{m}_{\text{fuel}} \cdot P_{LHV} \qquad \textit{(II.1-8)}$$

here $\dot{m}_{\text{fuel}}$ represents the mass flow rate of the inputted fuel, and P_{LHV} is the fuel's lower heating value.

Additionally, the effective thermal power released by micro combustion is calculated as:

$$P_{\text{Comb}} = P_{fuel} - P_{fuel,\ loss} \quad \textit{(II.1-9)}$$

Moreover, the heat loss ($P_{\text{fuel, loss}}$) is due to the incomplete combustion and it can be defined as:

$$P_{fuel,\ loss} = \dot{m}_{\text{fuel}} \cdot Y_{f,out} \cdot P_{LHV} \quad \textit{(II.1-10)}$$

II.2. Micro Thermophotovoltaic Systems

The emergence of micro combustion-based Thermophotovoltaic systems, commonly referred to as Micro Thermophotovoltaic (MTPV) systems, represents a significant breakthrough in the field of energy conversion and micro-scale power generation. It is crucial to delve into the fundamentals of MTPV systems and distinguish them from traditional Thermophotovoltaic (TPV) systems, emphasizing their basis on micro-scale combustion. Unlike traditional power generation systems that rely on large-scale components and complex design and structure, MTPV systems satisfy to the growing demand for compact, efficient, and portable power sources (**Figure II.2.1**). MTPV systems represent a pioneering rise by integrating the principles of thermodynamics, photonics, and materials science. They achieve the remarkable converting of thermal power from micro combustion into electricity at the micro-scale level. The significance of MTPV research is profound, primarily because it addresses the growing gap between conventional power sources and the power demands of modern microelectronics. In an era where small, autonomous devices play an increasingly pivotal role in our daily lives, the quest for efficient, self-sustaining power solutions has gained paramount importance. Another driving force behind MTPV research is the aspiration to discover sustainable and environmentally friendly power sources. Through optimized energy conversion processes, MTPV systems align with the global objective of mitigating carbon emissions and promoting clean energy technologies. Furthermore, MTPV systems offer a promising solution to overcome the limitations of traditional batteries and power storage devices with finite lifespans. MTPV holds the potential to provide a continuous and reliable power source across a diverse spectrum of micro-scale applications. These applications encompass remote sensors deployed in harsh and distant environments and implantable medical devices. This versatility underscores the transformative capacity of MTPV systems in the ongoing green energy revolution [63].

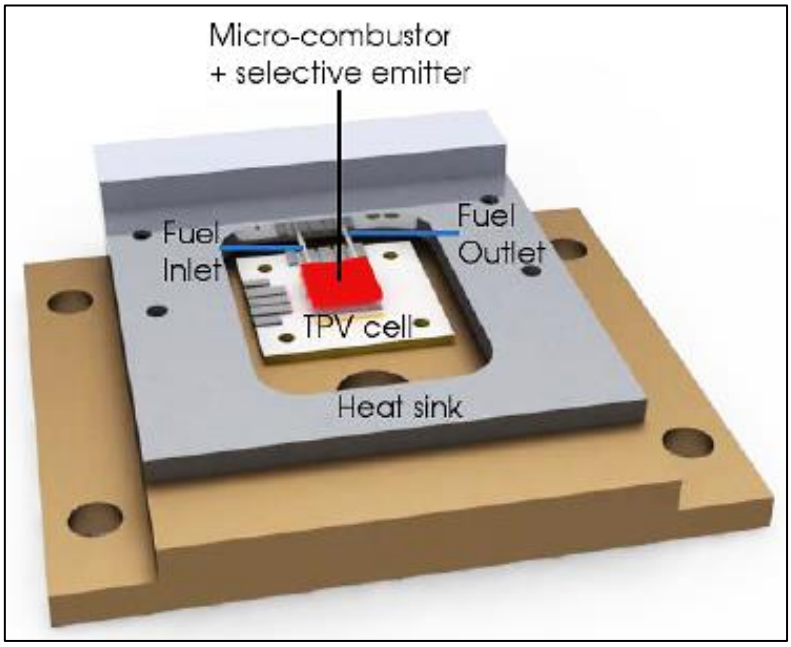

Figure II.2.1. *Micro Thermophotovoltaic (MTPV) portable generation system [63].*

II.2.1. Design and Structure

MTPV systems are a class of energy conversion systems that transform thermal energy into electricity through a combination of thermodynamic and photonic processes. The successful implementation of Micro Thermophotovoltaic (MTPV) systems relies on a well-thought-out design and a carefully constructed structure. These aspects are critical to systems and directly impact their performance, efficiency, and overall applicability. MTPV systems are engineered with a keen focus on maximizing energy conversion while considering factors such as materials, scalability, and thermal management. MTPV systems consist of several key components, each playing a vital role in the overall functionality and efficiency of the system. The exploration of Micro Thermophotovoltaic (MTPV) systems has seen a development of diverse designs and structures, each tailored to enhance overall system energy conversion efficiency and adaptability to various applications. This comprehensive study seeks to categorize these designs based on the cross-section of the micro combustors. Additionally, we delves into the structures of MTPV systems, elucidating variations and approaches adopted in the assemby of these systems.

- **Components**

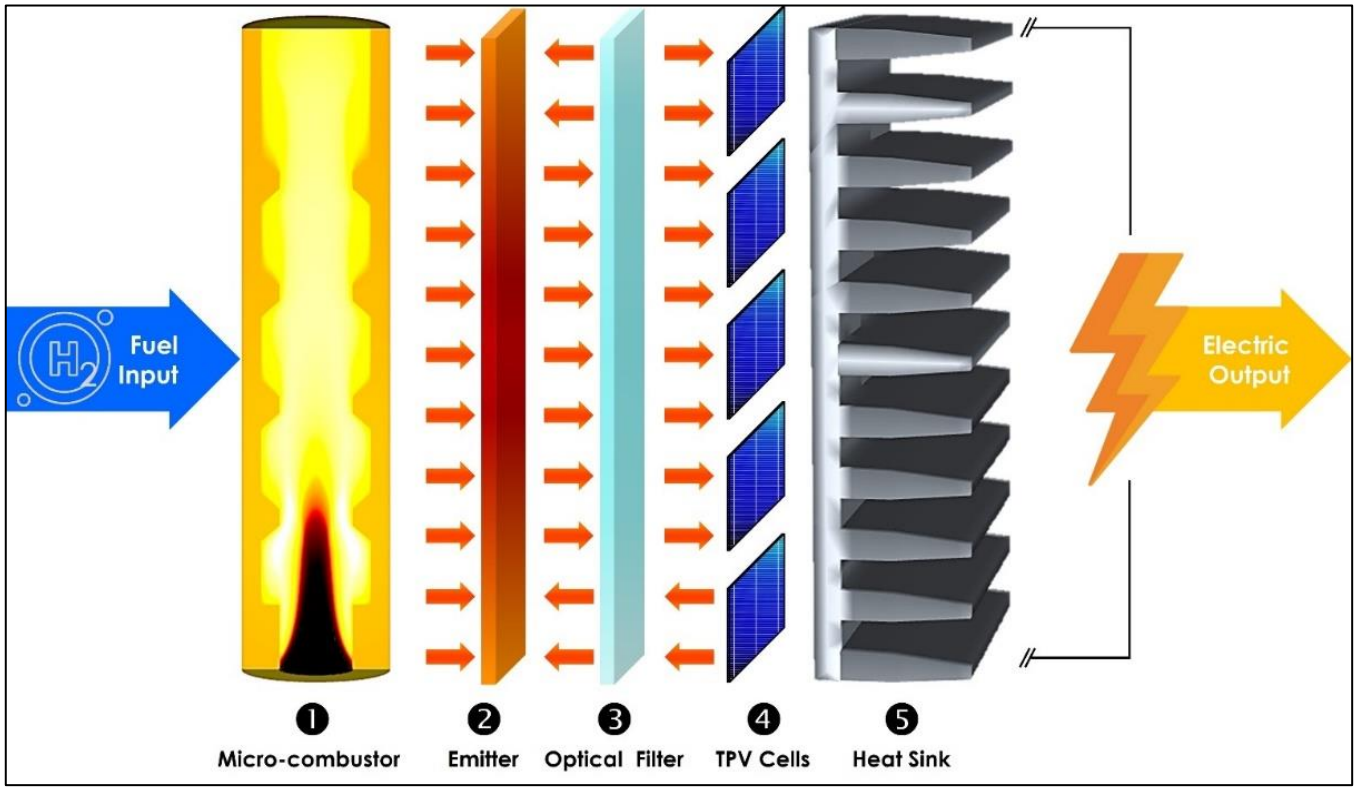

Figure II.2.2. *Schematic diagram of Micro Thermophotovoltaic System*

MTPV systems consist of several key components that work collaboratively to achieve efficient energy conversion. Understanding the role of each component is crucial for designing and optimizing MTPV systems [2]. The corresponding **Figure II.2.2** illustrates a schematic diagram for the MTPV system designed for this study.

❶ Micro Combustor

At the heart of the MTPV system lies the micro combustor as the heat source. This component is responsible for generating high-temperature thermal radiation. It typically utilizes a fuel-air mixture, which undergoes combustion, releasing heat. Exploring the design and operation conditions of micro combustors are critical for achieving stable, controlled, and efficient combustion while maintaining high

temperatures. Engineers often employ advanced materials and combustion techniques to optimize this component. The scope of our doctoral research is the micro combustor, which we consider the critical component toward high system performance, and specifically on its practical operation in MTPV systems.

❷ Emitter

The emitter is a crucial element responsible for emitting thermal radiation in the form of photons. The emitter function is to enhance the radiant heat transfer from the micro combustor into thermophotovoltaic cells and increase the emits of high energy photons [2]. Investigating emitter materials and their properties is crucial for enhancing photon emission. These materials must withstand high temperatures while efficiently emitting radiation in the desired wavelength range, ensuring maximum compatibility with thermophotovoltaic cells. Advanced materials, such as refractory metals or specially designed ceramics, are employed to achieve this.

❸ Optical Filter

To enhance energy conversion efficiency, MTPV systems incorporate an optical filter. This filter selectively transmits the radiation emitted by the emitter while reflecting unwanted wavelengths back into the emitter. This spectral control ensures that the photovoltaic cells receive radiation within their absorption spectrum, optimizing energy conversion. Examining the selection and characteristics of optical filters is essential for tailoring photon emission.

❹ Generator (TPV Cells Array)

The generator in an MTPV system consists of an array of Thermophotovoltaic (TPV) cells. These cells are responsible for converting the absorbed photons into electrical energy. The selection of TPV cell materials and design considerations are critical to achieving high conversion efficiency. Silicon-based cells are commonly used, but emerging materials like compound semiconductors hold promise for improved performance. Understanding the design and arrangement of PV cell arrays is pivotal for optimizing energy conversion.

❺ Cooling System (Heat Sink)

Efficient cooling is essential to maintain the MTPV system's temperature within the desired range and prevent thermal degradation of components. Heat sinks or cooling fins are integrated into the design to dissipate excess heat generated during operation. The choice of cooling method, whether air or liquid-based, depends on the specific application and thermal requirements.

II.2.2. System Efficiency Analysis

The thermal analysis plays a critical role in ensuring that the heat generated during combustion is effectively harnessed for practical purposes. The ability to predict and control thermal performance in micro combustors is crucial for achieving the desired performance and ensuring the integrity of MTPV system components. Furthermore, efficiency analysis is essential for assessing the effectiveness of MTPV systems and evaluating their performance [63]. This analysis sheds light on the efficiency of energy conversion processes, helping identify areas for improvement. According to the MTPV operating mechanism, the thermal power generated or transferred and the efficiencies of the different MTPV system components are defined as follows:

- **Micro Combustor Efficiency**

3. Thermal Efficiency

The heat transfer efficiency of the micro combustor can be divided into two distinct regions: inner surface heat transfer efficiency, related to the micro combustion gas-phase, and outer surface heat transfer efficiency, related to the surrounding environment.

The micro combustor heat transfer efficiency (η_{MC}) is calculated as follows:

$$\eta_{MC} = \frac{P_{\text{Rad}}}{P_{\text{Comb}}} \qquad \textit{(II.2-1)}$$

where, P_{Rad} is the radiative heat transferred from the micro combustor's outer surface to the emitter and is calculated as follows:

$$P_{\text{Rad}} = \varepsilon \sigma A_o \left(T_{w,o}^4 - T_\infty^4\right) \qquad \textit{(II.2-2)}$$

here, σ is the Stephen Boltzmann constant of 5.67×10^{-8} $(W/m^2.K^4)$, ε is the emissivity of the micro combustor material, A_o is the outer wall surface area, $T_{w,o}$ is the outer surface temperature, and T_∞ is the ambient temperature of the surrounding air. Moreover, P_{Rad} can also be defined as:

$$P_{\text{Rad}} = P_{\text{w, o}} - P_{\text{Conv, o}} \qquad \textit{(II.2-3)}$$

where, $P_{w,o}$ is the total thermal power of the micro combustor's outer surface, and $P_{Conv,o}$ is the thermal power transferred by convection from the micro combustor's outer surface to the surrounding air, calculated as follows:

$$P_{\text{Conv, o}} = h_o A_o \left(T_{w,o} - T_\infty\right) \qquad \textit{(II.2-4)}$$

here h_o is the convective heat transfer coefficient of the outer wall surface, and A_o is the outer wall surface area. Furthermore, the outer surface thermal power, $P_{w,o}$ can be defined as follows:

$$P_{\text{w, o}} = P_{\text{Conv, i}} - P_{\text{Cond}} - P_{\text{sides}} \qquad \textit{(II.2-5)}$$

where, P_{sides} is the thermal power transferred through the side walls, and P_{Cond} is the thermal power losses due to the thermal resistivity of the micro combustor material, transferred by conduction as follows:

$$P_{\text{Cond}} = -\,k\,A_c\,\frac{(T_{w,i} - T_{w,o})}{t_1} \qquad \textit{(II.2-6)}$$

here, k is the thermal conductivity of the micro combustor material, $(W/(m.K))$, A_c is the cross-sectional area, $T_{w,i}$ is the inner surface temperature, and t_1 is the micro combustor wall thickness.

On the other hand, $P_{Conv,I}$ is the ratio of the effective micro combustion thermal power transferred by convection from the gas-phase to the inner wall of the micro combustor, and it can be defined as:

$$P_{\text{Conv, i}} = h_i A_i \left(T_{w,i} - T_f\right) \qquad \textit{(II.2-7)}$$

where h_i is the convective heat transfer coefficient of the inner wall surface, and A_i is the inner wall surface area. $P_{Conv,I}$ can also be defined as:

$$P_{\text{Conv, i}} = P_{Comb} - P_{Exh} - P_{Pre} - P_{Rad,\text{i}} \qquad \textit{(II.2-8)}$$

where, P_{Exh} is the micro combustion heat loss due essentially to the thermal power contained by the exhaust gases. In addition, the heat loss is also due to the convection heat transferred from the combustion

products to the cold reactants, P_{Pre}, also known as the preheating effect, which is actually responsible for the re-ignition of newly entering cold reactants. On the other hand, the heat loss is also due to the radiative heat loss essentially emitted by the H_2O and CO_2 species, denoted $P_{Rad,i}$.

4. Figure of Merit

Moreover, in the context of evaluating micro combustor thermodynamic performance, an additional efficiency parameter known as the "Figure of Merit" (FoM) is defined as the ratio of the heat transfer from the outer wall (output) to the sum of chemical heat release and the pumping power required (inputs) as follows:

$$FoM = \frac{P_{w,o}}{P_{fuel}+\dot{W}_p} \qquad \textit{(II.2-9)}$$

where, $\dot{W}_p$ is the pumping power provided for the supply of the mixture at the inlet of the micro combustor, defined as follows:

$$\dot{W}_p = \frac{\dot{Q}_v\, \Delta P}{\eta_{pump}} \qquad \textit{(II.2-10)}$$

here, $\dot{Q}_v$ is the volume flow rate, ΔP is the pressure differential between the inlet and outlet of the micro combustor, and η_{pump} is the pump efficiency. In the current doctoral research, the pump efficiency is taken to be 70%.

• Emitter Efficiency

For emitter efficiency we categorize the two distinct cases of single layer and double layered micro combustors. In the first single layer case, the radiant thermal power output from the selective emitter is defined equal to the radiative heat transferred from the micro combustor outer surface, $P_{\text{em}} = P_{\text{Rad}}$, and calculated following the **Expression (II.2.3)** above. On the other hand, in the case of using double-layered structure, the radiant thermal power output from the emitter is defined as follows:

$$P_{em} = \varepsilon_{em}\sigma A_{em}(T_{em}^4 - T_\infty^4) \qquad \textit{(II.2-11)}$$

Moreover, the P_{em} can be defined also as:

$$P_{\text{em}} = P_{\text{Rad}} - P_{em,cond} - P_{em,loss}$$

where, $P_{em,loss}$ represent the thermal power losses due essentially to convection heat transfer with the surroundings. While, $P_{em,cond}$ is the conductive resistivity of the emitter material, and it is calculated following the Fourier Law expression as:

$$P_{em,cond} = -\,k\,A_{em,c}\,\frac{(T_{em,i}-T_{em,o})}{t_2} \qquad \textit{(II.2-12)}$$

On the other hand, the radiant thermal power entering the optical filter is equal to the product of the selective emitter surface area by the radiant power density is expressed by Stefan-Boltzmann law:

$$P'_{em} = q'_{em} \times A_{em} \qquad \textit{(II.2-13)}$$

$$\begin{aligned} q'_{em} &= \varepsilon_{em} \cdot A_{em} \cdot 2\pi \int_0^\infty I(\lambda, T_{em})\, d\lambda \\ &= \varepsilon_{em} \cdot A_{em} \cdot 2\pi \int_0^\infty \frac{h\,c^2}{\lambda^5}\left[exp\left(\frac{h\,c}{\lambda\, k_{bT_{em}}}\right) - 1\right]^{-1} d\lambda \end{aligned} \qquad \textit{(II.2-14)}$$

ε_{em} is the emitter material's emissivity, A_{em} is the emitter surface area, λ is the selected emitter band gap wavelength, $k_{\mathrm{b}} = 1.380 \times 10^{-23}\ \left(\frac{\mathrm{J}}{\mathrm{K}}\right)$ is the Boltzmann constant, $h = 6.626 \times 10^{-34}$ (J) is the Planck constant, and $c = 2.99 \times 10^{8}\ (\mathrm{m/s})$ is the Speed of light.

The radiant efficiency of the selective emitter is defined as the ratio of emitter output radiant thermal power to the micro combustor outer surface radiant thermal power:

$$\eta_{em} = \frac{P'_{em}}{P_{Rad}} \qquad \textit{(II.2-15)}$$

- **Optical Filter Efficiency**

Consequently, the spectral selection efficiency of optical filter is expressed as follows:

$$\eta_{GAP} = \frac{P_F}{P'_{em}} \qquad \textit{(II.2-16)}$$

where, the spectral power from the optical filter is defined as:

$$P_F = P'_{em} - P_{reflect,\ loss} \qquad \textit{(II.2-17)}$$

$$P_F = \varepsilon_{em} \cdot A_{em} \int_0^{\infty} I(\lambda, T_{em})\, \tau(\lambda)\, d\lambda$$
$$= \varepsilon_{em} \cdot A_{em} \int_0^{\lambda} \frac{2\pi\, h\, c^2}{\lambda^5} \left[exp\left(\frac{h\, c}{\lambda\, k_{bT_{em}}}\right) - 1 \right]^{-1} \tau(\lambda)\, d\lambda \qquad \textit{(II.2-18)}$$

Hence, Optical filter efficiency can be expressed as

$$\eta_F = \frac{P'_F}{P_F} \qquad \textit{(II.2-19)}$$

$$P'_F = P_F - P_{abs} \qquad \textit{(II.2-20)}$$

P_{abs} are power losses by absorption. They are frequently neglected, and $\eta_{\mathrm{F}} \approx 1$.

- **TPV Cells Efficiency**

The usable radiant power entering the thermophotovoltaic cells can be defined as:

$$P_{TPV} = P'_F - P_{TPV,\ loss} \qquad \textit{(II.2-21)}$$

$P_{\mathrm{TPV,\ loss}}$ is the power loss from the optical filter to the photovoltaic cell when the spectral power passes through it. The electric power generated by the thermophotovoltaic cell is defined as follow:

$$P_{el,dc} = V_{oc} \cdot I_{sc} \cdot FF \cdot A_{cell} \qquad \textit{(II.2-22)}$$

where, V_{oc} is open circuit voltage, FF is the fill factor, I_{sc} is short circuit current, and $\mathrm{A_{cell}}$ is the surface area of TPV cell. Hence, the short circuit current density is calculated as:

$$I_{sc} = e \cdot \int_0^{\infty} \Phi(\lambda)\, QE_{ext}(\lambda) d\lambda \qquad \textit{(II.2-23)}$$

where QE_{ext} is the external quantum efficiency and is the photon probability value of the wavelength absorbed by the cell. $\Phi(\lambda)$ is the photon flux.

$$\Phi(\lambda) = \frac{E_{kb}\ \lambda}{h\ c} \quad \textit{(II.2-24)}$$

$$V_{oc} = \frac{k_b T_{cell}}{e} \cdot ln\left(\frac{I_{sc}}{I_0} + 1\right) \quad \textit{(II.2-25)}$$

T_{cell} is the TPV cell temperature and I_0 is the saturation current calculated as:

$$I_0 = 1.84 \times 10^3 \cdot T_{cell}^3 \cdot exp\left(-\frac{E_g\ q_0}{k\ T_{cell}}\right) \quad \textit{(II.2-26)}$$

where, q_0 is elementary charge, E_g is the TPV cell energy bandgap, for example GaSb TPV cell energy bandgap is 0.72 eV. Moreover, fill factor is calculated as:

$$FF = \frac{\upsilon - ln(\upsilon + 0.72)}{\upsilon + 1} \quad \textit{(II.2-27)}$$

where, υ is normalized V_{oc} calculated as:

$$\upsilon = \frac{V_{oc}\ q_0}{k\ T_{cell}} \quad \textit{(II.2-28)}$$

Visibility factor efficiency is the spectral ratio of the power entering the photovoltaic cell:

$$\eta_{VF} = \frac{P_{TPV}}{P_F'} \quad \textit{(II.2-29)}$$

The efficiency of thermophotovoltaic cell is the ratio of the electrical power to the photovoltaic cell

$$\eta_{TPV} = \frac{P_{el,dc}}{P_{TPV}} \quad \textit{(II.2-30)}$$

The AC inverter efficiency is defined as follow:

$$\eta_{AC} = \frac{P_{el,ac}}{P_{el,dc}} \quad \textit{(II.2-31)}$$

- **Overall System Efficiency**

The overall electrical efficiency of the MTPV system is equal to the product of all the above stated efficiencies:

$$\eta_{sys} = \eta_{Comb} \cdot \eta_{MC} \cdot \eta_{em} \cdot \eta_{GAP} \cdot \eta_F \cdot \eta_{VF} \cdot \eta_{TPV} \cdot \eta_{AC} \quad \textit{(II.2-32)}$$

Chapter III: Methodology

III.1. Problem Formulation

In recent decades, numerical modeling has become an indispensable approach of modern science, with Computational Fluid Dynamics (CFD) standing out as a specific subset of numerical modelling within the field of mechanical engineering. CFD is dedicated to the study of fluid flow, chemical combustion, and heat transfer. It has evolved into a powerful tool extensively employed in the design, investigation, and development of various engineering systems. Consequently, numerous open-source and commercial CFD software solutions, such as OpenFOAM and Ansys Fluent, have been developed, incorporating diverse iterative solver algorithms. These CFD codes provide powerful tools in hand of researchers and engineers to simulate Multiphysics phenomena, analyze complex systems, predict their behavior, and optimize their performance. However, the effective numerical modeling of Multiphysics problems presents a significant challenge, demanding a high level of expertise and a profound understanding of the complicated physical phenomena involved. Micro combustion, in particular, serves as a prime example of these complex Multiphysics problems, characterized by the complicated interaction of flow, chemical and heat transfer phenomena. To model these complex phenomena effectively, it is imperative to get a full theoretical description of the various underlying flow, combustion and heat transfer transport phenomena. The intersection of these phenomena fundamentally governs the behavior of micro combustion and exert a decisive influence on its efficiency and overall performance. However, to optimally utilize the capabilities of Computational Fluid Dynamics (CFD), a systematic methodology is imperative to ensure accurate modeling of Multiphysics problems, especially considering the complexity of micro-combustion problems. Therefore, in the context of our doctoral numerical study, we established a methodology aimed at developing a reliable, verified, and validated numerical model that guarantees optimal simulation of turbulent mixing with or without chemical reactions. Additionally, this model needed to be applicable across various geometrical configurations. The foundational step in our methodology for developing a validate numerical model lies in the theoretical formulation of the micro combustion and heat transfer processes across gaseous and solid phase of the micro combustors. This involves developing of a comprehensive analysis of transport phenomena, ensuring an in-depth investigation of combustion flow, chemical, and thermal phenomena behavior. This theoretical framework strives to present a comprehensive model of the physics involved in both non-reacting and reacting processes, encompassing gas-phase behavior and heat transfer within the solid phase of the micro combustor's geometric configurations. This understanding of the underlying transport phenomena lays the groundwork for the mathematical formulation of the governing transport phenomena, expressed as equations of conservation of mass, momentum, species, and energy. These governing equations constitute the core of our methodology, representing the behavior of non-reacting and reacting processes as well as the intersections of turbulence and chemical processes. Furthermore, the mathematical model encapsulates a set of partial differential equations that meticulously account for various flow dynamics, chemical reactions, and heat transfer phenomena through their respective terms.

III.1.1. Theoretical Formulation

Micro-scale combustion is a remarkable field where the integral complexities of fluid dynamics, chemistry, mass and heat transfer converge within confined geometries, as previously discussed in the fundamentals of micro combustion. However, within the scope of this doctoral thesis, our research objectives involve the introduction of a combination of a backward-facing step and trapezoidal-shaped ribs. These factors play a pivotal role in significantly reshaping flow patterns and influencing chemical reactions and thermal behaviors within the micro combustors. Furthermore, our research aims to explore various operating conditions, which also exert a substantial influence on the flow, chemical, and thermal characteristics of micro combustion, as well as the performance of Micro Thermophotovoltaic (MTPV) systems. As a result, additional transport phenomena emerge, underscoring the importance of turbulence, recirculation zones, vortices, and their roles in species mixing and enhancement of heat transfer.

Understanding these additional phenomena and transport processes in both non-reacting and reactive scenarios is of paramount importance for developing an accurate numerical model applicable for simulating turbulent mixing in various geometric configurations. To offer a comprehensive overview, we conduct an in-depth comparative examination between the different transport phenomena within the straight micro combustor and those associated with the introduction of a backward-facing step. The utilization of a backward-facing step as an enhancement technique has gained widespread acceptance within the micro combustion community due to its effectiveness in flame stabilization and the enhancement of MTPV system efficiency. Its simplicity makes it an invaluable tool for analyzing the additional transport phenomena introduced by the presence of a backward-facing step in micro combustion, affecting phenomena in both the gas phase and heat transfer in the solid phase of the micro combustor.

- ## Micro Combustion (Gas-Phase)

a. Non-reacting Flows

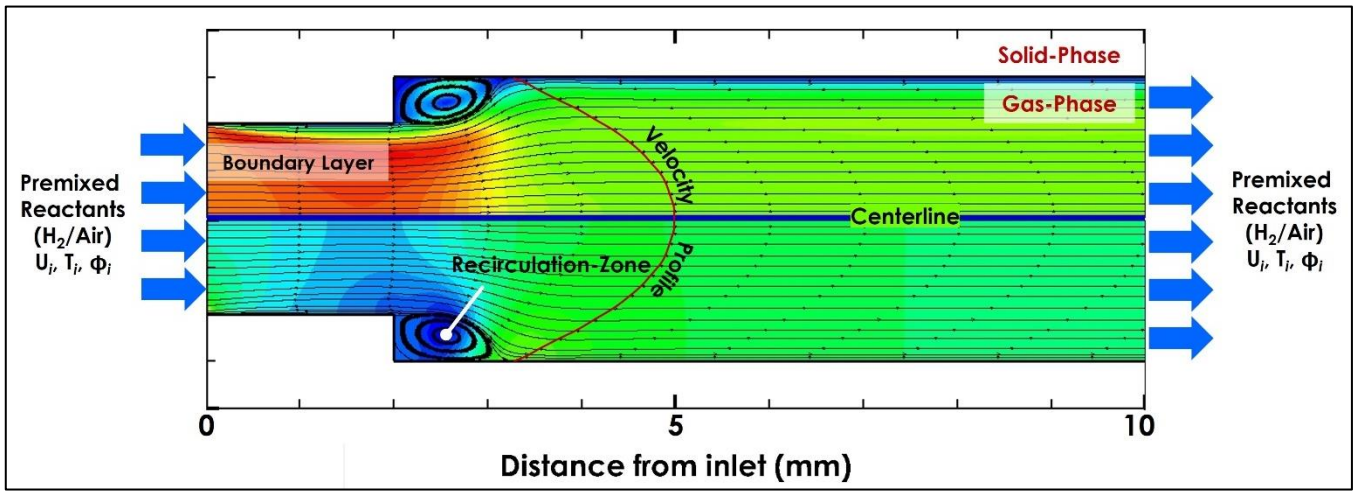

Figure III.1.1. *Schematic diagram of non-reacting flow within backward-facing step micro combustor.*

In the case of non-reacting flows, our primary focus is on examining fluid dynamics and flow behavior. This involves studying various aspects, including velocity profiles, pressure gradients, and the overall flow regime. Therefore, in the absence of chemical reactions, the premixed reactants flow within a straight micro combustor remains relatively uninterrupted, characterized by the smooth, predictable streamlined motion of the fluid. These flows exhibit a laminar regime marked by silky velocity profiles and minimal turbulence. Laminar flow predominates at lower Reynolds numbers, indicating a dominance of viscous forces over inertial forces. Velocity profiles across such straight micro combustor are shaped by flow conditions and boundary layer effects. The velocity profile is parabolic, with lower velocities near the wall and higher velocities at the center. Near the walls, velocity gradients are pronounced due to the wall friction and viscosity effects leading to the development of boundary layers. Additionally, a pressure gradient exists along the length of the micro combustor, contributing to the continuous flow of the fluid from the inlet to the outlet. In contrast, the introduction of a backward-facing step triggers chaotic flow patterns within the micro combustor. The step promotes a transition to a turbulent regime, leading to the emergence of various turbulence-related structures within the flow field, including turbulent eddies, vortices, and recirculation zones. This behavior differs markedly from what is observed in straight channels. As schematically represented in **Figure III.1.1**, the sudden change in diameter (or height) of the combustor at the backward-facing step decelerates the flow velocity, causing a discontinuity in the flow and initiating flow separation. This separation results in the formation of recirculation zones behind the step. This chaotic flow pattern is unique to the backward-facing step configuration. The formation is

associated with the development of shear layers and vortex shedding downstream of the step. Beyond the step, pressure recovery occurs as the flow reattaches and accelerates. This phenomenon significantly impacts pressure distributions and flow velocities downstream of the step. Furthermore, the recirculation zones introduce variations in velocity gradients within the micro combustor flow-field, affecting the overall flow behavior and creating a highly dynamic environment. Flow separation also leads to the creation of vortices within the recirculation zones. As flow dynamics are altered by the backward-facing step, boundary layers develop along the step's surface. This turbulent environment impacts velocity profiles and introduces variations across different regions of the micro combustor flow-field. The Reynolds number plays a significant role in determining the overall flow behavior. Turbulence intensity and Turbulent Kinetic Energy (TKE) exhibit significant variations across different regions of the combustor. However, it's important to note that despite the effect of a backward-facing step on shifting the flow regime towards a turbulent regime, the Reynolds numbers remain below the critical values typically associated with conventional macro-scale flows. This indicates that viscous forces continue to dominate over inertial forces in this micro-scale non-reactive flow.

b. Reacting Flows

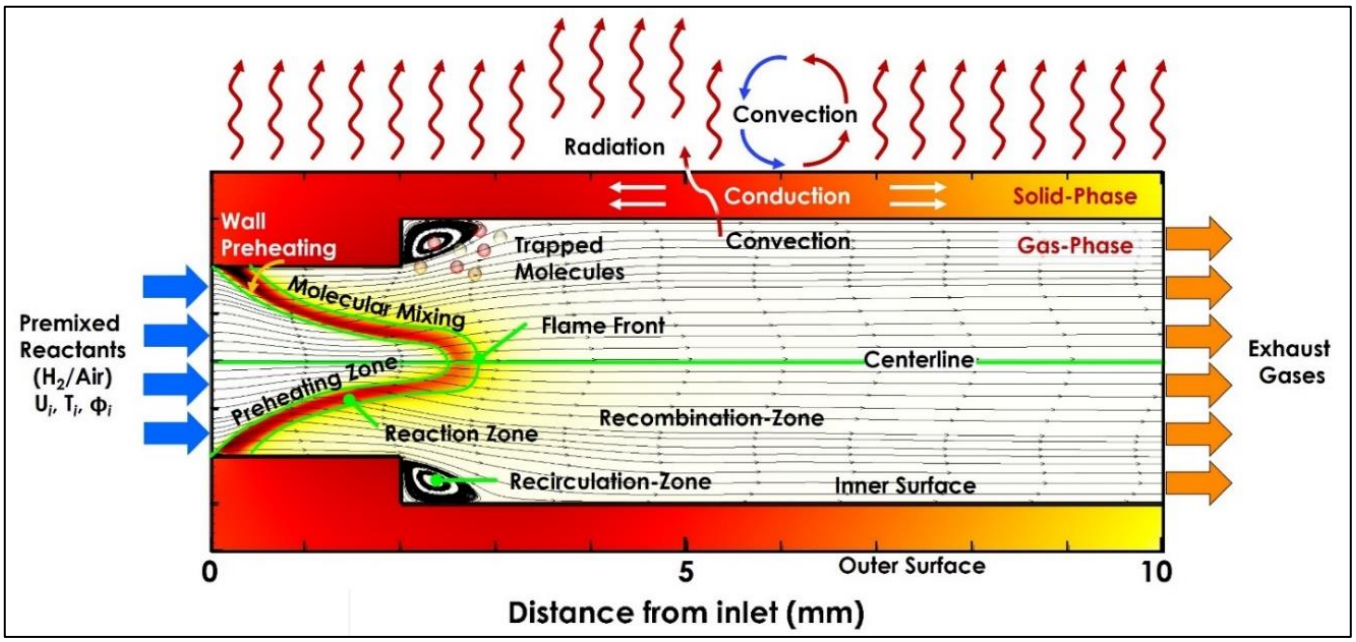

Figure III.1.2. *Schematic diagram of reacting flow within backward-facing step micro combustor.*

The ignition of chemical reactions within micro combustors introduces a new layer of complexity to fluid dynamics. Reacting flows are characterized by the interplay of fluid motion, species transport, chemical reactions and heat release. Combustion chemical reactions involve the consumption of fuel and oxidizer, leading to the production of reaction products and sometimes radicals. Combustion is an exothermic process, resulting in the release of heat. This heat raises the temperature of the surrounding gas and the micro combustor wall. Consequently, in-depth comparative examination of the transport phenomena governing the behavior of reacting flows within straight micro combustor and backward-facing step micro combustor.

- **Flow-field**

The ignition of chemical reactions within micro combustors plays a transformative role in shaping flow dynamics. In a straight channel micro combustor, chemical reactions serve as a key driving force, initiating a rapid alteration transforming the flow regime from laminar to turbulent. The initiation of chemical reactions introduces a high rate of energy release, which exert a profound influence on the stream field. As the flame consumes reactants, it tends to progress and elongate, altering the flow

streamlines. The reaction zone creates a low-pressure region, leading to the bending of streamlines towards the flame zone. This change in flow behavior leads to an increase in Reynolds numbers, where inertial forces become more pronounced, ultimately challenging the dominance of viscous forces. However, the transition to turbulent flow induces a more chaotic flow regime marked by intricate vortices and eddies within the flow field. The deformation of flow-field increases the velocity gradient, and boundary layers near the walls thin out, resulting in an accelerated pressure gradient. In this environment, pressure drop occurs at a different rate, with downstream flow acceleration being more pronounced. In the case of a backward-facing step micro combustor, the ignition of chemical reactions initiates a transformation, albeit with distinct spatial characteristics due to the step's presence. As reactants are consumed and transformed into products, the flow streamlines near the step and downstream display intricate patterns, introducing curvature into the streamlines. This curvature enhances molecular mixing of products and influences velocity gradients. Furthermore, the introduction of chemical reactions intensifies turbulence, leading to the development of turbulence-related structures such as turbulent eddies, vortices, and recirculation zones. The increased turbulence intensity results in additional bending and curvature of flow streamlines. The dynamic interplay between the flame, turbulence, and recirculation zones enhances molecular mixing, facilitating reactant distribution and promoting mass transfer.

Velocity profiles within this combustor become highly turbulent, influenced by the step-induced deceleration and the presence of recirculation zones. This altered flow behavior characterizes a turbulent regime, with significant increases in Reynolds numbers, indicating a shift toward greater inertial forces, partially counteracting the previously dominant viscous forces. Boundary layers form along the step's surface, further affecting velocity profiles, and the step introduces variations in pressure distributions and flow velocities downstream. The pressure recovery beyond the step is also influenced by the flame, subsequently impacting pressure gradients and flow velocities downstream. The increased pressure due to flame bending affects the behavior of boundary layers, causing them to evolve and impact velocity profiles across different regions of the combustor. The presence of the step and flame-induced variations create a complex interplay between geometric features, the flame, and fluid dynamics, ultimately determining the transport phenomena within the micro combustor. In micro combustors, where conditions can vary due to confinement and geometrical features, the pressure gradient plays a significant role in influencing the rate of reactions. The residence time of species within the combustion chamber is a critical parameter in reacting flows. It influences the extent to which species mix and interact. In straight channels, residence time is relatively predictable, with longer channels allowing for greater mixing. In turbulent flows, smaller eddies and vortices promote rapid mixing, even in shorter channels. In the presence of backward-facing step, residence time becomes more variable due to flow separation and recirculation zones. These zones can trap species for longer durations, leading to variations in concentration and temperature. This, in turn, can affect the ignition, re-ignition and combustion behavior when reactions are introduced.

- **Chemical Phenomena**

The chemical aspect of micro-scale combustion is a rich and complex domain governing fundamental reactions and species transformations. Ignition of these chemical reactions is a critical event, marking the initiation of combustion. It typically occurs at specific locations with favorable temperature and fuel-oxidizer concentrations. However, combustion involves the consumption of fuel and oxidizer, resulting in heat release and the formation of combustion products. The region where these chemical reactions take place is referred to as the reaction zone. This zone represents the boundary between the reactants' preheating zone and the recombination zone of products, as depicted in **Figure III.1.2**. It is characterized by high temperatures, significant species concentration gradients, and rapid chemical reactions. Combustion reactions are complex phenomena involving numerous intermediate species and elementary reactions. Radical species, such as hydroxyl radicals (OH•), atomic hydrogen (H•), and atomic oxygen

(O•), play crucial roles in chain reactions and species evolution during combustion. Their concentrations and distribution within the combustion zone are essential determinants of combustion efficiency. One of the central chemical transport phenomena in reacting flows is species transport. Spatial transport of species involves the movement and mixing of various chemical species, including fuel, oxidizer, and product gases. The spatial movement of species is influenced by factors such as concentration gradients, temperature gradients, flow velocities, and turbulence intensity. Concentration gradients of species are critical determinants of subsequent combustion behavior when reactions are initiated. The transport of species within microchannels is primarily governed by diffusive processes. The diffusion of molecules occurs due to thermal and concentration gradients, leading to the net movement of species from regions of higher temperature and concentration to regions of lower temperature and concentration, respectively. In straight channels, where flow remains relatively uniform, species transport primarily follows a one-dimensional diffusion model along the flow direction. The introduction of a backward-facing step significantly alters turbulence and mixing patterns. Flow separation, vortices, and recirculation zones induced by the step can enhance turbulence levels, facilitating better mixing and combustion efficiency.

The chemistry of reacting flows within micro combustors is a finely orchestrated interplay of various factors, with chemical kinetics at its core. Chemical kinetics refers to the study of reaction rates, that is, the rates at which reactants are transformed into products during combustion. These reaction rates are highly dependent on several key factors, including temperature, pressure, and reactant concentrations. Temperature plays a pivotal role in chemical kinetics. As the temperature increases, the rate of chemical reactions generally accelerates. Higher temperatures provide reactant molecules with more kinetic energy, enabling them to overcome energy barriers and participate in chemical reactions more readily. Consequently, in the high-temperature environment of micro combustors, the increased kinetic energy of molecules leads to faster reaction rates, driving the combustion process. Pressure is another crucial variable influencing chemical kinetics. Generally, increasing pressure tends to enhance reaction rates. This is because higher pressures result in molecules being packed more closely together, increasing the frequency of molecular collisions. These collisions are fundamental to chemical reactions, and at elevated pressures, they occur more frequently, expediting reaction rates. Reactant concentrations are yet another critical factor. Reaction rates are often directly proportional to the concentration of reactants. Higher concentrations of reactants mean more molecules available for reactions, leading to faster rates. In micro-scale combustion, fuel and oxidizer concentrations can vary due to flow patterns, mixing efficiency, and geometry. Understanding these concentration gradients and their impact on reaction rates is crucial for predicting and optimizing combustion processes within micro combustors. The interplay between these factors is highly complicated. In the confined environment of micro combustors, temperature, pressure, and reactant concentrations are closely intertwined. Temperature affects pressure, and vice versa, due to the ideal gas law. This interaction can significantly influence reaction rates. Moreover, the rapid changes in temperature and pressure gradients near the flame and within recirculation zones further complicate the situation. It requires precise mathematical modeling and simulation to accurately capture these interactions and predict the behavior of chemical kinetics within the complex micro-scale combustion environment.

- **Thermal Phenomena**

Within the realm of micro combustion, the thermal aspect plays a pivotal role in shaping the behavior of transport phenomena. As the mixture of reactants enters the confines of the micro combustor and ignition takes place, it heralds the onset of combustion, a dynamic process where the chemical energy stored in the reactants is converted into thermal energy. This transformation is fundamental to the operation of micro combustors, as it not only fuels the overall process but also dictates various transport phenomena within the system. The concept of the heat of reaction is central to understanding the thermal aspect of micro combustion. This parameter represents the amount of energy released or absorbed during a chemical

reaction, specifically during combustion. In the context of micro combustion, it is essential for explaining the heat generation within the system. As reactants combine and react, the heat of reaction plays a key role in determining the amount of thermal energy produced. This energy, in the form of heat, is responsible for raising the temperature of the combustion zone. A fundamental aspect of the thermal transport phenomena in micro combustion involves temperature profiles. These profiles offer insights into the distribution of thermal energy across different regions within the combustion zone. The combustion zone itself is typically divided into three key regions: the preheating zone, the reaction zone, and the recombination zone. Preheating zone is the region located just ahead of the flame front. Here, the incoming reactants are gradually heated as they approach the high-temperature flame. The temperature in this zone rises steadily as heat is conducted from the reaction zone. Preheating is a crucial process, as it helps prepare the reactants for the subsequent chemical reactions. The heart of the combustion process, the reaction zone is where the reactants undergo combustion. Here, the heat of reaction is released as a result of chemical reactions, raising the temperature significantly. It is in this zone that the reactants are transformed into combustion products, and it represents the peak of thermal energy generation within the micro combustor. Following the reaction zone, the recombination zone is where the combustion products mix and undergo further reactions. In this region, thermal energy is exchanged and redistributed among the various species present. The temperature may decrease as the products recombine and thermal energy is transferred.

Spatial transport of thermal energy is influenced by several factors, with convection being a dominant mechanism. Convection involves the transfer of heat by the actual movement of the fluid itself. In the context of micro combustion, this is particularly relevant in the preheating and reaction zones. As reactants approach the flame, they carry thermal energy with them, and this energy is then released as the reactants heat up in the preheating zone and subsequently undergo reactions in the reaction zone. Convection is a vital driver of spatial heat transport, impacting temperature gradients and velocity profiles within these regions. However, once combustion initiates, velocity profiles can undergo significant changes, especially in the reaction zone. The release of thermal energy in this region leads to a rise in temperature, which, in turn, alters the fluid properties and density. This effect can result in changes in velocity profiles, particularly in regions close to the flame front. Turbulence, a common occurrence in combustion systems, further influences thermal transport. The presence of turbulence intensifies the mixing of reactants and combustion products, leading to more efficient heat transfer through enhanced convection and, as a result, contributes to the establishment of more uniform temperature profiles, especially within the reaction zone. Turbulence, as an integral component of the combustion process, plays a dual role by not only enhancing the combustion efficiency but also actively influencing the thermal transport, which in turn affects various aspects of the system's performance. Simultaneously, the pressure field within a micro combustor is closely linked to the thermal aspect of combustion. As chemical reactions progress, pressure fluctuations occur, affecting the distribution of thermal energy. Especially in the preheating and reaction zones, variations in pressure exert a pronounced influence on the flow of reactants and the subsequent release of thermal energy. These pressure fluctuations lead to consequential effects, ultimately affecting the temperature gradients. The thermal radiative phenomena in micro combustion play a significant role in determining the heat transfer within the system. As the temperature rises in the reaction zone, gases emit thermal radiation. The properties of these gases, including their composition, affect the intensity and spectral distribution of radiation. Among the molecules present in the combustion products, water vapor (H_2O) exhibits unique radiative properties. Its role in radiative heat transfer is noteworthy, as its concentration and properties can significantly impact the radiative heat flux. One crucial aspect of radiative heat transfer is the concept of optical thickness. This parameter measures the extent to which a gas is capable of absorbing and emitting thermal radiation. In micro combustion, the optical thickness of gases, including water vapor, influences how effectively

radiation can traverse the combustion zone. Understanding optical thickness is essential for evaluating radiative heat transfer and optimizing the design and efficiency of micro combustors.

- ## Micro Combustor (Solid Phase)

In the realm of micro combustion, the transfer of heat is a multifaceted process that significantly influences the overall performance and efficiency of the MTPV system. The heat transfer within solid phase of a micro combustor can be categorized into three primary regions: the inner surface, wall material and the outer surface of the micro combustor. Understanding the different heat transfer mechanisms within the solid phase is crucial for ensuring structural integrity and overall system performance.

a. Inner Surface Area

As the combustion process unfolds, the hot gases, generated by the chemical reactions within the reaction zone, flow along the inner walls of the micro combustor. This direct contact between the high-temperature gases and the wall surfaces is where convective heat transfer takes place. Convective heat transfer at the inner surface of the micro combustor is a pivotal mechanism that significantly influences the combustion process. This heat transfer phenomenon involves the exchange of thermal energy between the hot combustion gases and the inner wall of the micro combustor. The convective heat transfer between the gas-phase and the inner surface of the solid walls is characterized by the heat transfer coefficient (h). It plays a crucial role in maintaining flame stability and impacting the temperature distribution within the walls. Convective heat transfer at the inner surface leads to the establishment of temperature gradients across the micro combustor walls. This temperature distribution within the walls is a critical factor for ensuring efficient combustion as the rise in wall temperature near the combustion zone has a preheating effect on the incoming reactants' mixture. This preheating phenomenon elevates the initial temperature of the reactants, thereby facilitating faster ignition and reaction rates. Moreover, this preheating effect is particularly significant in achieving repeated re-ignition of combustion. Convective heat transfer at the inner surface contributes also to the stability of the flame. By maintaining elevated wall temperatures, this heat transfer mechanism ensures that the necessary high-temperature environment for combustion is sustained. In addition to convective heat transfer, radiative heat transfer is another mechanism by which heat is transferred from the gas phase to the solid phase (the walls) within the micro combustor. However, radiative heat transfer plays a relatively minor role in micro combustion due to the low optical thickness of the majority of gases involved. The low optical thickness of gases within the micro combustor implies that they have limited ability to absorb and emit thermal radiation. In contrast, water vapor (H_2O) is an exception, possessing a higher optical thickness. This means that H_2O is responsible for the majority of heat transferred by radiation. However, its influence is still comparatively low when compared to the dominant convection.

b. Wall Material

Conductive heat transfer within a micro combustor's wall material is a pivotal aspect of its thermal dynamics. This fundamental transport phenomenon efficiently transfers combustion heat gained by convection from the inner surface to the outer surface of the micro combustor wall. The driving force behind conductive heat transfer is the temperature gradient existing between the inner surface temperature, where heat is gained through convection, and the outer surface temperature, where heat is released to be transferred toward the optical filter and TPV cells. The conductive heat transfer occurs essentially within the solid wall material. In addition to the dominant direction of heat conduction from the inner surface to the outer surface, some heat may also conduct sideways through the wall material. However, thermal conductivity, often referred to as the material's resistivity to heat transfer, determines how effectively heat is conducted through solid materials. Materials with high thermal conductivity are particularly efficient in facilitating the conductive heat transfer process. They allow for minimal

temperature gradients to develop along the outer surface of the micro combustor wall, resulting in a more uniform temperature distribution. This uniformity is crucial for reducing the likelihood of localized overheating and thermal stress, ultimately ensuring the safe and effective operation of the micro combustor. The thermal conductivity of the wall material is influenced by various factors, including its composition, structure, and temperature. The thermal conductivity of the material behaves with changing temperatures is essential for predicting its impact on heat transfer within the micro combustor. As temperature rises, the thermal conductivity of most materials increases, leading to more efficient heat conduction. This has a direct effect on the temperature distribution within the micro combustor wall material. The efficient conduction of heat helps maintain a uniform temperature profile along the outer surface of the micro combustor, preventing the formation of hotspots that could compromise its structural integrity. Moreover, the thickness of the micro combustor wall also plays a role in conductive heat transfer. Thicker walls may exhibit higher thermal resistance and, therefore, may introduce more significant temperature gradients. Consequently, material selection and wall thickness must be carefully considered during the micro combustor design process. The choice of wall material, with its specific thermal conductivity properties, directly impacts the micro combustor ability to manage temperature and thermal stress. It is essential to select materials that can for thinner walls withstand the elevated temperatures experienced during combustion while ensuring a uniform temperature distribution along the outer surface.

c. Outer Surface Area

The micro combustor's outer surface, acting as a critical interface, plays a crucial role in the overall thermal dynamics of the MTPV system. Once heat is conducted from the inner surface to the outer surface of the micro combustor wall, the next significant step is its transfer from the outer surface to the optical filter and Thermophotovoltaic (TPV) cells. The process involves convective and radiative heat transfer phenomena, each with distinct significance, as depicted in **Figure III.1.2**. Convective heat transfer is a vital mechanism governing the energy transformation at the micro combustor's outer wall. Convective heat transfer at the outer surface occurs due to the temperature difference between the micro combustor wall and the surrounding environment. The temperature gradient creates a motive force for the transfer of heat. This process involves the transfer of heat through the movement of a fluid, typically air, across the wall surface. The convective heat transfer coefficient (h) characterizes this phenomenon. It quantifies the rate of heat transfer per unit area for a given temperature gradient. Higher values of the convective coefficient indicate more efficient heat transfer through convection. The convective coefficient is intrinsically linked to the properties of the surrounding fluid, the fluid velocity, and the micro combustor material characteristics. Radiative heat transfer, on the other hand, complements convective heat transfer in its role at the micro combustor wall. It involves the exchange of thermal energy through electromagnetic waves from the micro combustor outer surface toward the optical filter and TPV cells. The efficiency of radiation depends on the emissivity (ε) of the wall material, which is a measure of how effectively the material emits thermal radiation. The selection of wall materials for the micro combustor is of utmost importance, as it directly affects both convective and radiative heat transfer. A material with high emissivity will efficiently radiate heat to the optical filter and TPV cells. Conversely, a material with low emissivity will absorb less thermal radiation and be more efficient in transferring heat through convection. The choice of material should align with the system's thermal requirements and the desired balance between convective and radiative heat transfer. The Stefan-Boltzmann Law governs this radiation, highlighting its dependency on temperature—the fourth power of the absolute temperature, to be precise. As temperature increases, radiation becomes the dominant mode of heat transfer due to its T^4 dependence. Radiation often dominates heat transfer in micro combustors due to their high operating temperatures. As the temperature increases, the intensity of thermal radiation grows significantly, overpowering the contribution from convective heat transfer. This phenomenon is particularly pronounced in micro combustors where high temperatures are prevalent, making radiation the dominant mechanism

for heat transfer. Furthermore, these heat transfer mechanisms are intricately linked to the temperature of the micro combustor. As the temperature of the system varies, the convective heat transfer coefficient and radiative emissivity of the wall material change. These alterations have a direct impact on the temperature distribution within the wall material, which, in turn, affects the temperature uniformity on the outer surface of the micro combustor. Managing the convective and radiative heat transfer is essential for optimizing the micro combustor's performance and ensuring the efficient operation of the overall MTPV performance.

III.1.2. Mathematical Formulation

Building upon the established fundamental understanding gained throughout the review of transport phenomena, we aim to mathematically model and express the physical phenomena intervening on both non-reacting and reacting flows. a set of partial differential equations that describes and quantifies the conservation of mass, momentum, species and energy, are formulated. First and foremost, the mass and momentum conservation equations take the lead, offering a comprehensive description of mass and momentum transport. These equations lay the foundation for understanding how mass moves through the system and how momentum is transferred within it. Simultaneously, we invoke the species transport equations, dedicated to elucidating mass transfer phenomena. These equations provide essential insights into how different chemical species are transported throughout the combustion chamber. In addition to mass, momentum, and species the energy equation terms are instrumental in depicting heat transfer and diffusion processes within the gas-phase. They allow us to explore the distribution of thermal energy and understand how it diffuses throughout the micro combustion chamber. To delve into the heat transfer mechanisms even further, we employ the Fourier law equation. This equation specifically defines conductive heat transfer within the solid phase of the micro combustor. It reveals how heat is conducted through the solid material that make up the chamber's structure. Simultaneously, In the context of heat transfer within the micro combustor, it's essential to consider conjugated heat transfer, which accounts for the thermal interaction between the gas phase and the inner surface of the micro combustor. Additionally, convective heat transfer plays a pivotal role in modeling the heat exchange process between the outer wall surface of the combustor and the optical filter and TPV cells. Lastly, the Stefan-Boltzmann equation takes the stage, providing a precise definition of radiative heat transfer from the outer surfaces of the micro combustor. This equation quantifies how thermal radiation is emitted from the chamber's outer walls, contributing to the overall heat transfer process.

- **Limitations and Assumptions**

Micro-combustion, as aforementioned, is a highly complicated process that emerges the intersection of fluid dynamics, chemical reactions, and heat transfer phenomena. To effectively model this complex process, streamline our approach and make meaningful progress in our doctoral research, we find it imperative to make several limitations and assumptions, each carefully justified to enhance the efficiency and practicality of our computational efforts. In our doctoral research, the micro-combustors we are designing feature a unique configuration with backward-facing and trapezoidal-shaped ribs that serve to induce turbulence. Given the importance of stability in our system, we make a deliberate choice to simplify our mathematical models and computational processes. Hence, a set of logical limitations and simplifying assumptions based on the theoretical understanding are made. We assume that the flow, whether it's non-reactive or reactive, remains in a state of equilibrium. By doing so, we prioritize the temporal stability of the flow within our micro-combustor design. As a result, we employ a steady-state model for all cases. This approach simplifies the consideration of time-dependent factors, allowing us to concentrate on spatial variations and gain a more comprehensive understanding of the micro combustion

behavior. One of the pivotal considerations in our research is the characteristic scale of micro-combustion chambers relative to the molecular mean free path (λ_f), quantified by the Knudsen number[1] (Kn). Our investigations reveal that the Knudsen number remains comfortably below the critical threshold of 0.001. This crucial finding allows us to maintain the continuum theory as a viable and pragmatic assumption. The implications of this are profound; the mass and momentum equations, which form the bedrock of fluid dynamics, retain their relevance and applicability in our micro-combustion simulations.

In both non-reacting and reacting flow scenarios, we maintain the Mach number[2] (Ma) below 0.1, ensuring subsonic flow conditions. This choice enables us to neglect the compressibility effects of the flows, facilitating a streamlined analysis. Consequently, we assume a constant density of the fuel-oxidizer mixture at the inlet of the combustor. Furthermore, we assume the negligible influence of gravitational forces on transport phenomena. This assumption is scientifically justified for several compelling reasons. First, the microscale nature of the combustion chambers itself means that gravitational forces are relatively weak compared to other dominant forces at play. The characteristic timescales of processes within the micro-combustor are typically short, rendering gravitational effects on fluid motion, such as buoyancy-driven flows, inconsequential. In essence, the rapid dynamics of micro-combustion processes prevent gravity from inducing substantial pressure variations. Moreover, the high flow velocities within the confined geometry of micro-combustors emphasize the importance of convective forces, further reducing the significance of gravitational effects. Additionally, our micro-combustor designs feature a horizontal alignment of components, effectively mitigating pressure variations along the vertical axis due to gravity. Hence, the cumulative effect of these factors supports the valid neglect of gravity's influence on momentum calculations within our micro-combustor configurations. As previously mentioned, radiation is a primary mechanism for transferring the heat generated during combustion. However, our analysis has shown that most gases exhibit extremely low optical thickness, making gas-phase radiation a negligible factor within our micro-combustion chamber. It's important to note that this conclusion is grounded in the limited significance of gas-phase radiation in our specific combustion process [49]. Additionally, we should acknowledge that the numerical model used for simulating gas-phase radiations remains limited and poses an expensive computational cost. We further assume that the fuel-oxidizer mixture is fully premixed before entering the micro-combustor chamber, characterized by an equivalence ratio (ϕ). This assumption provides a simplified representation of the combustion process, allowing us to focus on critical aspects without introducing unnecessary complexities associated with partial premixing. Lastly, we assert that the inner surface of the micro combustor is inert, ruling out surface oxidation reactions. This simplifies the chemical interactions at this interface, allowing for a cleaner focus on other crucial aspects of the combustion process.

Assumptions List:

(1) The flow, whether non-reactive or reactive, is assumed to remain in a state of equilibrium to prioritize temporal stability within the micro-combustor design.

(2) A steady-state model is employed for all cases to simplify consideration of time-dependent factors and focus on spatial variations for a comprehensive understanding of micro combustion behavior.

(3) The Knudsen number remains comfortably below 0.001, allowing the continuum theory assumption to be maintained for fluid dynamics equations, ensuring their relevance in simulations.

[1] The Knudsen number (Kn) is a dimensionless parameter that quantifies the ratio between the molecular mean free path length **(λ_f)** and a characteristic physical length scale within a flow field.

[2] The Mach number (Ma) is a dimensionless quantity that represents the ratio between the velocity of a flow to the speed of sound in the surrounding medium, and provides a crucial measure of the compressibility effects within a fluid flow field.

(4) The Mach number is kept below 0.1 in both non-reacting and reacting flow scenarios to neglect compressibility effects and facilitate streamlined analysis.

(5) Gravitational forces are assumed to have negligible influence on transport phenomena due to the microscale nature of combustion chambers and rapid dynamics preventing substantial pressure variations.

(6) Gas-phase radiation is considered negligible due to low optical thickness of most gases, minimizing its impact on heat transfer within the micro-combustion chamber [49].

(7) The fuel-oxidizer mixture is assumed to be fully premixed before entering the micro-combustor chamber, simplifying the combustion process representation.

(8) The inner surface of the micro combustor is assumed to be inert, simplifying chemical interactions and allowing focus on other crucial aspects of combustion.

By carefully embracing these limitations and assumptions, we streamline our research efforts, achieving a balance between computational efficiency and scientific rigor.

- ## Governing Equations

The mathematical formulation of micro combustion in form of governing equations constitutes a pivotal step in comprehending and modeling the intricate Multiphysics phenomena inherent to micro-scale combustion. These governing equations are expressed in the conservation form, which serve as the fundamental framework for depicting the dynamics of micro combustion processes. This particular form stands out for its capacity to mathematically portray the behavior of the physical phenomena governing micro combustion, including the complicated interplay of fluid dynamics, chemical reactions, heat generation, and heat transfer. By precisely defining these phenomena, these equations provide a roadmap for numerically simulating micro combustion, enabling us to predict and examine the behavior of the incorporating transport phenomena. In comparison to other forms such as the differential form and integral form, the conservation form offers distinct advantages. While the differential form is more suitable for theoretical analysis and can be used to describe phenomena at the smallest scales, it often involves intricate mathematical derivations. On the other hand, the integral form provides a global view of the system and is suitable for certain types of problems, particularly those involving boundary conditions and fluxes. However, it can be challenging to apply in cases where local phenomena and pointwise variations are of significant interest. The conservation form strikes a balance by offering both a comprehensive view of the system and a more straightforward mathematical representation. It is particularly well-suited for numerical simulations and the analysis of complex systems like micro combustion. This mathematical representation is indispensable for a deeper comprehension of the processes involved, guiding the development of energy-efficient micro combustion systems and offering insights into how to optimize their performance.

Furthermore, these governing equations in the conservation form lay the groundwork for numerical methodologies like the Finite Volume Method (FVM). This method allows us to translate the continuous nature of these phenomena into discrete algebraic equations that can be solved through computational fluid dynamics (CFD) techniques. In essence, the formulation of these governing equations in Conservation Form is the key that unlocks the door to accurate and insightful simulations of micro combustion, making it a cornerstone in the pursuit of efficient and sustainable micro-scale energy generation. Hence, following the aforementioned limitations and assumptions, the steady-state governing equations of mass, momentum, species and energy are solved for the computational fluid domain, at the same time, the energy equation is considered for computational of conductive heat transfer within solid domain. The choice of which governing equations to consider depends on the specific conditions at hand.

In cases of non-reacting flow within the gaseous phase, the key focus revolves around the Navier-Stokes equations, encompassing both mass and momentum conservation, and the species conservation equation. These equations are paramount for understanding the dynamics of the fluid and the distribution of species within the micro combustor. They allow us to characterize the fluid's behavior and the impact of micro combustor geometric configuration. However, when the scenario shifts to reacting flow, the role of the energy equation becomes increasingly significant. This is due to the initiation of chemical reactions within the micro combustor. The energy equation takes on a central role in accounting for the heat released or absorbed during these reactions, shedding light on the overall thermal behavior of the system.

a. Gaseous-phase

- ***Mass Conservation Equation***

The mass conservation equation, also referred to as the continuity equation, is a fundamental component of the Navier-Stokes equations, which describe the behavior of mixture within fluid domain. This equation quantifies the transport of mass within a fluid domain, ensuring that the law of conservation of mass is satisfied in fluid flow simulations. The equation is expressed as follows:

$$\nabla \cdot (\rho \vec{u}) = 0 \qquad \textit{(III.1-1)}$$

- ***Momentum Conservation Equation***

The momentum transport equation, also known as the Navier-Stokes equation, describes the conservation of momentum for a fluid. It quantifies the transport of momentum within the fluid domain. The general form of the momentum transport equation is as follows:

$$\nabla \cdot (\rho \vec{u}\vec{u}) = -\nabla p + \nabla \cdot (\bar{\bar{\tau}}) + \rho \vec{g} \qquad \textit{(III.1-2)}$$

- ***Species conservation equation***

The species conservation equation, describes the preservation of species mass within a fluid mixture. It quantifies the transport of various chemical species within the fluid domain. The general form of the species conservation equation is as follows:

$$\nabla \cdot (\rho \vec{u} Y_i) = -\nabla \cdot \vec{J}_i + R_i \qquad \textit{(III.1-3)}$$

In this equation:

- **Mass Diffusion Flux ($\vec{J}_i$):** Represents the vector that points in the direction of the most rapid decrease in the concentration and temperature of each species *i*. It shows the path along which the species is moving due to both mass and thermal diffusion. Mathematically, Fick's Law (also known as the dilution approximation) is under which the diffusion flux is described. For turbulent flow the mass diffusion flux is formulated as follows:

$$\vec{J}_i = -\left(\rho D_{i,m} + \frac{\mu_t}{Sc_t}\right) \nabla Y_i - D_{T,i} \frac{\nabla T}{T} \qquad \textit{(III.1-4)}$$

- ***Energy conservation equation***

The energy conservation equation describes the preservation and transport of thermal energy within the fluid domain. It quantifies the transfer of energy, including heat conduction, convection, and radiation. The general form of the energy conservation equation is as follows:

$$\nabla \cdot \left(\rho \vec{u} \left(h + \frac{u^2}{2}\right)\right) = \nabla \cdot \left(\lambda_{eff} \nabla T - \sum_i h_i \vec{J}_i + \bar{\bar{\tau}} \cdot \vec{u}\right) + S_{h,rxn} + S_R \qquad \textit{(III.1-5)}$$

- $\boldsymbol{S_{h,rxn}}$**:** This term represents the heat source due to chemical reactions. It represents the additional heat generation associated with chemical reactions of fuel and oxidizer. It is typically expressed in

terms of the reaction rate, enthalpy change, and species concentrations involved in the reaction. The effective thermal conductivity is typically defined as follows:

$$S_{h,rxn} = -\sum_i \frac{h_i^0}{M_i} \mathcal{R}_i \qquad \textit{(III.1-6)}$$

where, M_i represent the molar mass of species i.

b. Solid Phase

The thermal gradient equation, commonly referred to as Fourier's law, governs the heat transfer within a solid wall. The heat transfer through the solid zone transport purely by steady-state conduction. It quantifies the thermal gradient or temperature variation within the micro combustor wall material. The general form of the thermal gradient equation is as follows:

$$\nabla \cdot (\lambda_w \cdot \nabla T) = 0 \qquad \textit{(III.1-7)}$$

The heat conduction equation is a fundamental equation in heat transfer. It describes how heat is conducted through a solid phase. The equation states that the rate of change of temperature within the micro combustor material is proportional to the temperature gradient, where the constant of proportionality is the thermal conductivity. If there are no internal heat sources or sinks, this equation ensures that heat is conserved within the system, and it is used to model heat transfer in various engineering and scientific applications, such as in heat conduction through materials or heat transfer in stationary objects. However, to ensure the compatibility and mathematical consistency necessary for our comprehensive doctoral research, which encompasses an extensive range of micro combustor geometrical configurations in both 2D and 3D models, as well as planar and cylindrical shapes, we have undertaken the development of governing equations. These equations, which serve as the foundation for our investigations into non-reacting and reacting flows, have been meticulously formulated in their differential form, which is particularly suited for describing the complex phenomena under investigation. The use of both Cartesian and cylindrical coordinates allows us to adapt the mathematical framework to the specific characteristics of each case. This meticulous approach ensures that our analysis remains methodologically rigorous and consistent across the diverse geometrical configurations and flow scenarios that constitute our study.

III.2. Numerical Modelling

In our pursuit of numerically simulating micro combustion within various geometrical configurations, we have taken a meticulous approach to formulate the governing equations that encapsulate the fundamental transport phenomena. These equations mathematically describe fluid dynamics, chemical reactions, as well as mass and heat transfer. By doing so, we gain insight into the complicated interplay of these phenomena within the micro combustion field. It's crucial to note that these equations are highly coupled and nonlinear, making analytical solutions impossible. This complexity arises from the interdependencies between parameters like pressure and velocity, necessitating substantial computational algorithms. Moreover, terms such as the net rate of production of species in the species transport equation and complex transport phenomena, such as turbulence and chemical reactions rate, necessitate employment of simplified parametric approaches, which involve numerically modeling. These simplified approaches allow for a more manageable and efficient simulation of micro combustion dynamics. Moreover, it is essential to account for the turbulence-chemistry interaction, where turbulence and combustion processes influence each other. The numerical modeling stands as a pivotal bridge between the mathematical formulation and the practical simulation of micro combustion. Thus, a set of numerical models serving as the means to incorporate and simulate these complex transport phenomena. Specialized models such as Direct Numerical Simulation (DNS), Large Eddy Simulation (LES), and Reynolds-Averaged Navier-

Stokes (RANS) models play a pivotal role in addressing turbulence within our doctoral research geometrical configurations. Micro combustion systems often exhibit intense turbulence, making it imperative to incorporate turbulence-related terms into the governing equations. These models provide an effective means to accurately capture turbulent flow behavior, which is vital for understanding and optimizing micro combustion flow dynamics. Furthermore, the realm of micro combustion is characterized by complex chemical kinetics involving numerous chemical species and reactions. The complex nature of these reaction mechanisms necessitates the use of numerical models to solve a large system of stiff differential equations. This approach ensures that we can precisely simulate the complex chemistry occurring within the combustor. Heat and mass transfer, being integral components of exothermic micro combustion phenomena, play a critical role. Numerical models are indispensable in predicting the transport of heat and species in and around the combustion zone. Accurate simulation of these processes is essential for optimizing combustion efficiency and gaining a comprehensive understanding of the micro combustion system. The governing equations for micro combustion are highly sensitive to boundary conditions, particularly heat transfer at solid surfaces. Precise modeling of these boundary conditions is indispensable for reliable simulations. These conditions are intricately linked to heat transfer within the gaseous phase and require careful consideration due to their complexity. In essence, the connection between these numerical models and the governing equations lies in the discretization process. This transformation involves representing the governing equations in discrete forms, utilizing finite difference and finite volume methods. The grid-based approach breaks down both the fluid and solid domains into discrete points, enabling the numerical solution of these complex equations. The accuracy and convergence of these numerical solutions are contingent on the thoughtful selection of grid resolution, numerical schemes, and boundary conditions. To delve deeper into the need for a solution procedure when dealing with reacting flows, it's important to highlight that micro combustion introduces another layer of complexity. The interaction between chemical reactions and fluid dynamics in reacting flows demands a systematic approach to solve these coupled equations. This involves iterative methods to find a self-consistent solution that considers the interaction between the chemistry and the flow, as chemical reactions change the fluid properties, affecting the flow field, and vice versa. Additionally, selecting the appropriate Computational Fluid Dynamics (CFD) software is paramount for our research. It must possess the capabilities to simulate both non-reacting and reacting flows within the diverse micro combustor geometrical configurations. The choice of software should align with the specific needs of our study, accommodating the intricacies of micro combustion. This entails robust support for handling complex chemical kinetics, turbulence modeling, and the ability to incorporate various boundary conditions. Moreover, the software should allow for scalability, ensuring efficient utilization of computational resources as we investigate different combustion scenarios. These numerical models not only facilitate simulations but also serve as a means to validate and compare results with experimental data. This validation process is crucial for enhancing our confidence in the models and, in turn, advancing our understanding of the underlying physics of micro combustion. It is through this integration of numerical models and experimental validation that we gain comprehensive insights into the intricacies of micro combustion.

III.2.1. Numerical Models

- **Turbulence Model**

The Navier-Stokes equations are fundamental in fluid dynamics and describe the behavior of fluid flows, ranging from laminar to turbulent. However, for practical purposes, solving these equations directly for turbulent flows is impossible due to the complexity of turbulence. Turbulent flows exhibit fluctuations in the form of small-scale turbulent structures, and these structures lack a known direct mathematical solution. As a result, a statistical approach is needed to model turbulent flow regimes effectively. One

common statistical approach is the Reynolds ensemble average, which decomposes flow variables into mean values and fluctuations with a zero-mean value.

$$\phi = \bar{\phi} + \phi' \qquad \textit{(III.2-1)}$$

Where, ϕ is any conserved scalar quantity, $\bar{\phi}$ is the mean component (ensemble-averaged or time-averaged), and ϕ' is the fluctuating component. Moreover, the next assumptions are made: $\bar{\phi} = \overline{\rho\phi}/\bar{\rho}$, and $\overline{\rho\phi''} = 0$, but $\overline{\phi''} \neq 0$. Applying the Reynolds averaging to the variables of Navier-Stokes equations, such as the velocity, pressure and other scalar quantities, except for density. For velocity:

$$u_i = \overline{u_i} + u_i' \qquad \textit{(III.2-2)}$$

where, u_I is the velocity components ($i = 1,2,3$), $\overline{u_I}$ is the mean velocity component, and u_i' is the velocity fluctuating component. Moreover, for pressure:

$$p = \bar{p} + p' \qquad \textit{(III.2-3)}$$

where, p is the pressure component, $\bar{p}$ is the mean pressure component, and p' is the pressure fluctuating component. The assumptions behind the method include the idea that the mean flow is steady or slowly varying and that the turbulent fluctuations are smaller in magnitude compared to the mean flow. By replacing expressions of the flow variables in the steady-state mass and momentum equations and then performing an ensemble averaging while applying the aforementioned assumptions, we obtain the ensemble-averaged equations. These represent the turbulent transport equations, and can be expressed in cartesian tensor notation as follows:

$$\frac{\partial(\rho u_i)}{\partial x_i} = 0 \qquad \textit{(III.2-4)}$$

$$\frac{\partial(\rho u_i u_j)}{\partial x_i} = -\frac{\partial p}{\partial x_i} + \frac{\partial}{\partial x_i}\left(\bar{\bar{\tau}}_{ij} - \rho\overline{u_i' u_j'}\right) \qquad \textit{(III.2-5)}$$

These equations are called Reynolds-averaged Navier-Stokes (RANS) equations for both non-reacting and reacting flows. However, as a result of the Reynolds averaging process, an additional term called the "Reynolds Stress", $\rho\overline{u_i' u_j'}$, is introduced. This stress represents the mean momentum transport by turbulent diffusion. This decomposition allows us to focus on the mean behavior of the flow while considering the fluctuating components that contribute to turbulence. This approach is particularly useful for avoiding the expensive computational cost of directly simulating small-scale turbulent fluctuations through methods like Direct Numerical Simulation (DNS). To close the equation set and make it solvable, the Reynolds stresses must be appropriately modeled. A common approach is to use the Boussinesq hypothesis to relate the Reynolds stresses to the mean velocity gradients, following the next expression:

$$-\rho\overline{u_i' u_j'} = \mu_t\left(\frac{\partial u_i}{\partial x_j} + \frac{\partial u_j}{\partial x_i}\right) = -\frac{2}{3}\left(\rho k + \mu_t \frac{\partial u_k}{\partial x_k}\right)\delta_{ij} \qquad \textit{(III.2-6)}$$

Where, k is the turbulent kinetic energy, and δ_{ij} is the Kronecker delta. However, numerical models are employed to parameterize the effects of turbulence, and additional equations are required to close the additional term of turbulent kinetic energy (k). The Boussinesq hypothesis is employed in models like the Spalart-Allmaras model, $k-\varepsilon$ models, and $k-\omega$ models, offering the advantage of relatively low computational cost for estimating turbulent viscosity (μ_t). In the Spalart-Allmaras model, only one extra transport equation, representing turbulent viscosity, is solved. In the case of $k-\varepsilon$ and $k-\omega$ models, two additional transport equations, one for turbulence kinetic energy (k) and the other for either turbulence dissipation rate (ε) or specific dissipation rate (ω), are solved, and (μ_t) is calculated based on the values of k, ε, and ω. The disadvantage of the Boussinesq hypothesis is that it assumes μ_t to be an isotropic scalar, which is not strictly accurate. Nonetheless, this assumption often works well for shear flows dominated by a single turbulent shear stress component, which includes many technical flows like wall

boundary layers, mixing layers, jets, and more. On the other hand, the alternative approach, exemplified by the Reynolds Stress Model (RSM), involves solving transport equations for each component of the Reynolds stress tensor. Additionally, an equation for another scale-determining variable (usually ε or ω) is required. This means that in 2D flows, five extra transport equations are needed, and in 3D flows, seven additional equations must be solved. In many scenarios, models based on the Boussinesq hypothesis perform admirably, and the increased computational expense of the Reynolds stress model is not warranted. However, the RSM excels in situations where turbulence's anisotropy significantly impacts the mean flow. Such cases encompass highly swirling flows and stress-driven secondary flows.

In view of the proposed micro-combustor geometric configurations, several recirculation zones and turbulent structures are expected to be formed by the backward facing step and the trapezoidal ribs. As aforementioned in the theoretical formulation, even though the micro combustors exhibit lower Reynolds number values compared to conventional combustion chambers, turbulence remains a significant factor that necessitates modeling. Up to now, a numerous of studies [35], [64], [65] have underscored the significance of the turbulence model in predicting micro-combustion characteristics. According to Kuo and Ronney [66], turbulence becomes more important when the Reynolds number exceeds 500. In the present doctoral research micro combustor configurations, the critical inlet velocity corresponding to $\mathrm{Re} \geq 500$ is approximately 5 m/s. Furthermore, indicated by Jun Li et al. experimental study [67], the inlet velocity should never fall below 6 m/s to prevent flashback into the upstream channel. Additionally, velocities exceeding 16 m/s may result in significant acoustic emissions. The Reynolds number is defined based on the upstream tube diameter. Therefore, for all the cases under investigation, the inlet velocity of the mixture exceeds the critical velocity. As it is widely recognized, the quality of simulations is significantly dependent on the choice of a suitable turbulence model. Consequently, several studies have been undertaken to identify the most appropriate model for micro-combustion applications [19], [46], [57]. In turbulence modeling, the $k-\varepsilon$ model is a popular choice due to its ability to capture the essential characteristics of turbulent non-reacting and reacting flows. However, it's important to note that several variants of the $k-\varepsilon$ model exist, each with its own set of equations and assumptions. These variants were developed to address specific flow conditions and have unique features that make them suitable for various applications. One such variant is the standard $k-\varepsilon$ model, which provides a robust and straightforward approach to turbulence modeling. This model is widely used for a range of micro combustor configurations and offers a good compromise between accuracy and computational efficiency. Another variant is the RNG $k-\varepsilon$ model, which utilizes a Reynolds stress transport equation to improve the representation of anisotropy in turbulent flows. This model is particularly useful for situations where turbulence anisotropy plays a significant role in the flow dynamics. The realizable $k-\varepsilon$ model, is yet another variant, which was developed to address some of the limitations of the standard $k-\varepsilon$ model, particularly in complex flows with adverse pressure gradients. The realizable $k-\varepsilon$ model incorporates additional equations and constraints to improve accuracy and stability in a wider range of flow conditions. It has been shown to provide better agreement with experimental data.

These different variants of the turbulence model cater to specific flow scenarios and offer varying levels of accuracy and computational cost. The choice of which model to use depends on the nature of the flow being simulated and the desired balance between accuracy and computational cost. It's essential for researchers and engineers to select the most appropriate variant based on the specific characteristics of the micro-combustion and the goals of the simulations. However, as aforementioned in the bibliographic study, during the current decade the micro combustion becomes a field of intense experimental and numerical research and some of these research’s findings are briefly used in the setup of our numerical computation model. To determine the most suitable turbulence model for our research, we conducted a rigorous comparison study encompassing a range of $k-\varepsilon$ turbulence models and the Reynolds Stress Model (RSM). This systematic evaluation was aimed at identifying the model that best captures the intricacies of micro-combustion flows. The numerical simulations performed with each of these models

were meticulously analyzed and compared against a benchmark reference—the findings of an experimental study. This comprehensive approach allowed us to assess the predictive accuracy and reliability of each turbulence model in simulating real-world micro-combustion scenarios. As shown in **Figure III.2.1**, by aligning the numerical results with the reference experimental data, we gained valuable insights into the strengths and limitations of each model, ultimately enabling us to make an informed selection of the most appropriate turbulence model for our specific research objectives. An increasing number have found that amongst different variants of $k-\varepsilon$ variants models, the realizable $k-\varepsilon$ produce an excellent agreement with the experimental data [19], [59]. Therefore, the two-equations model of realizable $k-\varepsilon$ is adopted for all the present doctoral research simulations [39].

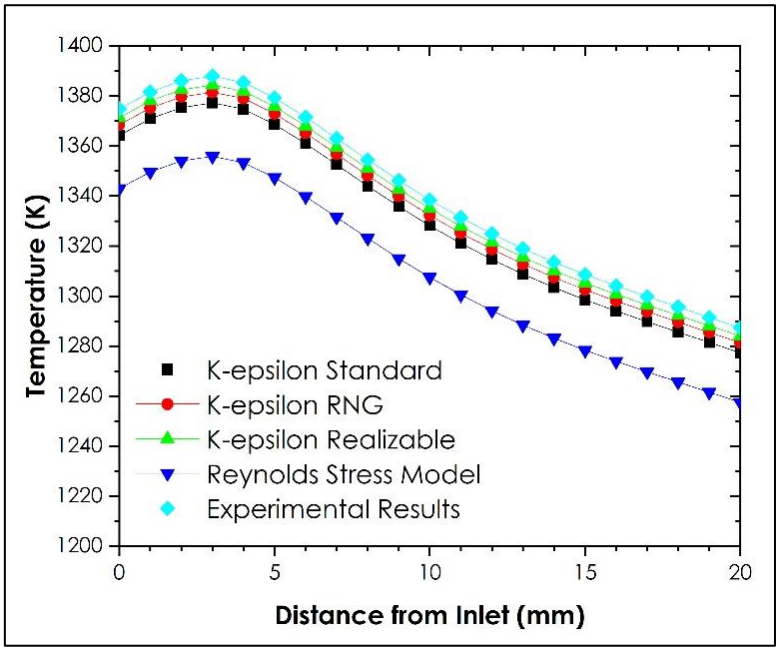

Figure III.2.1. *Verification of turbulence model: comparison of the outer wall temperature profile*

- **Near-Wall Treatment**

The presence of walls significantly influences turbulent flows, impacting both mean velocity and turbulence in complex ways. Close to the wall, viscous damping and kinematic blocking affect velocity fluctuations, and turbulence is augmented by the production of turbulence kinetic energy in the outer part of the near-wall region. Accurate modeling of the near-wall region is crucial for numerical solutions, especially considering walls as the main source of mean vorticity and turbulence. The near-wall region is divided into three layers: In the innermost layer, called the "viscous sublayer", the flow is almost laminar, and the (molecular) viscosity plays a dominant role in momentum and heat or mass transfer. In the outer layer, called the fully-turbulent layer, turbulence plays a major role. Finally, there is an interim region between the viscous sublayer and the fully turbulent layer where the effects of molecular viscosity and turbulence are equally important. **Figure III.2.2** illustrates these sublayers of the near-wall region.

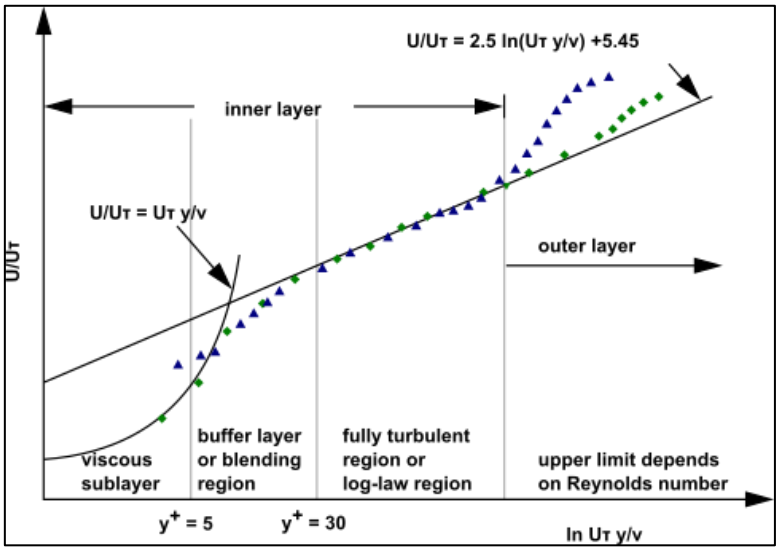

Figure III.2.2. *Sublayers of the Near-Wall Region*

This depiction is graphically represented on semi-logarithmic coordinates, providing a clear illustration of the different layers of the near the wall region. However, in order to establish a "universal" criterion, non-dimensional variables are introduced: u^+ for the normal velocity and y^+ for the distance to the wall, and can be defined as follows:

$$y^+ = \frac{\rho u_\tau y}{\mu} \tag{III.2-7}$$

where u_τ is the friction velocity, defined as:

$$u_\tau = \sqrt{\frac{\tau_w}{\rho}} \tag{III.2-8}$$

The evaluation of y^+ requires a comprehensive understanding of the wall shear stress τ_w. Various approaches, such as empirical expressions like the Colebrook law or reference tables exemplified by the Moody Chart, can be employed to compute the skin friction coefficient (C_f):

$$C_f = \frac{\tau_w}{\frac{1}{2}\rho U^2} \tag{III.2-9}$$

where, U represent velocity of the fluid parallel to the surface (freestream velocity). However, there are two main approaches for near-wall modeling:

Wall Functions

In this approach, the viscosity-affected inner region is not resolved. Instead, semi-empirical formulas called "Wall Functions" bridge the viscosity-affected region between the wall and the fully-turbulent region. This approach avoids modifying turbulence models to account for wall presence.

Near-Wall Modelling

In this approach, turbulence models are modified to resolve the viscosity-affected region with a mesh extending all the way to the wall, including the viscous sublayer. This allows for more accurate representation but requires specific adjustments in the turbulence model.

In the context of numerical modelling, it is crucial to carefully select and control the size of the first boundary layer cell, which corresponds to the magnitude of (y^+). The choice of an appropriate approach depends on the specific requirements of the simulation and the available data. Utilizing such methods ensures an accurate evaluation of (y^+) and, consequently, a reliable representation of the near-wall region in the computational domain. Properly controlling (y^+) is fundamental for achieving accurate and

efficient simulations, particularly in situations where the near-wall physics significantly influences the overall flow behavior such as non-reacting and reacting flows within micro combustors. In the current doctoral research, the decision to employ the standard wall function as the chosen wall function is rooted in careful consideration of the trade-offs between computational efficiency and accuracy in capturing near-wall effects. The standard wall function approach simplifies the treatment of the near-wall region by incorporating semi-empirical formulations, thus avoiding the need for resolving the inner region influenced by viscosity. This choice aligns with the balance between numerical efficiency and fidelity in predicting wall-bounded turbulent flows. The standard wall function is particularly well-suited when computational resources are a critical consideration, as it allows for a more streamlined simulation of the flow field near surfaces without sacrificing essential near-wall physics. This decision acknowledges the practical challenges associated with resolving the complexities of the viscous sublayer and buffer layer while ensuring that the overall accuracy of the numerical predictions remains robust within the constraints of the chosen turbulence modeling approach.

- **Combustion model**

The species transport equation formulated above model the convection, diffusion and reactions sources for each component species in the fluid phase. The reaction source term (R_i) stands for the net rate of formation or consumption of each component species in every elementary reaction of the reduced mechanism. In order to model the reaction source term (R_i) and close the species mass transport equation, the eddy dissipation concept model (EDC) is chosen. The model is suitable for turbulent reacting flows with fast chemistry and capture the turbulence effect on the reaction rate [19], [53]. EDC model assumes that reactions occur within small turbulent structures, called fine scales. Meanwhile, the length fraction ξ^* of the fine scales is modeled as:

$$\xi^* = C_\xi \left(\frac{\nu\varepsilon}{k^2}\right)^{\frac{1}{4}} \qquad \textit{(III.2-10)}$$

where, * denotes fine-scale quantities, ν stands for the kinematic viscosity and C_ξ is defined as volume fraction constant ($C_\xi = 2.1377$), Moreover, the reactions proceed in the fine scales over a time scale τ^*:

$$\tau^* = C_\tau \left(\frac{\nu}{\varepsilon}\right)^{\frac{1}{2}} \qquad \textit{(III.2-11)}$$

where, C_τ is a time scale constant equal to $C_\tau = 0.4082$. Therefore, the reaction source term (R_i) is calculated by:

$$R_i = \frac{\rho(\xi^*)^2}{\tau^*[1-(\xi^*)^3]}(Y_i^* - Y_i) \qquad \textit{(III.2-12)}$$

where, Y_i^* is the fine-scale species mass fraction after reacting over the time scale τ^*. On the other hand, the reaction rates are specified by the Arrhenius rates, and are integrated numerically using the ISAT algorithm. For the first reaction step, the stiff chemistry solver is considered in order to determine the first ISAT table entry.

III.2.2. Materials Properties

The micro-combustor is chosen to be made of 316 stainless-steel because of its significant thermostability capabilities and ability to withstand the high temperature (> 2000 °C) resulting from the reacting flows without degradation of its structure strength. Moreover, it has density ρ_s of 8000 (kg/m^3), and a specific heat capacity $C_{p,s}$ of 500 (J/kg.K). Meanwhile, due to the reacting flows high temperatures ($T_f \sim 2000\ K$), the oxidizing environment and the thinness of the wall thickness, the thermal conductivity is no longer a uniform property, which influences the outer wall temperature distribution. Therefore,

following the experimental and numerical results presented by J. Li et al. in 2009 [49], the thermal conductivity is ranging between $\lambda_w = 5$ (W/m.K) at $T = 300$ (K) and $\lambda_w = 20$ (W/m.K) at $T = 800$ (K). Therefore, the thermal conductivity is given as a function of temperature following the equation reported by K.C. Mills in 2002 [50] as:

$$\lambda_w = -7.301.10^{-6}T^2 + 2.716.10^{-2}T + 6.308 \quad \textit{(III.2-13)}$$

However, according to Jun Li et al., the outer wall temperature distribution profile peak value is largely influenced by the magnitude of the thermal conductivity [51]. Simultaneously, the ribs thickness is very carefully chosen in order to be both, too thin but enough to hold the high temperatures rates [52]. Besides, comparing to conventional hydrocarbons, hydrogen has a wider flammable range, high heating value, short reaction time scale and high flame speed which made it more suitable for combustion at micro-scale [23] [49]. Therefore, hydrogen and air were chosen as the fuel and oxidant, respectively. Furthermore, the skeletal reaction mechanism proposed by J. Li et al. for H_2-air mixtures is applied in the computational modelling of combustion [53], [54]. The mechanism consists of 9 species and 21 reversible elementary reactions, as listed in the **Table III.2.1**. The mechanism has been proved to be valid in the simulation of micro-[53], [54]. Meanwhile, the chemical reactions kinetics were set up using the CHEMKIN format. The ANSYS Fluent materials database is used to define the thermodynamic and transport properties of the mixture species.

On the other hand, in the case of reacting flows the physical properties of hydrogen-air mixture become dependent to the temperature and the composition of the mixture. Therefore, the mixture properties will be defined as temperature and composition dependent functions provided by the ANSYS Fluent [53], [54]. In respect of the assumption made above, the mixture density is calculated using the incompressible ideal gas law. Considering the mixture of fuel, oxidant and products as an incompressible ideal gas, the equation of state can be written as [53]–[55]:

$$\rho = \frac{P_{op}M}{RT} \quad \textit{(III.2-14)}$$

where, R is the universal gas constant (R=8.314 (kJ/kmol . k)).

In mixtures, $\boldsymbol{C_{p,i}}$ is often calculated as a weighted average considering mass fractions. Accurate knowledge for various species is critical for precise modeling and predicting the system's thermal behavior. While the molar mass M, specific heat c_p, viscosity μ and thermal conductivity k_f were calculated using the mass fraction weighted average of the species properties, which is expressed respectively as:

$$M = \left(\sum_{i=1}^{n} \frac{Y_i}{M_i}\right)^{-1} \quad \textit{(III.2-15)}$$

$$c_p = \sum_{i=1}^{n} Y_i c_{p,i} \quad \textit{(III.2-16)}$$

$$\mu = \sum_{i=1}^{n} Y_i \mu_i \quad \textit{(III.2-17)}$$

$$\lambda_f = \sum_{i=1}^{n} Y_i k_i \quad \textit{(III.2-18)}$$

Accordingly, the specific heat and both viscosity and thermal conductivity of each species are computed by piecewise polynomial and kinetic theory methods, respectively. The mass diffusivity of the mixture ($D_{i,m}$) is computed using the kinetic theory. The solver will use a modification of the Chapman-Enskog formula to compute the diffusion coefficient as following [54]:

$$D_{i,m} = 0.00188 \frac{\left[T^3\left(\frac{1}{M_i}+\frac{1}{M_j}\right)\right]^{\frac{1}{2}}}{P_{abs}\sigma_{ij}^2\Omega_D} \quad \textit{(III.2-19)}$$

Where, P_{abs} is the absolute pressure, Ω_D is the diffusion collision integral, which is a measure of the interaction of the molecules in the system [54]. On the other hand, the thermal diffusion coefficients can be defined following empirically-based composition-dependent expression derived from this form of the Soret diffusion coefficient will cause heavy molecules to diffuse less rapidly, and light molecules to diffuse more rapidly, towards heated surfaces. This form can be written as follows:

$$D_{T,i} = -2.59 \times 10^{-7} T^{0.659} \left[\frac{M_{w,i}^{0.511} X_i}{\sum_{i=1}^{N} M_{w,i}^{0.511} X_i} - Y_i\right] \cdot \left[\frac{\sum_{i=1}^{N} M_{w,i}^{0.511} X_i}{\sum_{i=1}^{N} M_{w,i}^{0.489} X_i}\right] \qquad \textit{(III.2-20)}$$

Table III.2.1. *Chemical Reaction mechanism of H_2-Air combustion* [53], [54]

N°	Reaction	A_k	β_k	E_k (J/kmol)
H_2/O_2 chain reactions				
1.	$H+O_2=O+OH$	3.55E+15	-0.40	1.66E+04
2.	$O+H_2=H+OH$	5.08E+04	2.70	6.29E+03
3.	$H_2+OH=H_2O+H$	2.16E+08	1.50	3.43E+03
4.	$O+H_2O=OH+OH$	2.97E+06	2.00	1.34E+04
H_2/O_2 dissociation/recombination reactions				
5.	$H_2+M=H+H+M^a$	4.58E+19	-1.40	1.04E+05
6.	$O+O+M=O_2+M^b$	6.16E+15	-0.50	0.00
7.	$O+H+M=OH+M^c$	4.71E+18	-1.00	0.00
8.	$H+OH+M=H_2O+M^d$	3.80E+22	-2.00	0.00
Formation and consumption of HO_2				
9.	$H+O_2+(M)=HO_2+(M)^e$	1.48E+12	0.60	0.00
10.	$HO_2+H=H_2+O_2$	1.66E+13	0.00	8.23E+02
11.	$HO_2+H=OH+OH$	7.08E+13	0.00	2.95E+02
12.	$HO_2+O=O_2+OH$	3.25E+13	0.00	0.00
13.	$HO_2+OH=H_2O+O_2$	2.89E+13	0.00	-4.97E+02
Formation and consumption of H_2O_2				
14.	$HO_2+HO_2=H_2O_2+O_2$	4.20E+14	0.00	1.20E+04
15.	$HO_2+HO_2=H_2O_2+O_2$	1.30E+11	0.00	-1.63E+03
16.	$H_2O_2+(M)=OH+OH+(M)^f$	2.95E+14	0.00	4.84E+04
17.	$H_2O_2+H=H_2O+OH$	2.41E+13	0.00	3.97E+03
18.	$H_2O_2+H=HO_2+H_2$	4.82E+13	0.00	7.95E+03
19.	$H_2O_2+O=OH+HO_2$	9.55E+06	2.00	3.97E+03
20.	$H_2O_2+OH=HO_2+H_2O$	1.00E+12	0.00	0.00
21.	$H_2O_2+OH=HO_2+H_2O$	5.80E+14	0.00	9.56E+03

Rate constants are given in the form of $\boldsymbol{k = A_k T^{\beta_k} \exp\left(-\frac{E_k}{RT}\right)}$.

[a,b,c,d,f] Enhancement factors: H_2=2.5 and H_2O = 12.0.

[e] Enhancement factors: H_2 = 2.0, H_20 = 11.0, O_2 = 0.78.

III.2.3. Boundary Conditions

For the problems of interest here, a set of mathematical conditions that must be satisfied in the solution of the governing equations. These conditions are assigned to the exterior edges of the computational domain. Therefore, the boundary conditions of the modelled micro-combustor are set as follows:

- **Fluid Zone**

For the current problems, the micro-combustor operates under standard atmospheric conditions, at ambient pressure and temperature of 1 atm and 300 K, respectively.

— Inlet: Mixture with uniform inlet velocity, temperature, pressure and mass fractions of the mixture components are specified. Besides, the hydraulic diameter and turbulent intensity at the boundary are arranged. Different inlet velocities and equivalence ratio[3] will be investigated.

— Outlet: Pressure-outlet boundary condition is selected, and the pressure is set to zero. Furthermore, the species and temperature gradients are taken to be zero too. For the turbulence calculation, the backflow hydraulic diameter and turbulent intensity are set as shown in **Table III.2.2** below.

- **Solid Zone**

— Interior surface: The no-slip condition is applied, and it is assumption of zero diffusive flux species is made on the gas-solid interface of the micro-combustor. In addition, the conjugated heat transfer between the fluid domain and the solid domain is considered. The convective heat transfer is considered only and surface-to-surface radiation in our analysis is neglected based on the findings reported by Li et al. [64]. According to their research, the influence of surface-to-surface radiation between the inner walls is minimal. This implies that the heat exchange through radiation between different surfaces within the micro combustor has a negligible impact on the temperature distribution of the outer wall. As a result, for the sake of simplicity and to streamline our calculations, we have chosen to exclude surface-to-surface radiation from our considerations, focusing on convective heat transfer mechanism. This simplification allows us to concentrate on the key factors influencing the outer wall temperature without compromising the accuracy of our predictions. Hence, the coupled interface method is applied. The convective heat transfer at inner surface is calculated as follows:

$$-\lambda_w \nabla T = h_{i,w}\left(T_g - T_w\right) \quad \text{(III.2-21)}$$

where, $h_{i,w}$ represent the convective heat transfer coefficient at the inner wall of micro combustor. T_g represents the temperature of the gaseous phase. The calculation of T_g is determined through the numerical solving of the energy equation specific to the gaseous phase.

— Exterior surface: The mixed (Robin) thermal condition is chosen, since the heat loss to the ambient surrounding is determined through both thermal radiation and natural convection. Therefore, the total heat loss rate is calculated as follow:

$$-\lambda_w \nabla T = h_{o,w}(T_w - T_\infty) + \varepsilon\sigma(T_w^4 - T_\infty^4) \quad \text{(III.2-22)}$$

[3] The equivalence ratio (ϕ) is a dimensionless parameter representing the ratio of the actual fuel-to-oxidizer mixture to the stoichiometric ratio for complete combustion. It's crucial for assessing combustion efficiency and emissions.

where, h is the natural convective heat transfer coefficient, T_w is the outer wall surface temperature, T_∞ is the ambient temperature, ε denotes the emissivity of the wall material mentioned earlier, and σ is the Stephan-Boltzmann constant. The natural convective heat transfer coefficient and the thermal emissivity of the wall represents a key parameter that have a high influence on the outer wall temperature distribution and the overall heat loss intensity [49]. According to the experimental results presented by Jun Li et al. [56], it is found that under the reacting flows high temperatures conditions, the emissivity of the wall is ranging between 0.5 and 0.9. On the other hand, the natural convective heat transfer coefficient ranges between 10 and 20 (W/m^{2}K). Therefore, following the experimental and numerical results presented in the literature or obtained by the numerical tests conducted during this study, an average value of $\varepsilon = 0.65$ and $h = 15\ \left(\frac{\mathrm{W}}{\mathrm{m^2K}}\right)$ are chosen to be used. The numerical values for the different parameters used at each of the physical boundaries are listed on the **Table III.2.2** below. The table specify the parameters and values that define the behavior of the micro combustor during the simulations. These parameters play a crucial role in determining how the fluid flows and interacts within the system. The table below outlines the specific components of our boundary conditions. These boundary conditions are essential for creating a realistic and controlled environment in our simulations, allowing us to investigate the behavior of the micro combustor under various operating conditions and geometries.

***Table III.2.2**. Boundary Conditions*

Boundary	Parameters	Unit	Values
Inlet	Velocity Inlet	(m/s)	Varied
	Temperature	(K)	300
	Gauge pressure	(Pa)	0
	Hydraulic diameter	(mm)	2
	Turbulent intensity	(%)	5
	Equivalence ratio ϕ	Non dimensional	Varied
Outlet	Gauge pressure	(Pa)	0
	Hydraulic diameter	(mm)	3
	Turbulent intensity	(%)	5
Wall	Material		316 Stainless-steel
	Thermal condition		Mixed
	Natural convective heat transfer coefficient (W/(m^2.K))		15
	External & internal emissivity		0.65

III.2.4. Computational Scheme

- **Numerical Methods**

In the numerical solution process, we employ a finite volume method to solve the set of governing equations implicitly. This method is implemented using a 2D segregated solver, and under-relaxation techniques are applied to enhance convergence. The numerical computations are carried out with a double-precision pressure-based steady-state solver to ensure accurate results. To handle the pressure-velocity coupling and enforce mass conservation, we utilize the "SIMPLE" algorithm, a widely accepted approach in computational fluid dynamics. This algorithm aids in obtaining the pressure field, which is crucial for the accurate simulation of fluid flows. In terms of spatial discretization, all the governing equations are discretized using the second-order upwind scheme. This choice of scheme helps maintain

accuracy in capturing flow behavior. Gradients, which play a significant role in these computations, are calculated using the Least Square Cell-Based method. To control the solution process and stabilize numerical errors, appropriate under-relaxation factors are set. These factors ensure that the solution converges effectively while avoiding instabilities in the numerical computations. Furthermore, for convergence assessment, we establish specific criteria for the residuals of the governing equations. The residuals, which indicate the difference between the calculated values and the expected values, are closely monitored during the simulations. The convergence criteria are set at 10^{-3} for all equations except for the energy equation, for which a stricter criterion of 10^{-6} is applied. This meticulous approach ensures that the numerical solution meets the desired level of accuracy and reliability in capturing the physical phenomena under consideration.

- **Solution Procedure**

In the simulation of reacting flows, achieving stable combustion requires a two-step procedure. Initially, the simulation commences by addressing the non-reacting flow, often referred to as the "cold-flow" stage. During this phase, only the flow and species mass conservation equations are solved, primarily because the system is isothermal. The results obtained from this step provide velocity and pressure fields, which serve as the initial solution for subsequent simulations of reacting flows. To initiate combustion, an initial temperature of 2000 K is applied to the fluid zone, igniting the mixture and kickstarting the chain reactions involved in combustion, as indicated in references [48], [59], [60]. For non-reacting cases, a different procedure is followed. The solver begins by solving the momentum equations, followed by the continuity equation, which in turn updates the pressure and velocity fields. Subsequently, the energy and species equations are computed, influencing the temperature and composition in both the solid and fluid zones. Iterations continue until a converged solution is obtained. It's worth noting that achieving numerical convergence in reacting flows can be particularly challenging due to the high nonlinearity and stiffness of the coupled equations that govern the computations. Additionally, the significant differences between the thermal properties of the walls and the fluid contribute to the complexity of the convergence process. Consequently, the energy equation is often the last to converge [61]. To handle these computations efficiently, all numerical simulations are performed on parallel computing platforms utilizing an 8-core processor running at 3.33 GHz with 24 GB of RAM. The computational time for each case varies depending on factors such as grid size and the complexity of the case, ranging from approximately an hour to several hours. This range accounts for the diverse computational demands of different scenarios, ensuring the accurate and thorough simulation of reacting flows.

III.2.5. Software Selection

At the outset of our doctoral research, we undertook a thorough comparative study to determine the most suitable software for our simulation needs. This evaluation focused on assessing the compatibility and capabilities of two prominent CFD tools: OpenFOAM and ANSYS Fluent. In the context of simulating turbulent flow within micro combustors, ANSYS Fluent emerged as the preferred choice for several compelling reasons. First and foremost, ANSYS Fluent offers a dedicated solver tailored for non-reacting turbulent flows. This specialization ensures robust and accurate results in modeling turbulent flow phenomena, making it ideal for our research. Moreover, Fluent excels in modeling chemical reactions under reacting conditions, providing comprehensive capabilities that align with our objectives. Fluent's strengths extend to its user-friendly interface, extensive predefined material libraries, and the availability of commercial support. These attributes collectively enhance accessibility and efficiency for users at various skill levels. The intuitive interface simplifies the setup of simulations, while the vast material libraries streamline the definition of properties, saving valuable time and effort. Furthermore, the presence of robust commercial support means that users can access assistance and guidance when needed, reinforcing its reliability as a simulation tool. Conversely, while OpenFOAM is a powerful open-source

solution, it has certain limitations for our specific research focus. Notably, it lacks a specialized non-reacting flow solver, and adapting it for reacting flow simulations may necessitate significant user customization. The text-based input approach, manual material property definitions, and reliance on open-source community support can pose challenges, particularly for users seeking a more user-friendly and well-documented solution. To summarize, both OpenFOAM and ANSYS Fluent have their respective merits, but ANSYS Fluent distinctly shines in simulating turbulent flows under non-reacting and reacting conditions within diverse micro combustor geometries. Its specialized solvers, advanced combustion models, efficient meshing capabilities, and user-friendly interface collectively make it an optimal choice for comprehensive and precise numerical studies in this domain.

III.2.6. Validation of Numerical Model

To assess the reliability and accuracy of the numerical approach employed in this study, a thorough validation process was conducted by comparing our simulations with experimental data from Tang et al. [68] and numerical simulations by Lu et al. [69]. The temperature distribution on the outer wall surface of the micro combustor was obtained through infrared thermal imaging, utilizing a Thermovision™ A40 camera equipped with a close-up lens for enhanced image clarity. Measurements were conducted in controlled conditions, in a windless and lightless environment, at an ambient temperature of approximately 20°C to minimize the influence of atmospheric radiation. **Figure III.2.3** illustrates the comparison between the present numerical simulations and the experimental data, revealing a noteworthy level of agreement. It's important to acknowledge that some minor discrepancies were observed in the upstream region (within 2 mm from the inlet). However, beyond this initial section, the maximum relative error was merely around 1% to 2%. These findings indicate that the numerical models and computational scheme employed in this study are reasonably reliable and exhibit a stronger agreement with the experimental data when compared to results from the existing literature. This validation process reinforces the confidence in our numerical methodology to be applied, confirming its capability to accurately represent the micro combustion phenomena in the given geometrical configurations and operating conditions. Such validation is a critical step in ensuring the credibility of the numerical model and its applicability to real-world scenarios.

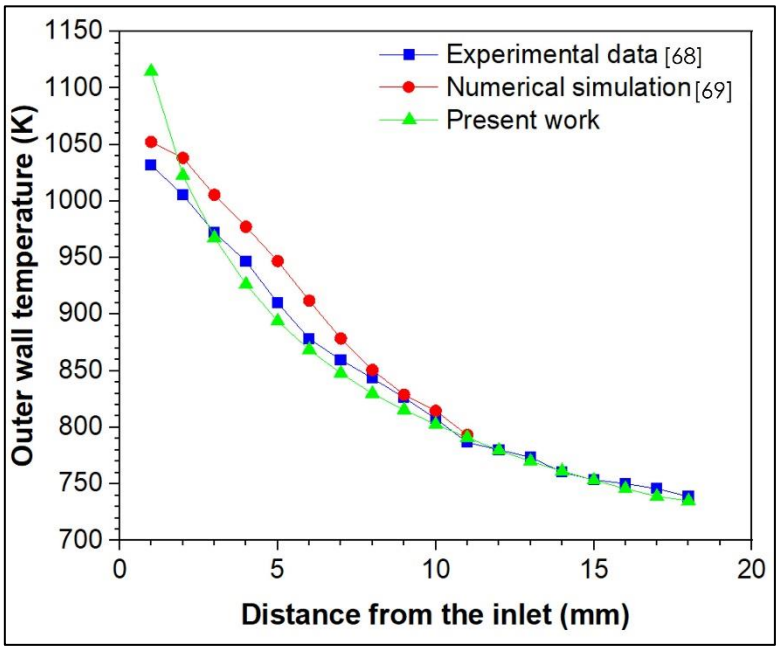

Figure III.2.3 *Comparison of the outer wall temperature profiles: experimental data [68] and numerical simulations [69].*

Chapter IV: Results

IV.1. 2D Numerical Simulation

This part of our doctoral research marks the practical application of our previously established numerical methodology. The transition from theory to practical application, involves the simulation of both non-reacting and reacting flows within our novel geometrical configurations. Our primary goal is to assess the impact of the newly proposed trapezoidal shaped rib enhancements on the overall efficiency of Micro Thermophotovoltaic (MTPV) systems, building on our established theoretical foundation. In line with our thesis's central focus, we conduct an extensive numerical analysis of turbulent mixing within the micro combustor for various geometrical configurations. Our numerical study is deeply rooted in the micro-combustion field and its enhancement strategies, holds promise for a variety of applications crucial to contemporary advancements. The ultimate aim is to contribute to the development of highly efficient energy systems, particularly focusing on Micro-Thermophotovoltaic (MTPV) systems.

The initial phase of our practical application focuses on 2D simulations. The choice to commence our investigation with 2D simulations is underpinned in aim to methodically separate the effect of trapezoidal shape rib on the main axial flow. This decision serves several essential purposes. Firstly, it provides us with a solid foundation to comprehensively assess the consequences of introducing trapezoidal-shaped ribs within the micro combustor's backward facing step. We seek to understand how this geometric configuration impacts various critical aspects of the micro combustion, including flow, combustion, and thermal characteristics. By initially focusing on 2D simulations, we aim to unravel the fundamental principles governing the interaction between the modified geometry and the fluid dynamics within the micro combustor, both for non-reacting and reacting flows. This approach allows us to separate the individual effect of geometric features to the observed changes in flow characteristics caused by the high-pressure reacting flows. It serves as a stepping stone toward a more comprehensive understanding that will be applied in subsequent 3D simulations.

However, this chapter is divided into two main phases. The first phase centers on investigating the effect of geometrical configurations on the flow, combustion and thermal characteristics. In the second phase of the 2D study, building on the insights gained in the first part, focusing on the chosen geometric configuration a deeper analysis allows us to systematically assess the influence of both the mixture inlet velocity and the hydrogen-to-air equivalence ratio on the thermal performance of the micro combustor. Our ultimate objective is to draw informed conclusions regarding the most suitable geometrical configuration and its compatible operating conditions. These studies offer valuable insights into the effects of geometric configurations and operating conditions on flow, combustion, and thermal characteristics. Furthermore, 2D simulations provide a computationally efficient means to explore a wide range of geometric configurations, operating conditions, and parametric variations, aiming to refine our knowledge for optimizing the application of our novel geometric enhancement technique. This comprehensive exploration equips us with valuable insights into the micro combustor's behavior under diverse scenarios.

Through these applications, we seek to demonstrate the potential of our proposed geometric modifications, specifically the trapezoidal shaped ribs. By quantifying their effects on flow, combustion, and thermal characteristics, we aim to underscore the value of integrating multiple equidistantly distributed ribs on the micro combustor's inner wall. Our study paves the way for their practical implementation in real-world systems. These applications hold the promise of revolutionizing energy systems, particularly within the realm of MTPV systems, by enhancing their efficiency, stability, and overall performance. The following sections will provide a comprehensive exploration of each aspect of our research, ensuring a clear and coherent presentation. Once these fundamental understandings are established, we can then transition to the more computationally demanding 3D simulations, where the complexity of the system is heightened.

IV.1.1. Effect of Geometry

- **Physical Model**

Introducing a rib is an enhancement technique used in aim to improve the micro-combustor performances in terms of flow-field, combustion and heat transfer characteristics. However, to clarify the novel proposed trapezoidal shaped rib figures of merit, a comparison study to the simple backward facing step micro combustor, is considered. In addition, we investigate the beneficial of the trapezoidal shape by comparison with rectangular, curved, and triangular shaped ribs. Building on our initial findings, we delve further into the study of the effect of number of ribs present within the micro combustor. Our exploration spans from a single rib to six ribs, maintaining equidistant spacing between them. Each rib configuration undergoes a thorough evaluation to determine its impact on flow field characteristics, combustion behavior, and thermal performance. In addition to the shape and number of ribs, our doctoral research includes a detailed analysis of the effect of rib height. Rib height is systematically varied within the range of 0.3 to 0.8, with a baseline of 0.5. This exploration allows us to assess how rib height influences key aspects such as flow field dynamics, combustion stability, and thermal behavior. A set of numerical simulations were performed using the aforementioned methodology. This study consists of comparing the different micro-combustors performances in terms of flow-field, combustion and heat transfer characteristics.

In the following, the dimensions of various geometrical configurations will be defined, encompassing the geometrical configuration to be used in the study of the effects of introducing ribs, the impact of different rib shapes, the influence of varying rib numbers, and the assessment of rib height effects, respectively. To align our research with established practices and maintain consistency with the micro-scale standards recognized by the research community, we adopted backward-facing step micro-combustor configuration with dimensions commonly employed in experimental studies. As shown in **Figure IV.1.1**, the backward-facing step micro-combustor configuration featured two channels, with the first having a height (or diameter, in the case of a cylindrical shape) of $d_1 = 2\,mm$ and a corresponding length of $L_2 = 2\,mm$. The second channel (or two cylinders in the case of a cylindrical shape) expanded to a height of $d_1 = 3\,mm$. Therefore, the backward-facing step has a height of $s = 0.5\,mm$. The micro combustor has a total length of the of $L_1 = 20\,mm$ and a thickness of $t_1 = 0.5\,mm$. The backward facing step micro combustor simple design will be denoted from now on using the next abbreviation (MCSD).

a. Effect of shape

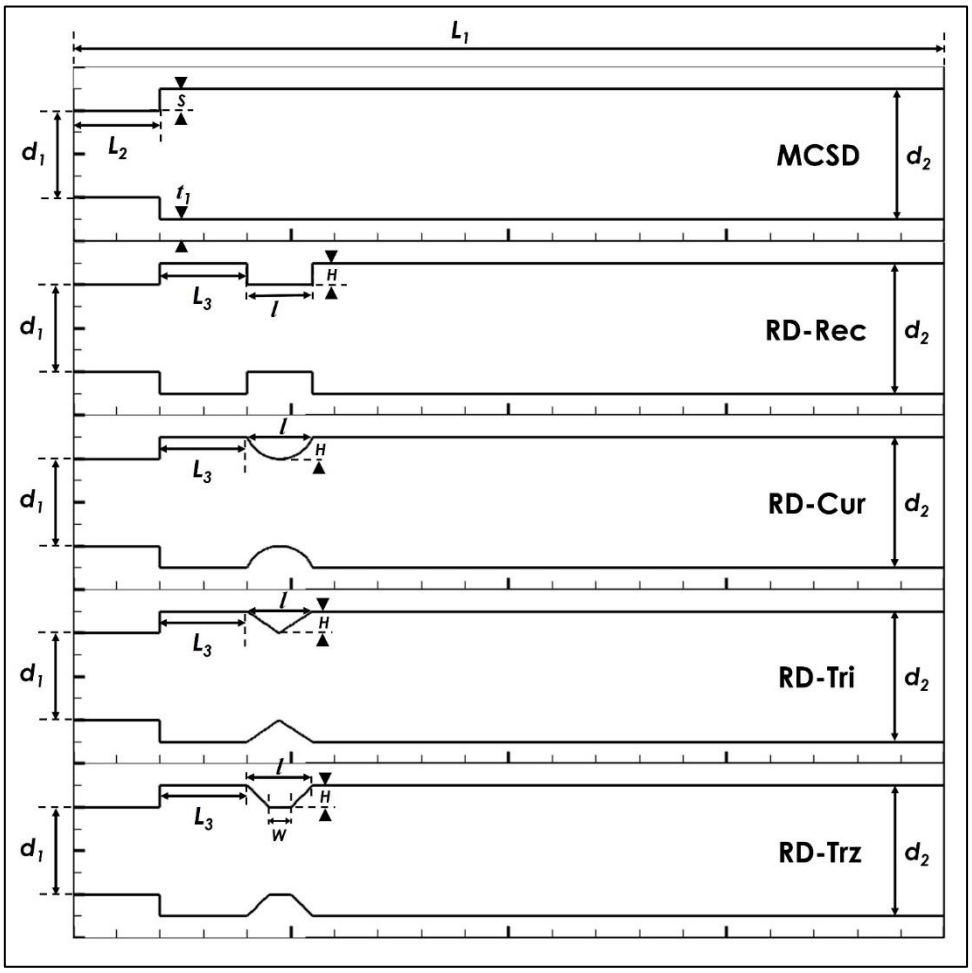

Figure IV.1.1. *Schematic diagram of the backward-facing step micro combustor with Simple (MCSD) rectangular (RD-Rec), curved (RD-Cur), triangular (RD-Tri), and trapezoidal (RD-Trz) shaped ribs design.*

Figure IV.1.1 shows the schematic view and dimensions of the proposed micro combustor with rectangular, curved, triangular, and trapezoidal shaped ribs design. The micro combustor featuring the rectangular-shaped rib design is identified as RD-Rec. Similarly, the micro combustor equipped with a curved-shaped rib is denoted as RD-Cur. The one with a triangular-shaped rib design is referred to as RD-Tri, and finally our new developed micro combustor incorporating the trapezoidal-shaped rib is labeled as RD-Trz. All the ribs are consistently positioned $L_3 = 2\,mm$ away from the step in all the micro combustor configurations with different rib shapes. For RD-Rec, the rectangular rib measures $l = 1.5\,mm$ in length and has a height of $H = 0.5\,mm$. For RD-Cur, the curved rib features a major axis of $l = 1.5\,mm$ and a minor axis (height) of $H = 0.5\,mm$. In the case of RD-Tri, the triangular rib has a base length of $l = 1.5\,mm$ and a height of $H = 0.5\,mm$. Lastly, in the case of RD-Trz, the trapezoidal rib is characterized by a long side of $l = 1.5\,mm$, a height of $H = 0.5\,mm$, a short side of $W = 0.5\,mm$, and an angle of $\theta = 45°$. The choice of a 45° angle for the trapezoidal rib edges and the spacing between the rib and the step in the micro-combustor design is driven by the aim to optimize fluid dynamics, combustion characteristics, and thermal performance. The selected angle and spacing enables improved flow behavior, enhances flame stability and species distribution, and improved convective heat transfer area and the outer wall temperature uniformity. Moreover, the height of the rib in the micro-combustor designs positively impacts fluid dynamics, combustion characteristics, and thermal performance. To describe the micro combustor's geometric parameters, **Table IV.1.1** offers a comprehensive summary of

the configurations. This table includes parameter names, their associated dimensions, and identifies the specific geometric parameters of interest for study, distinguishing them from the constant parameters.

Table IV.1.1. *Geometrical parameters of different micro combustor configurations.*

Geometrical Parameter	Parameter name	Value (mm)	Constant/ Variable
d_1	Inlet diameter (height)	2	Constant
d_2	Outlet diameter (height)	3	Constant
H	Rib(s) height	0.3 – 0.8	Variable
l	Rib(s) length	1.5	Constant
L_1	Combustor length	20	Constant
L_2	Inlet length	2	Constant
L_3	Distance between ribs	1 – 6	Variable
s	Step height	0.5	Constant
t_1	Combustor wall thickness	0.5	Constant
W	Trapezoidal rib short side	0.5	Constant

b. Effect of Number (spacing)

To study the effect of using multiple ribs within the micro combustor, we considered various configurations with different numbers of ribs and spacing, always ensuring an equidistant distribution of the ribs. As shown in **Figure IV.1.2**, the first micro combustor configuration incorporates one rib ($N = 1$) with a distance from the step equal to ($L_3 = 6\ mm$). In the second configuration, one rib is added and the micro combustor incorporates now two ribs ($N = 2$), while maintaining the equidistant distribution of the ribs with a distance from the step and between the ribs ($L_3 = 6\ mm$). For the third configuration, we moved the first rib 2 mm closer to the step, added another rib, and maintained the equidistant distribution, resulting in three ribs ($N = 3$) with a distance from the step and between the ribs of ($L_3 = 4\ mm$). In the fourth case, we moved the first rib 1 mm closer to the step, added another rib, and maintained the equidistant distribution, resulting in four ribs ($N = 4$) with a distance from the step and between the ribs of ($L_3 = 3\ mm$). In the fifth micro combustor configuration, the number of ribs remains the same, with four ribs ($N = 4$). However, the spacing between the ribs is reduced by moving the first rib 1 mm closer to the step. The equidistant distribution is maintained, with a distance from the step and between the ribs set at $L_3 = 2\ mm$. In the sixth case, we continued to refine the spacing by moving the first rib 0.5 mm closer to the step, adding another rib, and ensuring equidistant distribution, resulting in five ribs ($N = 5$) with a distance from the step and between the ribs of ($L_3 = 1.5\ mm$). In the seventh and final case, we again reduced the spacing by moving the first rib 0.5 mm closer to the step, adding another rib, and maintaining equidistant distribution, resulting in six ribs ($N = 6$) with a distance from the step and between the ribs of ($L_3 = 1\ mm$). To denote these micro combustor configurations, **Table IV.1.2** provides a comprehensive nomenclature of these micro combustors, including geometric parameters such as N (number of ribs), and L_3 (the distance of the first rib from the step and the distance between the different ribs), along with their respective values.

Table IV.1.2. *Nomenclature and dimensions of micro combustor configurations for the effect of number.*

Geometric Parameters	Unit	$MCRD_1$	$MCRD_2$	$MCRD_3$	$MCRD_4$	$MCRD_5$	$MCRD_6$	$MCRD_7$
N	/	1	2	3	4	4	5	6
L_3	(mm)	6	6	4	3	2	1.5	1

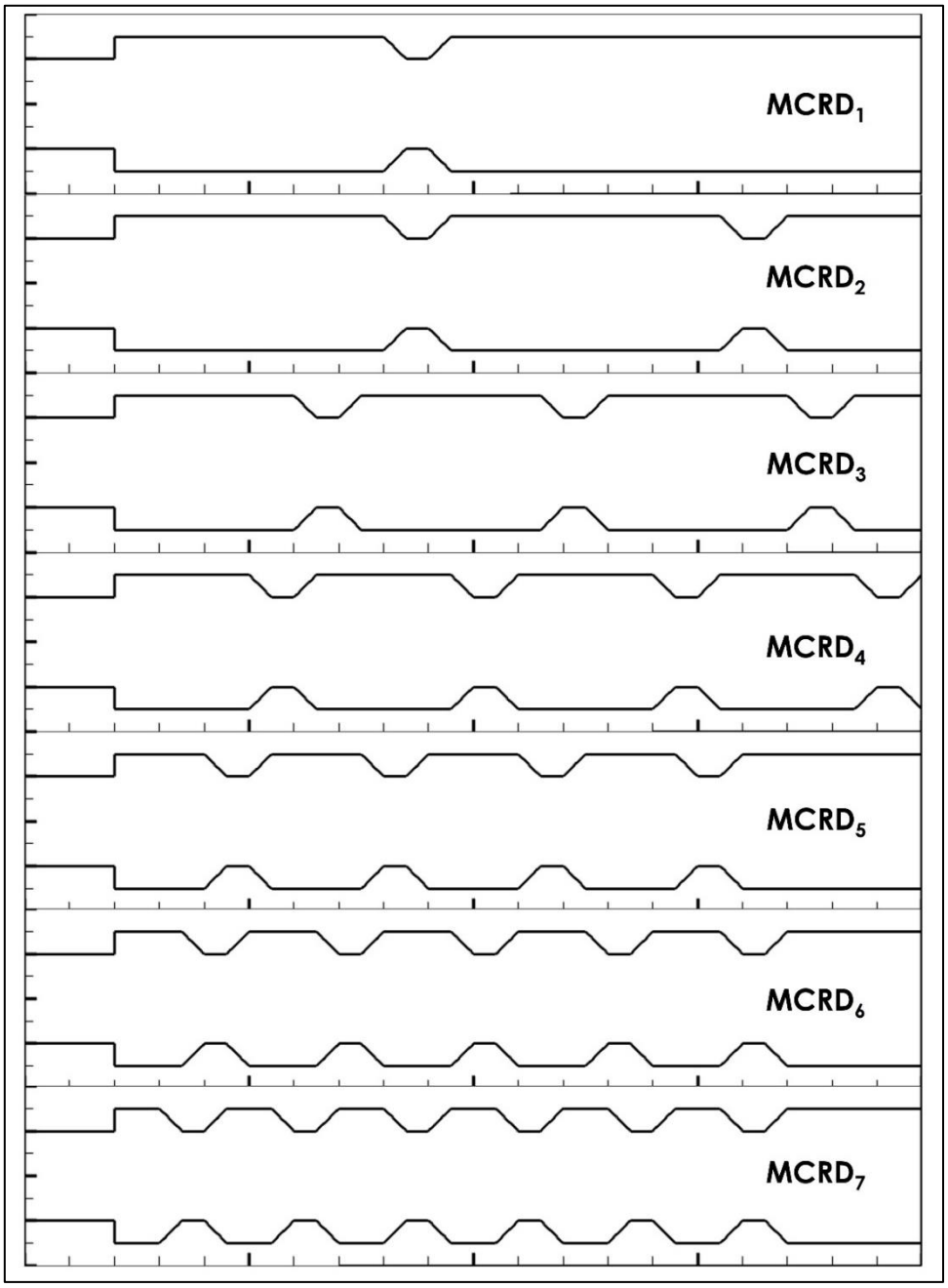

Figure IV.1.2. *Schematic diagram of micro combustor configurations for the effect of number (spacing).*

c. Effect of Height

To examine the influence of rib height within the micro combustor, we have explored various micro combustor configurations with equidistantly distributed trapezoidal ribs, each featuring different rib heights. In a systematic approach, we have varied the rib height within a range from 0.3 to 0.8, with 0.5 serving as the baseline reference. This exploration allows us to assess how changes in rib height impact critical aspects such as flow field dynamics, combustion stability, and thermal behavior. **Figure IV.1.3** illustrates the different micro combustors configurations with different ribs heights. Furthermore, **Table IV.1.3** presents a comprehensive nomenclature for the micro combustor configurations, including the height of the ribs in each configuration.

Table IV.1.3. *Nomenclature and dimensions of micro combustor configurations for the effect of height.*

Geometric Parameters	*Unit*	**RD-H1**	**RD-H2**	**RD-H3**	**RD-H4**	**RD-H5**	**RD-H6**
H	*(mm)*	0.3	0.4	0.5	0.6	0.7	0.8

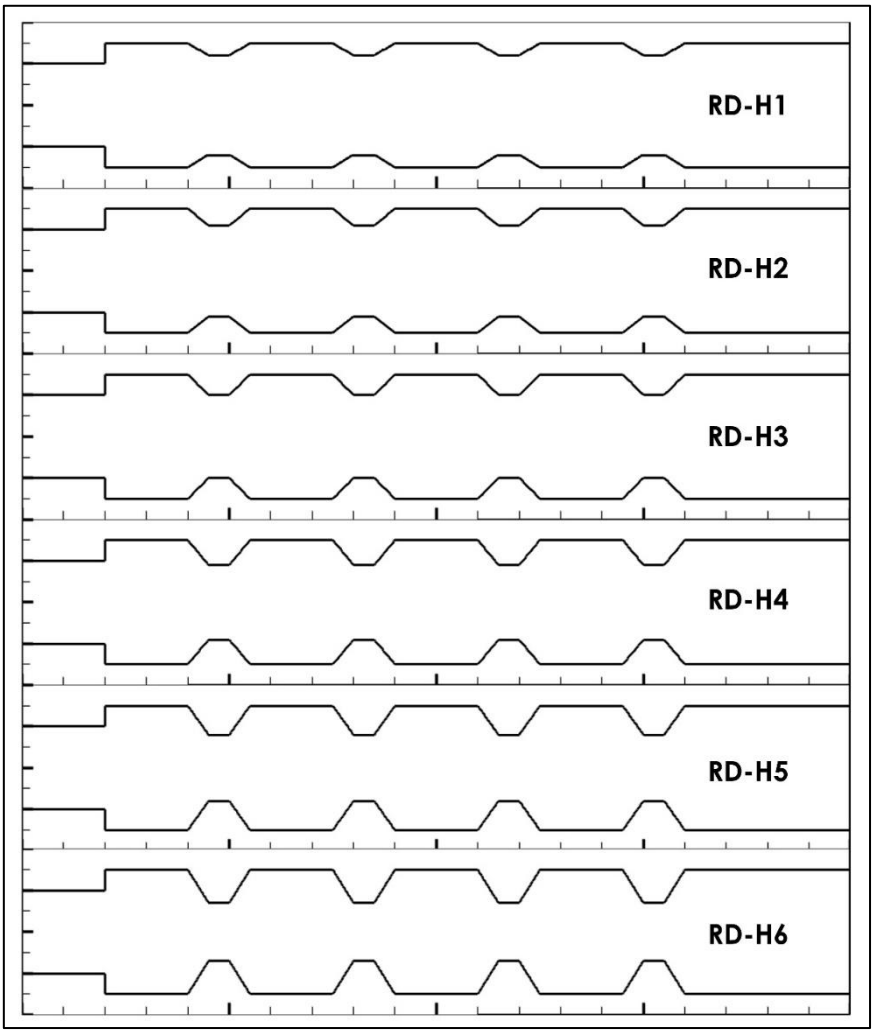

Figure IV.1.3. *Schematic diagram of micro combustor configurations for the effect of number (spacing).*

- **Computational Parameters**

Table IV.1.4. *Computational parameters for the effect of geometry*

Boundary	Parameters	Values
Inlet	Velocity Inlet (m/s)	6
	Temperature (K)	300
	Gauge pressure (Pa)	0
	Hydraulic diameter (mm)	2
	Turbulent intensity (%)	5
	Equivalence ratio ϕ	1
Outlet	Gauge pressure (Pa)	0
	Hydraulic diameter (mm)	3
	Turbulent intensity (%)	5
Wall	Material	316 Stainless-steel
	Thermal condition	Mixed
	Natural convective heat transfer coefficient (W/(m^2.K))	15
	External & internal emissivity	0.65

In the realm of numerical simulations for micro combustors, it is crucial to establish well-defined boundary conditions to ensure accurate and consistent results. In the study of geometry effect, we maintain stringent control over two key parameters during each simulation: the equivalence ratio (ϕ) and the inlet velocity (U_{in}). The equivalence ratio represents the ratio of the actual fuel-to-air mixture compared to the stoichiometric ratio required for complete combustion, and we consistently set it at 1.0. This value is fundamental in determining the fuel-air mixture's composition and its influence on combustion characteristics. Additionally, we maintain the inlet velocity at a constant 6 m/s. This parameter controls the rate at which fresh air and fuel enter the combustion chamber, directly affecting the flow dynamics and combustion behavior within the micro combustor. By maintaining these parameters at specified values throughout our simulations, we establish a consistent baseline for our study, allowing for meaningful comparisons and a thorough exploration of the effects of geometric configurations, including rib shape, number of ribs and ribs height on the micro combustor's performance. The details of these boundary conditions are summarized in **Table IV.1.4** for quick reference.

• Mesh Independency Study: 2D Approach

The accuracy and reliability of Computational Fluid Dynamics (CFD) results hinge not only on the validity of the computational models and methods employed but also on the presence of numerical errors. Among these errors, the most significant source is the numerical error arising from the discretization of the computational domain, often referred to as the grids. The quality and quantity of the elementary cells in the computational mesh significantly influence the results. Maintaining a delicate balance between the grid's size and structure and the computational load in terms of time and effort required to obtain a converged and accurate solution is critical. To address this, a grid independence study is conducted. In this study, six different grid systems, each with varying cell sizes (i.e., $\Delta x = \Delta y$), are generated using the ANSYS Workbench meshing software. It's worth noting that due to the geometrical shape of the micro-combustor, a structured grid composed of quadrilateral cells is chosen for this investigation. These grid systems are tested for both non-reacting and reacting flows, and the goal is to identify the mesh that ensures result independence, meaning that further refinement of the grid does not significantly affect the solution. This optimal mesh is the one that provides accurate results without excessive computational demands. For the sake of comparison and reference, a specific case with an inlet velocity of $U_{in} = 6\frac{m}{s}$ and an equivalence ratio of $\phi = 1.0$ is defined as a reference case. This case serves as a baseline to gauge the performance of different grid systems. By conducting this grid independence study, we can confidently select the most appropriate mesh for our simulations, ensuring both accuracy and efficiency in our CFD analyses.

a. Non-reacting Flow

In the context of non-reacting flows, the impact of grid refinement is assessed by using the outlet velocity as a comparative parameter. **Figure IV.1.4** provides a visual representation of how the outlet velocity varies with the number of elements in the grid. This analysis allows us to understand how the grid affects the flow results and helps identify trends and patterns in the data. To further ensure the mesh convergence and validate our findings, we apply Richardson extrapolation theory. This theory provides a systematic approach to determine if the refinement of the mesh leads to consistent and reliable results. In our case, we verify that the refinement ratio, as defined by references [62], [63], is greater than 1.3. **Table IV.1.5** presents the refinement ratios for the different generated meshes. These ratios serve as a quantitative measure of how the solution changes with grid refinement, allowing us to confirm that the mesh convergence is achieved and that the results become increasingly consistent as the grid is refined. This rigorous analysis ensures the reliability of our numerical simulations for non-reacting flows.

Table IV.1.5. *Non-reacting flow grid influence study: 2D Approach*

N	Mesh Size (mm)	Number of Elements	Refinement ratio	Outlet Velocity
1	0.04	51 000		3.982
2	0.03	90 180	1.768	3.994
3	0.025	128 000	1.419	3.999
4	0.02	200 000	1.563	3.999
5	0.015	352 980	1.765	4.001
6	0.0125	512 000	1.451	3.999

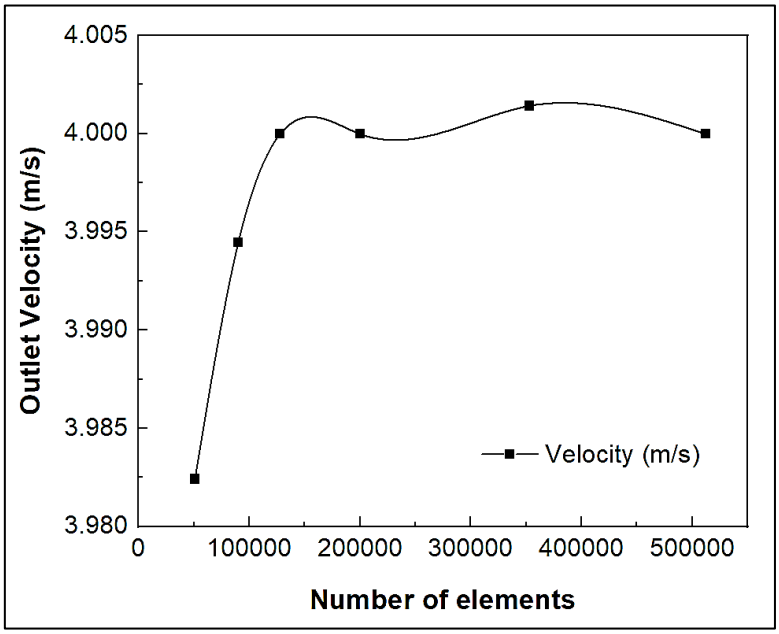

Figure IV.1.4. *Non-reacting flow grid influence study*

b. Reacting Flow

In the case of reacting flows, we conduct a grid independence study by examining the centerline temperature profiles of the micro-combustor at various mesh densities. **Figure IV.1.5** visually represents these profiles, providing insight into how the grid density impacts the temperature distribution within the micro-combustor. **Table IV.1.6**, on the other hand, provides a more detailed summary of the results of this grid independence study. It likely includes information on different mesh densities and their corresponding effects on the centerline temperature profiles. This comprehensive analysis allows us to determine the mesh density at which the results become independent of further grid refinement, ensuring accuracy and reliability in our simulations of reacting flows.

Table IV.1.6. *Reacting flow grid influence study: 2D Approach*

N	Mesh Size (mm)	Exhausted gas temperature (K)	Mean outer wall temperature (K)	Outlet Mass fraction of hydrogen (%)
1	0.04	1996.48	1323.58	0.001235704
2	0.03	1952.73	1202.08	0.001450730
3	0.025	1922.44	1183.40	0.001514652
4	0.02	1957.13	1209.68	0.001502347
5	0.015	1979.27	1276.99	0.001396664
6	0.0125	1907.14	1148.52	0.001607663

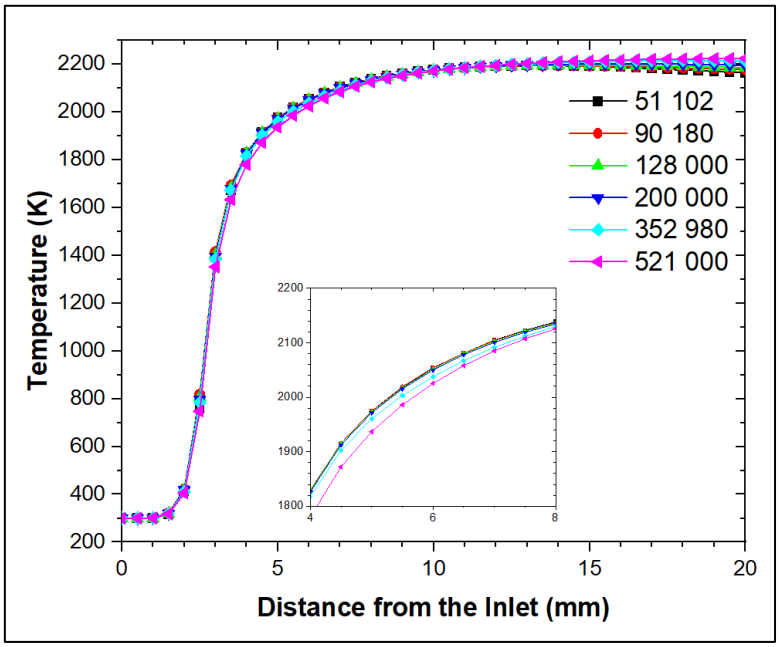

Figure IV.1.5. *Reacting flow grid influence study*

As presented in **Figure IV.1.4** & **Figure IV.1.5**, it can be observed that a medium mesh with 128,000 elements is sufficient to capture the velocity, temperature and species gradients between the fluid and solid zones.

- ## Results and Discussions: 2D Approach

Effect of Shape

a. Flow-field characteristics

To comprehensively investigate the effect of introducing ribs and their specific shapes on flow characteristics, we have employed a comprehensive approach in characterizing the challenges associated with micro combustion. As part of this analysis, we've delved into various aspects, including flow dynamics, flow stability, and flow efficiency. To achieve a comprehensive understanding of these aspects, we've utilized a set of metric parameters, allowing us to quantify and assess the performance of the micro combustion system accurately. This comprehensive approach enables us to gain valuable insights into the behavior and efficiency of the flow in response to rib introduction and shape variations.

- ***Flow Dynamics***

Flow dynamics encompass parameters involving velocity and pressure distribution and the turbulence level within the micro combustor. These parameters serve as critical indicators of the flow behavior. Hence, streamlines, velocity, static pressure and turbulent kinetic energy, turbulent intensity, and vorticity contours are used in order to uncover the flow-field characteristics. On the other hand, to clarify the influence of combustion, a set of numerical simulations under non-reacting and reacting flows were performed.

- ***Stream Field***

In general, the introduction of steps and ribs in a flow configuration leads to the roll-up of the shear layer, especially at the backward corner located behind these steps and ribs. In the context of our current study, where the distance between the ribs can be categorized as open cavities, a distinct flow pattern emerges. Here, the shear layer separates from the leading edge of the steps and ribs and subsequently reattaches downstream on the micro combustors inner surface wall. This flow behavior has significant implications,

notably resulting in the anticipation of large pressure losses and elevated turbulence levels within the system. Understanding these flow behaviors is crucial for a comprehensive analysis of the flow dynamics and the overall performance of the configurations under consideration. **Figure IV.1.6** *(a)* provides a valuable visual insight into the velocity contours of the hydrogen-air mixture flow within various micro combustor configurations, denoted MCSD, RD-Rec, RD-Cur, RD-Tri, and RD-Trz, all under non-reacting conditions. Furthermore, **Figure IV.1.6** *(b)* provides further zoomed-in view into the flow behavior within the different micro combustor configurations. This zoomed-in view focuses on the step and rib regions, allowing the analyze of velocity streamlines' behavior in specific areas. Understanding these flow behaviors is pivotal in comprehending the complex interactions within these micro combustors. First, we can observe areas of acceleration of flow velocity in the upstream channel of different micro combustor configurations. In the vicinity of the backward-facing step, we typically encounter deceleration of velocity, as the flow encounters a sudden expansion, resulting in a decreased velocity gradient. This deceleration zone is commonly associated with formation of recirculation zone behind the backward-facing step. Conversely, areas of acceleration are observed on the downstream channel of the micro combustors, especially for configurations incorporating ribs. When the flow passes over the ribs, it must navigate the geometric obstacles, causing an increase in velocity. The vena contracta occurs as a consequence of fluid acceleration due to the constriction caused by the rib. The fluid contracts at this point, resulting in an area of reduced cross-section and an associated increase in velocity magnitude.

Non-reacting flow

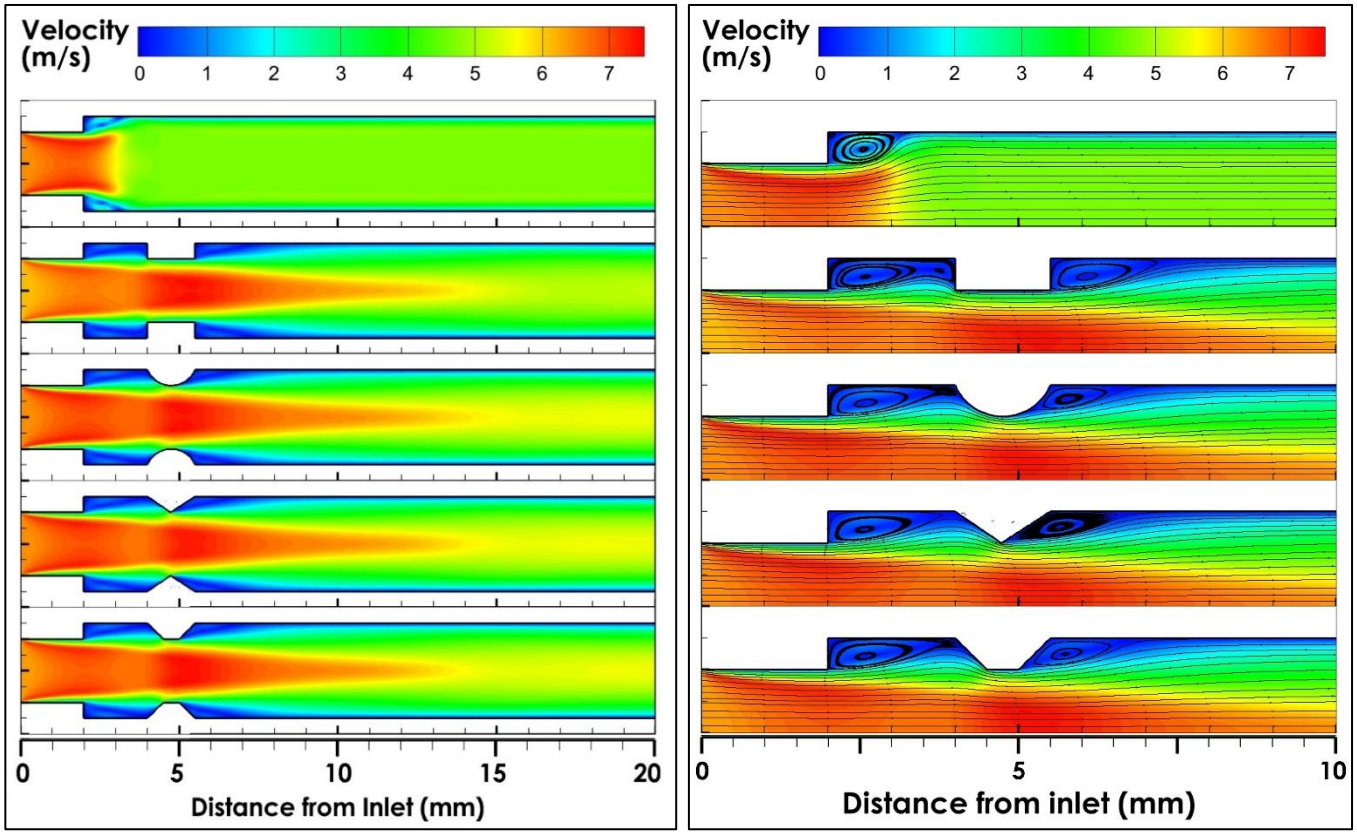

(a) *(b)*

Figure IV.1.6. *Non-reacting flow-field of different micro combustor configurations (a) velocity contour and (b) streamlines: effect of shape.*

The shape of ribs has a profound impact on the velocity distribution, as indicated by the velocity contours of different micro combustor configurations. The rectangular rib sharp corners create areas of recirculation, where the flow separates from the rib surface resulting in a low-velocity regions on the backward corner of the rib. While the rectangular rib design enhance mixing to some extent, it also introduces flow disturbances due to the abrupt geometry. In contrast, the curved rib, with its semicircular

shape, promotes smoother flow around the rib. The absence of sharp corners minimizes flow separation, reducing low-velocity regions. The curved rib's effect on velocity distribution is more favorable, as the flow adheres more closely to the rib's surface which facilitates better flow reattachment and reduced recirculation zone size. Meanwhile, the introduction of triangular shaped rib creates a unique flow pattern. The sharp tip encourages early separation, leading to localized low-velocity regions near the base. The trapezoidal rib, characterized by angled edges with a 45°-degree slope, exhibits an intermediate behavior between the other rib shapes. It creates vortices and recirculation zones, similar to the rectangular rib but with less intensity. However, the trapezoidal rib's design promotes better curvature and more effective flow redirection. In the wake of the rib's backward corner, a recirculation zone is present in all cases. The trapezoidal rib's elongated recirculation zone is advantageous as it maximizes the region of flow separation, effectively increasing residence time for enhanced mixing.

Reacting flow

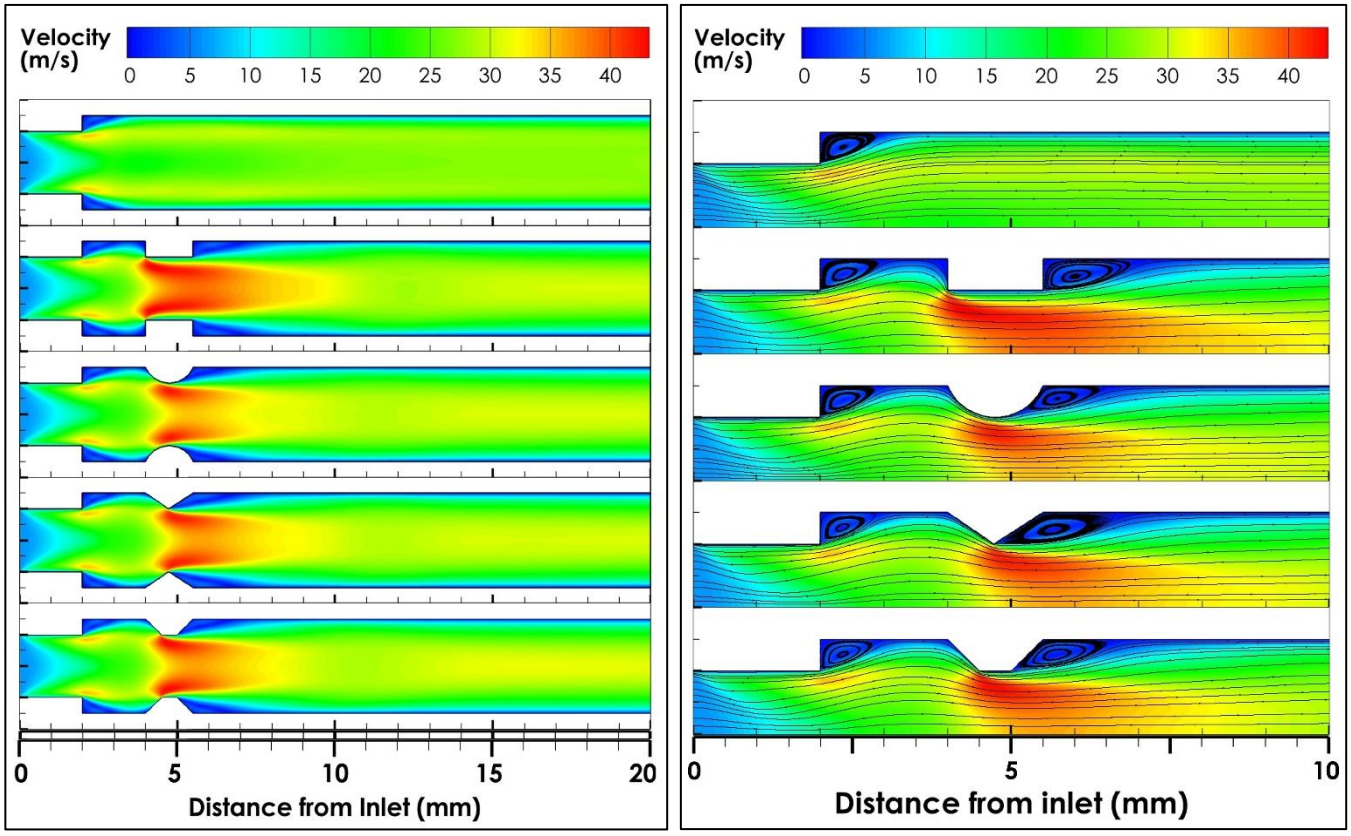

(a) *(b)*

Figure IV.1.7. *Reacting flow-field of different micro combustor configurations (a) velocity contour and (b) streamlines: effect of shape.*

The transition from non-reacting to reacting conditions reveals crucial aspects of combustion efficiency and stability. **Figure IV.1.7** *(a),* provides a visual insight into the velocity contours of the hydrogen-air mixture flow within various micro combustor configurations, namely MCSD, RD-Rec, RD-Cur, RD-Tri, and RD-Trz, all under reacting conditions. In the different configurations, the reacting flow patterns behind the step remain similar to the non-reacting conditions. A recirculation zone forms, characteristic of the sudden expansion at the step, and is a common feature in both non-reacting and reacting scenarios. Moreover, smooth acceleration of flow observed in the second channel. Conversely to non-reacting flows, the flame shape plays a pivotal role in influencing the flow field dynamics within the upstream channel. Specifically, the flame, with its elongated shape, exerts a pushing effect on the flow inside the downstream channel, altering the velocity contours and influencing the distribution of chemical species. Notably, the flame extends its influence, pushing the recirculation zones behind the backward-facing step further toward the corner of the step. This effect is particularly pronounced in RD-Rec, RD-Cur, RD-Tri,

and RD-Trz configurations, where the flame pushes product gases further toward the corner of the step and into the cavity between the step and the rib. Moreover, the ignition of chemical reactions plays a crucial role in determining the size of the vena contracta for different micro combustor configurations (RD-Rec, RD-Cur, RD-Tri, RD-Trz), with the reaction-induced changes in fluid properties affecting the contraction and acceleration of the flow over the ribs. As shown in **Figure IV.1.7** *(b)*, the chemical reactions' ignition has a profound effect on the reattachment of the shear layer on the inner surface of micro combustors. The initiation of combustion processes alters the temperature and pressure gradients, influencing the reattachment points and the overall recirculation zone length.

Considering the velocity magnitude and distribution, chemical reactions induce a quantifiable increase in flow velocity due to the release of thermal energy during combustion. This increase in velocity is particularly notable in region over the tip of the different ribs influenced by combustion, emphasizing the intimate coupling between chemical reactions and fluid dynamics in micro-scale combustion. **Figure IV.1.8** complements these observations by providing additional insights into the flow behavior within the different micro combustor configurations, offering a complete understanding of the complex interplay between chemical reactions and fluid dynamics in the studied systems. The velocity magnitude distribution along the center line of various micro combustor configurations reveals notable distinctions. RD-Rec stands out by presenting the highest velocity magnitude, a characteristic observed consistently under both non-reacting and reacting flows. The ignition of chemical reactions further amplifies this trend, showcasing a remarkable increase in maximum velocity magnitude for RD-Rec, escalating from 7.3 to 38.6 m/s. This trend is also evident in other configurations, with RD-Cur experiencing an increase from 6.9 to 34.75 m/s, RD-Tri from 6.84 to 36.2 m/s, and RD-Trz from 7.04 to 36.19 m/s. Importantly, the introduction of ribs induces a significant enhancement in the velocity distribution along the downstream channel compared to the velocity magnitude distribution under non-reacting flows.

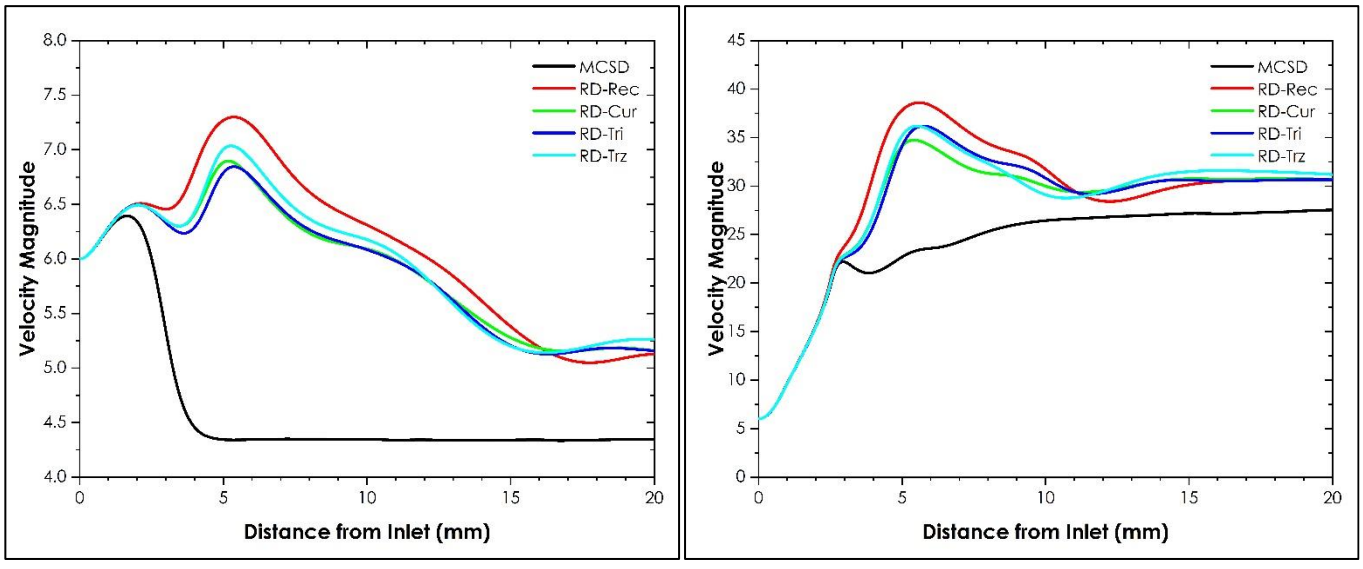

(a) *(b)*

Figure IV.1.8. *Velocity distribution along the centerline of different micro combustor configurations under (a) non-reacting and (b) reacting conditions: Effect of shape.*

To highlight the effect of chemical reactions ignition on the recirculation zones size, **Table IV.1.7** present the length of recirculation zones for the different micro combustor configurations under non-reacting and reacting flows. The presence of recirculation zones is evidenced by the negative values of the longitudinal speed. We determined the average length of the recirculation zones in the same previous way. However, the recirculation zones relative to reacting flows are shorter than those obtained under non-reacting flows conditions, which is in agreement with the visual insight shown by the velocity contours and streamlines. Indeed, for the reacting flows, a reduction in length of more than 50% for the recirculation zone length

behind backward-facing step and 10% for the recirculation zone behind the rectangular, curved, and trapezoidal ribs is observed compared to that obtained for the non-reacting flow. Conversely, for the reacting flows, the length of recirculation zone behind the triangular rib increases compared to that obtained for the non-reacting flow. Furthermore, the relationship between the velocity magnitude, rib shape, and the average length of the recirculation zones is found to be proportional.

Table IV.1.7. *Recirculation zones length of different micro combustor configurations under non reacting and reacting conditions.*

Geometric Configuration	MCSD	RD-Rec		RD-Cur		RD-Tri		RD-Trz	
		Step	Rib	Step	Rib	Step	Rib	Step	Rib
Non-reacting	1.2	2	1.8	2	1.5	2	1.9	2	1.84
Reacting	0.88	1	1.55	0.93	1.28	0.88	1.98	0.91	1.64
Effect of Reactions	- 0.32	- 1	- 0.25	- 1.07	- 0.22	- 1.12	0.08	- 1.09	- 0.2

in (mm)

- ***Pressure Fields***

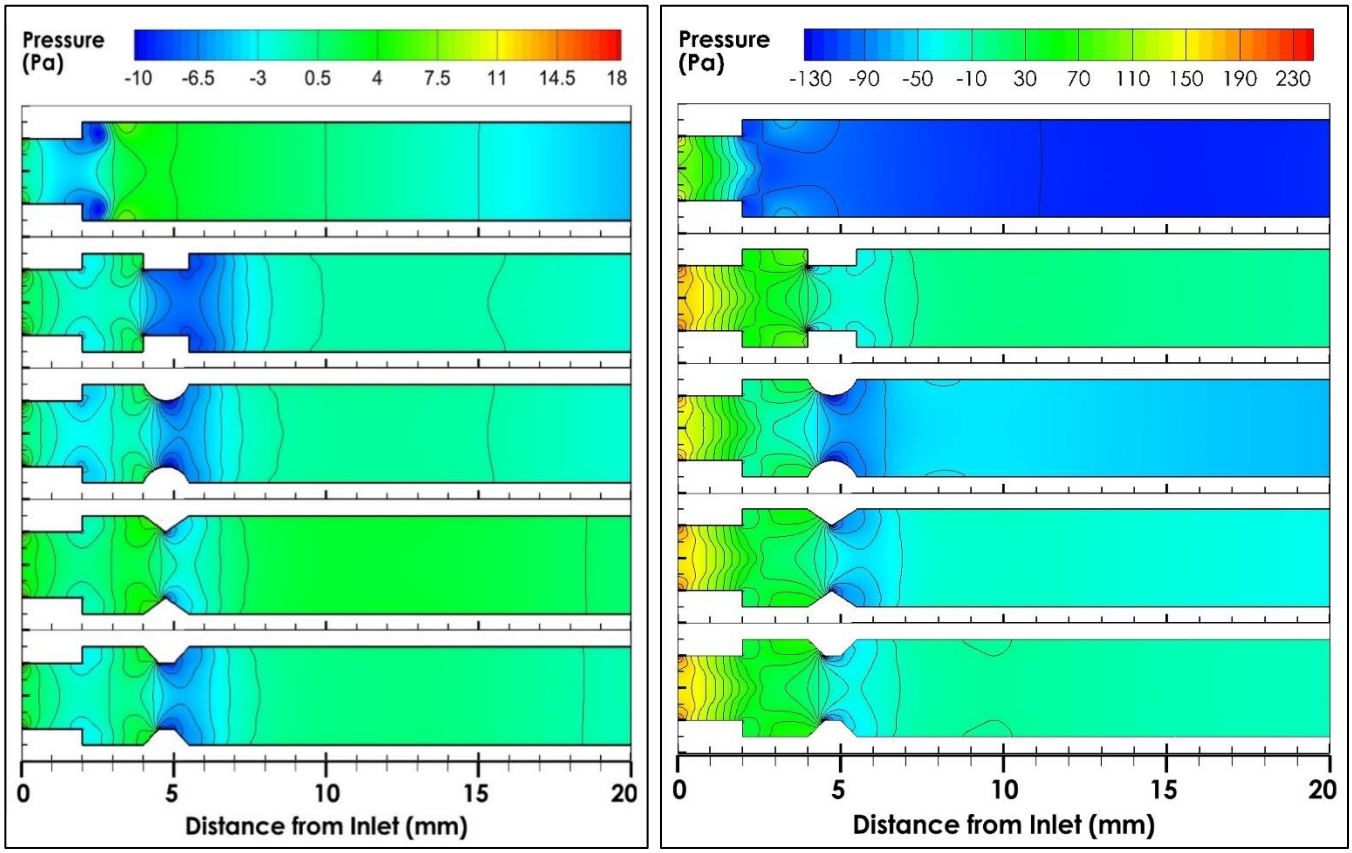

(a) *(b)*

Figure IV.1.9. *(a) Non-reacting flows, and (b) reacting flow static pressure contours for the different micro-combustor configurations: Effect of shape.*

Figure IV.1.9 provides an insightful exploration of pressure contours in both non-reacting and reacting flow conditions within various micro combustor configurations, offering a comprehensive understanding of pressure behavior and its implications for combustion stability and performance. In non-reacting conditions, we observe distinct pressure patterns in each configuration. For the MCSD configuration, the pressure contours reveal variations that correspond to the sudden expansion at the backward-facing step. A prominent pressure drop is observed in the recirculation zone behind the step, a typical feature of such geometric configurations. In the absence of ribs, the flow in the second channel exhibits relatively uniform pressure distribution, with minimal disruption. The RD-Rec configuration, characterized by sharp rectangular ribs, displays significant pressure changes. At the forward corner of the rib, we notice

areas of high pressure due to flow separation caused by the sharp edges. This localized increase in pressure can disrupt combustion stability and may lead to efficiency losses. At the rib tip, pressure variations indicate recirculation and separation, further highlighting the challenges posed by the rectangular rib's abrupt geometry. Behind the rib backward corner, a pronounced pressure drop signifies a long recirculation zone, indicating increased resistance to flow, which is unfavorable for combustion efficiency. Conversely, the RD-Cur configuration, featuring curved ribs, demonstrates a more favorable pressure distribution. The absence of sharp corners minimizes flow separation, resulting in reduced pressure fluctuations at the rib's forward corner. At the rib tip, pressure variations are less intense, indicating smoother flow attachment and less turbulent behavior. Behind the rib backward corner, the pressure drop is reduced, signifying better flow attachment and a more favorable pressure profile. These observations suggest that the curved rib promotes smoother pressure contours, which can contribute to enhanced combustion stability. The RD-Tri configuration, with its triangular rib, introduces unique pressure patterns. At the front forward corner of the rib, pressure variations indicate high-pressure areas due to early flow separation near the sharp tip. Behind the rib, pressure levels suggest flow reattachment, creating localized high-pressure regions. However, this configuration also exhibits notable pressure drops, signifying increased resistance to flow, which may impact combustion efficiency. The RD-Trz configuration, featuring trapezoidal ribs, displays pressure contours that strike a balance between the other rib shapes. At the rib's forward corner, moderate pressure variations suggest a compromise between flow attachment and separation, reducing pressure fluctuations. At the rib tip, pressure variations are less pronounced, indicating smoother flow attachment and redirection. Behind the rib backward corner, the pressure drop is moderate, suggesting efficient flow separation with less intensity compared to the rectangular and triangular ribs. These pressure contour observations imply that the trapezoidal rib design offers a favorable combination of combustion stability and efficiency.

Transitioning to reacting conditions in **Figure IV.1.9**, we can discern additional insights into pressure behavior. The MCSD configuration maintains pressure patterns similar to non-reacting conditions, with pressure fluctuations resulting from the sudden expansion at the step. These observations provide valuable information for combustion modeling and stability assessment. In the RD-Rec configuration under reacting conditions, the sharp corners of the rectangular rib continue to induce high-pressure zones at the forward corner, as seen in non-reacting conditions. At the rib tip, pressure variations indicate recirculation and separation, leading to increased pressure fluctuations. Behind the rib backward corner, the pronounced pressure drop persists, signifying the challenges associated with the rectangular rib's abrupt geometry in reacting flows. The RD-Cur configuration maintains its advantageous pressure distribution, with less pressure fluctuation at the rib's forward corner compared to the rectangular rib. At the rib tip, pressure variations remain less intense, suggesting smoother flow attachment and lower turbulence. Behind the rib backward corner, the pressure drop is reduced, indicating a more favorable pressure profile. These pressure contour observations underscore the potential benefits of the curved rib for combustion stability in reacting flows. The RD-Tri configuration exhibits pressure variations similar to non-reacting conditions, with high-pressure areas at the rib's forward corner and pressure drops behind the rib. These patterns are consistent with the challenges associated with the triangular rib's geometry in both non-reacting and reacting flows. Finally, the RD-Trz configuration showcases its balanced pressure behavior under reacting conditions. At the rib's forward corner, moderate pressure variations suggest a compromise between flow attachment and separation. At the rib tip, pressure variations are less pronounced, indicating smoother flow attachment and redirection. Behind the rib backward corner, the pressure drop is moderate, signifying efficient flow separation with less intensity compared to the rectangular and triangular ribs. These pressure contour observations reaffirm the advantages of the trapezoidal rib for promoting combustion stability and efficiency in reacting flows.

Analyzing the pressure distribution along the centerline of various micro combustor configurations (MCSD, RD-Rec, RD-Cur, RD-Tri, RD-Trz), as shown in **Figure IV.1.10**, provides valuable insights into

the flow characteristics and combustion behavior under both non-reacting and reacting conditions. In the absence of ribs (MCSD), under non-reacting conditions, static pressure gradually decreases along the length of the upstream channel, peaks behind the backward-facing step, to approximately 6 (Pa), and gradually descends to the outlet boundary, to outlet boundary condition of 0 (Pa). In reacting flow, pressure drops from 110 (Pa) upstream to a minimum level around 7.5 (Pa) after the step. rises to 11 (Pa), and then decreases downstream to the outlet boundary (0 Pa). The presence of ribs introduces additional complexity to the pressure distribution. Under both non-reacting and reacting conditions, pressure variations occur around the ribs, affecting the flow patterns and causing localized pressure changes. However, under non-reacting flow, pressure decreases within upstream channel, reaching negative values behind the step (around -1 Pa). The pressure distribution within RD-Rec configuration replicate MCSD, while RD-Cur, RD-Tri, and RD-Trz configurations show further pressure drops behind the step, followed by pressure increment in the cavity between the step and ribs. Behind the ribs, RD-Rec exhibits -4.5 (Pa), RD-Trz -3.5 (Pa), RD-Cur -3 (Pa), and RD-Tri -2.5 (Pa), then rises to around 10 (Pa), declining to 0 Pa at the outlet. Under reacting conditions, further amplified pressure level is recorded for different micro combustor configurations incorporating ribs. Combustion-induced pressure changes are prominent near the ribs and downstream, reflecting the interaction between combustion and geometric features. MCSD display lower pressure levels (between -10 to -20 Pa), with RD-Rec at -20 (Pa) and RD-Trz between RD-Rec and RD-Cur/RD-Tri. This observed behavior can be attributed to the interaction between the combustion process, fluid dynamics, and the introduced geometric features. The presence of ribs induces variations in flow patterns, creating regions of pressure deficit and excess, ultimately influencing the overall pressure distribution along the centerline. The specific shapes of the ribs contribute to unique pressure profiles, highlighting the significance of geometric configuration in shaping the pressure characteristics of micro combustors under different operating conditions.

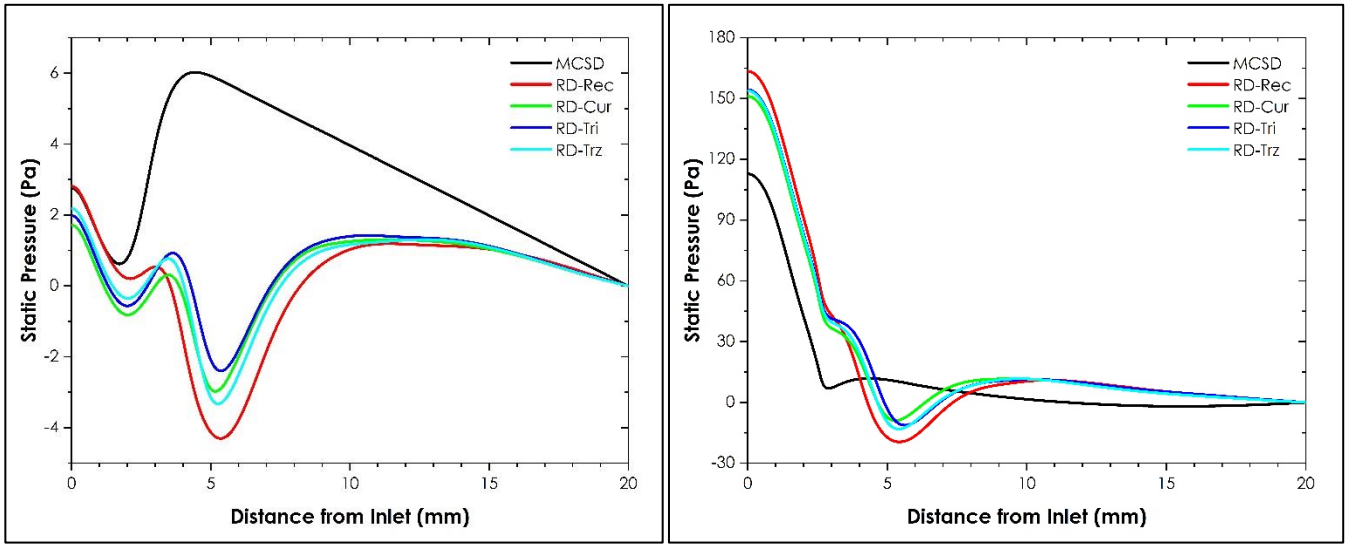

(a) *(b)*

Figure IV.1.10. *Pressure distribution along the centerline under of different micro combustor configurations (a) non-reacting and (b) reacting conditions: Effect of shape.*

- ***Turbulence Level***

Turbulence level of chemical reactions flow is known to play an important role in combustion performance and stability. Since the flow and chemical reactions are coupled processes, the chaotic dynamics of turbulent flow will cause the enhancement of mixing between the unburnt and burnt reactants. Thus, the turbulent environment increases the burning velocity of the cold reactants which then accelerates the reactions heat releasing. This reveals the mutual effect of turbulence present on both chemical and thermal processes of combustion. However, the introducing of ribs leads to direct increment of turbulence level. Hence, the turbulence level is characterized using: turbulent kinetic energy (k),

turbulence intensity (*I*) and turbulent vorticity. Turbulent Kinetic Energy (TKE) quantifies the overall energy associated with turbulent motion, Turbulent Intensity (TI) measures the relative strength of turbulence in relation to the mean flow, and Turbulent Vorticity describes the rotational aspects of turbulence within a fluid flow. Together, these parameters contribute to a comprehensive understanding of turbulent fluid dynamics. Therefore, to isolate the effect of the combustion and to elicit the effect of geometry, a comparative study of the level of turbulence under non-reaction and reacting conditions between the simple (MCSD) and the various micro combustor configurations, will take place.

Turbulence Kinetic energy

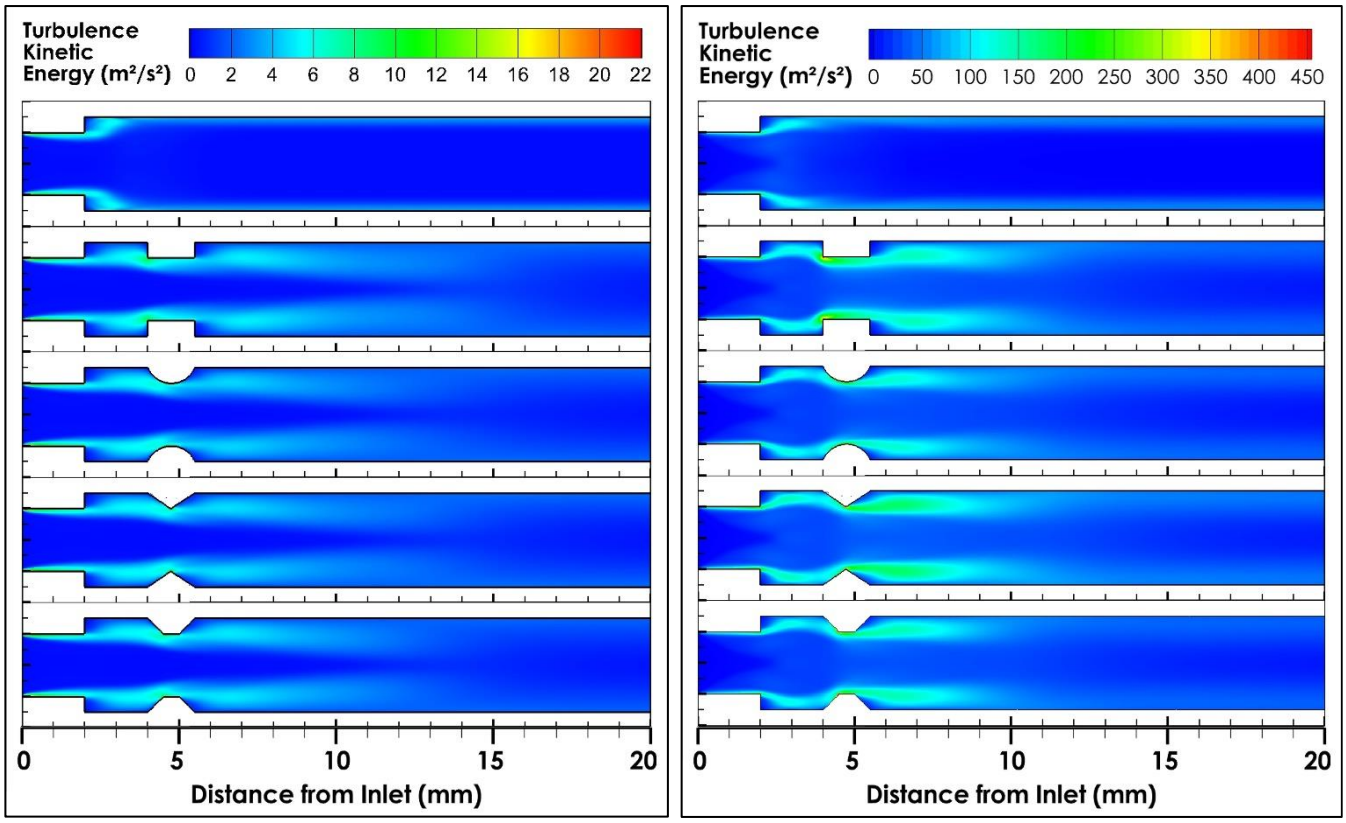

(a) *(b)*

Figure IV.1.11. *(a) Non-reacting flows, and (b) reacting flow Turbulent kinetic energy (TKE) contours for the different micro-combustor configurations: Effect of shape.*

Turbulent Kinetic Energy refers to the energy associated with turbulent motion within a fluid flow. In turbulent flows, fluid particles exhibit random and chaotic motion at various scales. TKE quantifies the kinetic energy associated with these turbulent fluctuations. Mathematically, TKE is calculated as the sum of the kinetic energy contributions across different turbulent velocity components. **Figure IV.1.11** presents turbulent kinetic energy (TKE) contours for both *(a)* non-reacting and *(b)* reacting flow conditions within the various micro combustor configurations, offering crucial insights into turbulence levels and their implications for combustion processes. In non-reacting conditions, TKE contours reveal distinct turbulence patterns in each configuration. For the MCSD configuration, we observe elevated TKE levels in the recirculation zone behind the backward-facing step. This region is characterized by increased turbulence resulting from flow separation and recirculation. In the downstream channel without ribs, TKE levels are relatively lower, reflecting smoother and more uniform flow behavior with minimal disruption. The RD-Rec configuration, with its sharp rectangular rib shape, exhibits intensified TKE levels at the forward corner of the rib. The sharp corners induce turbulent flow separation, leading to elevated TKE in this region. At the rib tip, TKE levels are also elevated, signifying turbulence associated with flow separation and recirculation. Behind the rectangular rib backward corner, TKE levels are notably high, indicating intense turbulence and energy dissipation in the recirculation zone. These observations suggest

that the rectangular rib design introduces significant turbulence levels, which may significantly impact combustion stability and efficiency. In contrast, the RD-Cur configuration, featuring curved ribs, displays more favorable TKE contours. TKE levels at the rib's forward corner are lower compared to the rectangular rib, indicating reduced turbulence resulting from the absence of sharp corners. At the curved rib tip, TKE levels are also lower, producing smoother flow attachment and reduced turbulence associated with flow separation. Behind the curved rib backward corner, TKE levels are reduced, signifying more favorable turbulence levels in this region. These TKE contour observations highlight the potential benefits of the curved rib in reducing turbulence and promoting combustion stability. The RD-Tri configuration introduces unique TKE patterns. At the forward corner of the triangular rib, TKE levels are elevated due to turbulent flow separation near the sharp tip. Behind the rib, TKE levels indicate turbulence associated with flow reattachment and recirculation. However, this configuration also exhibits elevated TKE levels in the recirculation zone, reflecting the challenges posed by the triangular rib's geometry. These elevated TKE levels may impact combustion efficiency. The RD-Trz configuration, with its trapezoidal ribs, showcases a balanced TKE distribution. TKE levels at the rib's forward corner indicate a compromise between flow attachment and separation, resulting in moderate turbulence levels. At the rib tip, TKE levels are also moderate, signifying reduced turbulence associated with flow separation. Behind the rib backward corner, TKE levels remain moderate, indicating more favorable turbulence levels compared to the rectangular and triangular ribs. These TKE contour observations reaffirm the advantages of the trapezoidal rib in maintaining balanced turbulence levels and promoting combustion stability.

Transitioning to reacting conditions in **Figure IV.1.11** *(b)*, we can distinguish additional insights into TKE behavior. The MCSD configuration maintains TKE patterns similar to non-reacting conditions, with elevated turbulence levels in the recirculation zone behind the step. In the RD-Rec configuration, the sharp corners of the rectangular rib continue to induce elevated TKE levels at the rib's forward corner, as seen in non-reacting conditions. At the rib tip, TKE levels are also elevated, signifying turbulence associated with flow separation and recirculation. Behind the rib backward corner, TKE levels remain notably high, reflecting the challenges posed by the rectangular rib's geometry in reacting flows. The RD-Cur configuration maintains its advantageous TKE distribution, with lower turbulence levels at the rib's forward corner compared to the rectangular rib. At the rib tip, TKE levels remain lower, suggesting reduced turbulence associated with flow separation. Behind the rib backward corner, TKE levels are reduced, indicating more favorable turbulence levels. These TKE contour observations highlight the potential benefits of the curved rib for combustion stability in reacting flows. The RD-Tri configuration exhibits TKE patterns similar to non-reacting conditions, with elevated turbulence levels at the rib's forward corner and behind the rib. These patterns align with the challenges associated with the triangular rib's geometry in both non-reacting and reacting flows. Finally, the RD-Trz configuration showcases balanced TKE behavior under reacting conditions. TKE levels at the rib's forward corner indicate a compromise between flow attachment and separation, resulting in moderate turbulence levels. At the rib tip, TKE levels remain moderate, signifying reduced turbulence associated with flow separation. Behind the rib backward corner, TKE levels remain moderate, indicating more favorable turbulence levels compared to the rectangular and triangular ribs. These TKE contour observations reaffirm the advantages of the trapezoidal rib in promoting combustion stability and efficiency in reacting flows. In summary, the figures showcasing Turbulent Kinetic Energy (TKE) provide critical insights into the interplay between chemical reactions and fluid dynamics within the micro combustor configurations. The TKE magnitude experiences a substantial surge upon the ignition of combustion, escalating by a factor of 20. This remarkable increase highlights the profound impact of combustion initiation on the energetic characteristics of the micro combustors.

Turbulence Intensity

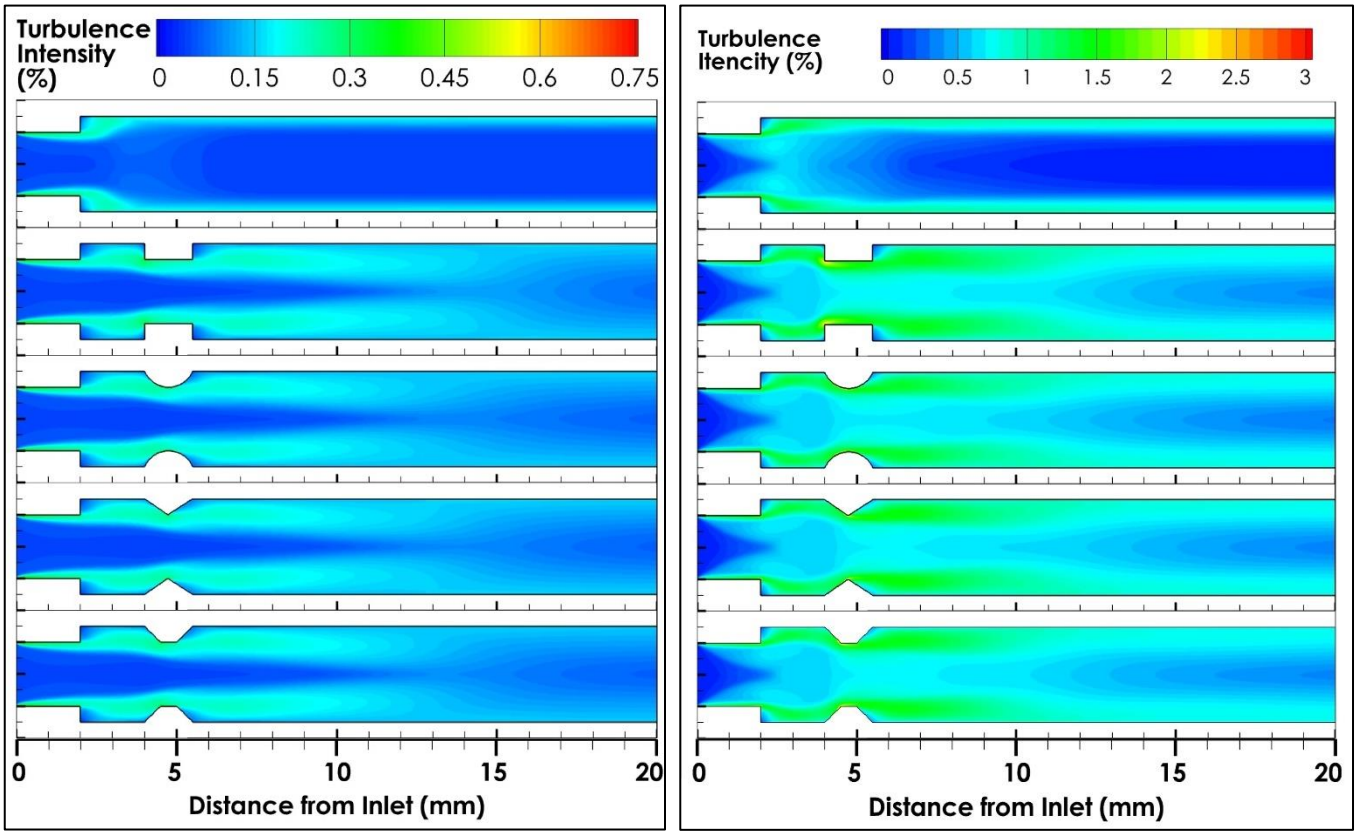

(a) *(b)*

Figure IV.1.12. *(a) Non-reacting flows, and (b) reacting flow Turbulence Intensity contours for the different micro-combustor configurations: Effect of shape.*

Turbulence Intensity is a dimensionless parameter that characterizes the strength and magnitude of turbulence within a flow. It is expressed as the ratio of the root-mean-square velocity of turbulent fluctuations to the mean velocity of the flow. Turbulence Intensity is represented as a percentage. Higher turbulence intensity values indicate a greater degree of turbulence in the flow. It is a valuable parameter for assessing the dynamic nature of turbulent flows. **Figure IV.1.12** presents turbulence intensity contours for both non-reacting and reacting flow conditions within various micro combustor configurations, shedding light on the turbulence levels and their implications for combustion processes. Under non-reacting conditions, the turbulence intensity contours offer distinct insights into the turbulence patterns of each configuration. For the MCSD configuration, elevated turbulence intensity levels are evident in the recirculation zone behind the backward-facing step. This region experiences increased turbulence due to flow separation and recirculation, aligning with the typical behavior of sudden expansions. In the downstream channel of MCSD, turbulence intensity levels are relatively lower, indicating smoother and more uniform flow behavior with minimal disruption. On the other hand, the RD-Rec configuration, with its sharp rectangular edges, exhibits intensified turbulence intensity levels at the forward corner of the rib. The presence of sharp corners induces turbulent flow separation, leading to elevated turbulence intensity in this region. At the rib tip, turbulence intensity levels are also elevated, signifying turbulence associated with flow separation and recirculation. Behind the rib backward corner, notably high turbulence intensity levels indicate intense turbulence and energy dissipation in the recirculation zone. These observations emphasize that the rectangular rib design introduces significant turbulence levels, which may impact combustion stability and efficiency. Conversely, the RD-Cur configuration, featuring curved ribs, presents more favorable turbulence intensity contours. Turbulence intensity levels at the rib's forward corner are lower compared to the rectangular rib, indicating reduced turbulence resulting from the absence of sharp corners. At the rib tip, turbulence intensity levels are also lower, suggesting smoother flow attachment and reduced turbulence associated with flow separation. Behind the rib backward corner, reduced turbulence

intensity levels indicate more favorable turbulence conditions in this region. These turbulence intensity contour observations highlight the potential benefits of the curved rib in reducing turbulence and promoting combustion stability. The RD-Tri configuration introduces unique turbulence intensity patterns. At the forward corner of the triangular rib, turbulence intensity levels are elevated due to turbulent flow separation near the sharp tip. Behind the rib, turbulence intensity levels indicate turbulence associated with flow reattachment and recirculation. However, this configuration also exhibits elevated turbulence intensity levels in the recirculation zone, reflecting the challenges posed by the triangular rib's geometry. These elevated turbulence intensity levels may impact combustion efficiency. The RD-Trz configuration, with its trapezoidal ribs, showcases a balanced turbulence intensity distribution. Turbulence intensity levels at the rib's forward corner indicate a compromise between flow attachment and separation, resulting in moderate turbulence levels. At the rib tip, turbulence intensity levels are also moderate, signifying reduced turbulence associated with flow separation. Behind the rib backward corner, turbulence intensity levels remain moderate, indicating more favorable turbulence conditions compared to the rectangular and triangular ribs. These turbulence intensity contour observations reaffirm the advantages of the trapezoidal rib in maintaining balanced turbulence levels and promoting combustion stability.

Transitioning to reacting conditions in **Figure IV.1.12**, we can discern additional insights into turbulence intensity behavior. The MCSD configuration maintains turbulence intensity patterns similar to non-reacting conditions, with elevated turbulence levels in the recirculation zone behind the step. These observations provide critical information for combustion modeling and stability assessment. In the RD-Rec configuration under reacting conditions, the sharp corners of the rectangular rib continue to induce elevated turbulence intensity levels at the rib's forward corner, as observed in non-reacting conditions. At the rib tip, turbulence intensity levels are also elevated, signifying turbulence associated with flow separation and recirculation. Behind the rib backward corner, turbulence intensity levels remain notably high, reflecting the challenges posed by the rectangular rib's geometry in reacting flows. The RD-Cur configuration maintains its advantageous turbulence intensity distribution, with lower turbulence levels at the rib's forward corner compared to the rectangular rib. At the rib tip, turbulence intensity levels remain lower, suggesting reduced turbulence associated with flow separation. Behind the rib backward corner, turbulence intensity levels are reduced, indicating more favorable turbulence conditions. These turbulence intensity contour observations highlight the potential benefits of the curved rib for combustion stability in reacting flows. The RD-Tri configuration exhibits turbulence intensity patterns similar to non-reacting conditions, with elevated turbulence levels at the rib's forward corner and behind the rib. These patterns align with the challenges associated with the triangular rib's geometry in both non-reacting and reacting flows. Finally, the RD-Trz configuration showcases balanced turbulence intensity behavior under reacting conditions. turbulence intensity levels at the rib's forward corner indicate a compromise between flow attachment and separation, resulting in moderate turbulence levels. At the rib tip, turbulence intensity levels remain moderate, signifying reduced turbulence associated with flow separation. Behind the rib backward corner, turbulence intensity levels remain moderate, indicating more favorable turbulence conditions compared to the rectangular and triangular ribs. These turbulence intensity contour observations reaffirm the advantages of the trapezoidal rib in promoting combustion stability and efficiency in reacting flows. The turbulence intensity behavior depicted in the figures illustrate a noteworthy increase in Turbulence Intensity by a factor of 4 following the initiation of combustion. This fourfold rise underscores the substantial influence of chemical reactions on the turbulent characteristics within the micro combustors. The heightened Turbulence Intensity post-ignition signifies a more chaotic and dynamic flow environment, aligning with expectations during the combustion process. The observed behavior holds significant implications for the overall flow dynamics and combustion efficiency of the micro-scale systems. This insight is invaluable in our quest to comprehend the intricate interactions

within micro combustors and emphasizes the need for precise control over combustion processes to optimize performance.

Vorticity dynamics

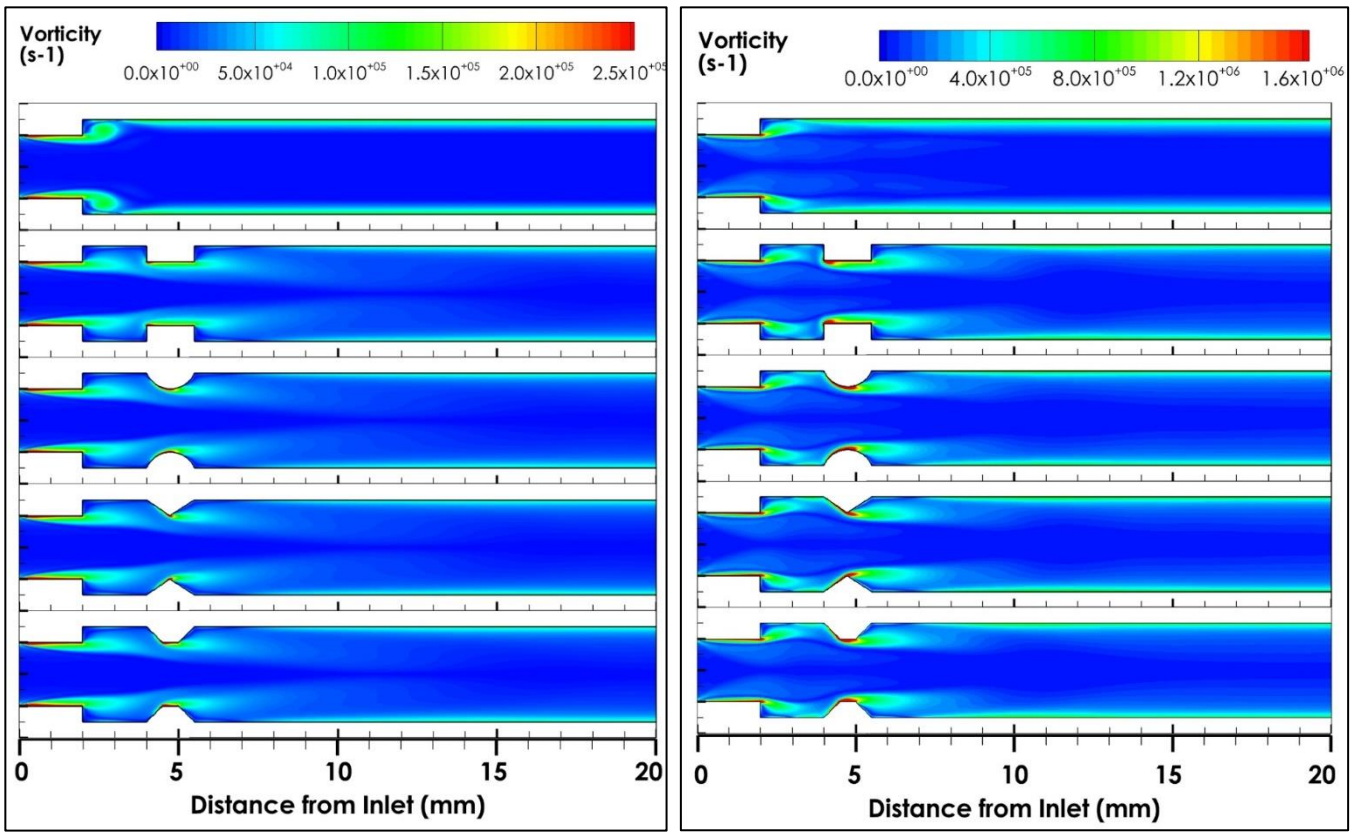

(a) *(b)*

Figure IV.1.13. *(a) Non-reacting flows, and (b) reacting flow Turbulence Vorticity contours for the different micro-combustor configurations: Effect of shape.*

Turbulent Vorticity refers to the rotational motion of fluid particles within a turbulent flow. Vorticity is a vector quantity representing the local spinning motion of fluid elements. In turbulent flows, vorticity is generated and sustained by the complex interactions between different fluid layers. Turbulent vorticity provides insights into the rotational behavior of the fluid, and its distribution helps in understanding the structure and dynamics of turbulence. The presence of turbulent vorticity contributes to the mixing and transport of momentum, heat, and other scalar quantities in turbulent flows. **Figure IV.1.13** presents turbulence vorticity contours for both non-reacting and reacting flow conditions within various micro combustor configurations, shedding light on the vorticity patterns and their implications for combustion processes. In non-reacting conditions, the turbulence vorticity contours provide critical insights into the vorticity distribution of each configuration. In the MCSD configuration, vorticity contours reveal distinct patterns in the recirculation zone behind the backward-facing step. This region experiences increased vorticity due to flow separation and recirculation, aligning with the typical behavior of sudden expansions. In the second channel without ribs, vorticity levels are relatively lower, indicating smoother and more uniform flow behavior with minimal disruption. The RD-Rec configuration, characterized by sharp rectangular ribs, exhibits intensified vorticity levels at the forward corner of the rib. The presence of sharp corners induces vorticity due to turbulent flow separation, leading to elevated vorticity in this region. At the rib tip, vorticity levels are also elevated, signifying vorticity associated with flow separation and recirculation. Behind the rib backward corner, notably high vorticity levels indicate intense vorticity and energy dissipation in the recirculation zone. These observations highlight that the rectangular rib design introduces significant vorticity, which may impact combustion stability and efficiency. Conversely, the RD-Cur configuration, featuring curved ribs, presents more favorable vorticity

contours. Vorticity levels at the rib's forward corner are lower compared to the rectangular rib, indicating reduced vorticity resulting from the absence of sharp corners. At the rib tip, vorticity levels are also lower, suggesting smoother flow attachment and reduced vorticity associated with flow separation. Behind the rib backward corner, reduced vorticity levels indicate more favorable vorticity conditions in this region. These vorticity contour observations emphasize the potential benefits of the curved rib in reducing vorticity and promoting combustion stability. The RD-Tri configuration introduces unique vorticity patterns. At the forward corner of the triangular rib, vorticity levels are elevated due to turbulent flow separation near the sharp tip. Behind the rib, vorticity levels indicate vorticity associated with flow reattachment and recirculation. However, this configuration also exhibits elevated vorticity levels in the recirculation zone, reflecting the challenges posed by the triangular rib's geometry. These elevated vorticity levels may impact combustion efficiency. The RD-Trz configuration, with its trapezoidal ribs, showcases a balanced vorticity distribution. Vorticity levels at the rib's forward corner indicate a compromise between flow attachment and separation, resulting in moderate vorticity. At the rib tip, vorticity levels are also moderate, signifying reduced vorticity associated with flow separation. Behind the rib backward corner, vorticity levels remain moderate, indicating more favorable vorticity conditions compared to the rectangular and triangular ribs. These vorticity contour observations reaffirm the advantages of the trapezoidal rib in maintaining balanced vorticity levels and promoting combustion stability.

Transitioning to reacting conditions in **Figure IV.1.11**, we can discern additional insights into vorticity behavior. The MCSD configuration maintains vorticity patterns similar to non-reacting conditions, with elevated vorticity in the recirculation zone behind the step. These observations provide critical information for combustion modeling and stability assessment. In the RD-Rec configuration under reacting conditions, the sharp corners of the rectangular rib continue to induce elevated vorticity at the rib's forward corner, as observed in non-reacting conditions. At the rib tip, vorticity levels are also elevated, signifying vorticity associated with flow separation and recirculation. Behind the rib backward corner, vorticity levels remain notably high, reflecting the challenges posed by the rectangular rib's geometry in reacting flows. The RD-Cur configuration maintains its advantageous vorticity distribution, with lower vorticity levels at the rib's forward corner compared to the rectangular rib. At the rib tip, vorticity levels remain lower, suggesting reduced vorticity associated with flow separation. Behind the rib backward corner, vorticity is reduced, indicating more favorable vorticity conditions. These vorticity contour observations highlight the potential benefits of the curved rib for combustion stability in reacting flows. The RD-Tri configuration exhibits vorticity patterns similar to non-reacting conditions, with elevated vorticity at the rib's forward corner and behind the rib. These patterns align with the challenges associated with the triangular rib's geometry in both non-reacting and reacting flows. Finally, the RD-Trz configuration showcases balanced vorticity behavior under reacting conditions. Vorticity levels at the rib's forward corner indicate a compromise between flow attachment and separation, resulting in moderate vorticity. At the rib tip, vorticity levels remain moderate, signifying reduced vorticity associated with flow separation. Behind the rib backward corner, vorticity levels remain moderate, indicating more favorable vorticity conditions compared to the rectangular and triangular ribs. These vorticity contour observations reaffirm the advantages of the trapezoidal rib in promoting combustion stability and efficiency in reacting flows.

- ***Flow Efficiency***

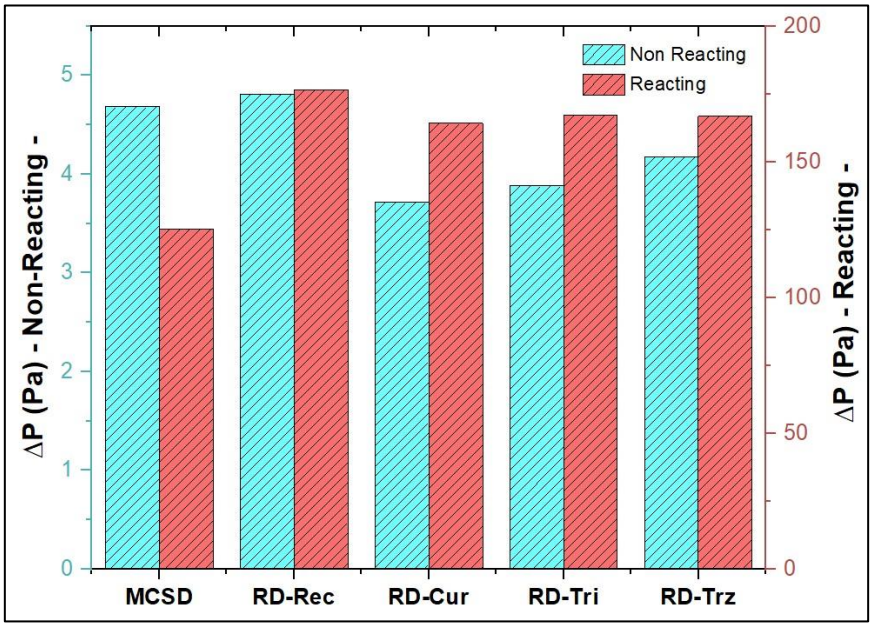

Figure IV.1.14. *Non-reacting flows and reacting flow pressure difference (⊿P) for the different micro-combustor configurations: Effect of shape.*

Quantifying the flow efficiency of various micro combustor configurations is crucial for assessing their performance, and one significant metric for this evaluation is the pressure difference across the micro combustor. The pressure difference serves as an indicator of the resistance the fluid encounters as it traverses the micro combustor, reflecting the efficiency of the flow through different geometries**. Figure IV.1.14** visually illustrates the pressure differences (ΔP) between the inlet and outlet for each micro combustor configuration under both non-reacting and reacting flows. Notably, the pressure differences exhibit a substantial increase with the ignition of chemical reactions. This is attributed to the additional resistance introduced by combustion, resulting in elevated pressures within the micro combustor. Analyzing the results presented in the figure, it's evident that under non-reacting conditions, all configurations exhibit relatively low-pressure differences. Under non-reacting conditions, MCSD exhibits pressure difference of 4.6834 Pa, indicating the pressure drop across the micro combustor. When chemical reactions are initiated (reacting conditions), the pressure difference significantly increases to 125.2781 Pa. However, when chemical reactions are initiated, a significant surge in pressure differences occurs. This increase is particularly pronounced for RD-Rec, where ΔP rises from 4.80935 Pa to 176.6114 Pa, indicating the substantial impact of combustion on flow resistance. Meanwhile, RD-Cur displays a non-reacting pressure drop (ΔP) of 3.71262 Pa, which increases to 164.1302 Pa under reacting conditions. This configuration demonstrates the lowest pressure difference compared to the rest of configurations under both non-reacting and reacting flows. Moreover, under non-reacting conditions, RD-Tri exhibits a ΔP of 3.88138 Pa, which rises to 167.0484 Pa in the presence of reacting flows. Furthermore, RD-Trz presents a non-reacting ΔP of 4.17787 Pa, which experiences a minor change to 166.8635 Pa under reacting conditions. Thus, the significant effect of chemical reactions released products temperature on the pressure field is revealed.

However, the pumping energy required for each micro combustor configuration, is essential for evaluating the energy needed to supply the mixture at the micro combustor's inlet. In addition, the pumping power is a critical parameter for calculating the figure of merit parameter, which is directly influenced by these pressure differences. To calculate the pumping energy in the context of 2D simulations, we consider a reference depth of $\Delta Z = 1$ mm. Given that the height of the inlet channel for all micro combustor configurations is equal to $d_1 = 2$ mm, this depth reflects the effective dimension for our calculations in the 2D domain. With an inlet velocity specified in the boundary conditions at 6 m/s,

the volume flow rate (Q_v) can be calculated using the formula $Q_v = A \cdot U_{in}$, where A is the cross-sectional area and U_{in} is the inlet velocity. For the current cases, $Q_v = 1 \cdot 10^{-6}\ (m^3/s)$. Hence, **Table IV.1.8** outline the pumping energy required for each micro combustor configuration. For the non-reacting scenarios, all configurations exhibit relatively low pumping energy requirements. Among the configurations, RD-Rec has the highest pumping energy demand, followed closely by RD-Trz. The differences in pumping energy among configurations in the non-reacting state are relatively subtle, reflecting the baseline energy needed to maintain fluid flow without the additional complexities of combustion. Upon introducing chemical reactions, a substantial increase in pumping energy is observed across all configurations. This augmentation is particularly pronounced in RD-Rec, indicating that the combustion process significantly raises the energy demands in this specific design. RD-Rec requires the highest pumping energy in both non-reacting and reacting scenarios, underscoring its heightened resistance to flow due to its geometric features. Despite the RD-Trz configuration doesn't present the most favorable pumping energy characteristics, this configuration strikes a balance between efficient flow dynamics, effective turbulence level and manageable pressure drops.

Table IV.1.8. *Pumping energy of micro combustor configurations under non reacting and reacting conditions: Effect of shape.*

Geometric Configuration	MCSD	RD-Rec	RD-Cur	RD-Tri	RD-Trz
Non-reacting	1.34E-05	1.37E-05	1.06E-05	1.11E-05	1.19E-05
Reacting	3.58E-04	5.05E-04	4.69E-04	4.77E-04	4.77E-04
Effect of Reactions	3.45E-04	4.91E-04	4.58E-04	4.66E-04	4.65E-04

in (W)

b. Combustion Characteristics

- ***Flame Dynamics***

- ***Flame Structure***

Flame structure, a fundamental aspect in the study of combustion, encompasses the physical and chemical attributes defining a flame. Understanding the intricate details of flame structure is paramount for optimizing combustion systems, ensuring efficient and clean energy conversion. Analyzing flame structure involves a comprehensive examination of key parameters such as species distribution, reaction rates, and mass fraction contours of specific chemical species. By delving into these factors, researchers gain insights into the underlying mechanisms of combustion, enabling the refinement of micro combustor designs for improved performance. The examination of intermediate chemical reaction kinetic rates further enhances our ability to gauge the impact of the micro combustor's geometry on micro combustion intensity. This holistic approach to flame structure analysis not only advances our understanding of combustion processes but also provides a basis for developing micro-scale combustion systems that are not only efficient but also environmentally sustainable.

In **Figure IV.1.15** the detailed analysis of major species' mass fractions and the heat of reaction along the centerline of the RD-Trz micro-combustor unveils a comprehensive understanding of the reacting flow-field. The profiles exhibit three distinct zones, each playing a crucial role in the combustion process. The preheat zone, the initial region along the centerline, serves as the area where cold reactants undergo preheating through heat diffusion from the nearby reaction zone. This preheating sets the stage for the initiation of destruction reactions of the fuel and the formation of intermediate radicals, creating conditions conducive to combustion ignition. Within the reaction zone, both the mass fractions of oxidizer and fuel decrease rapidly, indicating their consumption in the combustion process. Simultaneously, the mass fraction of product H2O and the intermediate radical OH increases proportionally, reaching their

peak values at the leading edge of the flame. Moving into the recombination zone, the mass fraction of reactants approaches zero, signifying their near-complete consumption, while the mass fraction of products continues to rise and stabilizes as the flow reaches the outlet of the combustor. This detailed analysis sheds light on the dynamic evolution of species' mass fractions, revealing the intricate interplay of chemical reactions and heat transfer processes within the RD-Trz micro-combustor.

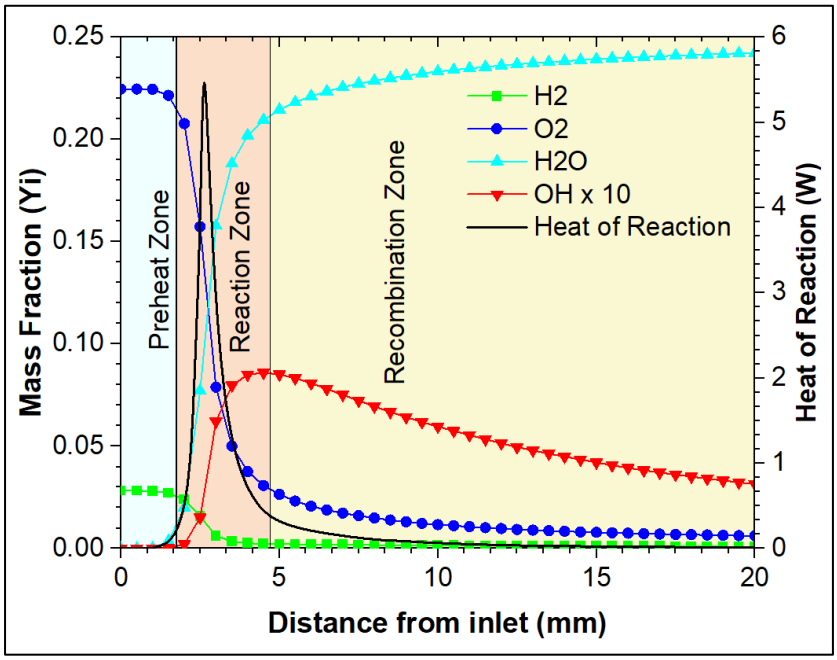

Figure IV.1.15. *Flame structure, major species and heat of reaction distribution along the RD-Trz micro combustor centerline.*

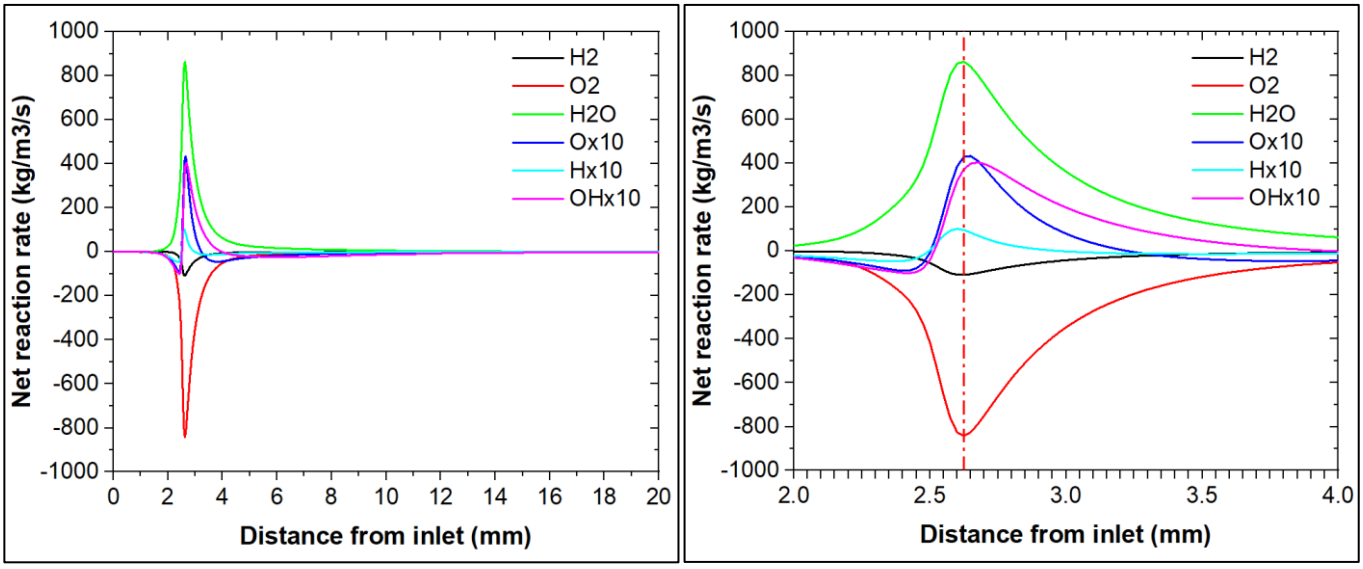

Figure IV.1.16. *The distribution of the net reaction rate of the major species along the RD-Trz micro combustor centerline.*

In **Figure IV.1.16**, the net reaction rate of major species, including H_2, O_2, H_2O, O, H, and OH, is depicted along the centerline of the RD-Trz micro-combustor configuration. The net reaction rate, expressed as negative for the consumption of reactant species and positive for the formation of products and intermediate species, provides crucial insights into the dynamic nature of the combustion process. The interplay between reactants and products is evident, revealing the locations and intensity of chemical reactions within the micro-combustor. Upon further analysis of **Figure IV.1.15** and **Figure IV.1.16**, a distinct reaction zone is identified, spanning from 2 mm to 4.3 mm from the inlet along the centerline.

Within this zone, the net reaction rates of various species undergo significant changes, indicating the core region where combustion reactions are most active. Notably, the net reaction rates reach their maximum values at approximately 2.625 mm from the inlet, signifying a critical point in the combustion process. This specific location highlights the region where the consumption of reactants and the formation of products and intermediate species are most pronounced, providing a focal point for understanding and optimizing the combustion dynamics within the RD-Trz micro-combustor configuration.

- ***Flame Propagation***

Flame Shape

To elucidate the impact of geometry on reaction zone and flame shape, **Figure IV.1.17** presents (a) hydrogen H_2 and (b) OH mass fraction contours for various micro combustor configurations, namely MCSD, RD-Rec, RD-Cur, RD-Tri, and RD-Trz. The analysis of hydrogen mass fraction contours reveals that, similar to the basic MCSD configuration, the reaction zone appears uniformly thin and conical in the upstream channel of all combustors, depicted in yellow. However, the distribution of hydrogen mass fraction within the different configurations exhibits slight variations influenced by geometry, particularly noticeable around the initial pairs of ribs, illustrated in dodger blue, indicating minimal geometry effects on the reaction zone. However, Li et al. [70] suggest that the OH mass fraction distribution inside a micro combustor can serve as an indicator of the flame. Examining the OH mass fraction distribution across all micro combustor configurations provides insights into the effect of rib shapes on flame shape, with distinct patterns observed. Therefore, the choice of rib shape becomes a crucial design parameter, requiring careful consideration to optimize combustion efficiency and prevent issues such as flame quenching or excessive stretching of the flame. The OH distribution serves as a valuable indicator of these combustion dynamics, offering insights into the interplay between geometric features and chemical reactions within micro combustors.

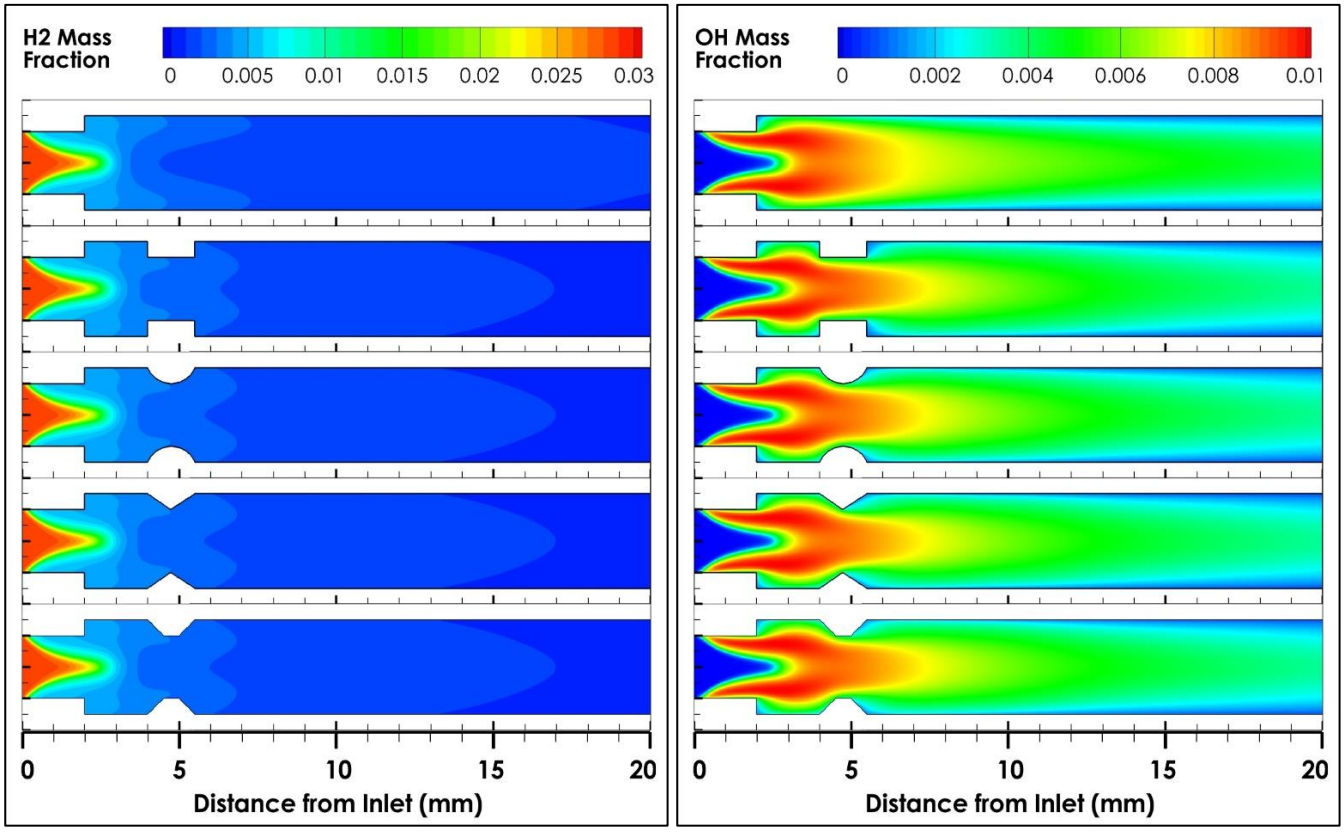

(a) *(b)*

Figure IV.1.17. *(a) hydrogen H_2 and (b) hydroxide OH mass fraction contours for the different micro-combustor configurations: Effect of shape.*

The introduction of ribs, whether rectangular (RD-Rec), curved (RD-Cur), triangular (RD-Tri), or trapezoidal (RD-Trz), plays a pivotal role in shaping the OH distribution patterns. Compared to the MCSD configuration, the introduction of ribs significantly affects the OH mass fraction distribution. As previously mentioned, each rib shape introduces unique fluid dynamics and flow characteristics, impacting the formation and behavior of OH radicals. For instance, recirculation zones generated behind the backward-facing step create low velocity zones behind ribs, which draw flame radicals (O, H, etc.) closer to the inner walls and contribute to the stretching of the flame. In the RD-Rec configuration, the sharp edges of rectangular ribs exert a pronounced influence on the flow dynamics. These sharp edges create stagnation zones and trap a significant number of reaction radicals within the cavity formed between the step and the forward-facing side of the ribs. Consequently, the flame shape undergoes a distinctive distortion, characterized by its deviation from its original shape due to the interaction with the flow recirculation zones established by the steps and ribs. This phenomenon underscores the intricate relationship between flow dynamics and chemical reactions in reacting flows and highlights how the ribs can alter flow dynamics, leading to changes in the path of the flame. Specifically, how the ribs shape changes induce deformations in both the shape of the flame and its front. In contrast, this phenomenon is efficiently moderated by the sloped edges of curved and triangular ribs, ensuring a streamlined flow profile and mitigating the risk of excessive flame stretching observed with rectangular-shaped ribs. Similarly, the trapezoidal ribs in RD-Trz, distinguished by their angled edges, play a pivotal role in promoting smoother flow dynamics and curbing the extent of flame elongation compared to RD-Rec. The inherent design of the trapezoidal ribs allows for more effective manipulation of flow patterns, minimizing disruptions and maintaining a more uniform flame distribution. This optimized flow behavior not only enhances combustion stability but also contributes to improved efficiency within the micro combustor. It underscores the significance of rib geometry in shaping combustion dynamics and underscores the advantages of employing trapezoidal ribs, such as those in the RD-Trz configuration, for optimizing micro combustor performance.

Flame front location

In order to clarify the effect of ribs shape on the combustion characteristics, the flame front location, ignition distance and the flame speed are used as a characteristic's parameters. OH mass fraction distribution inside a micro combustor can be seen as an indicator of the combustion intensity as it was stressed by Li et al. [70]. Consequently, the location of the OH mass fraction profile peak value is used as a characteristic parameter and defined as the flame front location in the present study. **Figure IV.1.18** plotted the OH mass fraction distribution profiles along the different combustors' centerlines under the same operating conditions. As shown, the OH mass fraction profiles exhibit a similar trend, but are shifted relative to each other. Moreover, the OH mass fraction profiles increase rapidly once the chemical reactions are initiated. However, the production rate of OH radical is almost similar for the different cases. **Figure IV.1.19** also demonstrates that the peak values of the OH radical profile are obtained at specific locations within each micro combustor. In the case of MCSD, the peak value occurs at a distance of 3.977 mm from the inlet. For RD-Rec, the peak is observed at 4.492 mm, while for RD-Cur, RD-Tri, and RD-Trz the peaks are located at 4.406 mm, 4.378 mm, and 4.435 mm from the inlet, respectively. Furthermore, the mass fraction of the produced radical OH decreases then gradually within the rest of the downstream channel following different rates. Comparing to MCSD, the introduction of ribs shifted the flame front location by 12,95 %, 10.79 %, 10.08 % and 11.52 % for RD-Rec, RD-Cur, RD-Tri, and RD-Trz, respectively. These outcomes reveal the direct effect of the recirculation zones (low velocity zones) generated by the pair of the steps and ribs. Moreover, the rib shape slips the flame front location from the inlet. Hence, the rib shape can also be used as a passive control technique to adjust the flame front location. According to Chattopadhyay et al. [71], the ignition distance is defined as the distance from inlet at the combustor axis where half of the hydrogen fuel is consumed. Therefore, the ignition distance is located about 2.55 mm from the inlet for the different micro combustor configurations.

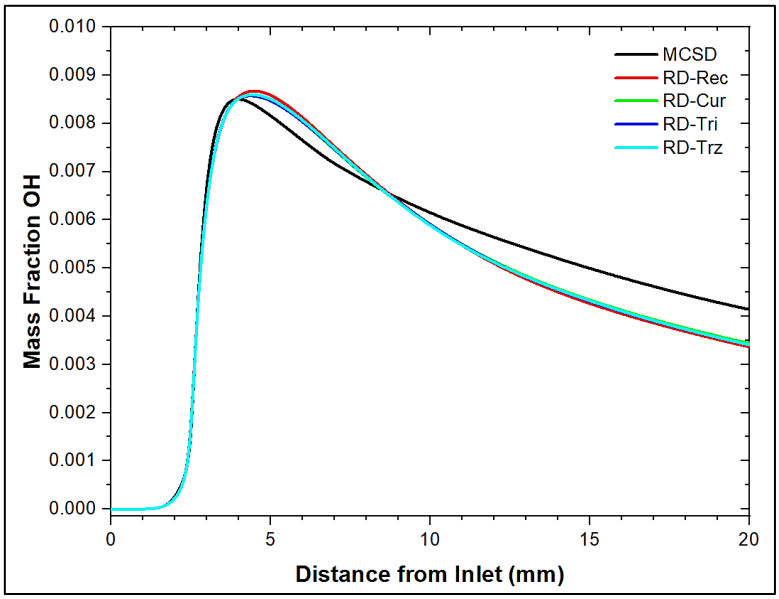

Figure IV.1.18. *OH mass fraction distribution centerline along the different micro-combustor configurations: Effect of shape.*

Flame speed

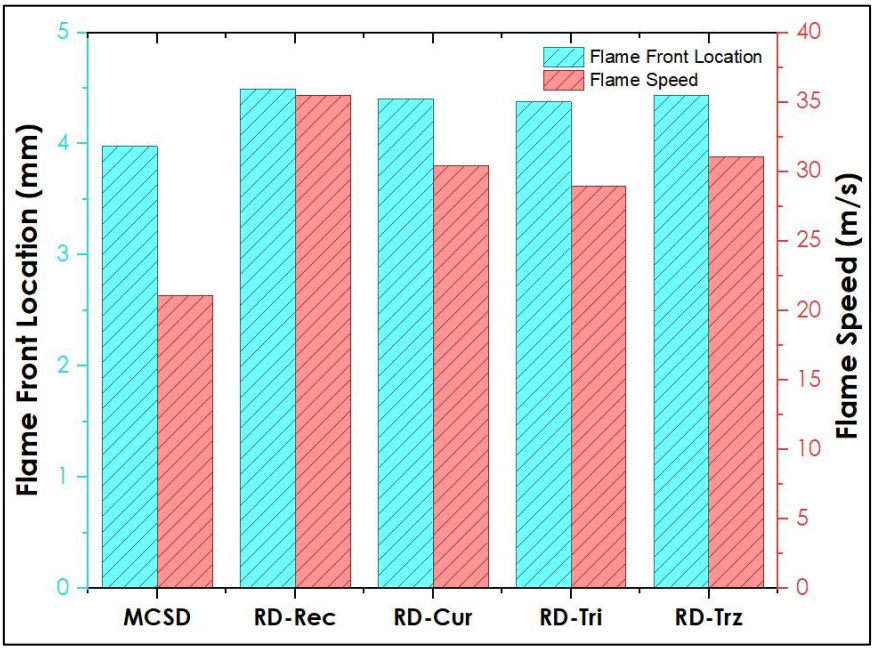

Figure IV.1.19. *Flame location and Flame speed for micro-combustor configurations: Effect of shape.*

To measure the flame speed parameter in this study, the method proposed by Li et al. [70] is employed. This method relies on the linear relationship established by Yamamoto et al. [72] between the peak of OH concentration profile and the flame speed. The method involves analyzing the OH concentration profiles obtained in order to obtain the position of the peak concentration. The peak of the OH concentration profile corresponds to the location of the flame front, and the magnitude of the flow velocity at this location is directly correlates with the speed at which the flame propagates. **Figure IV.1.19** shows the variations of the flame speed for the different geometry designs. As shown, the flame speed increases from 21.08 m/s to 35.5 m/s for the MCSD and RD-Rec, respectively. On the other hand, the flame speed increases to 30.44 m/s, 28.95 m/s and 31.06 m/s for the ribs shape, RD-Cur, RD-Tri and RD-Trz, respectively. This comparison to MCSD illustrates that the flame speed increases by approximately 68.41%, 44.4%, 37.33%, and 47.34% for RD-Rec, RD-Cur, RD-Tri, and RD-Trz, respectively. The observed increase in flame speed can be attributed to the heightened level of turbulence induced by the

presence of the backward-facing step and the different ribs shapes. This increased turbulence intensity has a significant impact on the diffusion rate of reactants and products within the reaction zone. The turbulent flow created by the geometry promotes a faster and enhanced mixing and interaction between the reactants and combustion products result in a more dynamic reaction zone. As a result, the incoming reactants are preheated to a greater extent, facilitating their rapid ignition and promoting a sustained and vigorous combustion process. The enhanced turbulent level and combustion intensity contributed also to the acceleration of the flame propagation speed.

- ***Combustion Efficiency***

- ***Combustion Intensity***

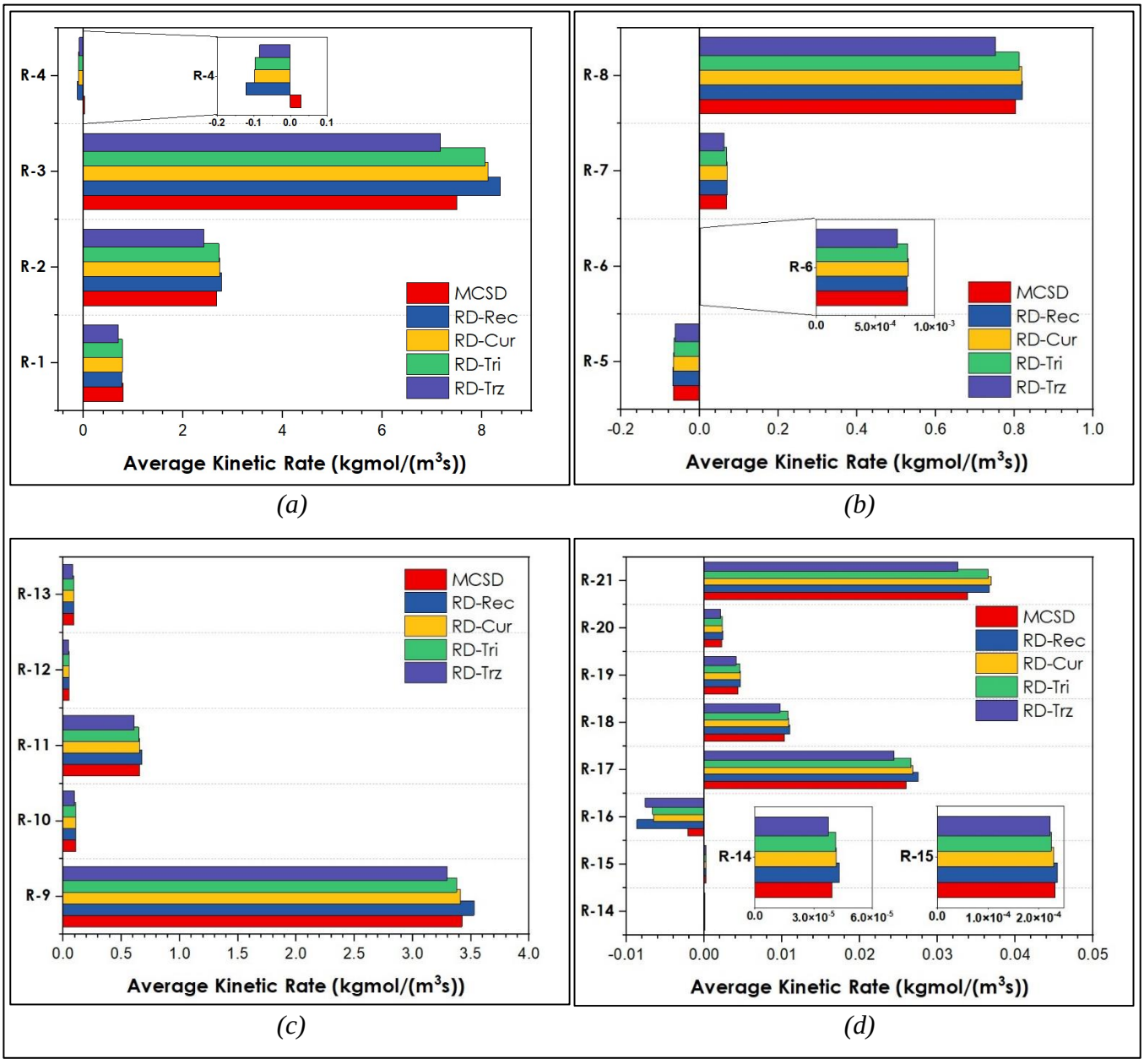

Figure IV.1.20. *Average kinetic rate of different elementary reactions for the different micro-combustor configurations: Effect of shape.*

Figure IV.1.20. illustrates the average kinetic reaction rates of different elementary reactions within each micro combustor configuration. These rates represent the speed at which chemical reactions occur within the combustors. Negative values suggest a net consumption of reactants, while positive values indicate product formation. The average kinetic rates of elementary reactions reveal distinctive patterns among micro-combustor configurations, emphasizing the impact of different geometric shapes on combustion

processes. Particularly, MCSD, RD-Rec, RD-Cur, RD-Tri, and RD-Trz exhibit clear differences, especially in reactions R-3, R-4, R-8, R-9, R-16, R-17, and R-21. Notably, reaction 3 consistently shows a significant positive rate across all configurations, signifying active combustion, aligning with expectations for its role in the combustion process. However, the combustion rates for MCSD serve as a reference case. Comparing configurations, the presence of ribs reduces combustion rates, with RD-Cur, RD-Tri, and RD-Trz exhibiting decreased rates compared to MCSD, suggesting that ribs promote more efficient chemical reactions. RD-Rec displays particularly increased combustion rates. The rates gradually decrease for RD-Cur, RD-Tri, and RD-Trz, suggesting nuanced effects of trapezoidal ribs on combustion intensity compared to other rib shapes. Comparing with MCSD, RD-Rec shows differences in rates for various reactions, emphasizing the influence of rib shape. RD-Cur exhibits varying combustion rates across different reactions, highlighting the impact of curved rib shapes. RD-Tri, like RD-Cur, displays a similar range of combustion rates. Interestingly, RD-Trz displays minimal combustion rate patterns, showcasing differences in reactions associated with trapezoidal rib shapes. These findings underscore the intricate relationship between micro-combustor geometry and combustion dynamics, providing valuable insights into how specific features, especially ribs, influence and optimize combustion efficiency. Further investigations into the mechanisms behind these trends will contribute to a comprehensive understanding of micro-combustion processes.

- ***Conversion Efficiency***

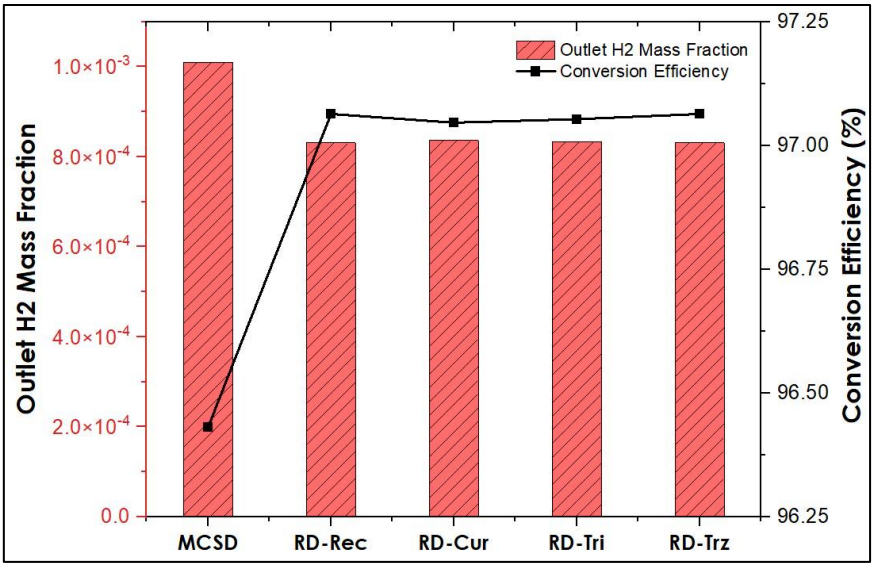

Figure IV.1.21. *Outlet H_2 mass fraction and Combustion efficiency for the different micro-combustor configurations: Effect of shape.*

In order to assess the performance of combustion, the conversion efficiency (chemical efficiency) η_{chem} is established as the evaluative parameter. Since hydrogen is the sole fuel in this study, the combustion efficiency can be directly associated with the rate at which hydrogen is consumed. **Figure IV.1.21** illustrates the average mass fraction of hydrogen at the outlet boundary of the different micro combustor configurations. Additionally, the figure presents the variations in micro combustion chemical efficiency. It is evident that the remaining hydrogen at the outlet is relatively low compared to the inlet mass fraction. The unconsumed hydrogen mass fraction decreases from 1.01 10^{-3} for MCSD to 8.31 10^{-4} for RD-Rec and RD-Trz, respectively. Furthermore, it is noteworthy that the mass fraction of unconsumed hydrogen for RD-Cur and RD-Tri are 8.36 10^{-4} and 8.34 10^{-4}, respectively. On the other hand, the same figure reveals an increase in combustion efficiency for different micro combustor configurations incorporating ribs compared to MCSD. With conversion efficiency increases from 96.42% for MCSD to 97.06% for RD-Rec, RD-Cur, RD-Tri and RD-Trz, respectively. These findings reflect one of the advantageous outcomes of incorporating a rib in terms of combustion efficiency. Hence, the introduction of ribs into the micro combustor has a discernible impact on flame stability and combustion efficiency, as the ribs serve

to enhance mixing and contribute to a more uniform fuel-air distribution. However, intriguingly, our comprehensive analysis indicates that the specific shape of the ribs exhibits no significant influence on flame stability or combustion efficiency, suggesting that the overall presence of rib structures plays a more pivotal role in optimizing these combustion characteristics. This observation underscores the robustness of flame stabilization and combustion efficiency achieved through rib implementation, irrespective of the particular geometric configuration of the ribs themselves.

c. Thermal Characteristics

- ***Temperature Distribution***

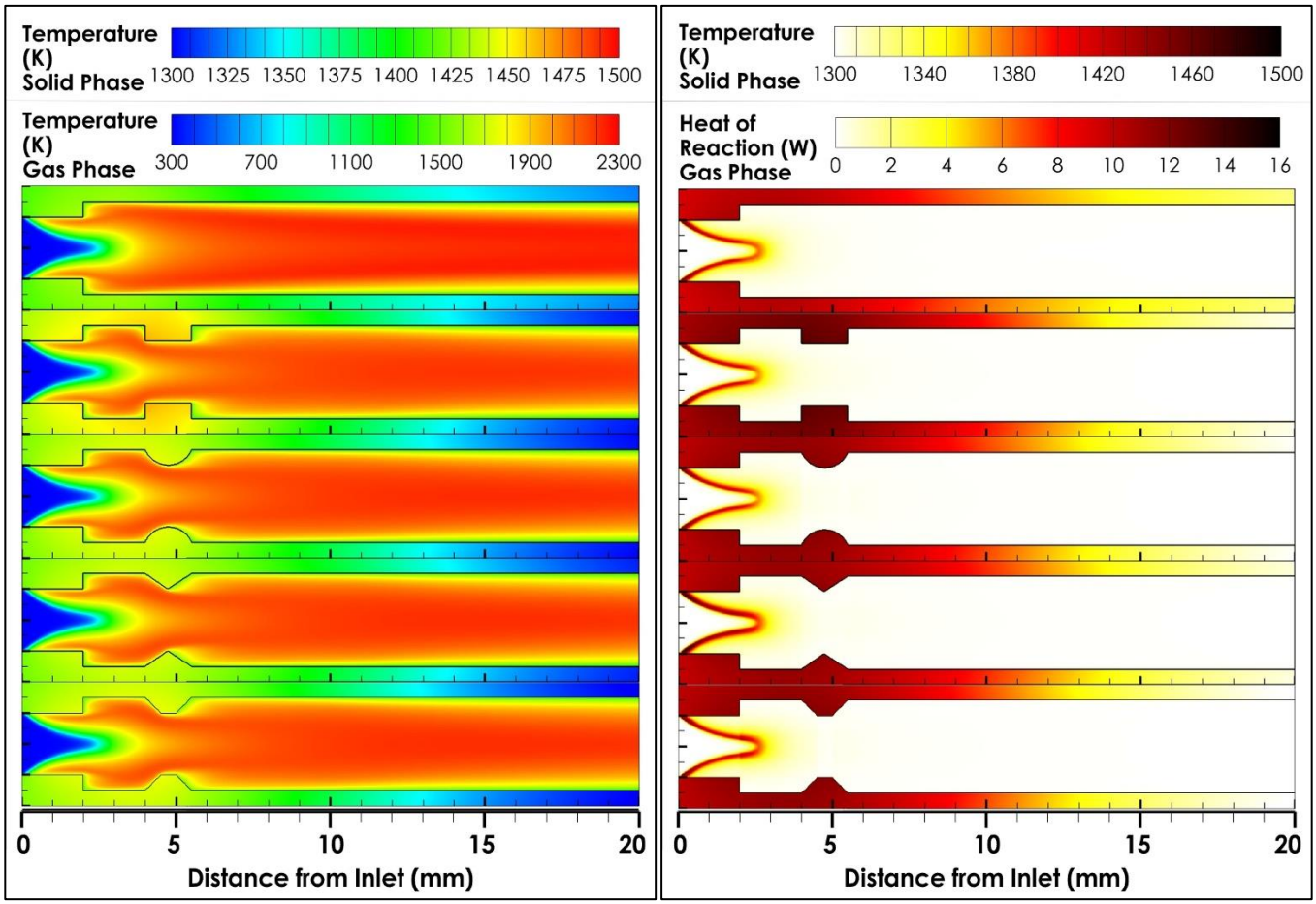

(a) *(b)*

Figure IV.1.22. *(a) Temperature and (b) Heat of reaction contours for fluid phase and solid phase of the different micro-combustor configurations: Effect of shape.*

Figure IV.1.22 *(a)* illustrates temperature contours for the different micro combustor configurations under discussion. The contours provide insight into the temperature distribution and the effect of introducing different rib shapes on the heat transfer within both fluid phase and solid phase. In the gas-phase, the contours depict the uniformity of temperature distribution within the different micro combustor configurations. As shown, the reactions zone manifests increasing temperatures owing to exothermic combustion reactions. The region proximal to the aforementioned recombination zone exhibits heightened temperatures, representing the hot product gaseous region, while areas closer to aforementioned preheating zone constitute the cold reactant gaseous region. The heat released by chemical reactions is mainly transported by the product gaseous. The heat transfer dynamics within these gas phase involve the diffusion of hot gases and the preheating of colder gases, facilitating continuous combustion reactions. Heat transfer mechanisms are predominantly convective, occurring between cold reactants, intermediate species, and hot products. Ribs, by inducing turbulence and enhancing fluid mixing, contribute to

improved convective heat transfer. This interaction extends to the micro-combustor's inner walls, where convective heat transfer between the gas phase and the solid structure is influenced by rib shapes. The effects of rib shapes on fluid dynamics and heat transfer efficiency are notable. Rib configurations, such as rectangular (RD-Rec) and trapezoidal ribs (RD-Trz), induce significant enhancement of turbulence level, thereby improving convective heat transfer compared to configurations featuring curved (RD-Cur) or triangular ribs (RD-Tri). The temperature distribution around the reaction zone reveals the effect of introducing ribs on the reaction zone shape. The acceleration zone at the ribs tip tends to shift the flame downstream and elongated the reactions zone. The introduction of ribs trapped more the hot product gaseous and concentrated them within the cavity between the backward facing step and the ribs, also around the inner wall surface. Compared to the traditional MCSD configuration, the hot products residence time near the reaction zone increases importantly which improves the combustion efficiency significantly and increases the conversion efficiency. Downstream of micro combustor configurations we observe a concentration of hot product gases in the center of combustors due to the resistance (skin friction) near the inner walls. This concentration effect affects considerably the heat transfer of the hot products gases to the micro combustors' inner walls. The analysis of temperature distribution within solid phase for each configuration sheds light on how ribs shape impacts the available surface area for convective heat transfer, offering insights into the significance of heat transfer enhancement made by each shape. The configurations with rectangular and trapezoidal ribs shape, with its longer edges, contributes to an expanded convective heat transfer area compared to configurations featuring curved (RD-Cur) or triangular ribs (RD-Tri), respectively. The choice of a 90° and 45° angle for the trapezoidal rib edges increased surface area allows for more effective heat transfer from the gas phase to the solid structure, promoting higher thermal efficiency. In the solid phase, heat transfer primarily occurs through conduction from the gas phase to the outer wall of the micro combustor configurations. The introduction of ribs modifies the conduction paths within the solid material, increasing heat transfer to the outer wall. The shape of the ribs becomes a key factor in dictating how heat is conducted through the solid material, impacting temperature gradients and thermal uniformity. Horizontal heat conduction within the micro-combustor material is influenced by the presence of ribs. This effect further contributes to the redistribution of heat within the wall material, impacting thermal gradients and overall performance.

Furthermore, **Figure IV.1.22** *(b)* provides a distinct depiction of the reaction zone within the different micro combustor configurations. The reaction zone is the visible, luminous, and hot gas that is produced during the combustion of a substance. It is the region where the most significant heat release from combustion reactions is actively occurring, resulting in the emission of light and heat. Reaction zones are typically characterized by their distinct colors. This portion of the gas phase is crucial as it represents the locus of intense chemical transformations, where fuel and oxidizer combine to produce hot combustion products. The clarity of the reaction zone allows for a detailed observation of the spatial distribution and intensity of heat release. This is particularly important as it enables a precise understanding of the areas within the combustion chamber where the majority of chemical energy is being converted into thermal energy. As depicted, the introduction of various rib shapes appears to have minimal impact on the shape of the reaction zone within the different micro combustor configurations. Despite the alterations in the geometrical arrangement caused by different rib shapes, the fundamental structure of the reaction zone remains relatively unchanged. Contrastingly, a simple distinction emerges when comparing the level of heat release among different micro combustor configurations. Specifically, the RD-Tri and RD-Trz configurations exhibits a higher level of heat release compared to RD-Rec and RD-Cur configurations. Similarly, they surpass MCSD in terms of the amount of heat released during combustion. These findings underscore the sensitivity of heat release to specific rib configurations. The triangular (RD-Tri) and trapezoidal (RD-Trz) ribs designs appear to enhance combustion efficiency, leading to a more pronounced heat release when compared to the rectangular (RD-Rec), curved (RD-Cur), and especially with simple

design (MCSD) counterparts. The observed differences in heat release highlight the intricate interplay between combustion dynamics and geometric features within the micro combustor.

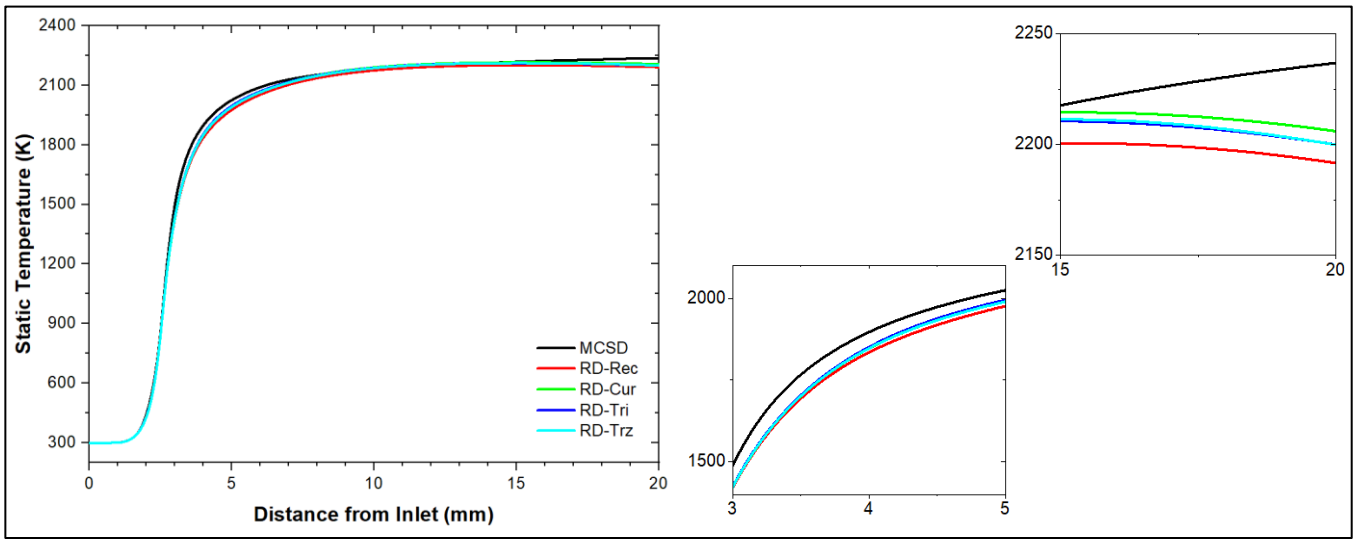

Figure IV.1.23. *Temperature distribution along the micro-combustor centerline for the different micro-combustor configurations: Effect of shape.*

To precisely evaluate the temperature distribution within the gas-phase, **Figure IV.1.23** has been presented, offering a detailed illustration of the temperature along the centerline across different micro-combustor configurations. The temperature profile initiates a noticeable ascent approximately 2 mm from the inlet, rapidly peaking in the proximity of the reaction zone, reaching around 2200 K. Following this peak, the temperature profile undergoes a transition, displaying an almost uniform distribution along the recombination zone. To further highlight the impact of rib configurations on temperature profiles, it is crucial to note that the Micro Combustor with Simple Design (MCSD) exhibits a distinct temperature profile along its centerline. Notably, the MCSD configuration displays a higher level of temperature, particularly after 10 mm from the inlet, and this disparity becomes more pronounced near the outlet when compared to micro combustor configurations incorporating different rib shapes. In specific comparison within the ribbed configurations, RD-Cur stands out by demonstrating a higher temperature level compared to RD-Tri, RD-Trz, and RD-Rec, respectively. This indicates that the curved rib shape is particularly effective in influencing the temperature distribution along the centerline, potentially due to its impact on fluid dynamics and heat transfer characteristics. Conversely, RD-Rec, featuring rectangular ribs, exhibits the lowest temperature level on the downstream of the second channel. This observed behavior aligns coherently with expectations, considering the introduction of ribs into the micro-combustor design. The ribs, strategically positioned, play a pivotal role in enhancing the turbulent flow field within the combustion chamber. This augmentation facilitates convective heat transfer and fosters efficient mixing of gases, particularly in proximity to the inner wall surface. Consequently, the observed shift in temperature profiles becomes indicative of an amplified convective heat transfer occurring between the combustion gases and the inner wall. It is noteworthy to emphasize that despite the significant changes in convective heat transfer induced by the ribs, the flame temperature remains remarkably stable across the various proposed geometric configurations. This stability underscores the minimal adverse effects of convective heat transfer on the flame temperature. The efficient convective heat transfer facilitated by the ribs contributes to improved mixing and combustion characteristics without compromising the stability of the combustion process. In essence, the detailed temperature profiles and the consistent flame temperature across different micro-combustor configurations provide valuable insights into the intricate interplay between geometric features, convective heat transfer, and combustion dynamics within these combustion systems.

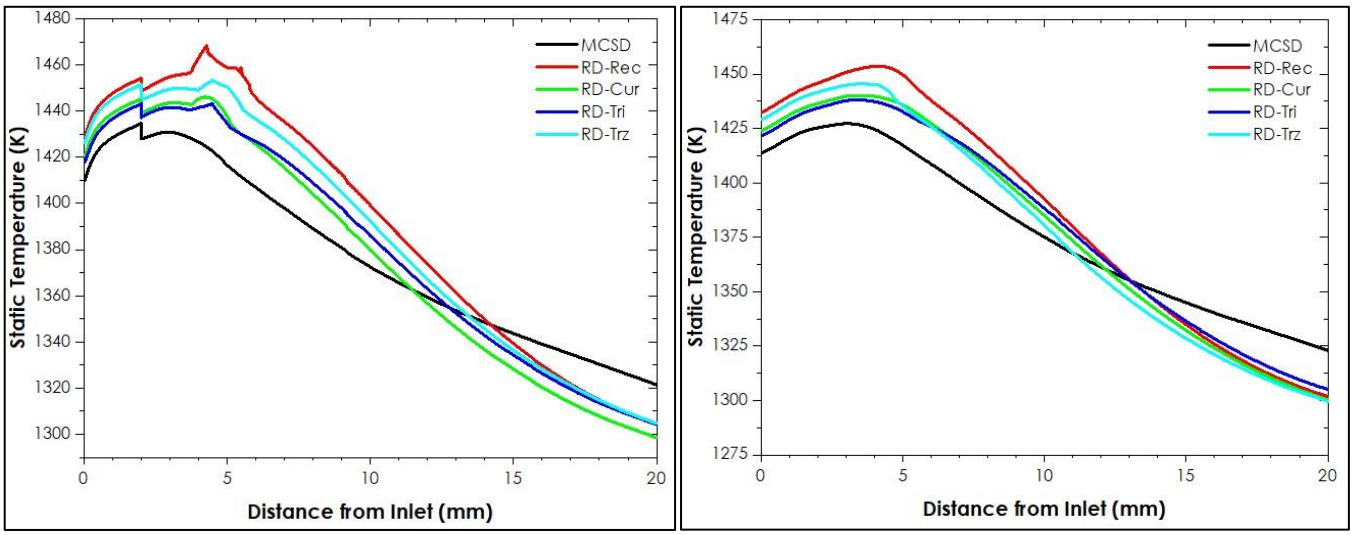

(a) *(b)*

Figure IV.1.24. *(a) Inner and (b) Outer wall temperature distribution for micro-combustor configurations: Effect of shape.*

The comprehensive analysis of temperature distribution along the inner and outer walls of different micro combustor configurations, as outlined in **Figure IV.1.24**, provides valuable insights into the intricate heat transfer phenomena occurring within these combustion systems. This comprehensive examination reveals distinctive behaviors among the various configurations. Firstly, the introduction of ribs is observed to significantly enhance convective heat transfer, a phenomenon evident in **Figure IV.1.24** *(a)* depicting the temperature profile along the inner wall. The temperature profiles can be dissected into four main regions: upstream, cavity, ribs, and downstream, each influenced by the presence of ribs. Notably, all ribbed configurations demonstrate higher temperatures level than the MCSD configuration, throughout the entire length of different micro combustor configurations. In the upstream inlet channel and cavity regions, RD-Rec and RD-Trz configurations exhibit the highest temperatures, surpassing RD-Cur and RD-Tri configurations. Within the cavity region, a slight temperature drop is observed near the backward-facing step, followed by an increase along the cavity between the step and the ribs. On the rib's region, while the temperature profile in MCSD exhibits a decreasing trend, RD-Rec, RD-Trz, RD-Cur, and RD-Tri configurations show an increasing behavior, reaching peak values at the rib's tips related to the aforementioned first recirculation zone (As shown in **Table IV.1.9**). RD-Rec and RD-Trz configurations display an additional peak behind the ribs related to the second recirculation zone, emphasizing the complex thermal dynamics induced by rib geometry. Comparison of peak temperatures at the ribs tips indicates that RD-Rec and RD-Trz configurations achieve higher values than MCSD, signifying the effectiveness of rib shapes in augmenting convective heat transfer. RD-Cur and RD-Tri configurations exhibit slightly lower peak temperatures, reflecting variations in turbulence levels induced by different rib shapes. Downstream, the overall trend of temperature profiles decreasing as the distance from the step and ribs regions increases is consistent across all configurations, indicative of the expected cooling effect along the flow path. This gradual decrease is a result of heat dissipation along the outer wall. The temperature profiles of ribbed configurations consistently surpass MCSD until 12 mm from the inlet, showcasing the enduring impact of enhanced convective heat transfer. Notably, RD-Cur demonstrates a higher decreasing rate, crossing the MCSD profile first, followed by RD-Tri, RD-Trz, and RD-Rec, respectively. At the outlet, MCSD exhibits the highest temperature, followed by RD-Rec, RD-Trz, and RD-Tri, with RD-Cur displaying the lowest outlet temperature. These trends underscore the substantial effect of increasing the convective heat transfer surface through rib configurations. Of particular note is the advantageous performance of RD-Trz, which stands out as the second-highest temperature configuration. Its trapezoidal rib shape not only contributes to increased turbulence and convective heat transfer but also demonstrates a remarkable uniformity in temperature distribution, a crucial objective in

the enhancement technique under discussion. This aligns seamlessly with the goals of both our doctoral research and the MTPV research community, highlighting the potential of RD-Trz for achieving improved thermal performance in micro-scale combustion systems.

Moving to the analysis of outer wall temperature profiles, **Figure IV.1.24** *(b)* provides a comprehensive comparison between Micro Combustor with Ribs (MCRD) configurations and the traditional Micro Combustor with Straight Duct (MCSD), emphasizing the favorable effects of the novel proposed designs. The temperature trends within these configurations exhibit distinctive characteristics, marked by a gradual increase in the upstream, cavity, and ribs regions. In the downstream direction, the temperature trends demonstrate a rapid decrease with increasing distance from the inlet, reflecting the convective effects along the flow path. The observed temperature variations among different configurations suggest a systematic influence of geometric features, particularly rib shapes, on the thermal characteristics of micro combustors. A comparison between different configurations consistently reveals lower temperature levels for MCSD along the entire outer wall. This aligns with expectations, as the absence of ribs minimizes convective heat transfer, resulting in lower temperature distribution along the outer wall. Notably, micro combustor configurations with curved ribs (RD-Cur) and triangular ribs (RD-Tri) exhibit relatively lower temperature levels across the upstream, cavity, and ribs regions compared to configurations with rectangular (RD-Rec) and trapezoidal (RD-Trz) ribs. The specific flow dynamics introduced by rectangular and trapezoidal ribs contribute to efficient heat transfer, highlighting the impact of rib shape on temperature distribution. Furthermore, in the upstream, cavity and rib regions, RD-Trz consistently demonstrates slightly lower static temperatures compared to RD-Rec and exhibits tendencies similar to other rib-shaped configurations in the downstream region. Variations in rib shape contribute significantly to temperature level, as outlined in **Table IV.1.9**, which details the maximum temperatures of MCSD and MCRD configurations on inner and outer walls, including the conduction effect. For all micro combustor configurations, the maximum temperature aligns with the inner wall temperature profile. RD-Rec, with rectangular ribs, exhibits the highest temperature around the first recirculation zone, reaching a maximum of 1453.732 K. RD-Trz, with trapezoidal ribs, follows with the second-highest temperature of 1445.422 K. Configurations with curved (RD-Cur) and triangular (RD-Tri) ribs show lower temperature levels, with maximum temperatures of 1440.17 K and 1438.07 K, respectively. In contrast, the MCSD configuration exhibits the lowest temperature among all configurations, with a maximum of 1427.192 K. Moreover, examining the temperature differences between the maximum temperatures at the inner wall and outer wall reveals the conduction effect of each rib shape. **Table IV.1.9** distinctly illustrates that the micro combustor configuration with trapezoidal-shaped ribs (RD-Trz) exhibits the lowest conduction effect among all other configurations. This observation leads to the conclusion that trapezoidal-shaped ribs significantly enhance the outer wall temperature distribution through improved inner wall convective heat transfer and conductive heat transfer of the micro combustor wall. The presence of higher ribs contributes to increased heat transfer rates, further elevating the outer wall temperature level and promoting uniformity. Consequently, the distinctive characteristics of trapezoidal-shaped ribs, exemplified by RD-Trz, impact heat transfer and combustion differently compared to other rib shapes.

Table IV.1.9. *Conduction effect of the different micro combustor configurations: Effect of Shape*

Geometric Configuration	MCSD	RD-Rec	RD-Cur	RD-Tri	RD-Trz
Inner Wall	1434.62	1468.29	1446.07	1443.15	1447.22
Outer Wall	1427.19	1453.73	1440.17	1438.07	1445.42
Conduction Effect	7.43	14.56	6.1	5.08	2.2

in (K)

- ***Thermal Efficiency***

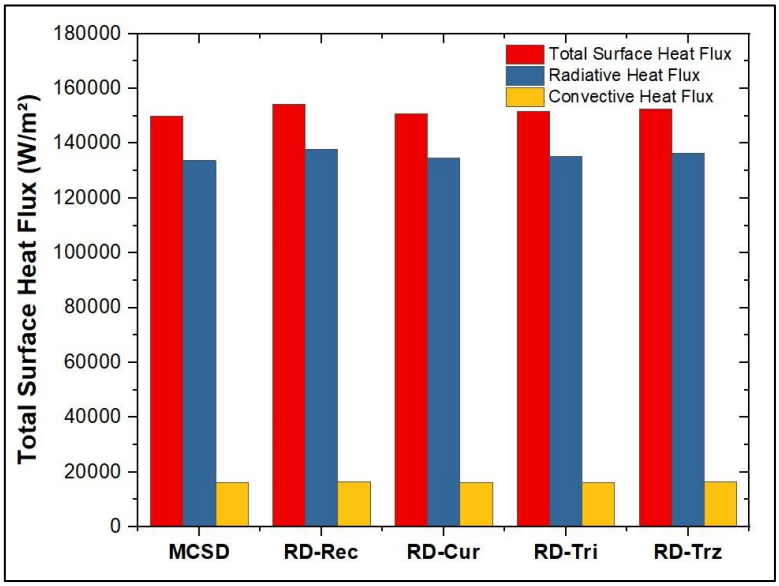

Figure IV.1.25. *The convective and radiative heat fluxes ratio to the total heat flux emitted via the outer wall for the different micro-combustor configurations: Effect of shape*

Figure IV.1.25 illustrates the convective and radiative heat fluxes ratio to the total heat flux emitted via the outer wall for the different micro combustors. The results indicate that the implementation of ribs increases the total heat flux transferred via the outer wall compared to the MCSD configuration. Specifically, the RD-Rec shows an increase of approximately 2.86 %, while the total heat flux increases by 0.59 %, 1.16 % and 1.84 % for RD-Cur, RD-Tri and RD-Trz, respectively. The majority of the heat losses are due to radiation, as indicated by the high radiation heat fluxes for all the micro combustor configurations. Moreover, the increase in the radiation heat flux is responsible for the variation of the total heat flux, while the convective heat flux remains almost constant for the different combustors proposed. Quantitatively, the radiation heat flux accounts for approximately 89.3 % of the total heat flux for MCSD, RD-Rec, RD-Cur, RD-Tri and RD-Trz, respectively. In contrast, the convective heat flux represents only about 10.7 % of the total heat transferred via the outer wall for the different proposed combustors.

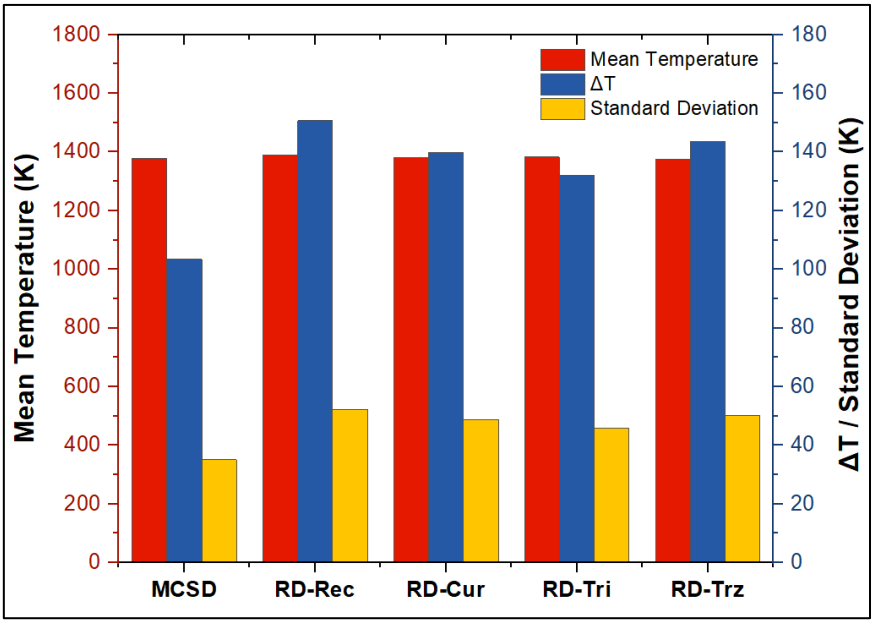

Figure IV.1.26. *The outer wall: Average temperature, temperature difference and Standard deviation for the different micro-combustor configurations: Effect of shape*

To assess the influence of introducing trapezoidal ribs and their shape on the thermal performance of different micro combustor configurations, a set of characteristic parameters was defined, as illustrated in **Figure IV.1.26**. The results show a notable increase in the mean temperature of the outer wall temperature profile with the introduction of ribs, rising from 1378.64 K for MCSD to 1388.39 K for RD-Rec. Additionally, the mean temperature for RD-Cur, RD-Tri, and RD-Trz increases to 1380.34 K, 1382.77 K, and 1385.54 K, respectively. These findings align with previous discussions indicating that the recirculation zones created by the ribs enhance convective heat transfer to the inner wall. Consequently, the temperature level at the outer wall is influenced proportionally by the rib shape. To further evaluate the thermal performance of the micro combustors, the outer wall temperature differences were analyzed. The results indicate a significant increase in outer wall temperature differences with the introduction of ribs and their shape. Specifically, the outer wall temperature distribution differences escalated from 103.47 K to 150.693 K for MCSD and RD-Rec, respectively. Furthermore, the differences increased to 139.801 K, 132.116 K, and 143.499 K for RD-Cur, RD-Tri, and RD-Trz, respectively. This resulted in an augmented outer wall temperature distribution deviation, calculated using the statistical parameter "standard of deviation." Hence, the RD-Rec and RD-Trz exhibits a noteworthy deviation of 52.11 K and 50.16 K, respectively, compared to MCSD, which reveals a deviation of 35 K. Similarly, the micro combustor with curved and triangular-shaped ribs shows a deviation of 48.83 K and 45.74 K, respectively. These findings highlight the impact of rib shapes on the outer wall temperature distribution and emphasize the significance of careful consideration in optimizing the rib design for enhanced thermal performance in micro combustors.

However, achieving a delicate equilibrium between augmented heat transfer and potential heat loss drawbacks is paramount in micro combustor design. This balance is especially crucial when integrating ribs with sharp corners, as while they expand the convective heat transfer area, they also elevate the risk of heat dissipation to the surroundings. Excessive heat loss can compromise thermal efficiency and even lead to flame quenching. Equally critical is the thoughtful selection of the backward-facing step's expansion ratio to prevent excessive stretching of the reaction zone, which could also result in flame quenching. In addressing these challenges, the trapezoidal shape of rib angled edges emerges as a strategic passive control technique. This design element enables the regulation of trapped gases along the combustor's inner wall, achieving a balanced compromise between heat transfer requirements and objectives while mitigating the risks associated with flame stretching and quenching. The RD-Trz configuration stands out as a nuanced solution, offering enhanced heat transfer capabilities and effective control over combustion dynamics in micro combustors. In particular, RD-Trz configuration demonstrates superiority and ability to effectively manage heat transfer while minimizing adverse effects on combustion efficiency and flame stability.

Effect of Number (Spacing)

a. Flow-field characteristics

To thoroughly explore the impact of incorporating different numbers of trapezoidal shaped ribs and their respective configurations on flow characteristics, we have adopted a comprehensive approach. Within this analysis, we've examined diverse factors such as flow dynamics and efficiency. Employing a set of metric parameters has facilitated a meticulous assessment of the geometric effect, ensuring an accurate quantification. This comprehensive approach affords us valuable insights into how the flow responds to variations in the number of ribs.

- ***Flow Dynamics***

- ***Stream Field***

Figure IV.1.27 offers a visual insight into the velocity contours of the flow within various micro combustor configurations under non-reacting and reacting conditions, denoted as MCRD1, MCRD2, MCRD3, MCRD4, MCRD5, MCRD6, and MCRD7. Observations reveal areas of acceleration in the upstream channel of different micro combustor configurations. In the vicinity of the backward-facing step, deceleration of velocity is typical due to the sudden expansion, resulting in a decreased velocity gradient and the formation of a recirculation zone. Conversely, acceleration occurs on the downstream channel of micro combustors incorporating ribs, as the flow passes over the rib's tips, causing an increase in velocity. The vena contracta, resulting from fluid acceleration due to ribs constriction, leads to reduced cross-section and increased velocity magnitude. The number of trapezoidal ribs significantly influences velocity distribution, as evidenced by the velocity contours of various micro combustor configurations. The increase of ribs number and reduction of space between the ribs increases the velocity magnitude and the number of recirculation zones, directly.

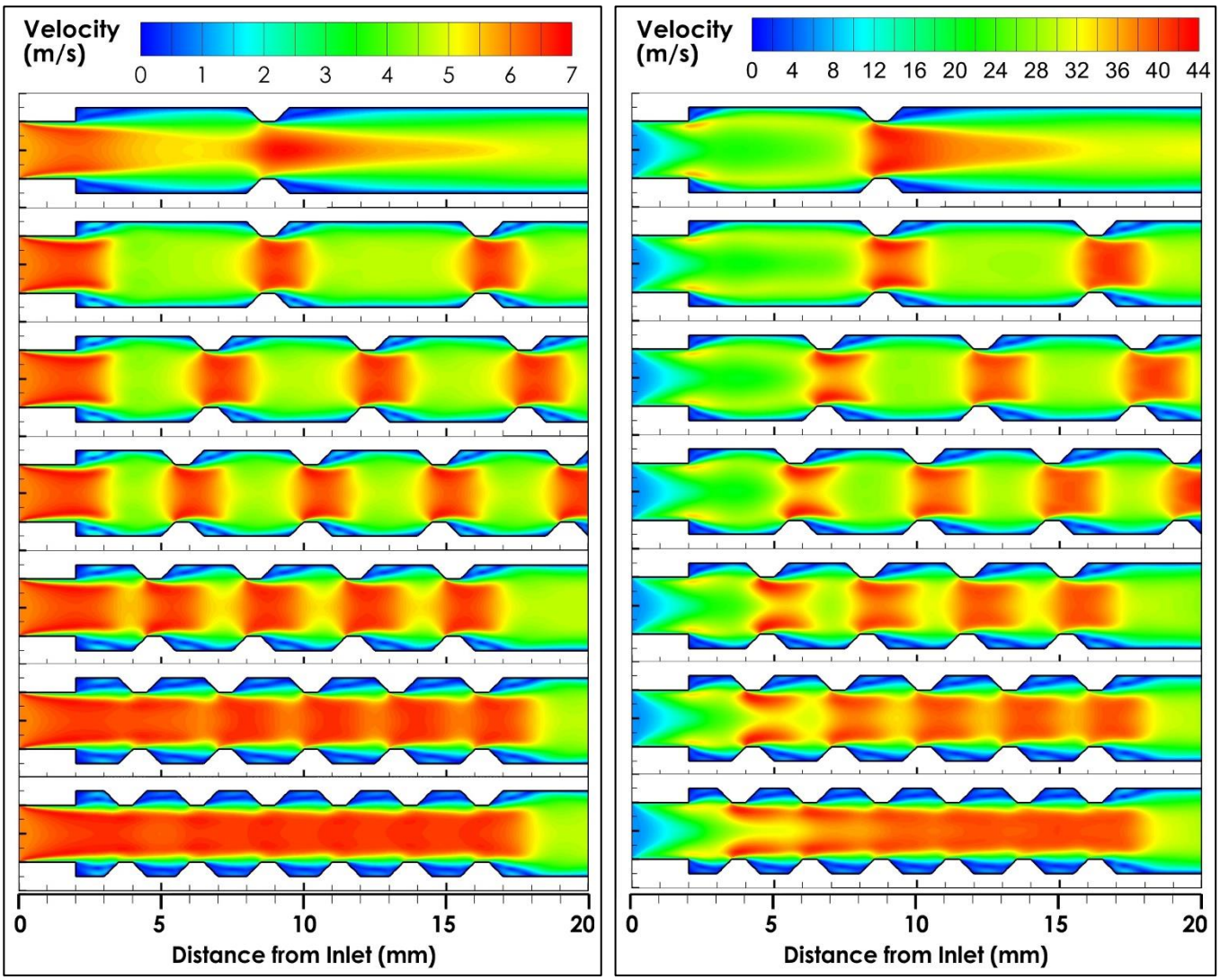

(a) *(b)*

Figure IV.1.27. *Flow-field velocity contours of different micro combustor configurations under (a) non-reacting and (b) reacting conditions: effect of number (spacing).*

The transition from non-reacting to reacting conditions reveals essential aspects of combustion efficiency and stability. **Figure IV.1.27** *(b)* provides a visual insight into the velocity contours of the flow within

various micro combustor configurations under reacting conditions. In these different configurations, the reacting flow patterns behind the step remain akin to the non-reacting conditions, forming a recirculation zone behind each step and rib. Additionally, acceleration of flow over the rib's tips is observed in the second channel. Contrary to non-reacting flows, the flame shape significantly influences the flow field dynamics within the upstream channel. The elongated flame exerts a pushing effect on the flow inside the downstream channel, altering velocity contours and influencing the distribution of chemical species. Furthermore, the ignition of chemical reactions plays a crucial role in determining the size of the vena contracta for different micro combustor configurations (MCRD1-7). The increase of ribs number and decreasing of spacing has a profound effect on the reattachment of the shear layer on the inner surface of micro combustors. The increase of ribs number alters flow-field and velocity gradients, influencing reattachment points and the overall length of the recirculation zone. Considering velocity magnitude and distribution, the micro combustor configurations with one, two and three ribs (MCRD1, MCRD2, MCRD3) exhibit moderate velocity magnitude and distribution. Meanwhile, the micro combustor configuration with four ribs and 3 mm spacing MCRD4, show an acceleration zone by the outlet which may present a bad effect on both combustion stability and thermal performance. On the other hand, MCRD5 configuration with four ribs and 2 mm spacing show a reasonable balance between increasing the number of recirculation zone and keeping the residence time reasonable with chemical reactions time scale. In contract, the micro combustor configurations with 5 and 6 ribs and space of 1.5 mm and 1 mm, MCRD6 and MCRD7, induce a quantifiable increase in flow velocity due to the reduced spacing between the ribs. This increase is particularly notable in the region over the tip of the different ribs which may reduce the residence time considerably and cause blowoff of flame.

- ***Pressure Fields***

Figure IV.1.28 provides a comprehensive examination of pressure contours in both non-reacting and reacting flow conditions within various micro combustor configurations (MCRD1-7), offering insights into pressure behavior and its implications for combustion stability and performance. In non-reacting conditions, distinctive pressure patterns are observed for each configuration. In MCRD1, MCRD2 and MCRD3 the pressure contours show variations corresponding to the sudden expansion at the backward-facing step, with a prominent pressure drop in the recirculation zone behind the ribs. The increase of ribs number results in a relatively non uniform pressure distribution. The different configurations exhibit significant pressure changes, including high-pressure areas at the first rib forward corner and a pronounced pressure drop behind the last rib backward corner. This indicates potential challenges to combustion stability and efficiency. MCRD5, with four ribs and 2 mm spacing, demonstrates a more favorable pressure distribution compared to MCRD4, emphasizing the impact of spacing on pressure behavior. MCRD6, and MCRD7 configurations, featuring five and six ribs with varying spacing, display distinct pressure patterns corresponding to their trapezoidal shape of ribs. Notably, the pressure contours in MCRD6 and MCRD7 suggest a high flow separation, indicating potential disadvantages for combustion stability. Transitioning to reacting conditions, pressure behavior provides additional insights. While MCRD1, MCRD2, MCRD3, MCRD5 maintains pressure patterns similar to non-reacting conditions. In MCRD4 under reacting conditions, the presence of rib at the outlet induce high-pressure zones at the inlet, posing challenges for flow efficiency and pumping energy required. MCRD6 and MCRD7 configurations maintains a similar high pressure drops, showcasing the impact of rib spacing on combustion stability.

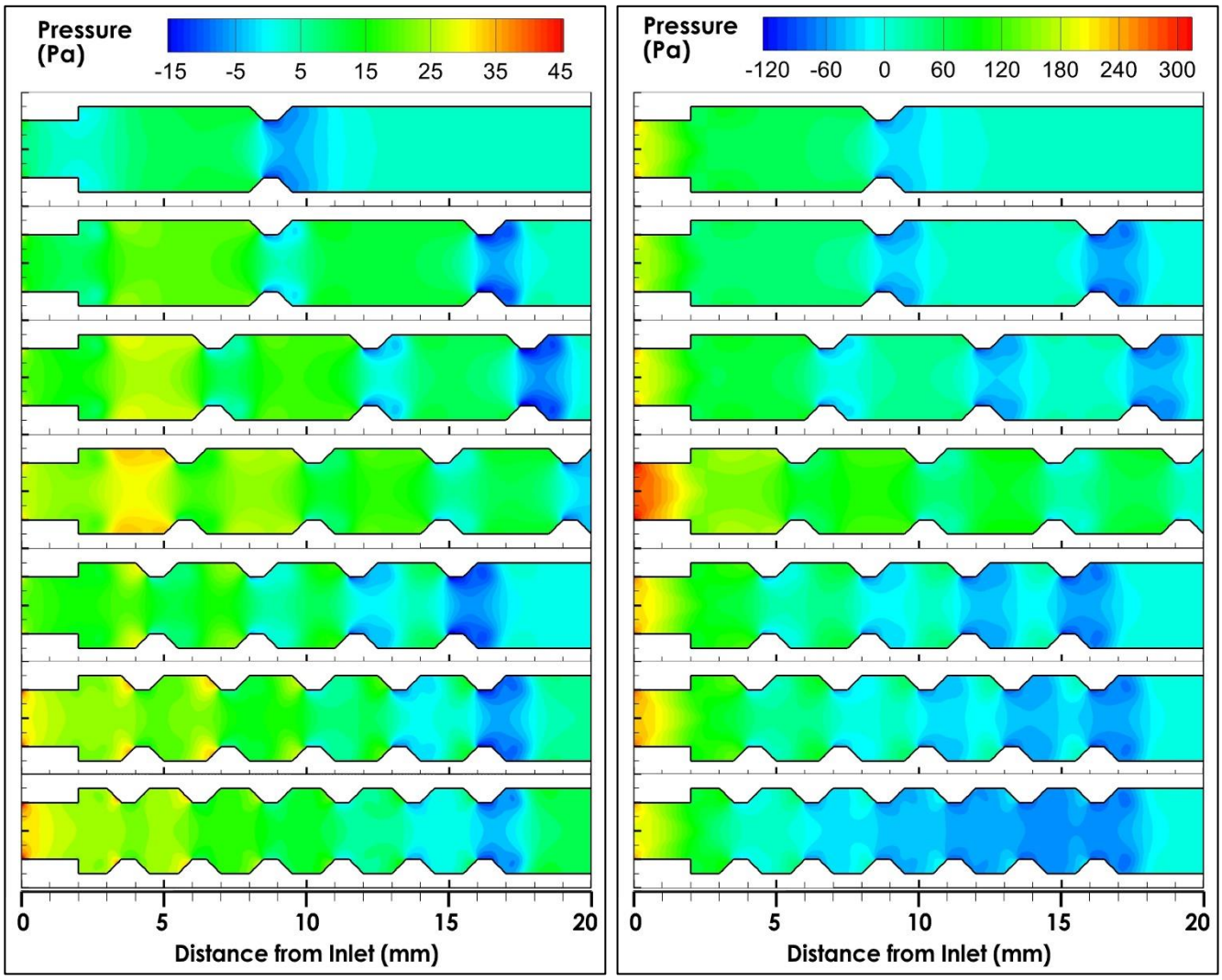

(a) *(b)*

Figure IV.1.28. *(a) Non-reacting flows, and (b) reacting flow static pressure contours for the different micro-combustor configurations: Effect of number (spacing).*

- ***Turbulence Level***

Turbulence Kinetic energy

Figure IV.1.29 illustrates turbulent kinetic energy (TKE) contours for both non-reacting and reacting flow conditions within various micro combustor configurations (MCRD1-7). In the non-reacting flow conditions, the TKE contours exhibit distinct patterns, particularly in the recirculation zones behind the backward-facing steps and trapezoidal-shaped ribs. As the number of ribs increases from MCRD1 to MCRD7, a discernible trend emerges. The additional ribs contribute to heightened TKE levels in the recirculation zones, indicating increased kinetic energy resulting from enhanced flow separation. Moving from MCRD1 to MCRD7 involves a systematic reduction in the distance between ribs, showcasing a refined configuration. This refinement is evident in the more intricate TKE contours, reflecting a more intricate flow field influenced by the arrangement of ribs. The reduced spacing intensifies the recirculation zones' impact, emphasizing the crucial role of rib geometry in shaping turbulence dynamics. Transitioning to reacting flow conditions, it becomes apparent that the modifications in rib number and spacing also impact combustion-related TKE. The TKE contours under reacting conditions illustrate the intricate interplay between combustion processes and the modified flow field. The increased TKE levels persist, suggesting that the alterations in rib configuration not only influence flow separation but also have implications for combustion efficiency.

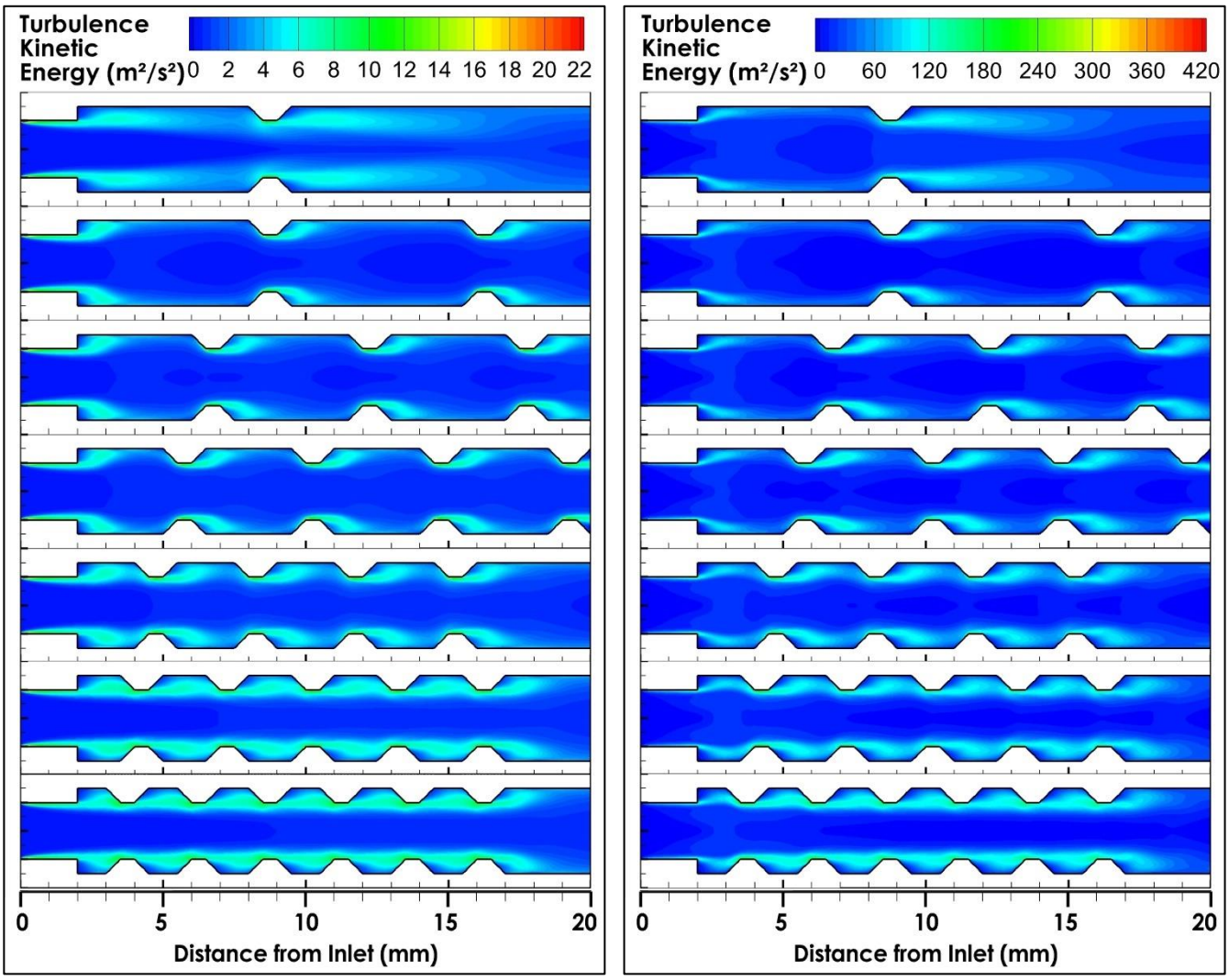

Figure IV.1.29. *(a) Non-reacting flows, and (b) reacting flow Turbulent kinetic energy (TKE) contours for the different micro-combustor configurations: Effect of shape.*

Turbulence Intensity

Figure IV.1.30 illustrates turbulence intensity (TI) contours for both non-reacting and reacting flow conditions within various micro combustor configurations (MCRD1-7), providing insights into turbulence levels and their implications for combustion processes. The exploration of turbulence intensity across different micro combustor configurations (MCRD1-7) sheds light on the intricate relationship between the number of ribs and the spacing between them in both non-reacting and reacting flow scenarios. In non-reacting conditions, the turbulence intensity contours exhibit distinct patterns, particularly accentuated in the recirculation zones behind the backward-facing steps and trapezoidal-shaped ribs. As the number of ribs increases from MCRD1 to MCRD7, a discernible trend emerges, indicating a heightened level of turbulence intensity associated with the introduction of additional ribs. The reduction in the distance between ribs, as seen in the transition from MCRD1 to MCRD7, contributes to a more intricate and intensified turbulence intensity. The refined configurations underscore the impact of rib trapezoidal shape on turbulence dynamics, with the reduced spacing accentuating the turbulence levels in key regions, especially around the ribs. Transitioning to reacting flow conditions, the influence of ribs number and spacing on turbulence intensity become significant. The contours of turbulence intensity under reacting conditions reveal an increased level of turbulence and complex interplay between combustion processes and the modified flow field. The increased turbulence intensity, particularly around

the ribs and recirculation zones, suggests that the alterations in rib number and spacing have a dual effect, influencing both flow dynamic.

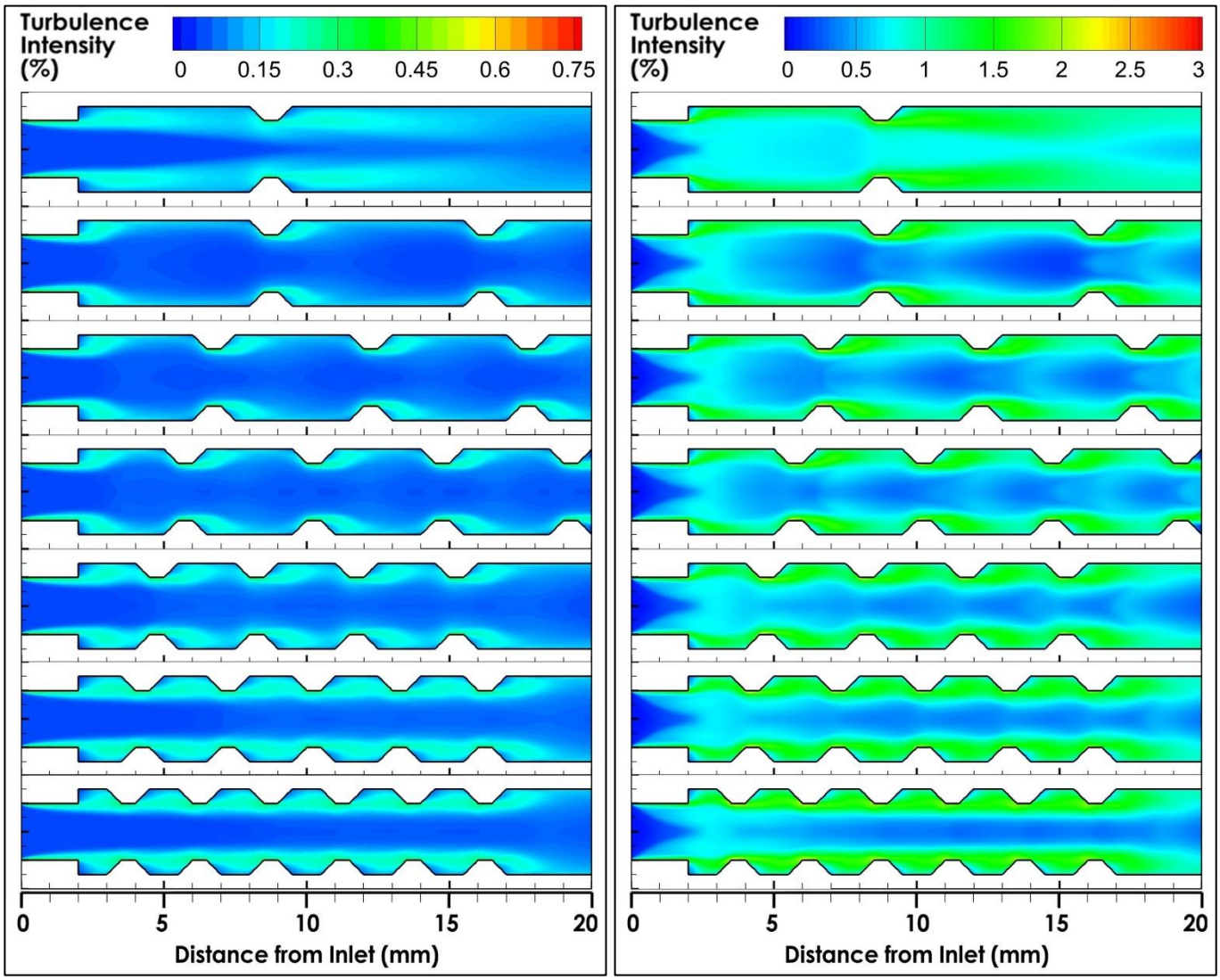

(a) *(b)*

Figure IV.1.30. *(a) Non-reacting flows, and (b) reacting flow Turbulence Intensity contours for the different micro-combustor configurations: Effect of number (spacing).*

Vorticity dynamics

Figure IV.1.31 displays vorticity contours for both non-reacting and reacting flow conditions within various micro combustor configurations (MCRD1-7), revealing vorticity patterns and their impact on combustion processes. In non-reacting scenarios, these contours offer crucial insights into the vorticity distribution of each configuration. MCRD1 exhibits distinctive patterns in the recirculation zone behind the backward-facing step, showing increased vorticity due to flow separation. In the absence of ribs in MCRD1's second channel, vorticity levels are comparatively lower, indicating smoother and more uniform flow behavior. As the number of ribs increases, vortices become pronounced and complex, especially behind the steps and ribs. The reduction in distance between ribs enhances vortices magnitude, emphasizing the role of trapezoidal geometric features in shaping flow vorticity dynamics. The absence of ribs on the outlets is advantages, as it mitigates the proportion of reverse flow occurrence. Furthermore, the increase of ribs number and reduction of distance between them beyond four ribs and 2 mm, respectively shows a stretching effect and causes a non-uniform flow disrupting the intended streamline and may induce flow instabilities which may lead to disrupting the combustion process and may affect combustion stability. The ignition of chemical reactions, elevated levels of vorticity in the recirculation

zones, posing challenges for combustion efficiency. These vorticity contour observations underscore the significance of rib design, number and spacing in shaping vorticity levels, providing valuable information for combustion modeling and stability assessment in micro combustors.

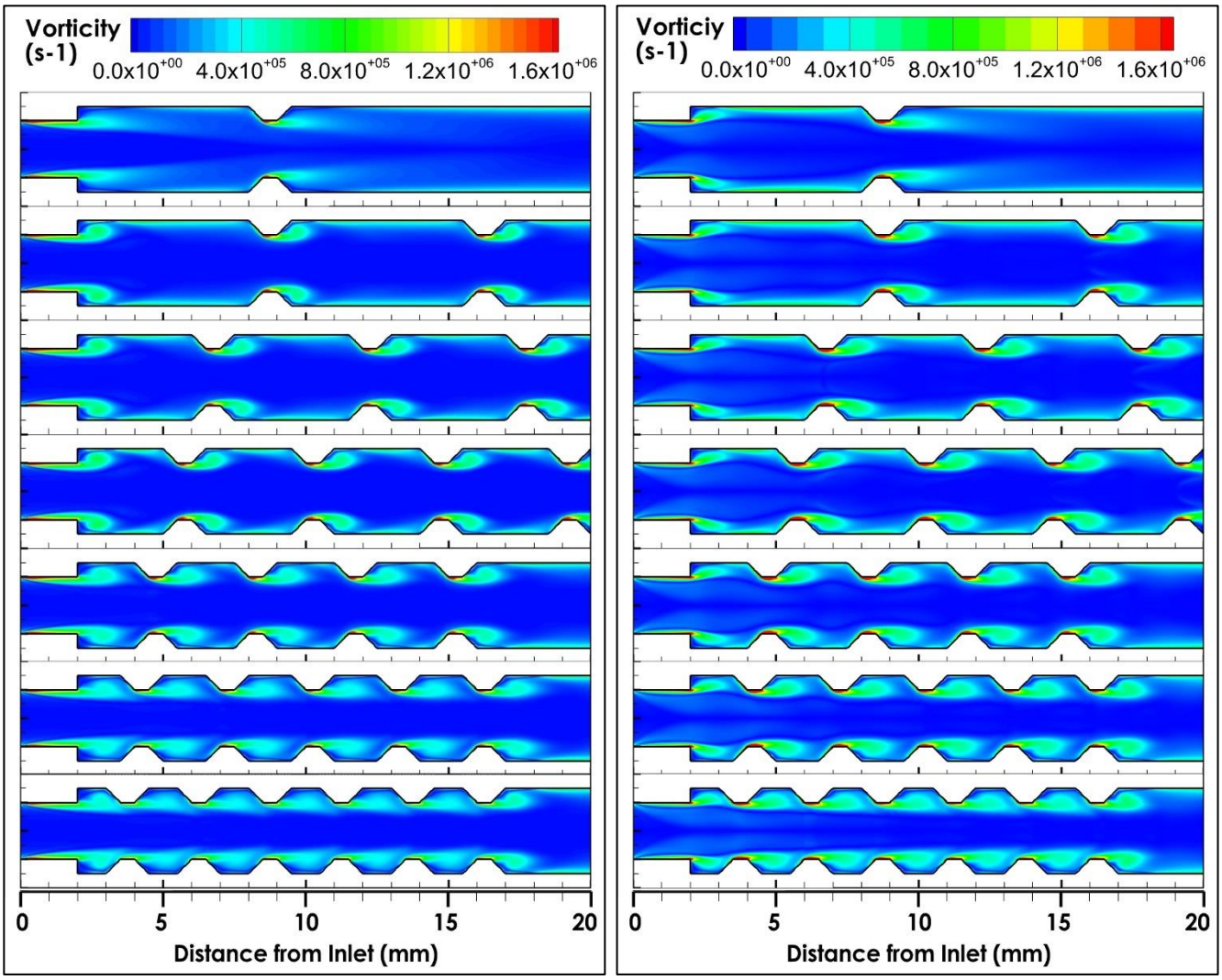

Figure IV.1.31. *(a) Non-reacting flows, and (b) reacting flow Turbulence Vorticity contours for the different micro-combustor configurations: Effect of number (spacing).*

The micro combustor configuration with four ribs (MCRD5) and a spacing of 2 mm between them stands out as a favorable design, showcasing distinct advantages when compared to other configurations (MCRD1-7). The choice of four ribs, strategically equidistantly positioned with a 2 mm spacing, results in a balanced and optimized flow field with enhanced turbulence characteristics. MCRD5 demonstrates superior control over the flow field, with the four ribs effectively manipulating the turbulent kinetic energy (TKE) distribution. The equidistant spacing ensures a well-defined recirculation zone behind each rib, promoting efficient mixing of reactants and combustion products. The deliberate reduction in spacing between ribs to 2 mm enhances the impact of recirculation zones, emphasizing the critical role of rib geometry in shaping turbulence dynamics. This refined spacing contributes to a more intricate and effective flow control mechanism. MCRD5 strikes an optimal balance between the number of ribs and their spacing, avoiding the extremes observed in configurations with fewer or more ribs. This balanced design showcases the importance of careful consideration of geometric parameters for micro combustor optimization.

- ***Flow Efficiency***

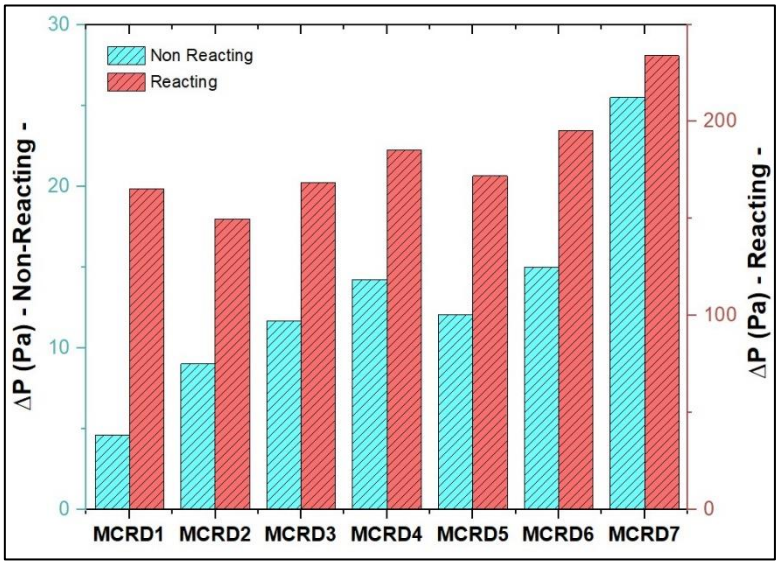

Figure IV.1.32. *Non-reacting flows and reacting flow pressure difference (ΔP) for the different micro-combustor configurations: Effect of number (spacing).*

Figure IV.1.32 visually represents the pressure differences (ΔP) between the inlet and outlet for each micro combustor configuration under both non-reacting and reacting flows. Analyzing the results presented in the figure, it's evident that under non-reacting conditions, all configurations display relatively low-pressure differences. Remarkably, the pressure differences exhibit a substantial increase with the initiation of chemical reactions which is attributed to the additional resistance introduced by combustion, resulting in elevated pressures within the micro combustors. Under non-reacting conditions, the configurations exhibit varying degrees of pressure drop, with MCRD1 showing the lowest ΔP of 4.62907, followed by MCRD2 at 9.01864, MCRD3 at 11.67611, MCRD4 at 14.22706, MCRD5 at 12.05296, MCRD6 at 14.98772, and MCRD7 with the highest ΔP of 25.4947. Upon initiation of chemical reactions (reacting conditions), a significant increase in pressure differences is observed across all configurations, indicating the impact of combustion on flow resistance. Specifically, MCRD1 experiences a notable surge in ΔP to 165.4966, followed by MCRD2 at 149.8848, MCRD3 at 168.7181, MCRD4 at 185.5081, MCRD5 at 172.0043, MCRD6 at 195.4815, and MCRD7 with the highest ΔP of 234.0016. These quantified pressure differences provide a comprehensive understanding of how each micro combustor configuration responds to reacting flows, highlighting the influence of design parameters on flow stability and efficiency. Notably, MCRD5 demonstrates favorable flow-field characteristics, particularly the 2 mm interspace between the ribs succeed in managing pressure differences, with showing relatively lower values compared to configurations MCRD4, MCRD6, and MCRD7 which exhibit higher pressure differences, implying increased flow resistance and energy dissipation under both non-reacting and reacting conditions. These configurations may experience challenges in maintaining stable flow conditions and optimizing combustion stability and efficiency. The configuration MCRD5 indicates not only better flow control and reduced energy losses, but also a relatively similar residence time compared to configurations MCRD1, MCRD2, and MCRD3 suggesting enhanced efficiency and performance. Overall, the findings underscore the importance of ribs number and interspace between them in optimization of micro combustor design to mitigate pressure losses and improve operational effectiveness.

However, **Table IV.1.10** presents the pumping energy values for various micro combustor configurations under both non-reacting and reacting conditions, along with the corresponding effect of reactions. The differences in pumping energy among configurations under non-reacting conditions are relatively subtle, reflecting the baseline energy needed to maintain fluid flow without the additional complexities of

combustion. It is observed that the pumping energy increases progressively with the introduction of additional ribs and refinement of spacing between them. Furthermore, all configurations exhibit relatively low pumping energy requirements. Among the configurations, MCRD6 has the highest pumping energy demand, followed closely by MCRD7. This trend suggests that the increasing of ribs number and reducing the distance between them, impose higher resistance to flow, necessitating greater energy input. Interestingly, the effect of reactions amplifies this trend, indicating that the combustion process further exacerbates the energy requirements. This can be attributed to the additional energy demands associated with fuel combustion, leading to heightened flow resistance. This augmentation is particularly pronounced in MCRD6 and MCRD7, indicating that the combustion process significantly raises the energy demands in these specific number of ribs and spacing between them. Furthermore, MCRD4, MCRD6 and MCRD7 requires the highest pumping energy under both non-reacting and reacting conditions, underscoring its heightened resistance to flow due to its geometric features. Conversely, MCRD5 exhibits the most favorable flow-field characteristics, achieving a delicate equilibrium between efficient flow dynamics, optimal turbulence levels, and manageable pressure drops. These findings emphasize the complex interplay among geometric configuration parameters, rib number, spacing, and flow-field attributes, accentuating the significance of optimizing design parameters to elevate both overall performance and efficiency.

Table IV.1.10. *Pumping energy of micro combustor configurations under non reacting and reacting conditions: Effect of number (spacing).*

Geometric Configuration	$MCRD_1$	$MCRD_2$	$MCRD_3$	$MCRD_4$	$MCRD_5$	$MCRD_6$	$MCRD_7$
Non-reacting	1.32E-5	2.58E-5	3.34E-5	3.44E-5	4.06E-5	4.28E-5	7.28E-5
Reacting	4.73E-4	4.28E-4	4.82E-4	4.91E-4	5.30E-4	5.59E-4	6.69E-4
Effect of Reactions	4.6E-4	4.02E-4	4.48E-4	4.57E-4	4.89E-4	5.16E-4	5.96E-4

in (W)

b. Combustion Characteristics

- ***Flame Dynamics***

Flame Shape

The investigation into the combustion characteristics and flame dynamics in reacting flows among micro combustor configurations (MCRD1-7) provides critical insights into the interplay between geometric features and chemical reactions. **Figure IV.1.33,** displaying hydrogen H_2 and hydroxide OH mass fraction contours, facilitates the elucidation of reaction zone and flame shape, respectively. By visualizing H_2 and OH mass fraction contours, the reaction zone and flame shape are elucidated, respectively. Across all configurations, the reaction zone in the upstream channel consistently appears thin and conical, denoted in yellow, indicating minimal geometry effects on its shape. However, variations in the remaining hydrogen distribution, represented by H_2 mass fraction contours in dodger blue, are observable, particularly around backward-facing steps and initial pairs of ribs in MCRD3-7. The interspace in these configurations, referred to as the cavity, significantly influences the flow dynamics by effectively trapping remaining hydrogen residues. This trapped hydrogen residue near the reaction zone plays a crucial role in enhancing combustion efficiency. The impact of the interspace becomes particularly pronounced when it ranges from 3mm to 1mm. Notably, the MCRD5 configuration, featuring 4 ribs and 2mm interspace, exhibits superior patterns and effectively maintains the trapped hydrogen residues within the cavity which may promotes combustion efficiency. Consequently, the selection of ribs number and inter-rib spacing emerges as crucial design parameters, as it influences combustion efficiency and the prevention of issues such as flame quenching or excessive stretching of flame become important.

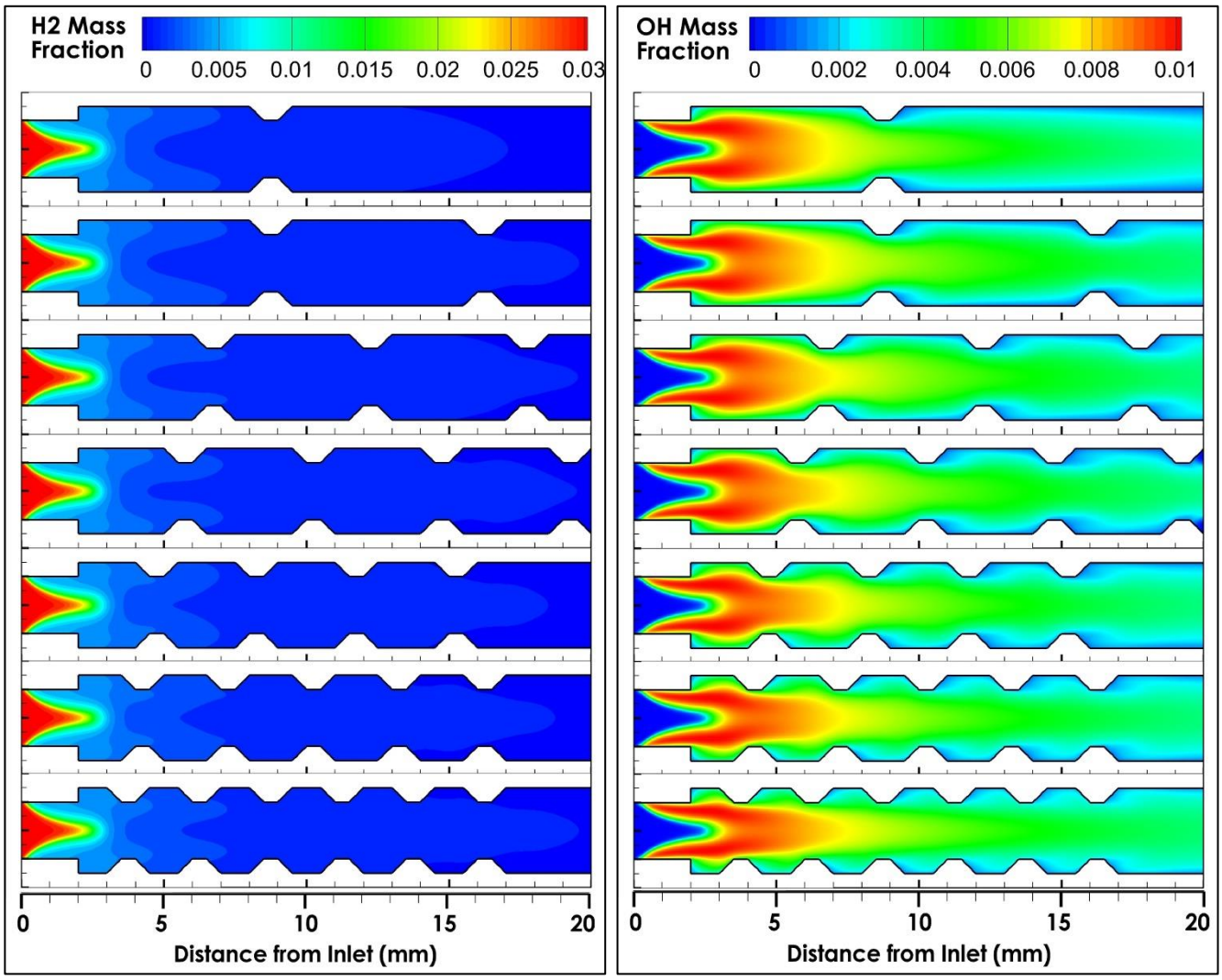

(a) *(b)*

Figure IV.1.33. *(a) Hydrogen H_2 and (b) Hydroxide OH mass fraction contours for the different micro-combustor configurations: Effect of number (spacing).*

Hence, the OH mass fraction contours, representing the flame shape, provide further insights into these combustion dynamics. In configurations MCRD1, MCRD2, and MCRD3, where the first rib is positioned sufficiently far from the flame front, exhibit minimal influence on its shape. Conversely, in MCRD4, with an inter-rib spacing of 3mm, leads to the entrapment of reaction gases, drawing them towards the inner wall of the micro combustor. This phenomenon subtly alters both the shape and front of the flame, inducing a slight distortion. Furthermore, MCRD5, with an inter-rib spacing of 2mm, exhibits a similar effect, trapping reaction gases slightly closer to the inner wall and pushing the flame front further. Notably, the vena contracta phenomenon, in combination with the angled edges of the first trapezoidal rib, affects the flame width, reducing it significantly compared to previous configurations. This effect becomes more pronounced in MCRD6 and MCRD7, where the second rib is also closer to the flame front, resulting in a sharper and narrower front shape. However, the recirculation zones generated behind the backward-facing steps, contribute to the stretching of flame. This stretching is efficiently moderated by the angled edges of trapezoidal ribs. Comparing to MCRD1, the introduction of more ribs significantly impacts the OH mass fraction distribution, with each additional rib introducing unique fluid dynamics that influence the formation and behavior of OH radicals. The positioning of the first rib and the choice of an appropriate inter-rib spacing of 2mm, as seen in MCRD5, play a crucial role in ensuring smooth flow and preventing excessive stretching of flame compared to configurations with smaller spacing. Overall, this comprehensive analysis underscores the intricate relationship between micro combustor geometrical

configuration, flow and combustion dynamics, emphasizing the need for meticulous consideration of the ribs number and interspace as geometrical parameters to optimize combustion efficiency and prevent issues like flame quenching or excessive stretching.

Flame front location

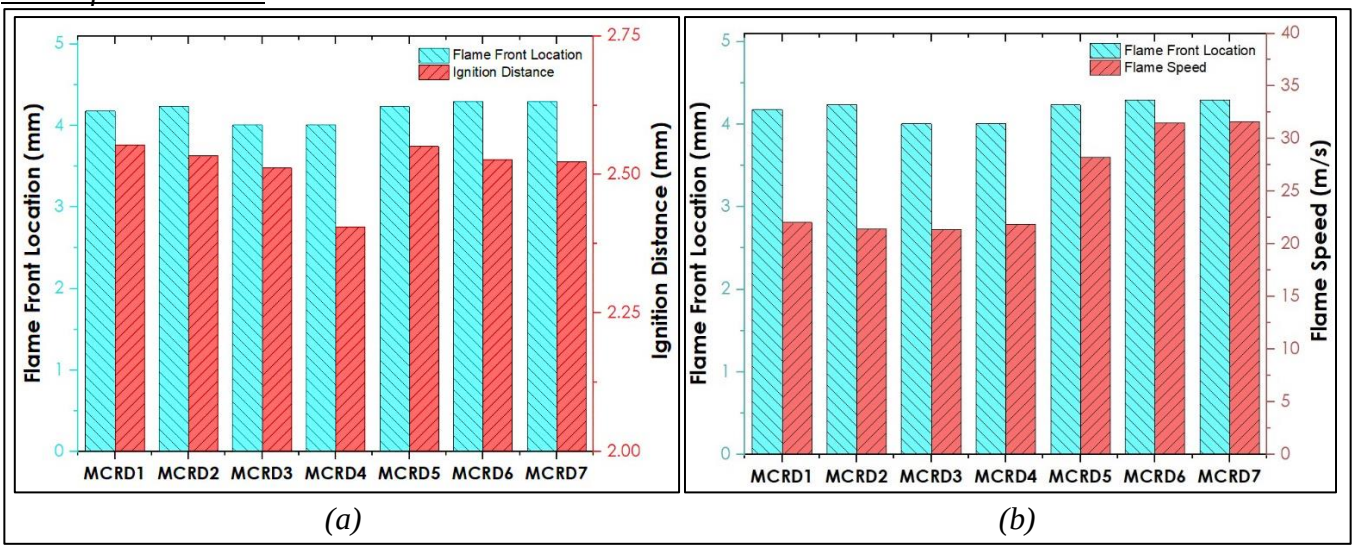

Figure IV.1.34. *Flame front location, ignition distance (a) and flame speed (b) for different micro-combustor configurations: Effect of number (spacing).*

Analyzing the flame front location, ignition distance and flame speed across the various micro combustor configurations (MCRD1-7) provides valuable insights into the influence of ribs number and interspacing on combustion dynamics. Following the method stressed by Li et al. [70] **Figure IV.1.34** illustrates these characteristic parameters, revealing notable trends and behaviors. However, the flame front location is a critical parameter indicating where the combustion process initiates and progresses within the micro combustor. Looking at the results, it is evident that across all configurations (MCRD1-7), slight variations in flame front location are present. For instance, MCRD1 and MCRD2 exhibit similar flame front locations, with values around 4.2 mm. However, MCRD3 and MCRD4, shows a slightly shorter flame front location at approximately 4.0 mm, indicating a quicker initiation of combustion compared to previous configurations. This trend suggests that variations in rib number and interspacing can affect the spatial distribution of combustion within the micro combustor. However, MCRD5, with four trapezoidal ribs and 2 mm interspace, exhibits a more significant impact on flame front location, with value exceed 4.23 mm. Moving to MCRD6 and MCRD7, with further reduced interspacing, display slightly longer flame front locations at 4.29 mm. This indicates that reducing the interspace between the ribs does not significantly affect the flame front location. On the other hand, the ignition distance represents the distance from the micro combustor inlet to the point where combustion initiates. Examining the results in the **Figure IV.1.34** *(a)*, it's evident that the ignition distances vary slightly across the different configurations. MCRD1, MCRD2, and MCRD3 exhibit ignition distances ranging from 2.55 mm, 2.53 mm, to 2.51 mm, respectively. These configurations demonstrate relatively consistent ignition behavior, with minor variations attributed to differences in ribs number and interspacing between them. Furthermore, MCRD4 and MCRD5, display ignition distances of approximately 2.41 mm and 2.55 mm. Moving to MCRD6 and MCRD7, the ignition distances decrease to 2.53 mm and 2.52 mm. These findings indicate that the presence of ribs and their spacing has a negligible effect on the ignition distance, indicating that ignition primarily depends on other factors such as fuel-air mixture composition and ignition source characteristics.

Flame speed

Figure IV.1.34 *(b)* illustrates the variations in flame speed at which the fuel-air mixture is consumed through the various micro combustor configurations (MCRD1-7), reflecting the rate of combustion and energy release. Regarding the results, notable variations in flame speed are observed across the configurations. MCRD1, MCRD2, and MCRD3 demonstrate decreasing flame speeds, ranging from approximately 22.04 m/s and 21.43 m/s to 21.36 m/s, respectively. These configurations exhibit consistent combustion behavior, with minor fluctuations attributed to variations in geometric features and flow dynamics. On the other hand, MCRD4 showcases a flame speed of approximately 21.87 m/s, while MCRD5 demonstrates a significantly higher flame speed of approximately 28.23 m/s. This disparity suggests that the geometric features, particularly the rib shape and interspace, play a crucial role in influencing combustion dynamics and flame propagation. Moreover, MCRD6 and MCRD7 demonstrate flame speeds of approximately 31.52 m/s and 31.62 m/s, respectively, indicating there's a more pronounced variation among the configurations. This indicates that the number and spacing of ribs have a considerable impact on flame propagation, with configurations featuring closer ribs resulting in faster flame speeds. However, the heightened flame speed observed is attributed to increased turbulence resulting from the higher number of ribs and reduced inter-rib spacing. This intensified turbulence enhances the diffusion rate of reactants and products facilitating faster mixing and interaction between reactants, leading to a faster combustion process. Consequently, incoming reactants experience greater preheating, promoting rapid ignition and accelerate flame propagation speed.

- ***Combustion Efficiency***

- ***Combustion Intensity***

Figure IV.1.35 presents the average kinetic reaction rates for various elementary reactions within each micro combustor configuration (MCRD1-7). Each configuration exhibit’s distinct reaction rates across the range of chemical processes involved. Analyzing these results provides insights into how the geometric features and design parameters influence combustion intensity and efficiency. For instance, there is a consistent pattern of reaction rates across the configurations for various elementary reactions. Certain reactions exhibit higher rates, indicating their prominence in the combustion process. Notably, the elementary reactions 3, 8, 9, and 16 consistently demonstrate elevated rates across all configurations. However, reactions 16 and 17 exhibit negative rates, suggesting a depletion or inhibition effect within the reaction mechanism. On the other hand, the elementary reaction 20 consistently exhibits a negligible rate or even a negative value, suggesting its limited contribution to combustion. The variations in rates for other elementary reactions can be attributed to the geometric differences in the micro combustor configurations. Examining the results, reveals that the MCRD5 configuration demonstrates generally higher reaction rates across most elementary reactions compared to all other configurations except MCRD7. This suggests that the specific design features of MCRD5, possibly related to the ribs' number and spacing, facilitate more efficient combustion processes and higher reaction rates. On the other hand, MCRD7 shows the most elevated rates across various reactions, underscoring its effectiveness in enhancing combustion kinetics. Moreover, the contrast in reaction rates between configurations underscores the importance of optimizing micro combustor design to enhance combustion efficiency and performance. By adjusting parameters such as ribs' number and interspacing, it's possible to influence reaction kinetics and improve overall combustion characteristics.

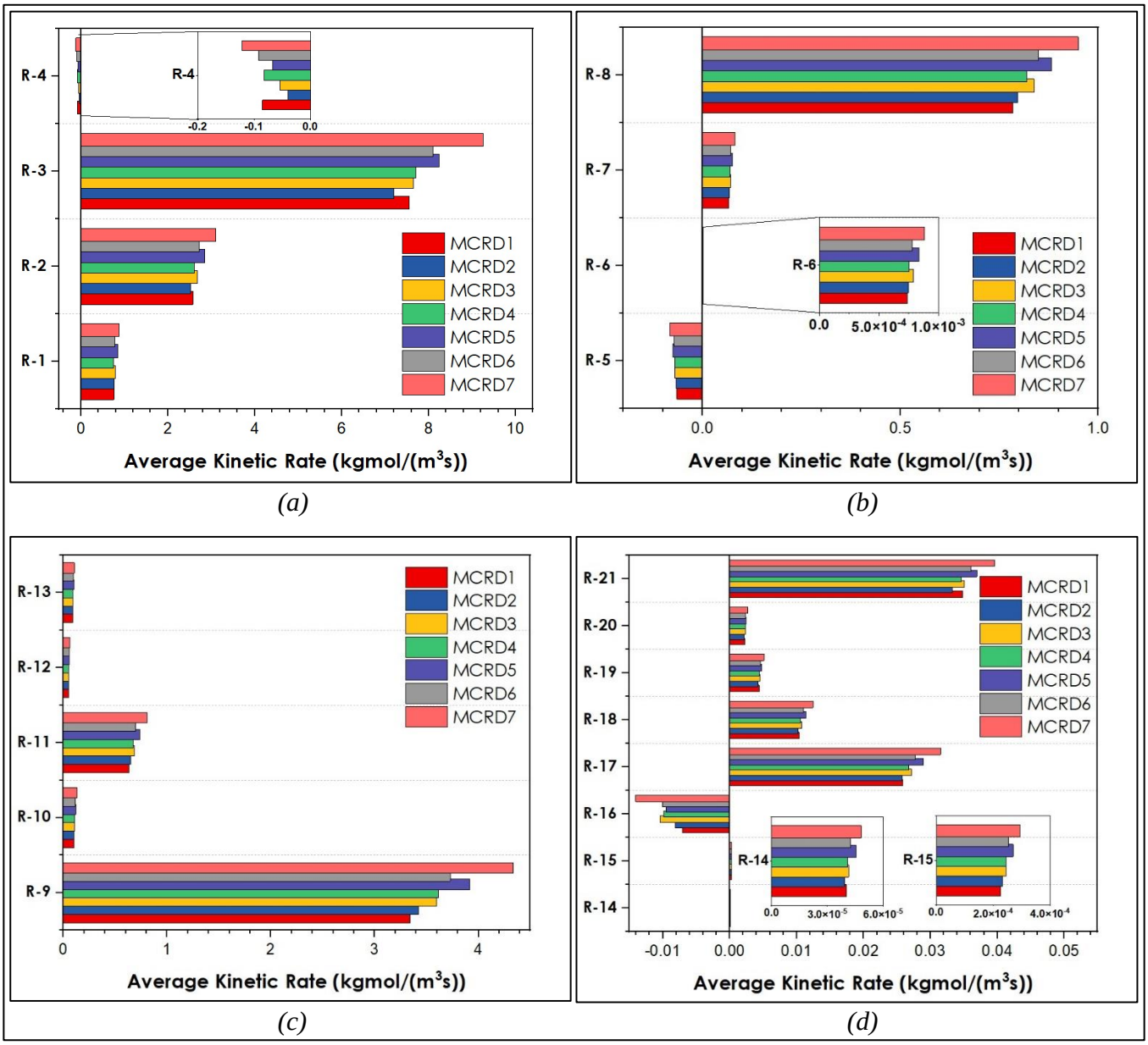

Figure IV.1.35. *Average kinetic rate of different elementary reactions for the different micro-combustor configurations: Effect of number (spacing).*

- ***Conversion Efficiency***

Figure IV.1.36 illustrates the average mass fraction of hydrogen at the outlet boundary for various micro combustor configurations (MCRD1-7) and the corresponding variations in micro combustion conversion efficiency. These metrics are crucial in assessing the combustion performance and efficiency of each configuration. Analysis of results reveals that MCRD5 stands out with the lowest outlet hydrogen mass fraction, indicating more complete combustion compared to other configurations. Correspondingly, MCRD5 exhibits the highest conversion efficiency, nearing 98%. This suggests that the design features of MCRD5 promote efficient combustion and maximize the utilization of hydrogen fuel. While MCRD1, MCRD2, MCRD3, MCRD4, and MCRD6 also demonstrate relatively high conversion efficiencies above 96%, their outlet hydrogen mass fractions are slightly higher compared to MCRD5. Moreover, MCRD7 shows a similar outlet hydrogen mass fraction to MCRD5, but with a slightly lower conversion efficiency. The superior performance of MCRD5 in terms of both outlet hydrogen mass fraction and conversion efficiency highlights the effectiveness of its design features, such as ribs number and spacing, in promoting complete combustion and maximizing fuel conversion. These findings emphasize the

importance of ribs number and spacing as geometrical parameters in optimizing micro combustor to enhance combustion efficiency and overall performance.

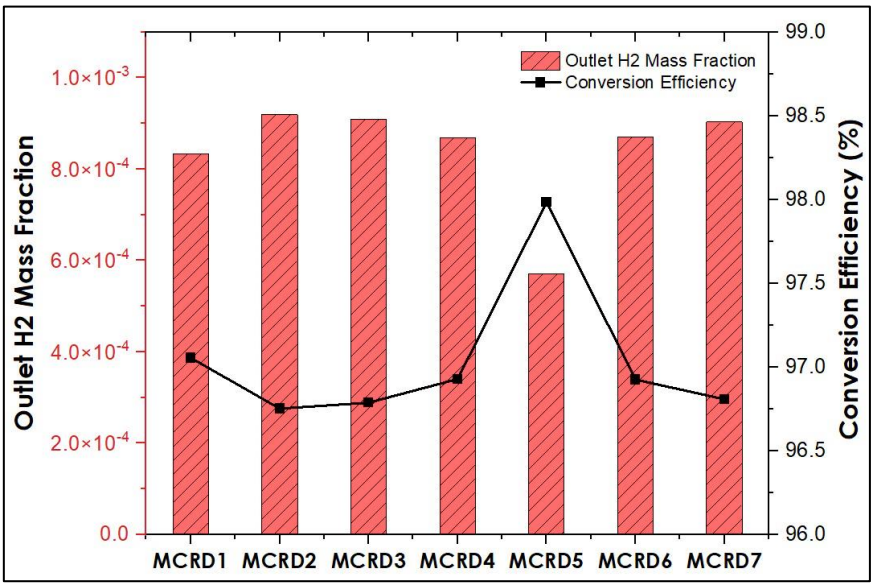

Figure IV.1.36. *Outlet H_2 mass fraction and Combustion efficiency for the different micro-combustor configurations: Effect of number (spacing).*

c. Thermal Characteristics

- ***Temperature Distribution***

Figure IV.1.37 *(a)* presents temperature contours for both gas and solid phases across various combustor configurations, employing distinct legends for each phase to enhance visibility. These contours provide valuable insights into the effects of increasing rib number and reducing inter-rib spacing on temperature distribution within both gas and solid phases. Additionally, they elucidate the influence of heat transfer mechanisms, particularly convective and conductive mechanisms, within and between the gas and solid phases. The temperature distribution within the gas phase across different configurations is observed to be well-distributed, with the ribs effectively shifting heat closer to the inner wall surface compared to traditional MCSD designs. This phenomenon is more pronounced with higher rib numbers and reduced inter-rib spacing. The turbulent flow generated by the ribs creates vortices that retain hot combustion gases in recirculation zones, enhancing gas mixing and increasing the presence of hot spots within the micro combustors. Furthermore, the increase in rib number and reduction in interspacing significantly impact the temperature distribution within the solid phase. As a result, solid phase temperature contours become more uniform, particularly showing higher temperatures near the outlet. The increased rib number also amplifies the surface area available for convective heat transfer, leading to more efficient heat transfer from combustion gases to the inner walls of the combustor. Consequently, MCRD1 exhibits the lowest solid phase temperatures among all configurations. However, MCRD4 displays slightly lower solid phase temperatures near the outlet compared to MCRD3 and MCRD5, which can be attributed to the positioning of the last rib near the outlet and unfavorable flow dynamics. On the contrary, MCRD2, MCRD3, MCRD5, MCRD6, and MCRD7 all demonstrate increasing solid phase temperatures and slightly decreasing gas phase temperatures with the increase in rib number and reduction in inter-rib spacing. This observation highlights the intricate relationship between flow dynamics, combustion dynamics, and heat transfer mechanisms, especially convective mechanism. This indicates the complex interplay between rib configurations, flow dynamics, combustion dynamics, and convective heat transfer mechanisms. Furthermore, **Figure IV.1.22** *(b)* provides a distinct depiction of the reaction zone within the different micro combustor configurations (MCRD1-7). As illustrated, the increase in rib number and reduction in interspacing between them seem to have minimal impact on the shape of the reaction zone

across the various micro combustor configurations. Despite the lack of significant alterations in reaction zone shape, the geometrical arrangements resulting from the increase in rib number reveal important differences in the amount of heat released by each reaction zone. For instance, the heat released by the reaction zones varies slightly from 12.93 W for MCRD1 and MCRD2 to 12.98 W for MCRD3. Conversely, MCRD4 exhibits the lowest generated heat of reaction, with a value of 10.97 W. Furthermore, MCRD5, MCRD6, and MCRD7 demonstrate increased heat released by chemical reactions with the increase in rib numbers and reduction of inter-rib spacing, reaching values of 13.144 W, 13.21 W, and 13.34 W, respectively. These observed differences in heat release underscore the intricate interplay between combustion dynamics, heat transfer, and geometric features within the micro combustor.

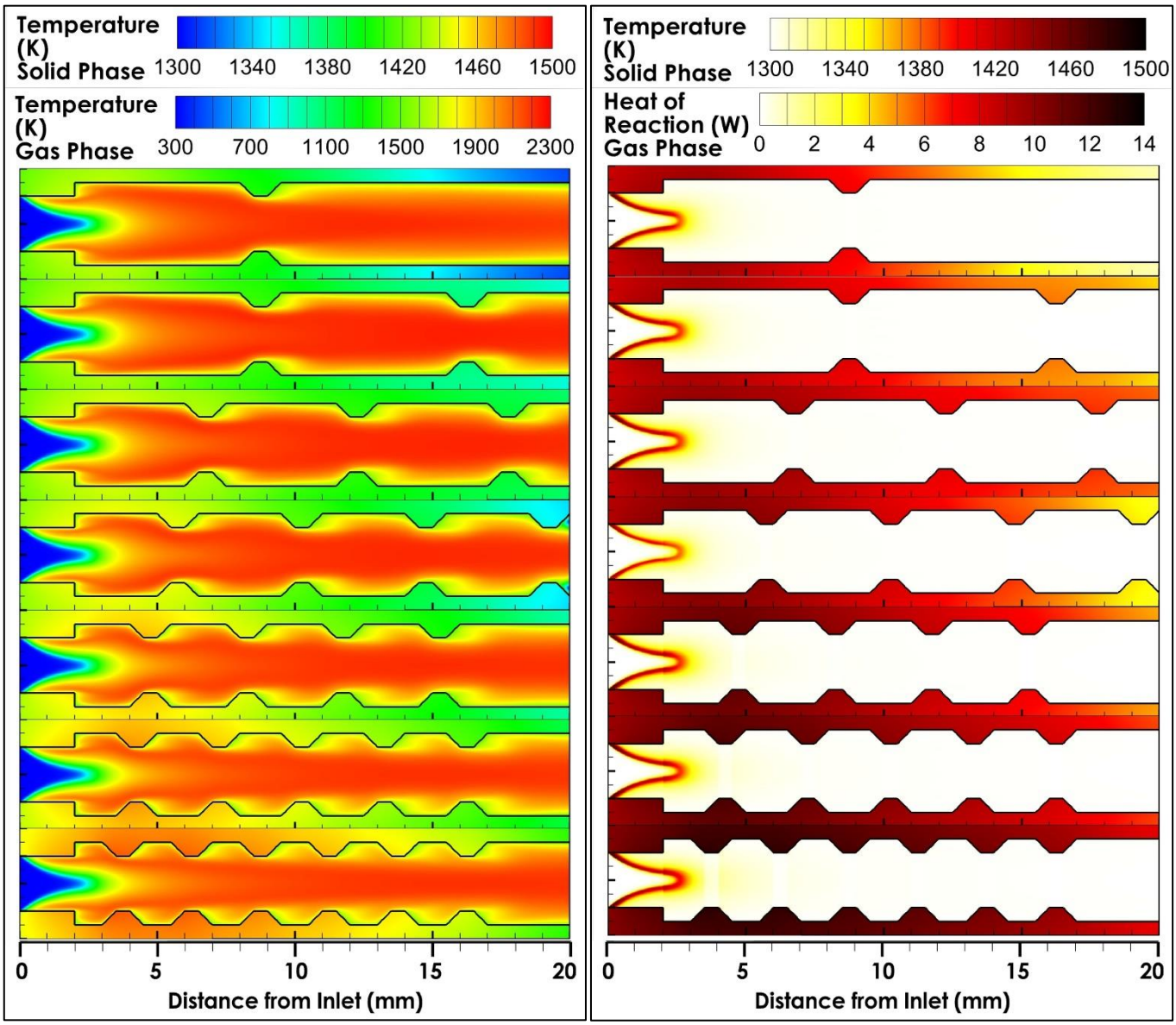

Figure IV.1.37. *(a) Temperature and (b) Heat of reaction contours for fluid phase and solid phase of the different micro-combustor configurations: Effect of number (spacing).*

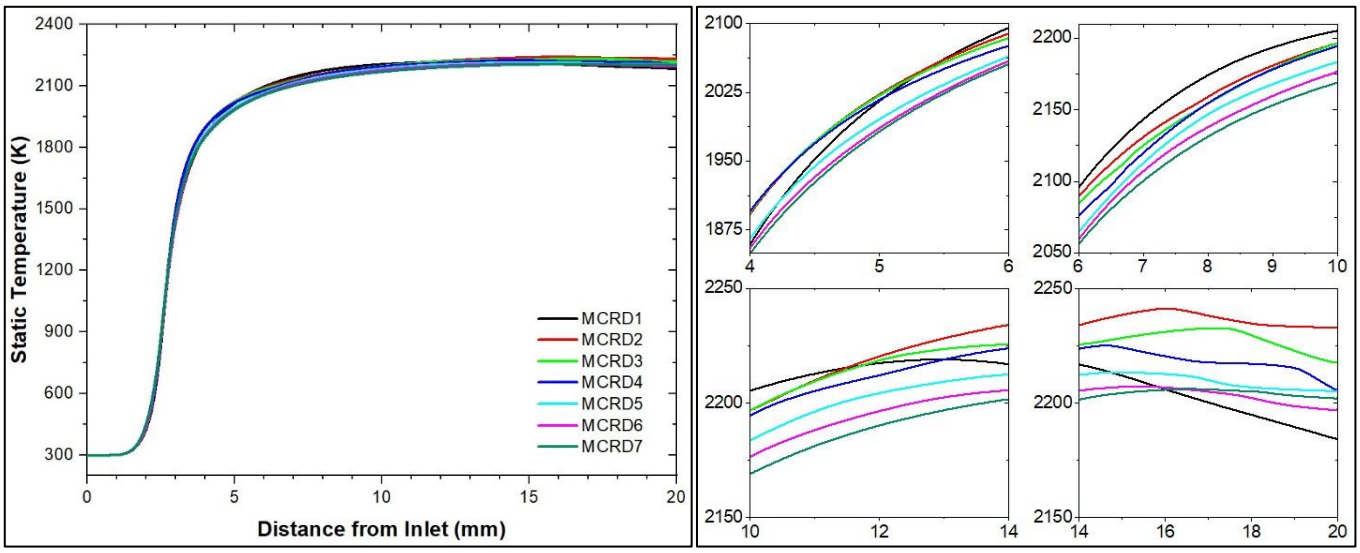

Figure IV.1.38. *Temperature distribution along the micro-combustor centerline for the different micro-combustor configurations: Effect of number (spacing).*

Figure IV.1.38 illustrates the temperature distribution along the centerline of various micro combustor configurations. However, the temperature profiles across the gas phase of different configurations shows approximately uniform distributions along the centerline. Despite, the zoom view to the different regions of micro combustor reveals slight differences between the profile's temperature levels. It is evident that the temperature profiles of different micro combustor configurations (MCRD1-7), exhibit a gradual decreasing levels starting from 10 mm to the outlet of the various micro combustor configurations. The temperature profiles shift slightly from each other and decreases respectively with the increase of ribs numbers. This observation is consistent with the aforementioned effect of ribs number in promoting a turbulent flow field, enhancing convective heat transfer, and facilitating the mixing of gases closer to the inner wall surface. Hence, the temperature profiles tendencies directly result from the enhancement of the inner wall surface area by increasing ribs numbers and reducing inter-rib spacing. Consequently, the gas phase temperature remains approximately stable for the various proposed configurations, indicating minimal adverse effects of convective heat transfer on combustion stability.

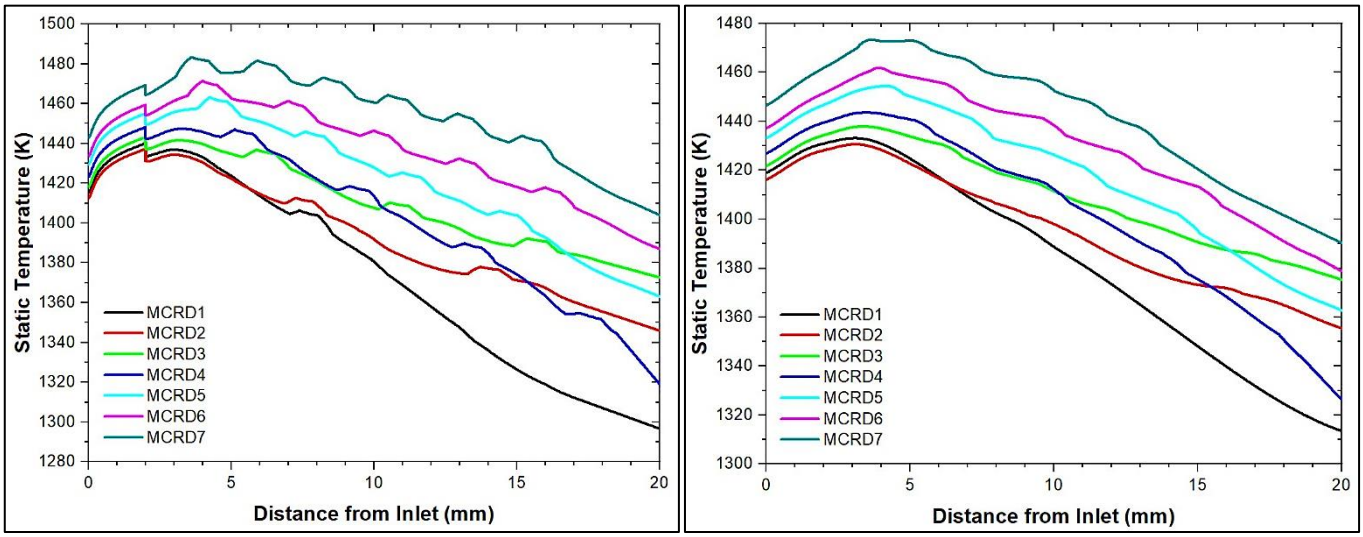

(a) *(b)*

Figure IV.1.39. *(a) Inner and (b) Outer wall temperature distribution for micro-combustor configurations: Effect of number (spacing).*

Figure IV.1.39 depicts the temperature distribution along both the inner and outer wall surfaces of different micro combustor configurations (MCRD1-7) providing valuable insights into the impact of ribs number and inter-rib spacing on thermal performance. In terms of the inner wall surface, **Figure IV.1.39** *(a)* shows that as the number of ribs increases, the temperature level shows a noticeable rise. This trend is highlighted by the distinct trace of rib shapes in the temperature profiles, indicating points of highest temperature levels coinciding with the locations of the ribs. This observation underscores the role of ribs in intensifying convective heat transfer and augmenting temperature levels along the inner walls. Ultimately, the increase of ribs number, enhances temperature level and increase the distribution uniformity which contributes to improvement of combustion and heat transfer efficiency. Furthermore, on the outer wall surface depicted by **Figure IV.1.39** *(b)*, a similar trend is observed. As rib numbers increase, the temperature profiles indicate a higher level and more uniform distribution. This suggests that the enhancement of inner wall convective heat transfer create a more efficient heat transfer process in the outer wall of configurations increasingly and proportionally with the increase of ribs number and reduction of spacing. Considering conductive heat transfer through the solid phase, it is evident that configurations with higher rib numbers exhibit decreased conductive heat losses. This observation underscores the importance of geometric features, specifically the ribs number and spacing, in mitigating conductive heat losses and improving overall outer wall temperature level and distribution uniformity.

- ***Thermal Efficiency***

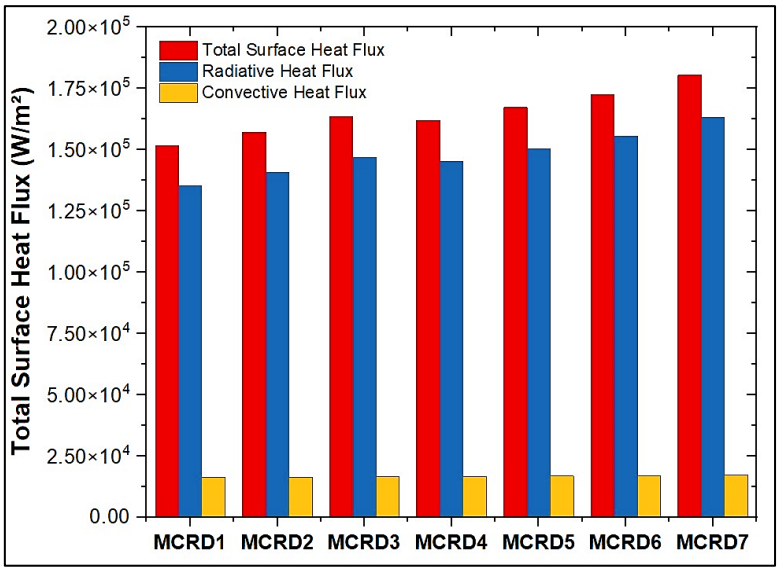

Figure IV.1.40. *The convective and radiative heat fluxes ratio to the total heat flux emitted via the outer wall for the different micro-combustors: Effect of number (spacing)*

Figure IV.1.40 provide a comprehensive overview on the heat transfer characteristics for different micro combustor configurations (MCRD1-7). The total surface heat flux, composed of convective and radiative components, is a critical parameter influencing the thermal performance of the micro combustors. The total surface heat flux, comprised of convective and radiative components, is a pivotal parameter dictating the thermal efficiency of micro combustors. Across the configurations, there's a discernible escalation in the total surface heat flux, in direct correlation with the increase in ribs number, signifying an overall enhancement in heat transfer within the combustor systems. Analyzing the individual heat flux components reveals a consistent upward trend in both convective and radiative heat fluxes across the configurations. Convective heat flux, representing heat transfer through fluid motion, maintains a relatively lower proportion of the total heat flux but exhibits a notable increase with the augmentation of ribs number and reduction in inter-rib spacing. This suggests that the presence of multiple ribs and reduced spacing fosters more efficient convective heat transfer between the outer wall and the surroundings, contributing significantly to the overall heat flux. In contrast, radiative heat flux, depicting

heat transfer through electromagnetic radiation, accounts for the highest proportion of heat transferred by the outer wall across various configurations and displays a similar increasing trend. The amplification in radiative heat flux underscores the improved thermal performance facilitated by the incorporation of multiple ribs and reduced inter-rib spacing. These observed trends in both convective and radiative heat fluxes align with expectations of enhanced heat transfer mechanisms in micro combustors. The prevalence of radiative heat flux as a proportion of the total heat flux is a particularly advantageous outcome, given its critical role in the operation of MTPV systems. The goal of enhancing MTPV system performance and conversion efficiency is thus supported by the augmentation of radiative heat flux, emphasizing the significance of optimizing micro combustor design to maximize radiative heat transfer capabilities.

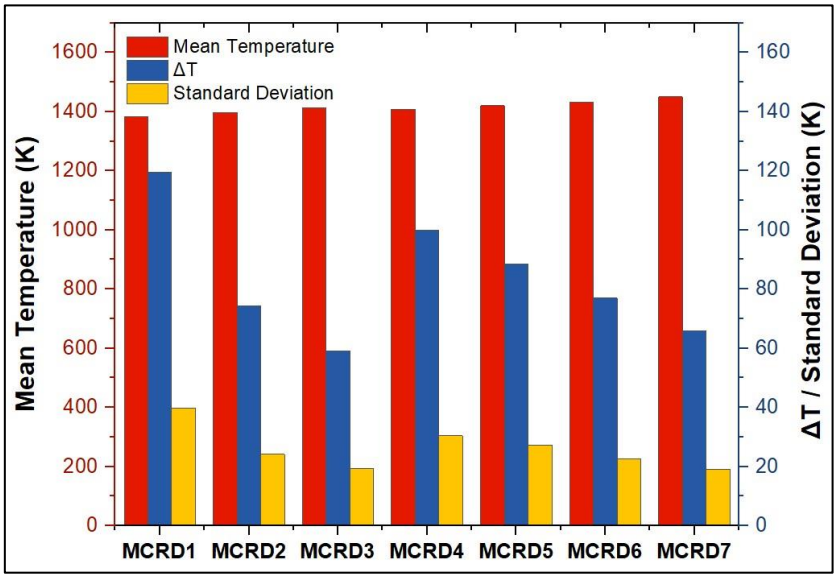

Figure IV.1.41. The outer wall: Average temperature, temperature difference and Standard deviation for the different micro-combustors: Effect of number (spacing)

In order to quantify the influence of ribs number and inter-rib spacing, the mean temperature, temperature difference, and standard deviation values presented in **Figure IV.1.41** depict the thermal performance of the outer walls of different micro combustor configurations (MCRD1-7). As observed, there is a consistent increase in mean temperature across configurations, indicating higher thermal energy levels along the outer walls with the introduction of multiple ribs and reduced inter-rib spacing. This increase in mean temperature correlates with the enhanced heat transfer facilitated by the geometric modifications. The results indicate that the mean temperature of the outer wall temperature profile slightly increases with the increase of ribs number, from 1383.23 K for MCRD1 to 1396.82 K for MCRD2. Additionally, the mean temperature of MCRD3, MCRD4, MCRD5, MCRD6, and MCRD7 increases to 1412.4 K, 1408.04 K, 1420.44 K, 1432.44 K, and 1450.12 K, respectively. Additionally, the temperature difference (ΔT) and standard deviation provide insights into the thermal stability and uniformity of the outer wall temperatures. MCRD3 and MCRD7, with lower temperature difference values of 59.05 K and 65.78 K, respectively, indicate more consistent temperature distributions, reflecting improved thermal stability. On the other hand, MCRD1 and MCRD4 show the highest temperature difference with values of 119.65 K and 100 K, respectively. However, MCRD2, MCRD5, and MCRD6 configurations show a moderate level of non-uniformity with temperature differences of 74.31 K, 88.42 K, and 76.91 K, respectively. The fluctuating trend in temperature difference (ΔT) across configurations reveals that ribs' positions had a high influence on thermal stability and uniformity along the outer walls of the micro combustors. On the other hand, the standard deviation values further emphasize the consistency and reliability of the thermal performance in configurations with higher ribs numbers. The decreased standard deviation of MCRD7 and MCRD3 of 19.17 K and 19.4 K, respectively, implies a more controlled and predictable thermal

behavior. Besides, MCRD1 and MCRD4 show the highest standard deviation with values of 39.75 K and 30.37 K, respectively. However, MCRD2, MCRD5, and MCRD6 configurations show a moderate level of non-uniformity with standard deviation values of 24.14 K, 27.26 K, and 22.6 K, respectively. These findings highlight the impact of ribs' positions on the overall thermal stability of micro combustors. Overall, the results underscore the advantageous effects of incorporating multiple ribs and reducing inter-rib spacing on the outer wall thermal performances of micro combustor configurations.

Effect of Height

a. Flow-field characteristics

To thoroughly investigate the influence of trapezoidal-shaped ribs, we adopt a comprehensive approach, delving into the additional effect of rib height on flow characteristics. In order to elucidate the combustion impact, we examine fluid flow dynamics, including velocity and pressure distribution, as well as turbulence levels, under both non-reacting and reacting flow conditions. Additionally, we quantify the efficiency of non-reacting and reacting flows across different configurations.

- ***Flow Dynamics***

- ***Stream Field***

Non-reacting flow

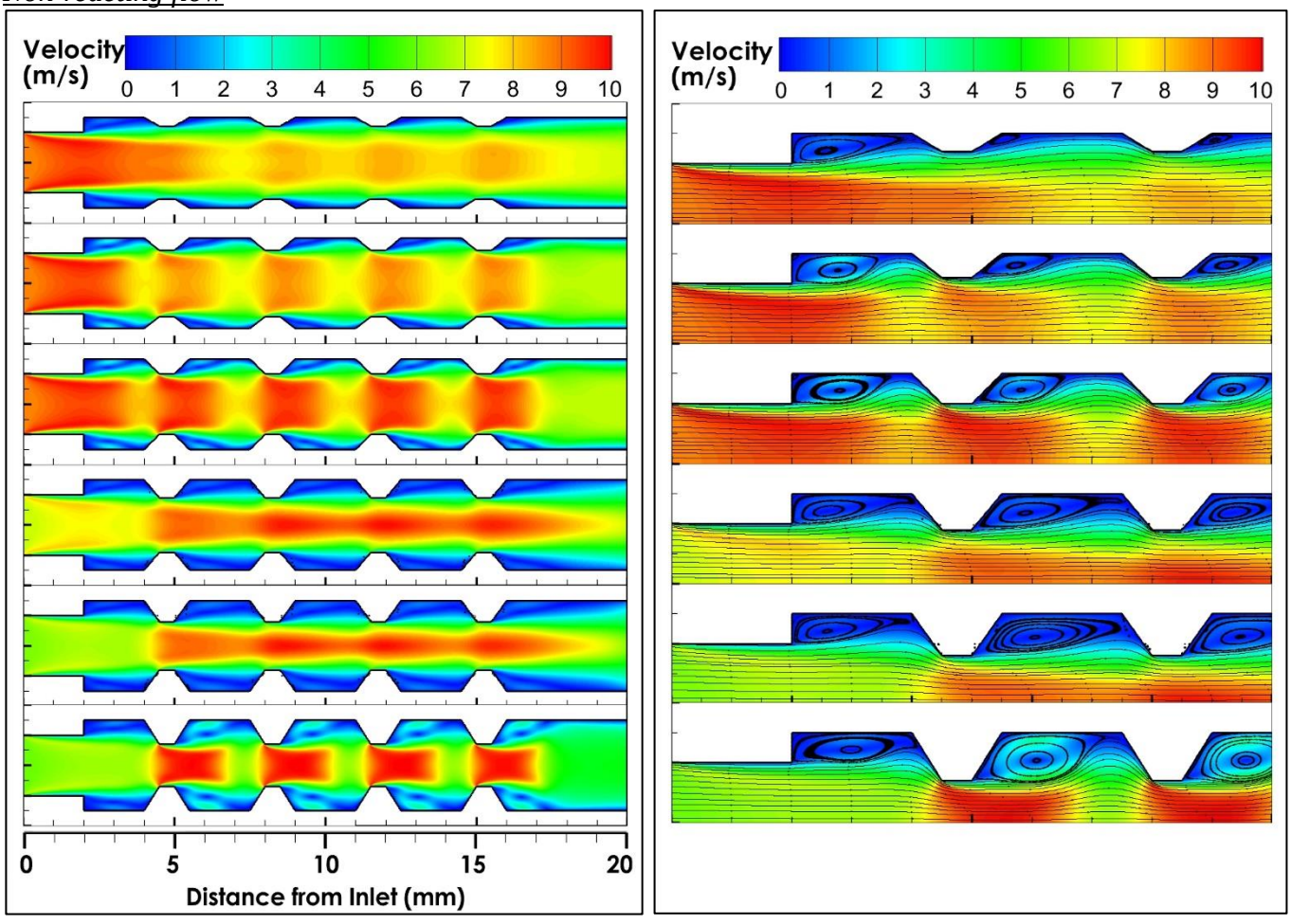

(a) *(b)*

Figure IV.1.42. *Non-reacting flow-field of different micro combustor configurations (a) velocity contour and (b) streamlines: effect of height.*

The analysis of **Figure IV.1.42** *(a)* offers valuable insights into the velocity contours of the hydrogen-air mixture within various micro combustor configurations under non-reacting conditions, with rib height as a variable. Initially, areas of flow velocity acceleration are evident upstream, consistent with previous observations on the impact of rib shape and number. However, as the flow encounters the backward-facing step and ribs, a typical deceleration occurs, resulting in the formation of recirculation zones. Notably, an increase in rib height is associated with larger recirculation zones, both in length and height, as illustrated by **Figure IV.1.42** *(b)*. This enlargement is attributed to the obstruction caused by taller ribs, which induces greater flow disturbance and recirculation. Additionally, acceleration zones are observed over the ribs, intensifying with increasing rib height, leading to the formation of multiple high-velocity zones. This acceleration is particularly evident for rib heights beyond 0.5 mm, with ribs taller than 0.8 mm exhibiting significantly intensified velocity magnitudes. Conversely, ribs with heights lower than 0.5 mm exhibit comparatively lower velocity magnitudes. The increase in rib height amplifies the phenomenon of vena contracta, potentially resulting in fluctuating flow-field dynamics and affecting flow stability. Furthermore, taller ribs contribute to the expansion of low-velocity zones, with some configurations experiencing complete cessation of flow. Overall, these findings underscore the substantial influence of rib height on flow-field dynamics, with taller ribs inducing complex flow patterns and velocity distributions.

Reacting flow

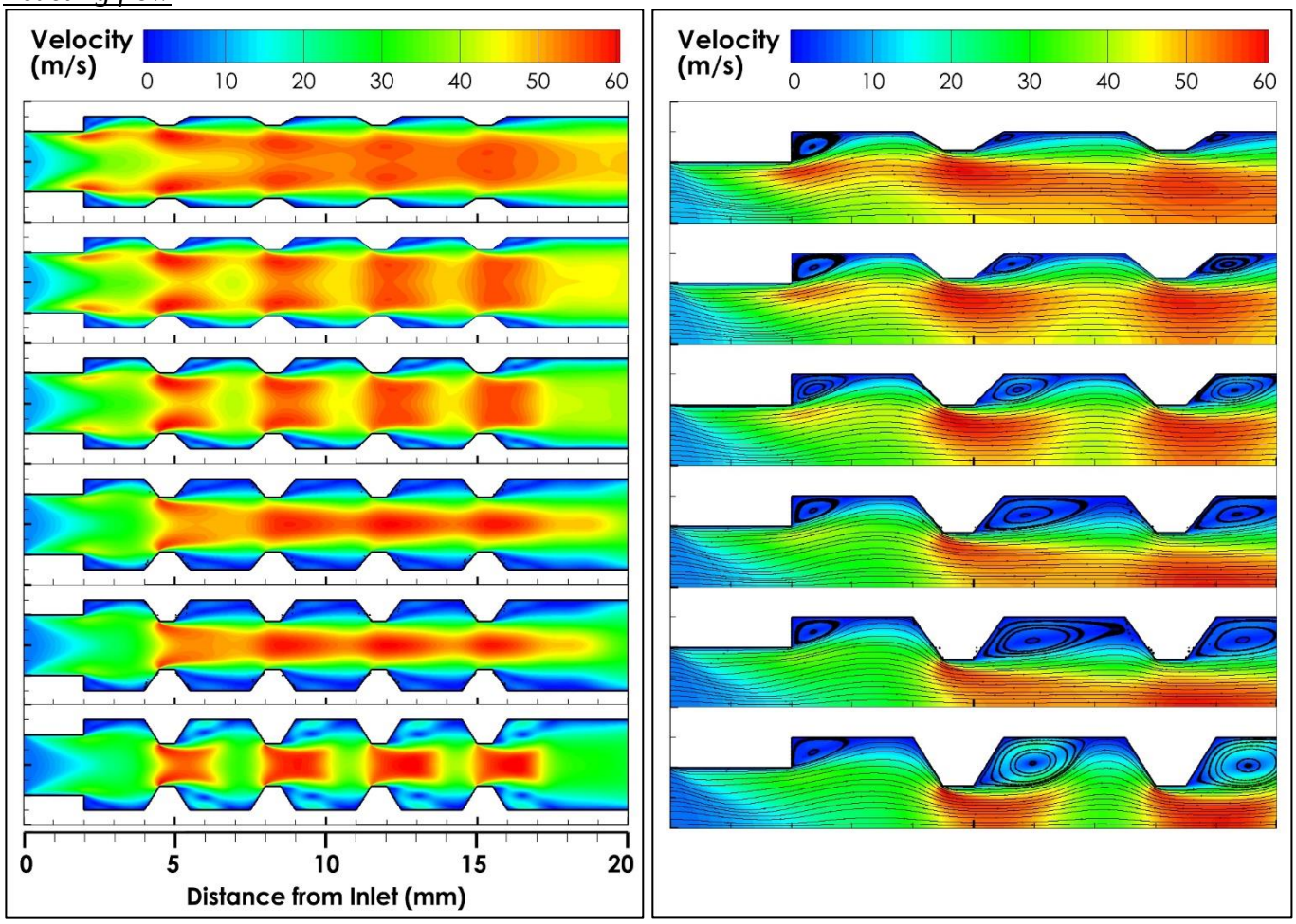

(a) *(b)*

Figure IV.1.43. *Reacting flow-field of different micro combustor configurations (a) velocity contour and (b) streamlines: effect of height.*

Transitioning to reacting flow **Figure IV.1.43**, provide invaluable insights into the dynamic interplay between chemical reactions and flow field characteristics within micro combustor configurations. As

chemical reactions are initiated, transitioning from non-reacting to reacting conditions, there's a notable surge in velocity magnitude across the configurations, reaching up to 60 m/s. Interestingly, despite this increase, the flow patterns behind the steps and ribs remain reminiscent of non-reacting conditions, maintaining characteristic recirculation zones formed by the abrupt expansion of these structures. Moreover, a distinct effect of combustion emerges within the flow field. The elongated flame, characteristic of reacting flows, exerts a pronounced pushing effect on the flow in the upstream channel, notably altering velocity contours and influencing the distribution of chemical species. Notably, this influence extends beyond the flame's immediate vicinity, pushing the recirculation zones further behind the backward-facing step towards the corner—a consistent observation across all configurations. The initiation of chemical reactions also plays a pivotal role in shaping the vena contracta phenomenon, a significant aspect of flow behavior over the ribs. As combustion occurs, there's a quantifiable increase in flow velocity, driven by the release of thermal energy. This increase is particularly pronounced over the ribs' tips, emphasizing the intricate coupling between chemical reactions and fluid dynamics at the microscale. Furthermore, the figure highlights how variations in geometric features, such as rib height, influence the flow-field dynamics under reacting conditions. The amplification of the vena contracta phenomenon with increased rib height underscores the potential for fluctuating flow-field dynamics, which in turn can impact both flow and combustion stability. Overall, the insights gleaned from this figure underscore the complex and tightly intertwined nature of chemical reactions and flow dynamics within micro combustors, offering valuable guidance for optimizing combustion efficiency and stability in these systems.

Pressure Fields

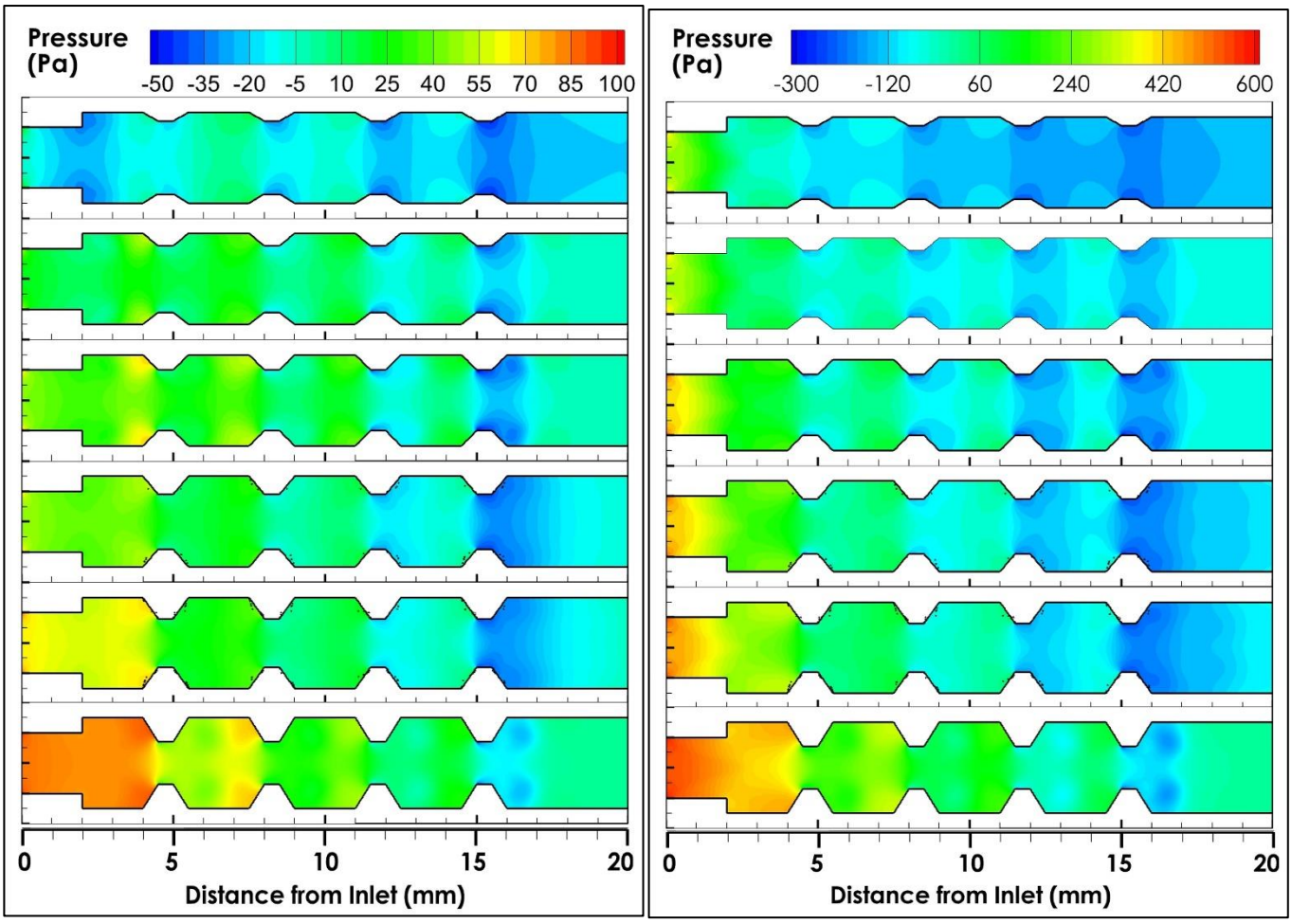

(a) *(b)*

Figure IV.1.44. *(a) Non-reacting flows, and (b) reacting flow static pressure contours for the different micro-combustor configurations: Effect of height.*

Figure IV.1.44 offers a comprehensive analysis of pressure contours in both non-reacting and reacting flow conditions across various micro combustor configurations (RD-H1 to RD-H6). The examination provides valuable insights into the effect of ribs height on pressure behavior, elucidating its implications for combustion stability and performance. Under non-reacting flow, distinctive pressure patterns are revealed for each configuration. For RD-H1, pressure contours exhibit variations corresponding to the step and ribs, with the highest pressure drop occurring in the recirculation zone behind the ribs. The increase in rib height leads to a relatively higher pressure drop. Additionally, notable pressure changes, such as high-pressure areas at the ribs forward corner and a pronounced pressure level behind the last rib backward corner, are observed, indicating potential challenges to combustion stability and efficiency. Configurations RD-H2 to RD-H4 demonstrate a more favorable pressure distribution compared to RD-H5 and RD-H6, highlighting the influence of rib height on pressure behavior. Particularly, RD-H4 to RD-H6 show indications of high flow separation, suggesting potential drawbacks for combustion stability. Transitioning to reacting conditions, pressure behavior reveals further insights. RD-H1, RD-H3, RD-H4, and RD-H5 under reacting conditions exhibit high-pressure zones at the inlet and low-pressure zones by the outlet, posing challenges for flow efficiency and increasing pumping energy requirements. RD-H1 and RD-H6 configurations demonstrate the lowest and highest pressures levels at the outlet and inlet, respectively, highlighting the impact of rib height on combustion stability. The thorough examination of pressure contours not only underscores the intricate interplay between geometric features and pressure dynamics but also provides valuable information for optimizing combustion efficiency and stability in micro combustors.

- ***Turbulence Level***

Turbulence Kinetic energy

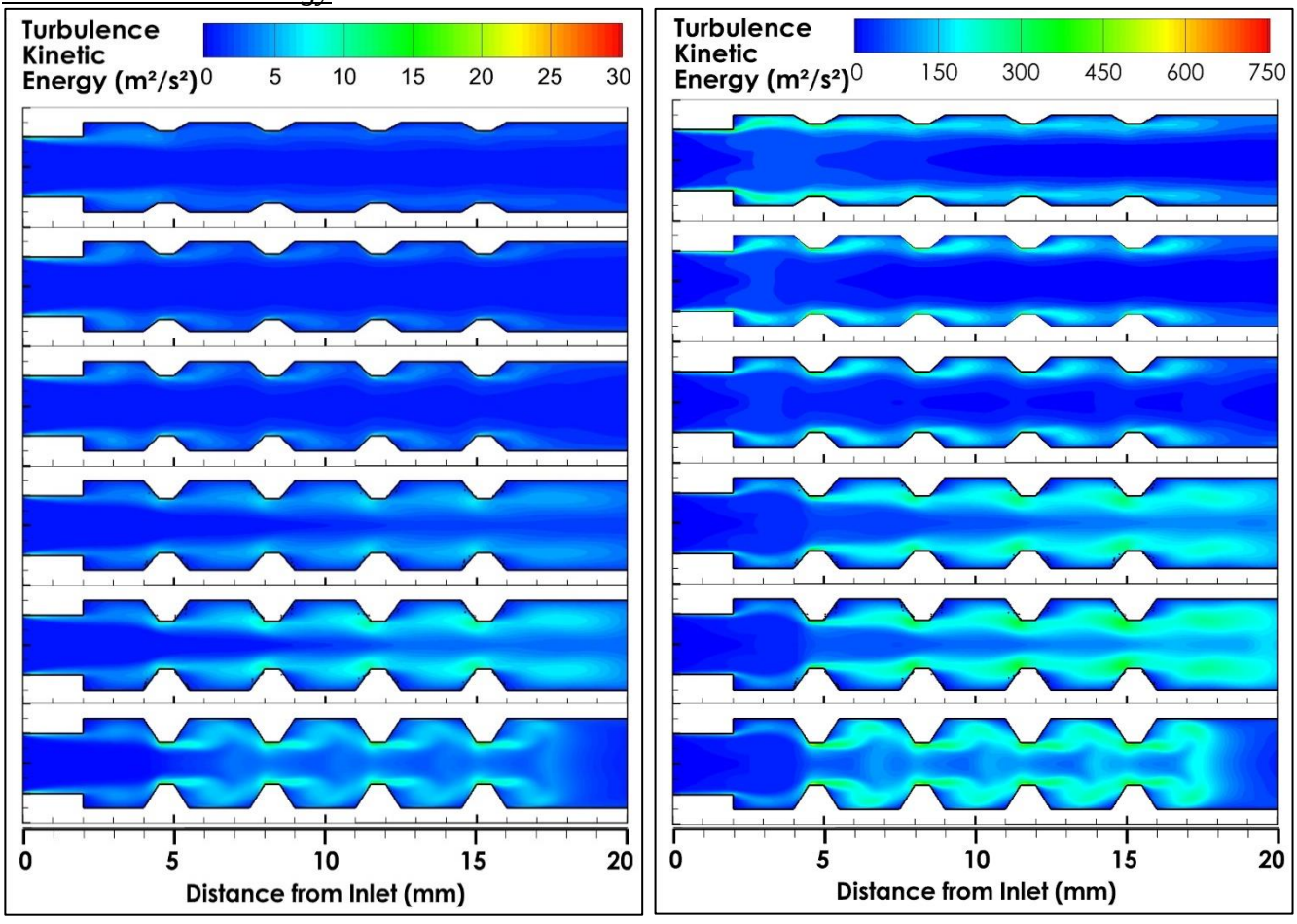

Figure IV.1.45. *(a) Non-reacting flows, and (b) reacting flow Turbulent kinetic energy (TKE) contours for the different micro-combustor configurations: Effect of height.*

Figure IV.1.45 provides an in-depth analysis of turbulent kinetic energy (TKE) contours, offering critical insights into turbulence levels and their implications for combustion processes in micro combustors. In the non-reacting conditions, configurations RD-H1 and RD-H2, characterized by ribs heights of 0.3 mm and 0.4 mm respectively, exhibit notably lower TKE levels compared to other configurations. Conversely, RD-H5 and RD-H6, featuring ribs heights of 0.7 mm and 0.8 mm, demonstrate elevated TKE levels attributed to turbulent flow separation near the front edges and behind the ribs, driven by flow reattachment and recirculation phenomena. In contrast, configurations RD-H3 and RD-H4, with ribs heights of 0.5 mm and 0.6 mm respectively, display a more balanced TKE level and distribution, suggesting a potential optimization of turbulence characteristics. Upon transitioning to reacting conditions, TKE levels escalate significantly across all configurations, particularly evident in the recirculation zones behind each step and rib. RD-H1, RD-H2, and RD-H3 configurations manifest elevated yet uniform TKE levels, indicative of efficient combustion dynamics. However, RD-H4, RD-H5, and RD-H6 configurations exhibit markedly higher TKE levels, suggesting potential challenges in maintaining combustion stability. These findings underscore the pivotal role of rib height in modulating turbulence levels, emphasizing the importance of meticulous rib height selection in optimizing passive control techniques for micro combustors.

Turbulence Intensity

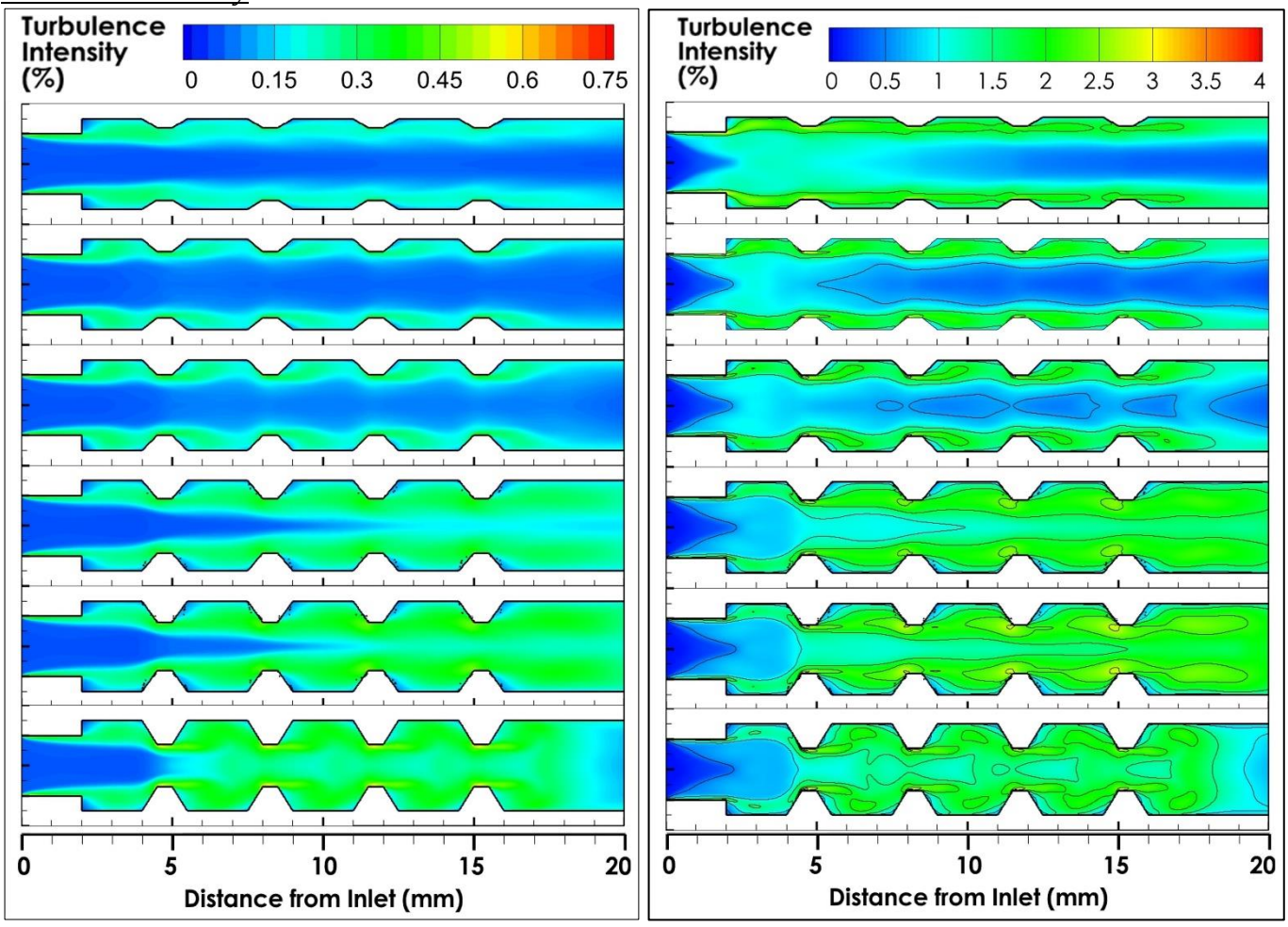

Figure IV.1.46. *(a) Non-reacting flows, and (b) reacting flow Turbulence Intensity contours for the different micro-combustor configurations: Effect of height.*

Figure IV.1.46 offers a detailed depiction of turbulence intensity (TI) contours across various micro combustor configurations (RD-H1 to RD-H6) under both non-reacting and reacting conditions. Turbulence intensity is a critical parameter in characterizing flow behavior and its impact on combustion processes. In the non-reacting conditions, we observe distinct patterns of TI distribution across the

configurations, influenced by the varying heights of the ribs. Configurations with lower rib heights, such as RD-H1 and RD-H2, exhibit comparatively lower TI levels, while configurations with higher rib heights, such as RD-H5 and RD-H6, display elevated TI levels, indicative of intensified turbulence within the flow field. Transitioning to reacting conditions, we observe a notable increase in turbulence intensity across all configurations, consistent with the activation of chemical reactions. This increase underscores the complex interplay between flow dynamics and combustion processes, with turbulence intensity playing a significant role in promoting efficient mixing and heat transfer. Furthermore, the influence of rib height on turbulence intensity becomes more pronounced under reacting conditions, with configurations featuring taller ribs exhibiting higher TI levels.

Vorticity dynamics

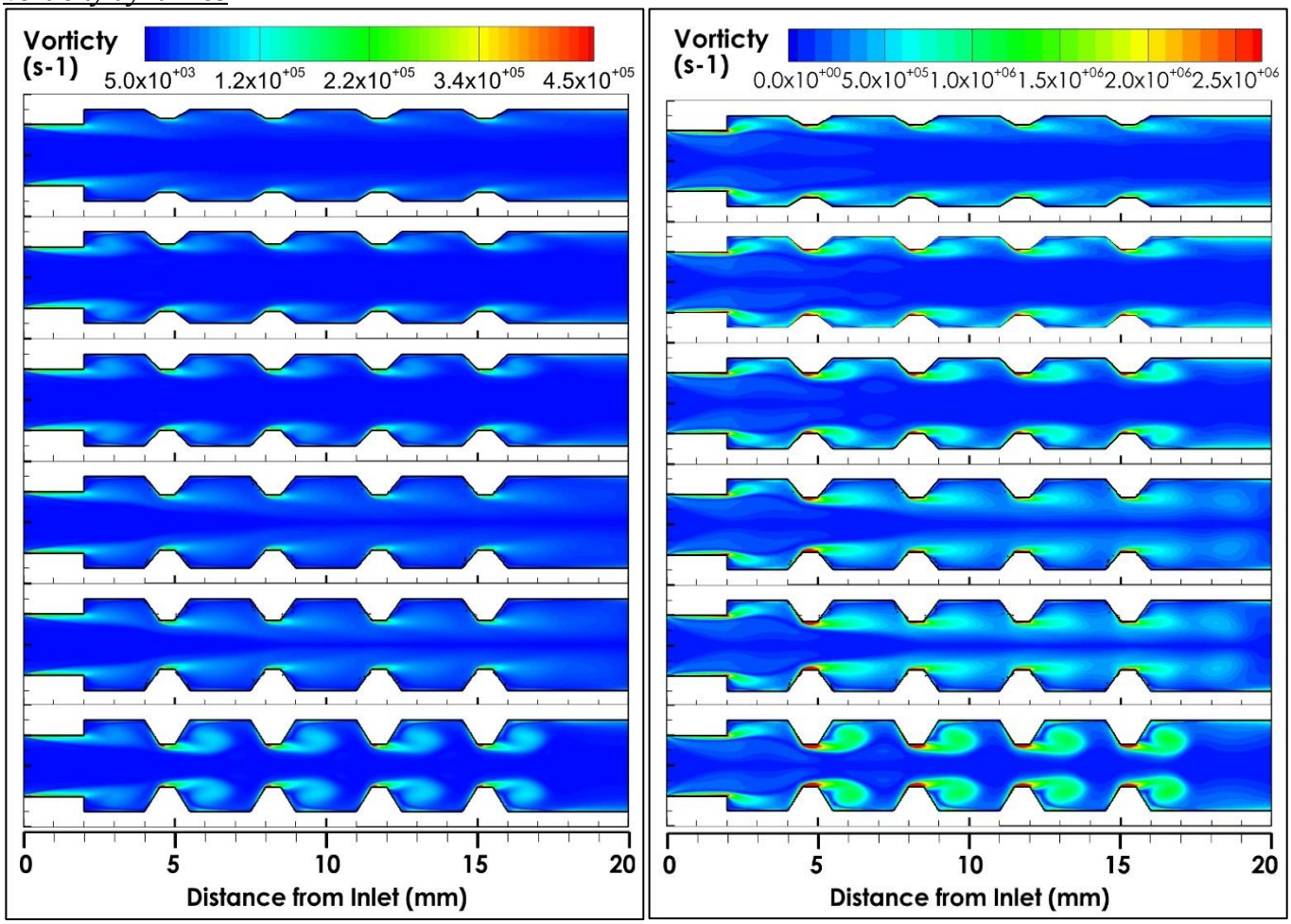

(a) *(b)*

Figure IV.1.47. *(a) Non-reacting flows, and (b) reacting flow Turbulence Vorticity contours for the different micro-combustor configurations: Effect of height.*

Figure IV.1.47 presents turbulence vorticity contours across configurations (RD-H1 to RD-H6), depicting the dynamic behavior of vorticity in micro combustors with varying rib heights under both non-reacting and reacting conditions. Vorticity, a measure of local rotation within a fluid flow, plays a crucial role in understanding flow dynamics and turbulence behavior. Under the non-reacting conditions, distinct patterns of vorticity distribution are observed across the configurations, influenced by the height of the ribs. Configurations with lower rib heights, such as RD-H1 and RD-H2, exhibit relatively lower vorticity levels, indicating less intense rotational motion within the flow. Conversely, configurations with higher rib heights, such as RD-H5 and RD-H6, display elevated vorticity levels, reflecting more vigorous vortical structures and increased turbulence intensity. Transitioning to reacting conditions, we observe significant changes in vorticity dynamics across all configurations. The activation of chemical reactions

introduces additional complexities to the flow field, resulting in alterations in vorticity patterns and behaviors. In configurations with taller ribs, such as RD-H5 and RD-H6, the vorticity contours exhibit intensified vortical structures, indicative of enhanced turbulence and mixing due to the interaction between combustion and flow dynamics. However, RD-H3 and RD-H4 configurations represent a middle ground in terms of vorticity behavior, offering a balanced approach to turbulence management in micro combustors. This highlights the importance of selecting an appropriate rib height to achieve optimal flow dynamics and combustion performance, considering factors such as turbulence intensity, mixing efficiency, and stability across various operating conditions.

- ***Flow Efficiency***

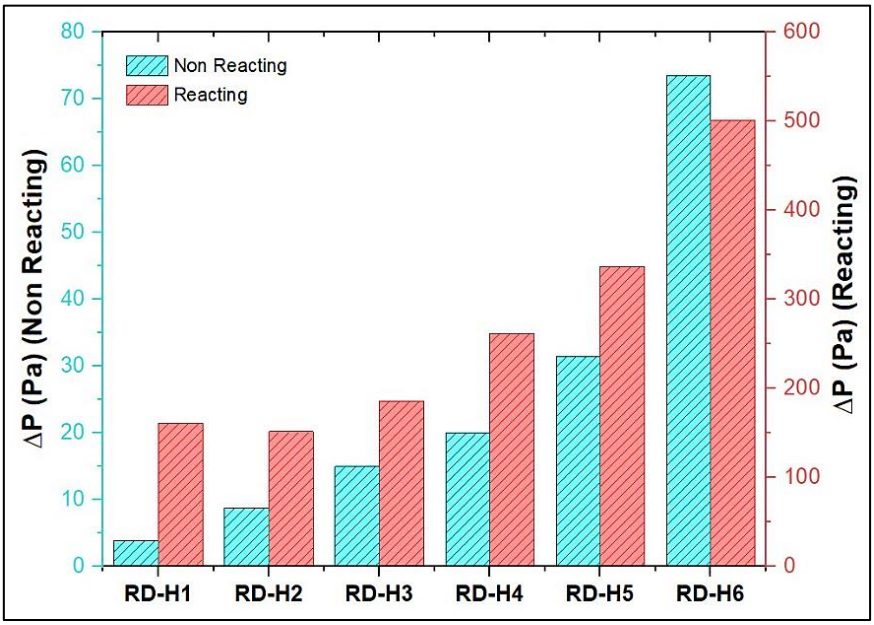

Figure IV.1.48. *Non-reacting flows, and reacting flow pressure difference (ΔP) for the different micro-combustor configurations: Effect of height.*

The pressure differences (ΔP) between the inlet and outlet of micro combustor configurations, as illustrated in **Figure IV.1.48**, offer valuable insights into flow efficiency under both non-reacting and reacting conditions. It's evident from the visual representation that the pressure differences increase significantly with the rise in ribs heights across the configurations. This observation underscores the influence of geometric features, particularly rib height, on flow resistance and pressure drop within the micro combustors. Moreover, the initiation of chemical reactions further amplifies the pressure differences across the micro combustor configurations. Comparing the static pressure values between non-reacting and reacting conditions reveals a substantial increase in pressure under reacting flows for all configurations. This phenomenon is particularly pronounced in configurations with taller ribs, where the pressure differences reach higher magnitudes due to the combined effects of flow resistance and combustion-induced pressure changes.

Table IV.1.11 offer valuable insights into the pumping energy required for micro combustor configurations under both non-reacting and reacting conditions. Pumping energy, expressed in terms of non-dimensional coefficients, provides a measure of the energy required to overcome flow resistance and maintain flow through the micro combustors. Under non-reacting conditions, the pumping energy increases progressively with the ribs' height across all configurations. This trend suggests that taller ribs impose greater flow resistance, requiring higher pumping energy to maintain flow. For instance, RD-H1 with the lowest ribs height exhibits the lowest pumping energy of 1.09 10^{-05}, while RD-H6 with the tallest ribs height requires the highest pumping energy of 2.10 10^{-04}. Transitioning to reacting conditions further exacerbates the pumping energy requirements across all configurations. The combustion-induced pressure

changes and flow disturbances significantly increase flow resistance, leading to higher pumping energy demands. Consequently, the pumping energy values under reacting conditions are substantially higher compared to non-reacting conditions for all configurations. These results highlight the importance of considering pumping energy requirements when designing micro combustors, especially concerning the selection of rib height. Optimal rib height should be carefully chosen to balance flow resistance and combustion efficiency, minimizing pumping energy requirements while ensuring adequate flow through the micro combustor.

Table IV.1.11. Pumping energy of micro combustor configurations under non reacting and reacting conditions: Effect of height.

Geometric Configuration	RD-H1	RD-H2	RD-H3	RD-H4	RD-H5	RD-H6
Non-reacting	1.09E-05	2.50 E-05	4.27E-05	5.69E-05	8.98E-05	2.10E-04
Reacting	4.59 E-04	4.33 E-04	5.30E-04	7.48E-04	9.62E-04	1.43E-03
Effect of Reactions	-4.48E-04	-4.08E-04	-4.87E-04	-6.91E-04	-8.72E-04	-1.22E-03

in (W)

b. Combustion Characteristics

- ***Flame Dynamics***

Flame Shape

The investigation into the combustion characteristics and flame dynamics in reacting flows among micro combustor configurations RD-H1 to RD-H6 provides critical insights into the interplay between geometric features, particularly ribs height, and chemical reactions. Figure IV.1.49, displaying hydrogen H2 and hydroxide OH mass fraction contours, facilitates the elucidation of reaction zone and flame shape, respectively. By visualizing H2 and OH mass fraction contours, the reaction zone and flame shape are elucidated, respectively. Across all configurations, the reaction zone in the upstream channel consistently appears thin and conical, denoted in yellow, indicating minimal geometry effects on its shape. However, variations in the remaining hydrogen distribution, represented by H2 mass fraction contours in dodger blue, are observable, particularly around the backward-facing steps and ribs across the various configurations RD-H1 to RD-H6. The ribs heights of 0.6 mm and less demonstrate advantageous behavior compared to ribs with heights of 0.7 mm and 0.8 mm. Ribs with heights of 0.6 mm and less effectively maintain the shape of the reaction zone and minimize excessive stretching of the flame. However, ribs with heights of 0.7 mm and 0.8 mm tend to disrupt the shape of the reaction zone and may contribute to the stretching of the flame, adversely affecting combustion efficiency. Ribs with heights of 0.7 mm and 0.8 mm create greater flow disturbances and recirculation zones due to their larger obstruction in the flow path. This leads to the entrapment of reaction gases and influences the behavior of OH radicals, consequently affecting the shape and behavior of the flame. In contrast, ribs with heights of 0.6 mm and less impose less disturbance on the flow, allowing for smoother flow dynamics and better preservation of the reaction zone shape. The consequences of ribs with heights of 0.7 mm and 0.8 mm potentially include flame quenching, inefficient combustion, and increased energy losses due to excessive stretching of the flame. Therefore, careful consideration of ribs height is essential to optimize combustion efficiency and prevent these adverse effects.

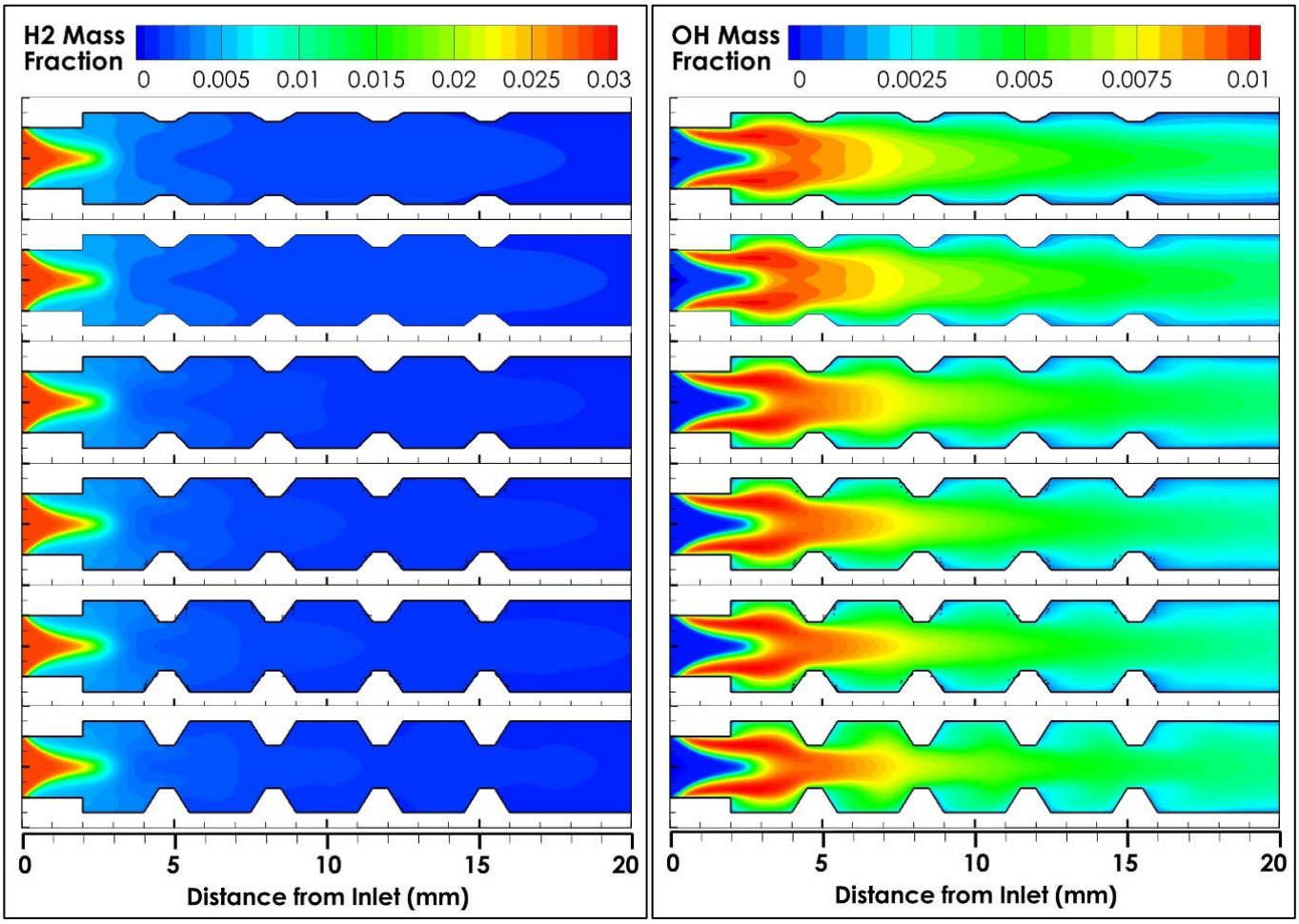

(a) *(b)*

Figure IV.1.49. *(a) hydrogen H_2 and (b) hydroxide OH mass fraction contours for the different micro-combustor configurations: Effect of height.*

Flame front location

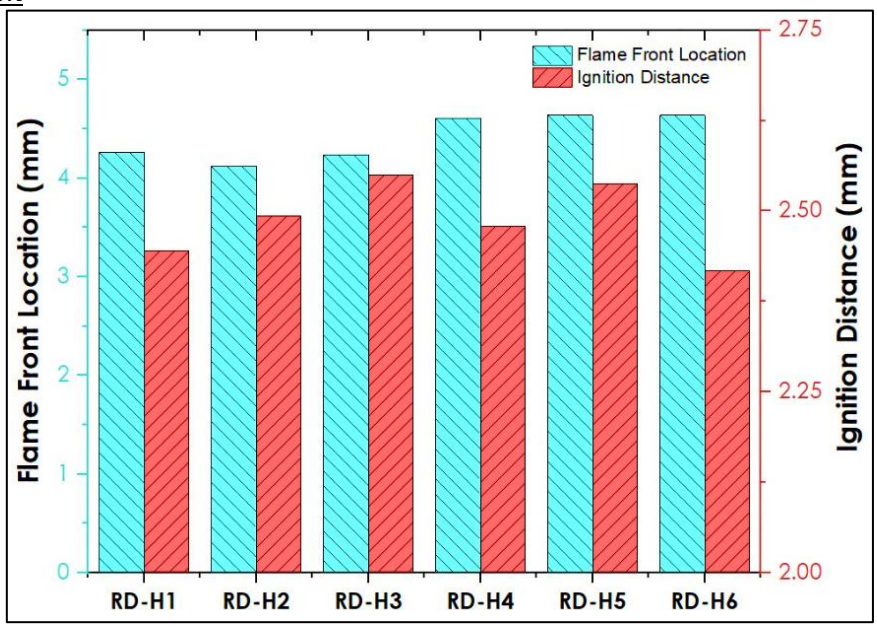

Figure IV.1.50. *Flame front location and ignition distance for different micro-combustor configurations: Effect of height.*

Analyzing the flame front location, ignition distance, and flame speed across micro combustor configurations RD-H1 to RD-H6 sheds light on the impact of ribs height on combustion dynamics.

Illustrated in **Figure IV.1.50**, these parameters unveil noteworthy trends and behaviors, providing insights into the influence of ribs height on combustion initiation and progression. The flame front location serves as a crucial indicator of combustion initiation and spatial distribution within the micro combustor. The flame front location serves as a critical indicator of combustion initiation and progression within the micro combustor. Observing the results, it is apparent that slight variations in flame front location are present across all configurations. For instance, RD-H1 and RD-H2 exhibit similar flame front locations, hovering around 4.26 mm and 4.12 mm, respectively. However, RD-H3 shows a slightly shorter flame front location at approximately 4.23 mm, suggesting a quicker initiation of combustion compared to previous configurations. Conversely, RD-H4 to RD-H6, with increasing ribs heights, display longer flame front locations, with RD-H6 reaching up to 4.64 mm. This indicates a slower initiation of combustion, potentially attributed to increased flow disturbance and altered flow patterns caused by taller ribs. Moving to ignition distances, which represent the distance from the micro combustor inlet to the point of combustion initiation, RD-H1 to RD-H6 configurations exhibit varying ignition distances. RD-H1, RD-H2 and RD-H3 configurations demonstrate relatively consistent ignition behavior with increasing distances values of approximately 2.45 mm, 2.49 mm, and 2.55 mm, respectively. However, RD-H4, RD-H5 and RD-H6 exhibit slightly shorter ignition distances compared to RD-H1, RD-H2 and RD-H3, with increasing distances values of approximately 2.48 mm, 2.54 mm, and 2.42 mm, respectively. This is due essentially to the increased flow disturbances and altered flame propagation dynamics caused by taller ribs. Overall, these results underscore the advantages of ribs with heights of 0.6 mm and less compared to ribs with 0.7 mm and 0.8 mm. Ribs with heights of 0.6 mm and less tend to promote smoother combustion initiation and propagation. Conversely, taller ribs introduce greater flow disturbances and alter flow patterns, leading to slower combustion initiation and potentially affecting overall combustion efficiency.

Flame speed

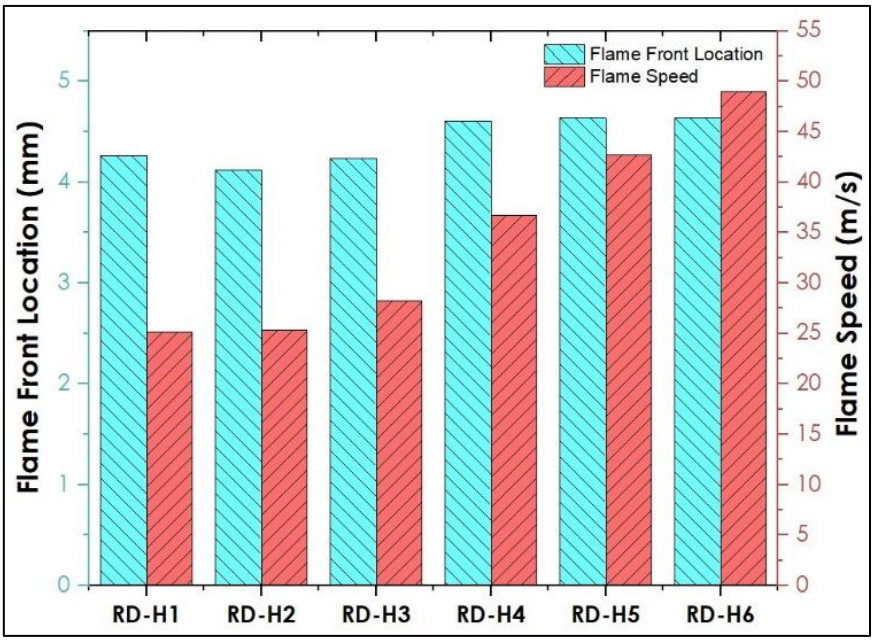

Figure IV.1.51. *Flame location and flame speed for different micro-combustor configurations: Effect of height.*

Figure IV.1.51 illustrates the flame speed variations across different ribs height configurations (RD-H1 to RD-H6) offer significant insights into the combustion dynamics and energy release within micro combustors. The observed flame speeds reflect the rate at which the fuel-air mixture is consumed, indicating the efficiency of combustion processes. Analyzing the results, we note distinct variations in flame speed across the configurations. RD-H1 and RD-H2 demonstrate relatively similar flame speeds,

with values around 25.12 m/s and 25.29 m/s respectively. Similarly, RD-H3 exhibits a slightly higher flame speed of approximately 28.23 m/s. These configurations display consistent combustion behavior, with minor deviations attributed to differences in ribs height. In contrast, RD-H4 and RD-H5 showcase substantially higher flame speeds, with values of approximately 36.72 m/s and 42.66 m/s respectively. RD-H6 exhibits the highest flame speed among all configurations, recording approximately 48.95 m/s. This considerable disparity suggests that ribs height significantly influences combustion dynamics and flame propagation. Scientifically, the observed variations in flame speed can be attributed to the impact of ribs height on flow dynamics and turbulence. Ribs with heights of 0.6 mm and less promote smoother flow and lower turbulence levels, resulting in relatively lower flame speeds. In contrast, ribs with heights of 0.7 mm and 0.8 mm create greater flow disturbances, leading to increased turbulence and faster flame speeds. Furthermore, configurations with taller ribs experience enhanced turbulence levels, facilitating faster mixing and interaction between reactants. This accelerated mixing promotes rapid ignition and combustion, resulting in higher flame speeds. Overall, these findings underscore the intricate relationship between ribs height, flow dynamics, and combustion efficiency, emphasizing the importance of ribs height optimization in achieving desired combustion performance within micro combustors.

- ***Combustion efficiency***

- ***Combustion Intensity***

Figure IV.1.52. illustrated the average kinetic reaction rates across different ribs height configurations (RD-H1 to RD-H6) provide valuable insights into combustion intensity and efficiency within micro combustors. These reaction rates shed light on how geometric features, particularly ribs height, influence combustion kinetics and efficiency. Analyzing the results reveals notable variations in reaction rates across elementary reactions for each configuration. Certain reactions consistently exhibit higher rates, indicating their significance in the combustion process. Notably, reactions 3, 8, 9, and 16 consistently demonstrate elevated rates across all configurations, suggesting their crucial roles in combustion. However, reactions 16 and 17 exhibit negative rates across all configurations, implying a depletion or inhibition effect within the reaction mechanism. Additionally, reaction 20 consistently exhibits negligible rates or even negative values, indicating its limited contribution to combustion. The variations in rates across configurations can be attributed to differences in ribs height. Configurations with shorter ribs, such as RD-H1 to RD-H4, generally exhibit lower reaction rates compared to configurations with taller ribs, such as RD-H5 and RD-H6. This suggests that ribs with heights of 0.6 mm and less promote more efficient combustion processes, resulting in higher reaction rates. In contrast, RD-H5 and RD-H6 demonstrates generally higher reaction rates across most elementary reactions compared to all other configurations except. This indicates that the specific design features, may affect the combustion stability. The contrast in reaction rates between configurations emphasizes the importance of ribs height selection in enhancing combustion efficiency and performance. Overall, the results highlight the intricate relationship between ribs height, combustion kinetics, and efficiency, emphasizing the need for careful consideration of ribs height in micro combustor design to optimize combustion performance.

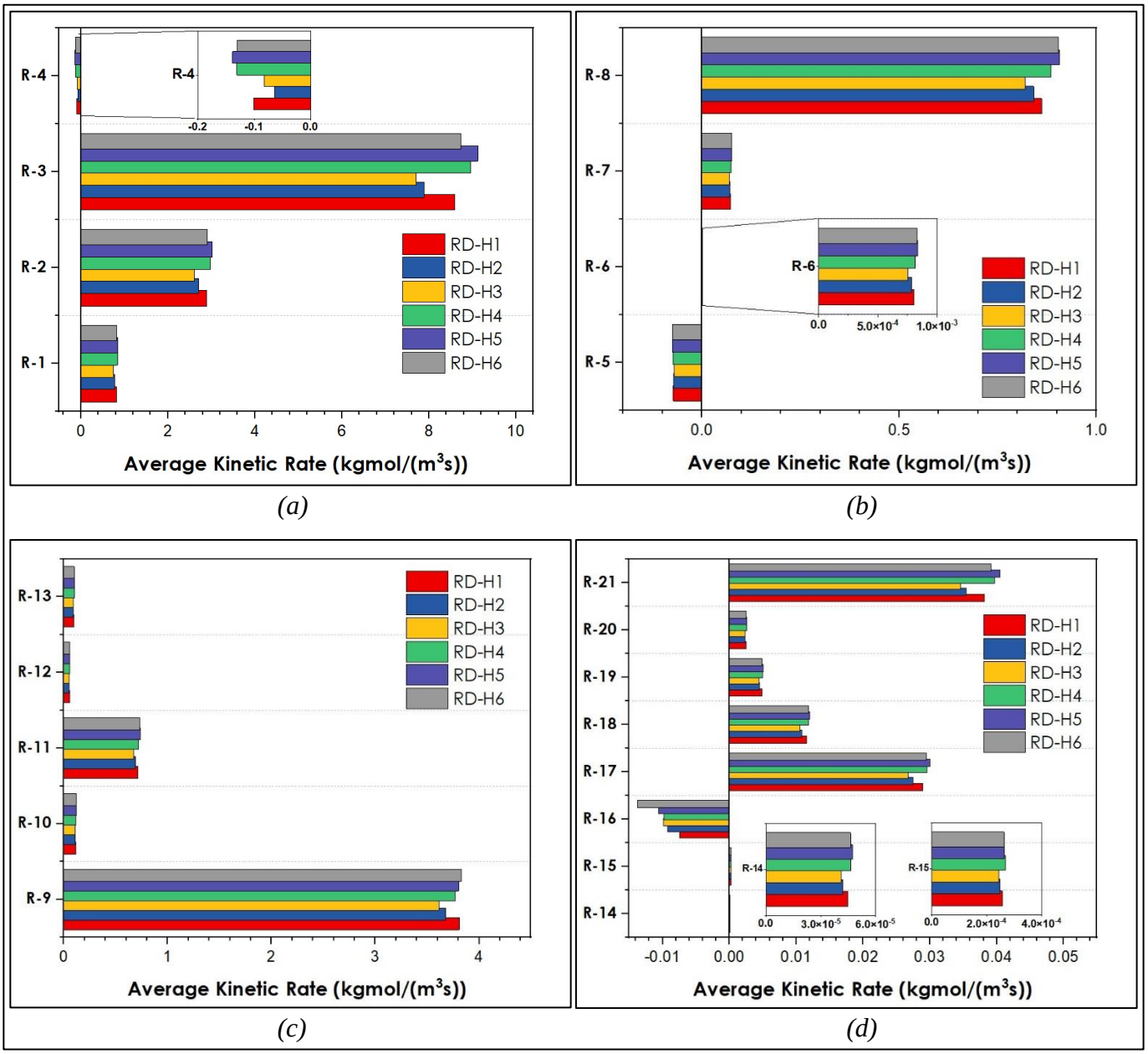

Figure IV.1.52. *Average kinetic rate of different elementary reactions for the different micro-combustor configurations: Effect of height.*

- ***Conversion Efficiency***

Figure IV.1.53 presents the average mass fraction of hydrogen at the outlet boundary for various ribs height configurations (RD-H1 to RD-H6), and corresponding variations in micro combustion conversion efficiency, offers valuable insights into the combustion performance and efficiency of each configuration. These metric parameters are pivotal for evaluating the conversion efficiency of hydrogen fuel in different micro combustor configurations under discussion. Analyzing the results reveals distinct variations in outlet hydrogen mass fraction and conversion efficiency across different ribs height configurations. Notably, RD-H3 stands out with the lowest outlet hydrogen mass fraction, indicating more complete combustion compared to other configurations. Correspondingly, RD-H3 exhibits the highest conversion efficiency, approaching 96.93%. This suggests that the ribs height of RD-H3, with 0.5 mm, promote efficient combustion and maximize the utilization of hydrogen fuel. While RD-H1, RD-H2, RD-H4, RD-H5, and RD-H6 demonstrate slightly higher outlet hydrogen mass fractions, and relatively lower conversion efficiencies compared to RD-H3. The configurations RD-H1, RD-H2 and RD-H4 exhibits conversion efficiencies of 96.72 %, 96.82 %, and 96.76 %, respectively. However, RD-H5 and RD-H6

both shows the higher outlet hydrogen mass fractions, resulting in the lower conversion efficiencies with values of 96.6 % and 96.52 %, respectively. This indicates that configurations with ribs height less or either higher than 0.5mm may create lower conversion efficiencies and less efficient combustion. In conclusion, the results emphasize the intricate relationship between ribs height, combustion efficiency, and conversion efficiency. The findings highlight the need for careful selection of ribs height as a geometrical parameter in optimizing micro combustor design to enhance combustion efficiency and overall performance.

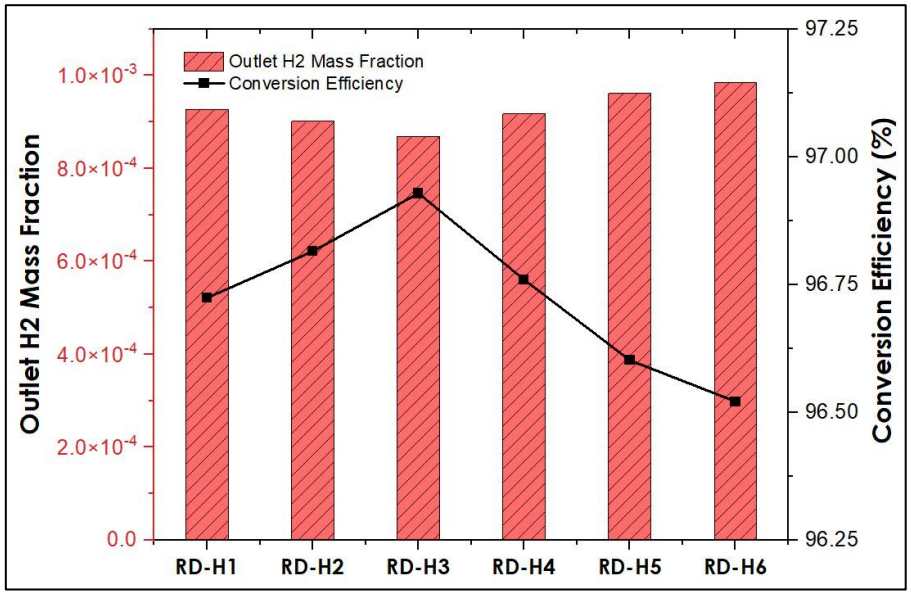

Figure IV.1.53. *Outlet H_2 mass fraction and Combustion efficiency for the different micro-combustor configurations: Effect of height.*

c. Thermal Characteristics

- ***Temperature Distribution***

Figure IV.1.54 *(a)* provides insights into the temperature distribution within both gas and solid phases across various micro combustor configurations (RD-H1 to RD-H6), employing distinct legends for each phase to enhance visibility. These temperature contours offer valuable insights into the effects of ribs height on temperature distribution and the interplay between turbulence level, combustion dynamics, and convective heat transfer mechanisms. Observations reveal that the variations in ribs height impact both gas and solid phase temperature distribution. Higher rib heights result in increased turbulence levels and more pronounced recirculation zones, enhancing gas mixing and creating hot spots within the combustor. Conversely, configurations with lower rib heights demonstrate more uniform gas phase temperature distribution. Furthermore, the increase in rib height influences solid phase temperature contours. Higher rib heights facilitate convective heat transfer, leading to more efficient heat transfer from combustion gases to the inner walls of the combustor. Consequently, configurations with higher rib heights exhibit higher solid phase temperatures, particularly near the outlet. Among the configurations, RD-H6 demonstrates the highest solid phase temperatures, indicating efficient convective heat transfer and enhanced combustion. RD-H5 follows closely, showing slightly lower solid phase temperatures. RD-H4 and RD-H3 exhibit also increasing solid phase temperatures with the increase in rib height, highlighting the impact of these configurations' ribs height on temperature level and distribution, compared to configurations with ribs height lower than 0.5 mm. **Figure IV.1.54** (b) provides insights into the distribution of heat generated by chemical reactions within the gas phase across different micro combustor configurations (RD-H1 to RD-H6). Despite the variations in ribs height, the shape of the

reaction zone appears to undergo minimal alteration, indicating the robustness of combustion dynamics to changes in this parameter. However, the amount of heat released by the reaction zones varies notably among the configurations, reflecting the influence of ribs height on combustion intensity and heat transfer mechanisms. Among the configurations, RD-H3 demonstrates the highest heat of reaction, with a value of 13.14 W, indicating efficient combustion and heat release. RD-H2 follows closely, exhibiting a heat of reaction of 13 W. These configurations likely benefit from optimal ribs height, promoting turbulence and enhancing combustion efficiency. On the contrary, RD-H5 displays a lower heat of reaction at 11.89 W, suggesting less efficient combustion. This could be attributed to suboptimal ribs height, which may disrupt flow dynamics and reduce turbulence levels, leading to incomplete combustion. RD-H6 exhibits a moderate heat of reaction at 12.46 W, indicating relatively efficient combustion compared to RD-H5 but less efficient than RD-H3 and RD-H2. This highlights the sensitivity of combustion dynamics to ribs height, emphasizing the importance of optimizing this parameter for maximizing heat release and combustion efficiency. Overall, these observations underscore the complex interplay between ribs height, flow dynamics, turbulence level, and combustion dynamics in micro combustors. They emphasize the need for careful consideration of ribs height to optimize combustion performance and heat release within the gas phase.

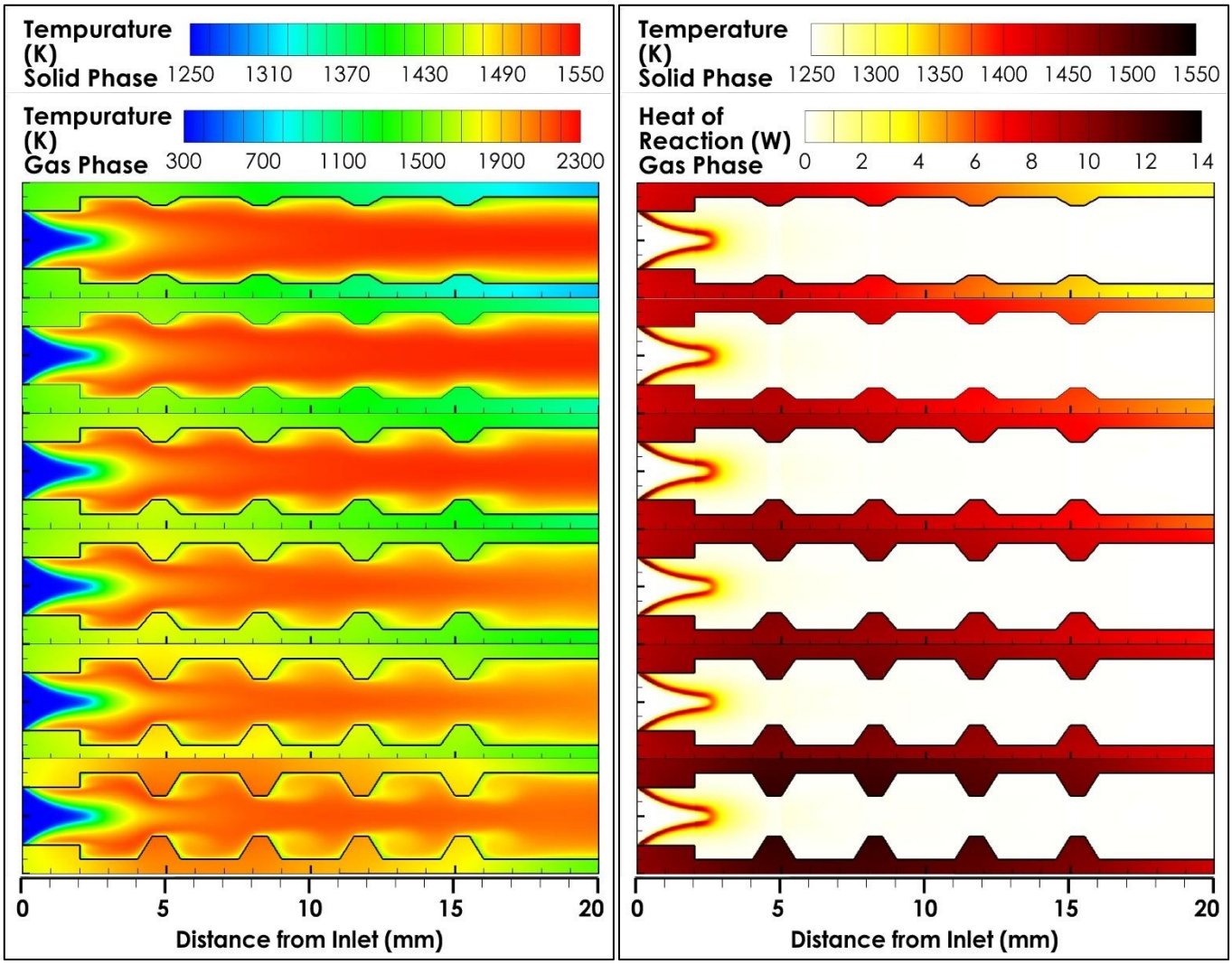

(a) *(b)*

Figure IV.1.54. *Temperature contours for the different micro-combustor configurations: Effect of height.*

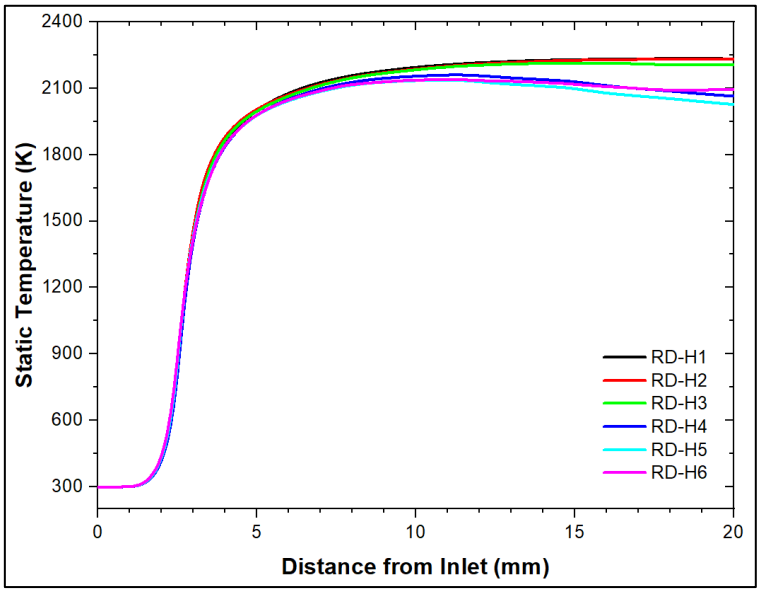

Figure IV.1.55. *Temperature distribution along the micro-combustor centerline for the different micro-combustor configurations: Effect of height.*

Figure IV.1.55 provides insights into the temperature distribution along the centerline of gas phases across different micro combustor configurations (RD-H1 to RD-H6). Despite variations in ribs height, the temperature profiles exhibit approximately uniform distributions along the centerline, indicating stable thermal behavior within the gas phase. Upon closer examination, slight differences in temperature levels are observed within different regions of the micro combustor configurations. Specifically, for the rib's height of 0.6 mm to 0.8 mm, a gradual decrease in temperature levels is noted along the centerline, particularly from 10 mm from the inlet to the outlet of the RD-H4, RD-H5, and RD-H6 configurations. These observations align with the known effect of ribs height on convective heat transfer towards the inner walls of micro combustors. Higher ribs height results in increased convective heat transfer, which leads to more efficient cooling of the gas phase along the centerline. Consequently, configurations with ribs height of 0.6 mm and higher exhibit lower temperature levels along their centerlines compared to configurations with lower ribs height. The trends in temperature profiles reflect the intricate interplay between ribs height, convective heat transfer, and gas phase temperature distribution. However, this underscores the importance of careful selection ribs height to achieve desired temperature distributions and thermal performance.

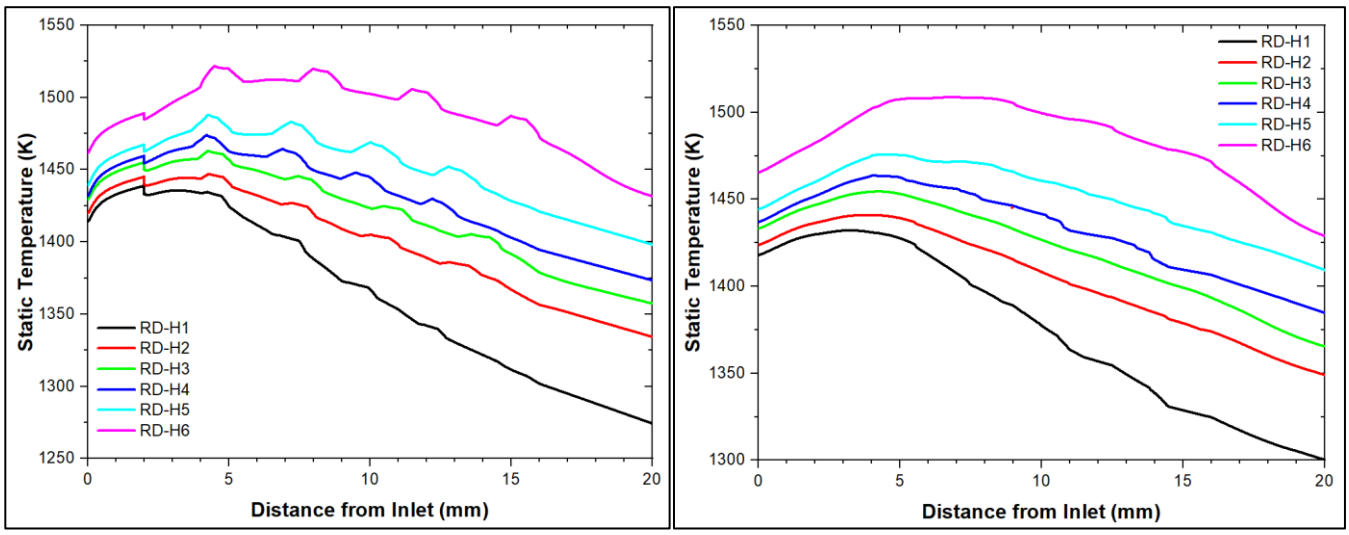

(a) *(b)*

Figure IV.1.56. *Outer wall temperature distribution for micro-combustor configurations: Effect of height.*

Figure IV.1.56 provides a comprehensive view of the temperature distribution along both the inner and outer wall surfaces of micro combustor configurations (RD-H1 to RD-H6), shedding light on the influence of ribs height on thermal performance. Examining the temperature distribution along the inner wall surface, as depicted in **Figure IV.1.56** *(a)*, it is evident that as ribs height increases, there is a noticeable rise in temperature levels. This trend is accentuated by the distinct presence of rib shapes in the temperature profiles, with points of highest temperature levels aligning with the locations of the ribs. Such observations underscore the pivotal role of ribs height in intensifying convective heat transfer, consequently augmenting temperature levels along the inner walls. Ultimately, the increase in ribs height enhances temperature levels and promotes distribution uniformity, contributing to improved combustion and heat transfer efficiency. Similarly, on the outer wall surface, as illustrated in **Figure IV.1.56** *(b)*, a parallel trend is observed. With an increase in ribs height, the temperature profiles depict higher levels and more uniform distribution along the outer wall. This indicates that the enhancement of convective heat transfer along the inner wall leads to a more efficient heat transfer process across the outer wall of configurations, scaling proportionally with the increase in ribs height. Considering conductive heat transfer through the solid phase, configurations with higher ribs height exhibit decreased conductive heat losses. This highlights the importance of geometric features, particularly ribs height, in mitigating conductive heat losses and enhancing overall temperature levels and distribution uniformity along the outer wall. However, the temperature distribution along both the inner and outer walls of micro combustor configurations is significantly influenced by ribs height, with configurations featuring higher ribs height demonstrating higher temperature levels and improved distribution uniformity. This underscores the critical role of optimizing ribs height to achieve desired temperature distributions and thermal performance within micro combustor configurations.

- ***Thermal Efficiency***

Figure IV.1.57 offers a comprehensive examination of the heat transfer characteristics along the outer wall of various micro combustor configurations (RD-H1 to RD-H6), shedding light on the influence of ribs height on heat transfer mechanisms. The total surface heat flux, comprising both convective and radiative components, emerges as a critical parameter dictating the thermal efficiency of micro combustors. Across the configurations, there is a discernible escalation in the total surface heat flux, directly correlated with the increase in ribs height. This indicates an overall enhancement in heat transfer within the micro combustor configurations, attributable to the optimized inner wall surface. Analyzing the individual heat flux components reveals a consistent upward trend in both convective and radiative heat fluxes across the configurations. Convective heat flux, representing heat transfer through fluid motion, maintains a relatively lower proportion of the total heat flux but demonstrates a notable increase with the augmentation of ribs height. This underscores the role of ribs height in promoting more efficient convective heat transfer between the outer wall and the surroundings. In contrast, radiative heat flux, depicting heat transfer through electromagnetic radiation, accounts for the highest proportion of heat transferred by the outer wall across various configurations and displays a similar increasing trend. The amplification in radiative heat flux underscores the improved thermal performance facilitated by the incorporation of higher ribs height, which is advantageous for the operation of MTPV systems. However, these findings underscore the importance of careful selection of ribs height as a key design parameter for optimizing heat transfer mechanisms and enhancing radiative thermal performance within micro combustor configurations.

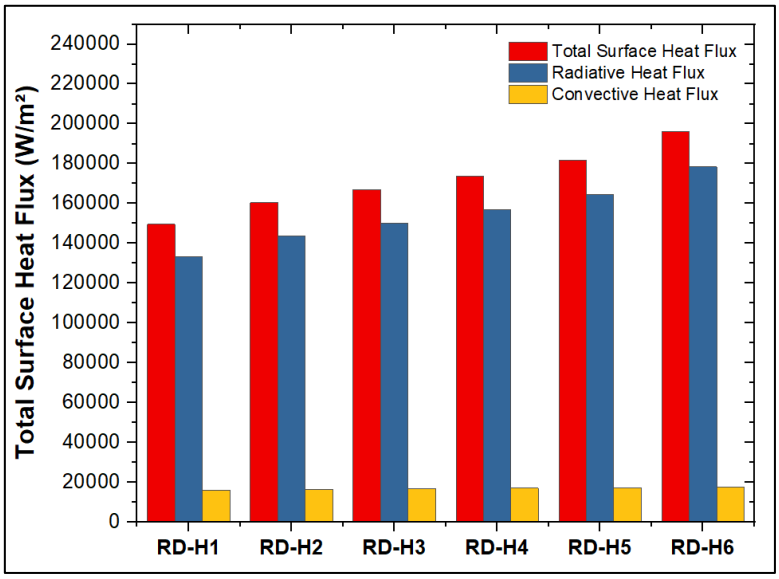

Figure IV.1.57. *The convective and radiative heat fluxes ratio to the total heat flux emitted via the outer wall for the different micro-combustors: Effect of height*

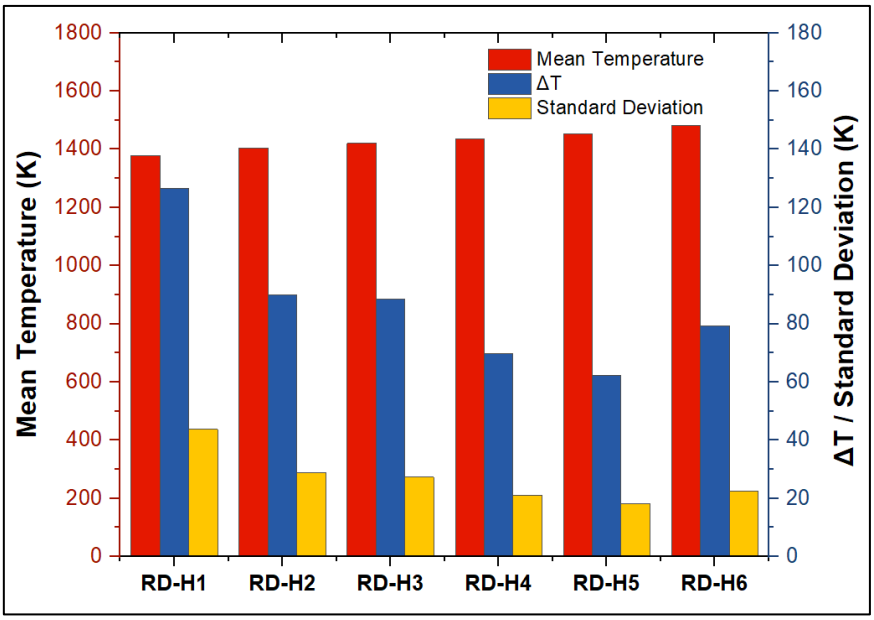

Figure IV.1.58. *The outer wall: Average temperature, temperature difference and Standard deviation for the different micro-combustors: Effect of height*

Figure IV.1.58 provides a detailed analysis of the outer wall thermal performance for various micro-combustor configurations (RD-H1 to RD-H6), focusing on the mean temperature, temperature difference (ΔT), and standard deviation values. Across the configurations, there is a consistent increase in the mean temperature along the outer walls, indicating higher thermal energy levels with the augmentation of ribs height. This rise in mean temperature correlates with improved heat transfer facilitated by the augmentation of ribs height. Specifically, the mean temperature progressively increases with higher ribs height, from 1378.139 K for RD-H1 to 1483.153 K for RD-H6. Temperature difference (ΔT) and standard deviation offer insights into the thermal level and uniformity along the outer walls. Configurations with lower ΔT and standard deviation values demonstrate more consistent temperature distributions and improved thermal uniformity. RD-H4 and RD-H5 exhibit the lowest ΔT values of 69.618 K and 62.156 K, respectively, indicating greater uniformity in temperature distribution. Additionally, RD-H4 has the lowest standard deviation of 21.08716 K, suggesting highly controlled and predictable thermal behavior. On the other hand, configurations like RD-H1 and RD-H2 show higher ΔT values, indicating a relatively

higher level of non-uniformity in temperature distribution. Similarly, RD-H1 has the highest standard deviation of 43.70731 K, reflecting lower thermal behavior compared to configurations with higher ribs height. Configurations with higher ribs height tend to exhibit lower ΔT and standard deviation, indicating more uniform temperature distributions and enhanced thermal stability. Overall, the results highlight the advantageous effects of incorporating higher ribs height on the outer wall thermal performances of micro-combustor configurations, leading to improved thermal efficiency and more uniform temperature distributions along the outer walls.

IV.1.2. Effect of Operating Conditions: Target Configuration

- **Physical Model**

This doctoral study not only aims to advance the micro-combustion field through an exploration of geometric configuration approaches but also delves into examining the impact of operating conditions on various facets of micro combustion and challenges in MTPV systems. The investigation specifically concentrates on defining the optimal operating range for inlet velocity (6-14 m/s) and equivalence ratio (0.8/1.2) in turbulent micro combustion mixtures. Employing a systematic numerical methodology and a meticulous analytical approach, we seek to deepen our comprehension of micro-combustion, encompassing flow dynamics, chemical processes, and thermal interactions. The overarching objective is to augment the overall performance and efficiency of micro combustors and MTPV systems. In the following, **Figure IV.1.59** illustrates the schematic representation and dimensions of the innovatively proposed micro-combustion chamber. In the operational phase, a uniformly flowing premixed H2-air mixture, with a velocity of 6 m/s, is introduced into the upstream channel of the expansion, characterized by a height (H1) of 2 mm, a length (L2) of 2 mm, and a thickness (t1) of 1 mm. The combustion byproducts are then expelled through the downstream channel, featuring a height (H_2) of 3 mm and a thickness (t2) of 0.5 mm. Additionally, the cavities within the system are defined by a length (L3) of 2 mm, and the angled ribs are specified by a height (h) of 0.5 mm and an angle (θ) of 45°. The overall length of the micro combustor is denoted as L1 and measures 20 mm. This configuration outlines a comprehensive design for the micro-combustion chamber, encompassing specific dimensions and angles, facilitating a controlled flow of the premixed fuel-air mixture and efficient expulsion of combustion products. The strategic placement of ribs and cavities, as described in the schematic, is intended to optimize combustion processes and enhance the overall performance of the micro combustor during operation.

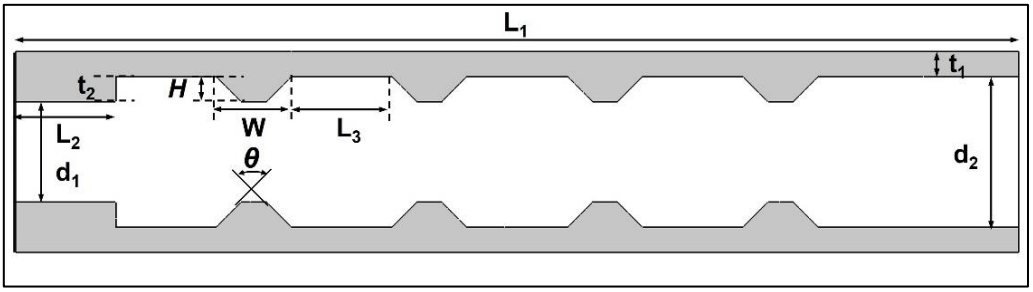

Figure IV.1.59. *Schematic diagram of the geometric configuration: Effect of Operating conditions*

- **Computational Parameters of Target Configuration**

In the context of numerical simulations applied to our developed micro combustor configuration, it is imperative to study the effect of boundary conditions to ensure the accuracy and consistency of configuration performance. In examining the impact of operating conditions, we rigorously control two pivotal parameters in each simulation: the inlet velocity (U_{in}) and the equivalence ratio (ϕ). The

equivalence ratio denotes the ratio of the actual fuel-to-air mixture to the stoichiometric ratio required for complete combustion, and we consistently change it from 0.8 to 1.2 by 0.1. This value plays a fundamental role in determining the composition of the fuel-air mixture and its effects on combustion characteristics. Moreover, we introduce variability in the inlet velocity, allowing it to range dynamically between 6 and 14 m/s. This parameter governs the speed at which fresh air and fuel enter the combustion chamber, directly influencing flow dynamics and combustion behavior within the micro combustor. By incorporating this variability, we aim to explore a broader spectrum of operational conditions, recognizing that the inlet velocity is a crucial factor in shaping combustion processes and MTPV systems performance. These adjustments in our approach aim to provide a more comprehensive understanding of the micro combustor's behavior under varying conditions, expanding the scope of our investigation beyond a fixed inlet velocity and stochiometric equivalence ratio. The specific details of these modified boundary conditions can be found in **Table IV.1.10** for quick reference.

Table IV.1.12. *Computational parameters for the effect of operating conditions of target configuration*

Boundary	Parameters	Values
Inlet	Velocity Inlet (m/s)	6-14
	Temperature (K)	300
	Gauge pressure (Pa)	0
	Hydraulic diameter (mm)	2
	Turbulent intensity (%)	5
	Equivalence ratio ϕ	0.8-1.2
Outlet	Gauge pressure (Pa)	0
	Hydraulic diameter (mm)	3
	Turbulent intensity (%)	5
Wall	Material	316 Stainless-steel
	Thermal condition	Mixed
	Natural convective heat transfer coefficient (W/(m^2.K))	15
	External & internal emissivity	0.65

- ## Results and Discussions: 2D Approach of target configuration

a. Effect of Inlet Velocity

a. Flow field Characteristics

Figure IV.1.60 illustrate the effect of inlet velocity variations (ranging from 6 to 14 m/s) on (a) the stream-field and (b) pressure field within the target micro combustor configuration is crucial in understanding the dynamics of combustion processes. As the inlet velocity increases, it directly influences the stream field, altering the distribution of flow patterns and velocities within the combustion chamber. Higher inlet velocities result in increased acceleration zones, particularly evident around the tips of the ribs, where the flow encounters obstacles, leading to intensified turbulent flow phenomena. This heightened turbulence enhances mixing and interaction between reactants, promoting more efficient combustion processes. Additionally, the pressure field within the micro combustor experiences notable changes with varying inlet velocities. As the inlet velocity increases, the pressure within the combustion chamber also rises, reflecting the increased momentum of the incoming flow. Conversely, higher velocities lead to more significant pressure drops across the micro combustor due to increased flow resistance and energy dissipation within the micro combustor. In terms of flow stability, certain inlet velocities may exhibit more favorable characteristics. While higher velocities contribute to enhanced mixing and combustion efficiency, excessively high velocities can lead to flow instabilities and

turbulence-related issues. Therefore, an optimal inlet velocity needs to be identified, balancing the benefits of increased mixing and combustion with the need for flow stability. Overall, the choice of inlet velocity profoundly influences the flow-field and pressure field within the micro combustor, affecting flow efficiency and stability.

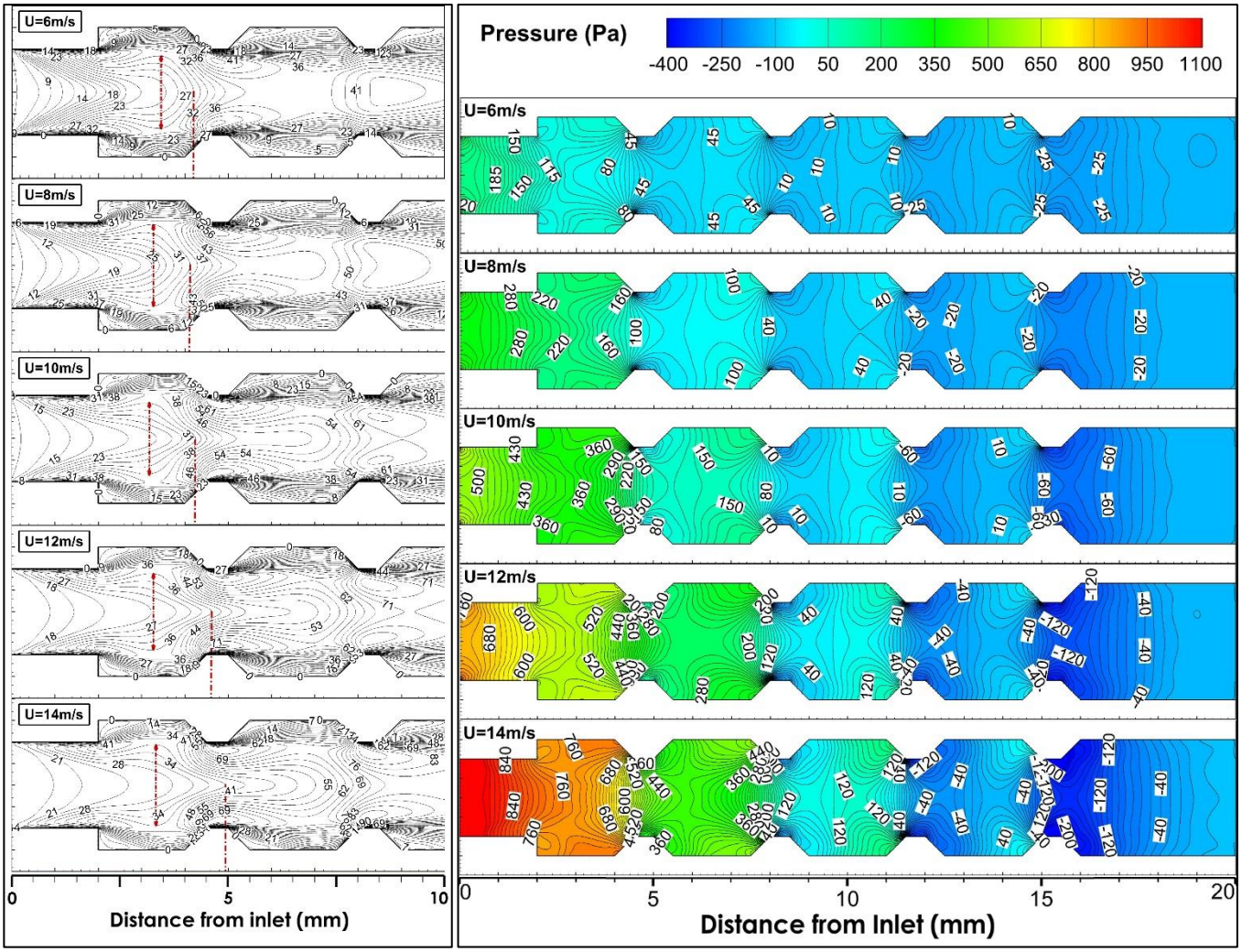

(a) *(b)*

Figure IV.1.60. *Flow-field streamlines (a) and pressure contour (b) for the different inlet velocities: Effect of operating conditions*

The impact of inlet velocities on turbulent kinetic energy, turbulence intensity, and vorticity contours is a critical aspect in understanding the dynamic behavior of micro combustors. As shown in **Figure IV.1.61**, as the inlet velocities vary within the specified range of 6-14 m/s, the turbulent kinetic energy undergoes significant changes, influencing the overall turbulence intensity and vorticity patterns within the combustion chamber. At lower inlet velocities within the range, there is a notable decrease in turbulent kinetic energy, resulting in a more laminar flow profile. This leads to lower turbulence intensity behind the steps and ribs, creating a smoother flow pattern. Conversely, as the inlet velocities increase towards the upper limit of the range, turbulent kinetic energy experiences a marked rise. This increase contributes to higher turbulence intensity, especially behind the steps and ribs, generating more pronounced turbulent structures in the flow field. The vorticity contours are intricately linked to the turbulent kinetic energy variations induced by the changing inlet velocities. At lower velocities, vorticity contours exhibit a more subdued and organized pattern, while higher velocities contribute to the formation of more intricate vortices. The distribution and size of these vortices play a pivotal role in the overall flow dynamics.

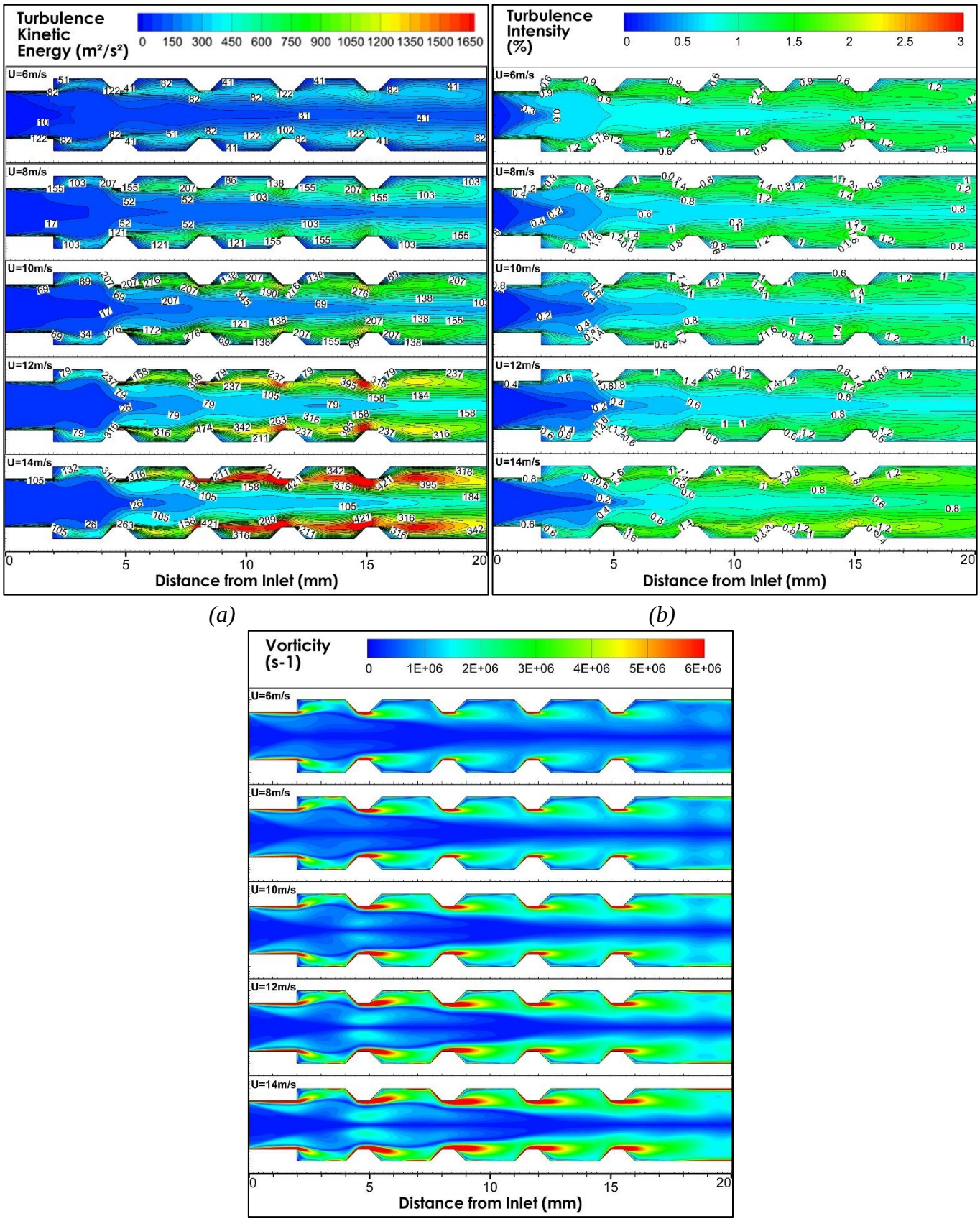

Figure IV.1.61. *(a) Turbulent kinetic energy (b) turbulence intensity contour (c)and turbulence vorticity for the different inlet velocities: Effect of operating conditions*

b. Combustion Characteristics

- ***Flame Propagation***

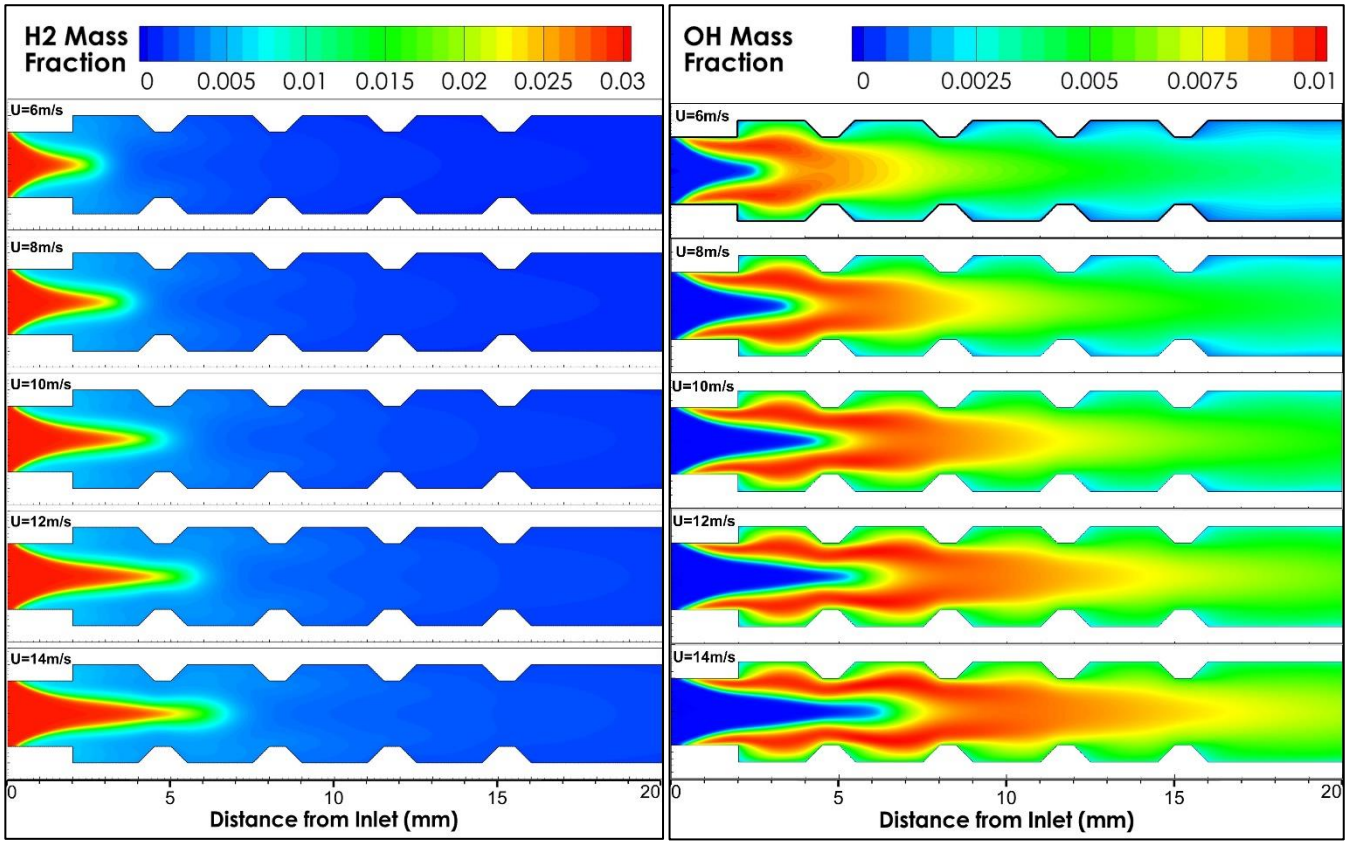

(a) *(b)*

Figure IV.1.62. *(a) Hydrogen H_2 and (b) hydroxide OH mass fraction contour for the different inlet velocities: Effect of operating conditions*

The modulation of inlet velocities within the prescribed range exerts a profound influence on the distribution of hydrogen H_2 and hydroxide OH mass fraction and the resultant flame shape in micro combustors, as shown in **Figure IV.1.62**. As the inlet velocities escalate from 6 to 14 m/s, discernible changes in the hydrogen mass fraction distribution and flame geometry emerge, specifically characterized by the elongation of the flame in the downstream channel. At lower inlet velocities, the hydrogen mass fraction distribution tends to exhibit a more confined and concentrated profile near the flame front. This is accompanied by a compact flame shape, indicating a controlled combustion process within the micro combustor. As the inlet velocities increase, the hydrogen mass fraction becomes more dispersed across the flame, reflecting enhanced mixing and interaction between the fuel and oxidizer. The elongation of the flame in the downstream channel with escalating velocities can be elucidated through the intricate interplay of fluid dynamics and combustion kinetics. Higher inlet velocities intensify the convective transport of reactants, promoting a more extensive mixing of hydrogen and air. This heightened mixing leads to an elongated flame structure as the combustion reactions progress downstream. The increased velocity facilitates a more thorough intermingling of fuel and oxidizer, resulting in a prolonged combustion zone. The elongation of the flame is indicative of the intricate balance between advection, diffusion, and chemical reactions in the combustion process. The convective transport of reactants plays a pivotal role in shaping the flame, and the increase in inlet velocities augments this transport, influencing the flame's spatial distribution. Moreover, the elongation signifies a more efficient utilization of reactants, contributing to a sustained combustion process in the extended downstream region.

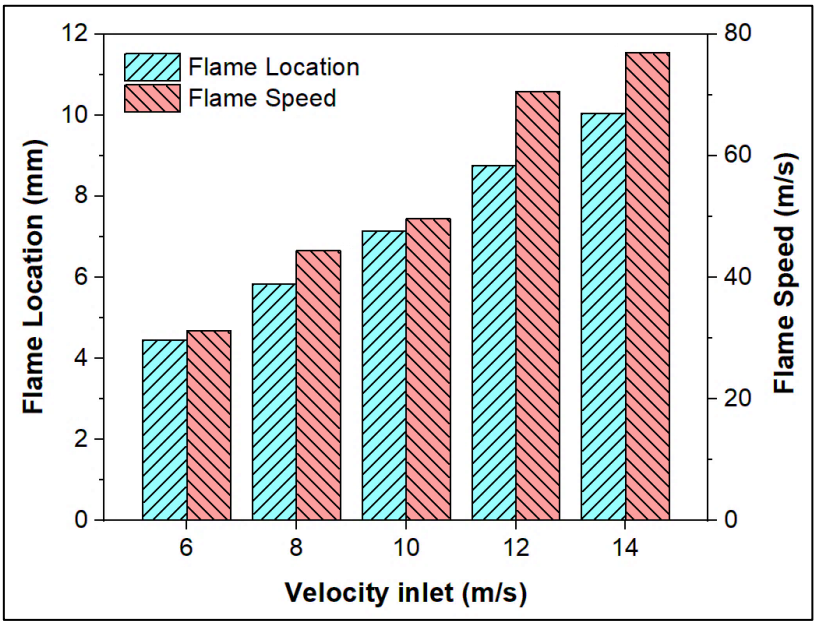

Figure IV.1.63. *Flame front location and flame speed for the different inlet velocities: Effect of operating conditions*

The flame front location and flame speed in a combustion system are notably influenced by the inlet velocity. As shown in **Figure IV.1.63, a**n increase in inlet velocity contributes to enhanced convective transport, expediting the arrival of fresh reactants to the combustion zone. This, coupled with quicker mixing of fuel and oxidizer, results in a more advanced flame location. Elevated inlet velocities also induce greater turbulence, fostering efficient combustion and dispersing heat effectively to sustain and propel the flame front. The optimized residence time, facilitated by increased convective transport, rapid mixing, and turbulence, ensures more reactants participate in combustion reactions, contributing to the advancement of the flame front. The collective effect leads to an overall increase in flame speed, representing the rate at which the combustion front advances through the reactant mixture. Understanding and manipulating these factors are crucial for optimizing combustion performance across various applications.

- ***Flame Efficiency***

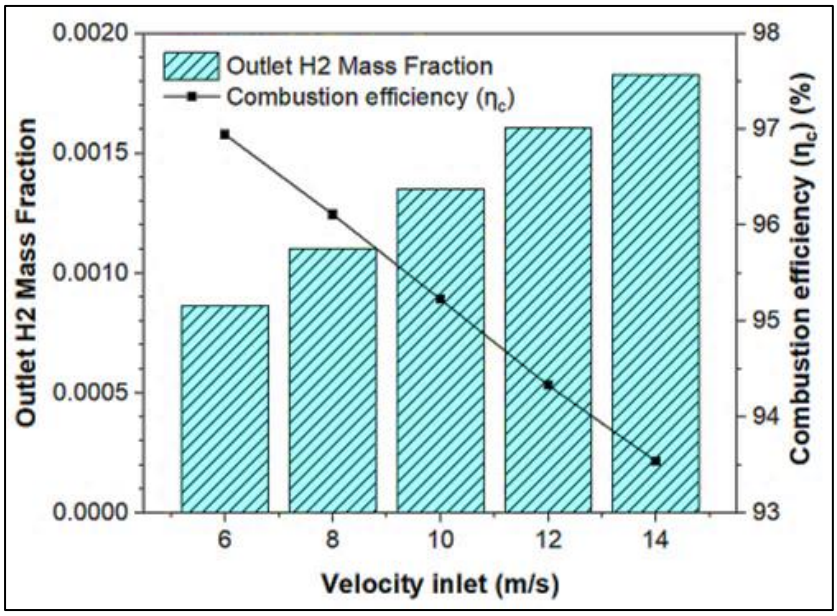

Figure IV.1.64. *Outlet H_2 mass fraction and Combustion conversion efficiency for the different inlet velocities: Effect of operating conditions*

The combustion conversion efficiency is intricately tied to the inlet velocity in a combustion system. Inlet velocity plays a crucial role in determining the rate at which fresh air and fuel are introduced into the combustion chamber. As shown in **Figure IV.1.64**, an increase in inlet velocity can positively impact combustion efficiency by promoting better mixing of fuel and oxidizer. This enhanced mixing, facilitated by higher inlet velocities, ensures a more uniform distribution of reactants, optimizing the conditions for combustion reactions. Moreover, elevated inlet velocities contribute to improved convective transport, facilitating the rapid transport of reactants to the combustion zone. This, in turn, increases the residence time of the reactants in the combustion chamber, allowing for more thorough and efficient combustion. The enhanced convective transport also helps in dissipating heat more effectively, preventing localized hotspots and ensuring a more uniform temperature distribution within the combustion chamber.

c. Thermal Characteristics

- ***Temperature Distribution***

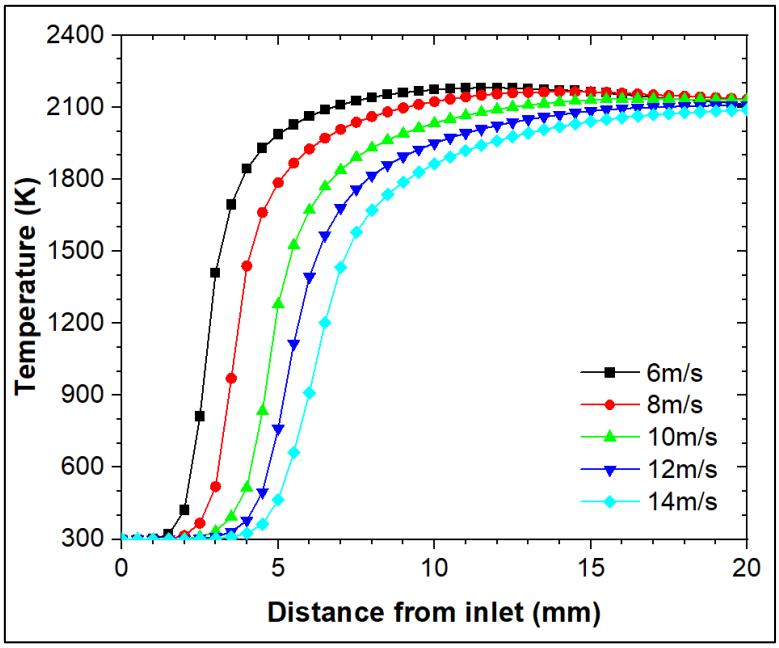

Figure IV.1.65. *Temperature distribution along the micro-combustor centerline for the different inlet velocities: Effect of operating conditions*

Figure IV.1.65 presents the temperature distribution along the centerline of the proposed micro-combustor for various inlet velocities (ranging from 6 m/s to 14 m/s). It can be observed that as the inlet velocity increases, the gas temperature rises rapidly at distances of 2 mm, 3 mm, 4 mm, 4.5 mm, and 5 mm from the inlet. The temperature then increases in a steep profile, reaching a maximum level around 2200°C. Furthermore, it is apparent that the temperature profiles shift away from the inlet of the micro-combustor with each subsequent increase in inlet velocity. These results demonstrate the impact of inlet velocity on the position of the reaction zone, which is generally characterized through the temperature distribution profiles within the combustor. The shift in the temperature profiles away from the micro-combustor inlet is attributed to the pressure increase of the cold reactants on the reaction zone as the inlet velocity is raised. This pressure increases forces the flame front away from the micro-combustor inlet. This phenomenon is due to the increase in the amount of fuel and oxidizer entering the combustor, leading to higher combustion rates and temperatures. Additionally, the pressure of the cold reactants contributes to the movement of the reaction zone by exerting a force on the flame front. The findings highlight the importance of regulating the inlet velocity to control the position of the reaction zone and ensure efficient combustion in micro-combustors.

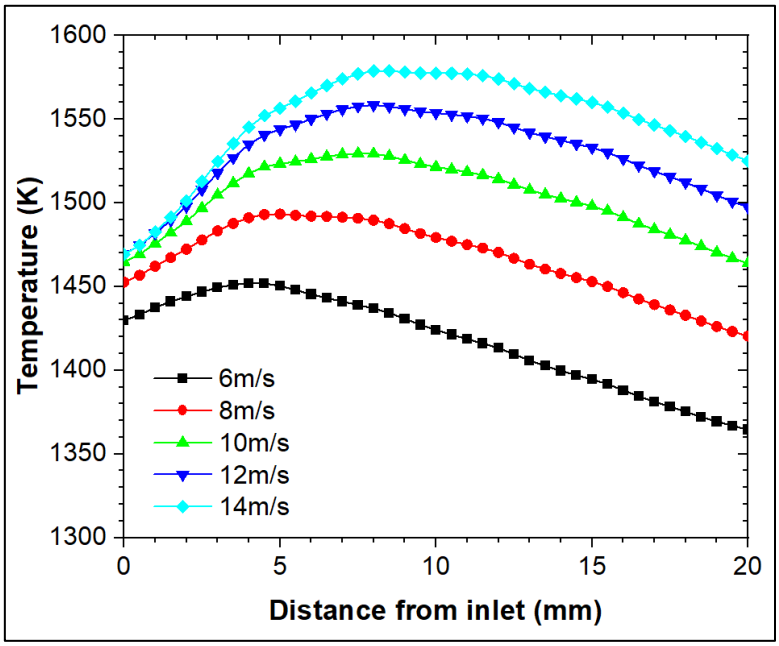

Figure IV.1.66. *Outer wall temperature distribution for the different inlet velocities: Effect of operating conditions*

Figure IV.1.66 presents the outer wall temperature distribution profiles for the different inlet velocity cases. The figure shows that the temperature profiles increase from the inlet to reach a peak value at different positions for each velocity case (4 mm, 5 mm, 7.5 mm, 8 mm, and 8.5 mm for velocities 6 m/s, 8 m/s, 10 m/s, 12 m/s, and 14 m/s, respectively). Afterward, the temperature profiles start to decrease gradually, but differently depending on the inlet velocity. It can also be noticed that the outer wall temperature level increases with the increase of the inlet velocity. Furthermore, it can be observed that the increase in temperature level slows down with each increase in the inlet velocity. However, the positive effect of the inlet velocity on the position of the reaction zone and the uniformity of the outer wall temperature level is clearly shown. Therefore, it can be deduced that at higher inlet velocities, the flow regime through the micro combustor becomes more turbulent, which enhances mixing of the hot combustion gases and brings them closer to the inner wall surface. This leads to an increase in the convective heat transfer rate between the hot combustion gases and the inner wall surface, resulting in higher temperatures near the wall. Moreover, at very high inlet velocities, there can be a decrease in the residence time of the combustion gases within the micro combustor. However, due to the presence of the trapezoidal shaped ribs, the combustion gases experience a longer residence time as they are forced to flow around the equidistant distributed ribs, which decrease the challenges of incomplete combustion and flame instability. Hence, at every increase of the inlet velocity, the outer wall temperature level rises are due to the increased chemical reactions rates resulting in the increase of the heat release rate from the combustion gases.

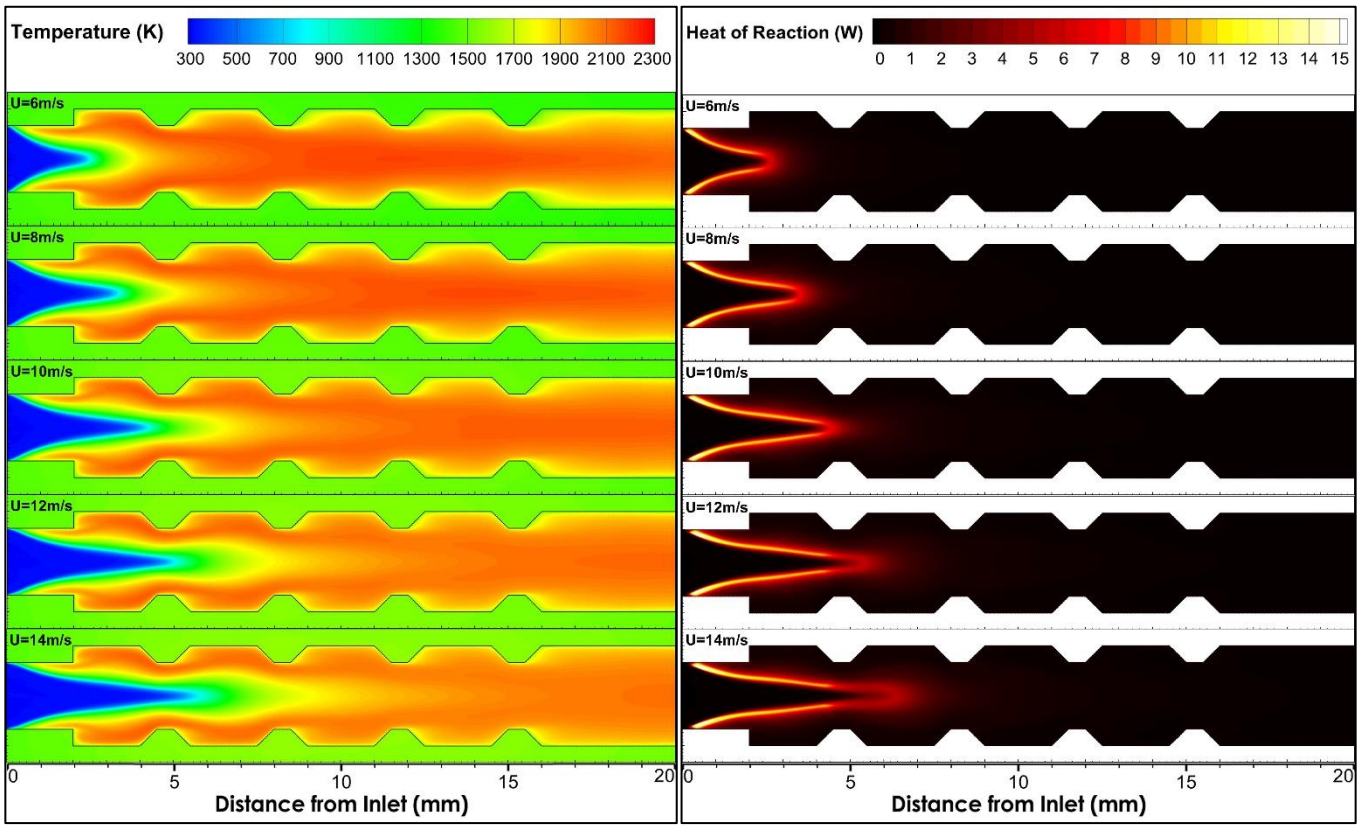

(a) *(b)*

Figure IV.1.67. *(a) Temperature and (b) heat of reaction contours for the different inlet velocities: Effect of operating conditions*

Figure IV.1.67 illustrates the temperature and heat of reaction contours for the various inlet velocities cases. The figure clearly shows that the flame shape become more stretched and elongated in the downstream direction, indicating that the combustion gases are being stretched and pulled by the stronger turbulent flow field. Consequently, as the inlet velocity increases, the cold reactants push the reaction zone away from the entrance as the inlet velocity increases. The stretched and elongated flame bring the combustion gases closer to the inner wall with each increase in the inlet velocity. Therefore, the vortices and recirculation zones become stronger and more intense, resulting in better mixing and enhance the combustion rate causing an increase in the heat release rate. In addition, the increased surface area due to the trapezoidal shape of the ribs improves the convective heat transfer of the inner wall. This upshots in a more uniform temperature distribution along the combustor outer wall length, with the peak temperature moving further downstream with each increase in the inlet velocity. These findings are consistent with the previous observations and explain the increase in the temperature level of the outer wall with each increase in the inlet velocity. However, the increase in the inlet velocity can also lead to some negative effects such as the increase in pressure drop across the combustor, which can reduce the efficiency of the system. It can also lead to excess heat transfer to the walls of the combustor, which can lead to thermal stress and potential failure of the system. Therefore, operate at higher inlet velocities is more beneficial in order to obtain greater thermal performance and better temperature uniformity.

- ***Thermal Efficiency***

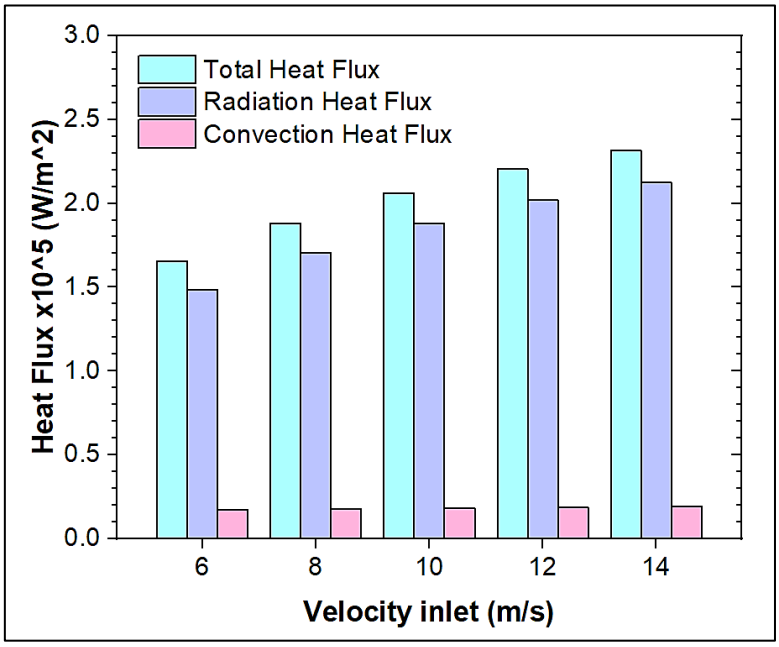

Figure IV.1.68. *The convective and radiative heat fluxes ratio to the total heat flux emitted via the outer wall for the different inlet velocities*

Figure IV.1.68 presents the comparison of the convective and radiative heat fluxes ratios to the total heat flux emitted via the micro-combustor outer wall for the various inlet velocity cases. The numerical results demonstrate a direct increase in total heat flux with the increase of inlet velocity. As shown, radiative heat flux is the dominant mechanism, consistent with previous findings. For instance, the total heat flux emitted for the inlet velocity of 8 m/s is approximately 14.54% higher than that emitted for the 6 m/s case. Furthermore, the total heat flux emitted for the inlet velocities of 10 m/s, 12 m/s, and 14 m/s are 24.85%, 33.93%, and 41.21% higher, respectively, compared to the 6 m/s case. In contrast, convective heat flux represents only 9.8% to 10.1% of the total heat flux emitted by the micro-combustor outer wall for all the inlet velocity cases. Meanwhile, the radiative heat flux represents 89.69%, 90.59%, 91.16%, 91.51%, and 91.71%, respectively, with the increase in inlet velocity.

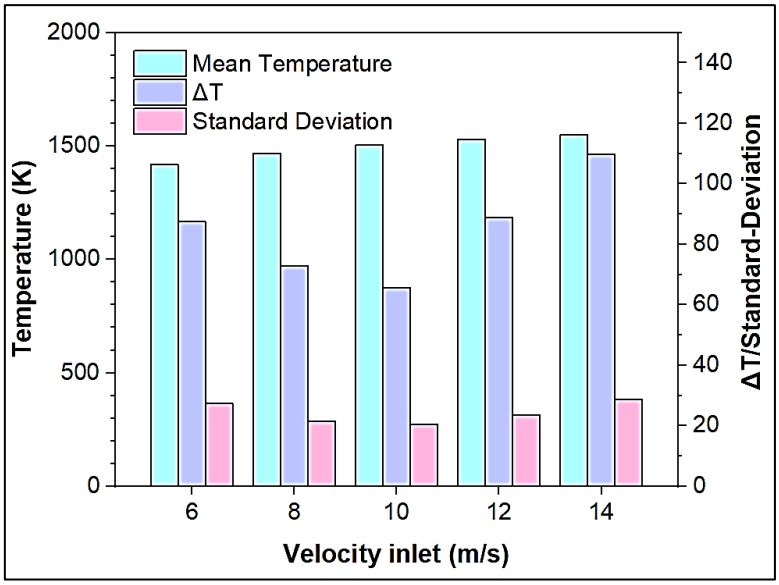

Figure IV.1.69. *The outer wall: Average temperature, temperature difference and Standard deviation for the different inlet velocities: Effect of operating conditions*

Figure IV.1.69 presents a comparison of the thermal performance key parameters for the different inlet velocities. Therefore, it can be observed that the outer wall mean temperature increases gradually from 1417.71 K to 1466.95 K, 1503.48 K, 1530.34 K, and 1549.78 K, As the inlet velocity increases from 6 m/s to 8 m/s, 10 m/s, 12 m/s, and 14 m/s, respectively. These results demonstrate the favorable effect of the inlet velocity on the thermal performance of the micro-combustor's outer wall. Specifically, increasing the inlet velocity increases the combustion chemical reactions rates, which in turn raises the temperature of the combustion products. This leads to increased convective heat transfer at the inner wall, which raises the temperature of the outer wall of the micro-combustor. On the other hand, Fig. 16 also presents the outer wall temperature differences for the different inlet velocities. As shown, the temperature difference decreases significantly for both inlet velocities of 8 m/s and 10 m/s compared to the basic case with the inlet velocity of 6 m/s. Quantitatively, the temperature difference decreases from 87.5 K to 72.9 K and 65.6 K, respectively. However, the temperature difference increases again with an increase in inlet velocity to 12 m/s and 14 m/s, to 88.79 K and 109.71 K, respectively. Therefore, the temperature difference for the inlet velocity of 10 m/s represents the lowest temperature difference among the different cases. The optimal inlet velocity for efficient thermal performance is then 10 m/s, which ensure also the temperature uniformity distribution on the outer wall of the micro-combustor. Indeed, Fig. 16 quantitatively presents the proportion of non-uniformity of the outer wall temperature profile for different inlet velocity cases using the aforementioned statistical parameter "standard of deviation". The results show that the outer wall non-uniformity significantly decreases for inlet velocities of 8 m/s and 10 m/s, respectively, compared to the 6 m/s reference case. However, the non-uniformity increases again for inlet velocities of 12 m/s and 14 m/s, respectively. Quantitatively, the standard of deviation parameter decreases from 24.41 for the inlet velocity of 6 m/s to 21.59 and 20.41 for inlet velocities of 8 m/s and 10 m/s, respectively. Figures 13 and 14 show that the peak temperature value shifts away from the inlet and downstream the combustor, resulting in higher temperature distribution differences. Accordingly, the temperature distribution at the outer wall surface becomes more non-uniform with the inlet velocities above 10 m/s.

b. Effect of Equivalence Ratio

a. Combustion Characteristics

- ***Flame Propagation***

- ***Flame Shape***

Figure IV.1.70 illustrates clearly that the variation in equivalence ratio has a profound impact on the distribution of hydrogen (H2) and hydroxyl (OH) mass fractions, as well as the flame shape in the micro-combustor. In lean mixtures (lower equivalence ratios), there is a noticeable decrease in the mass fractions of both H2 and OH. This phenomenon is intricately linked to the reduced availability of hydrogen, a key component in the combustion process. With less hydrogen present, the formation of OH radicals is hindered, leading to lower OH mass fractions. The decreased H2 and OH mass fractions correlate with a shorter flame length in lean mixtures. Conversely, in rich mixtures (higher equivalence ratios), there is an increase in both H2 and OH mass fractions. The surplus of hydrogen in rich conditions enhances the production of OH radicals, resulting in elevated OH mass fractions. The higher availability of hydrogen in rich mixtures also promotes a more complete combustion process, leading to increased H2 mass fractions. Importantly, the increase in H2 and OH mass fractions is associated with a decrease in flame length in rich mixtures. These observations can be explained through chemical kinetics. In lean conditions, the limited availability of hydrogen hampers the formation of OH radicals, crucial for sustaining combustion reactions. This limitation reduces the flame length due to a less active combustion zone. On the other hand, in rich conditions, the excess hydrogen facilitates a more extensive combustion reaction, generating

higher concentrations of H2 and OH species. The intensified combustion process results in a shorter flame length.

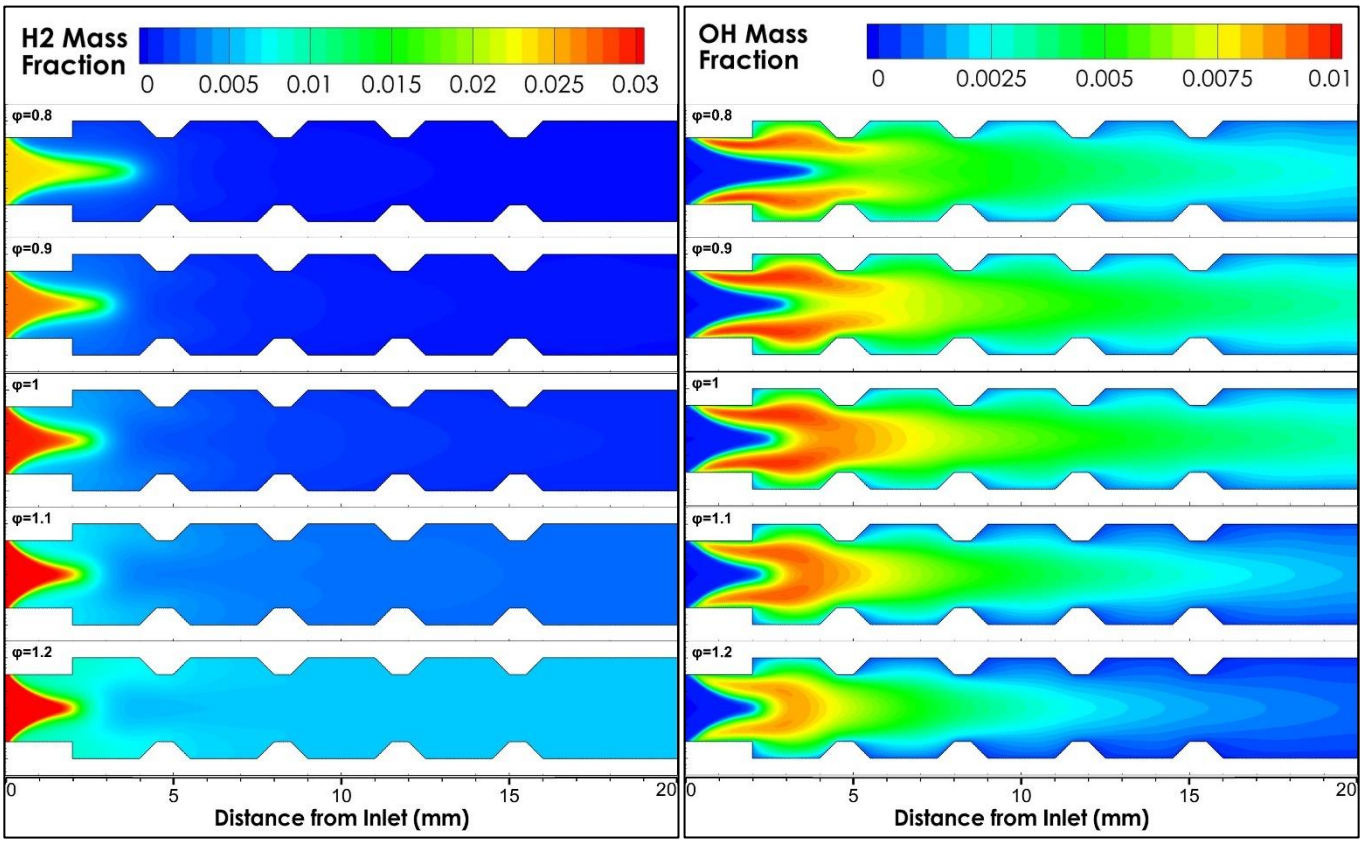

(a) *(b)*

Figure IV.1.70. *(a) Hydrogen H2 and (b) hydroxide OH mass fraction contour for the different equivalent ratios: Effect of operating conditions*

- ***Flame Front Location and Speed***

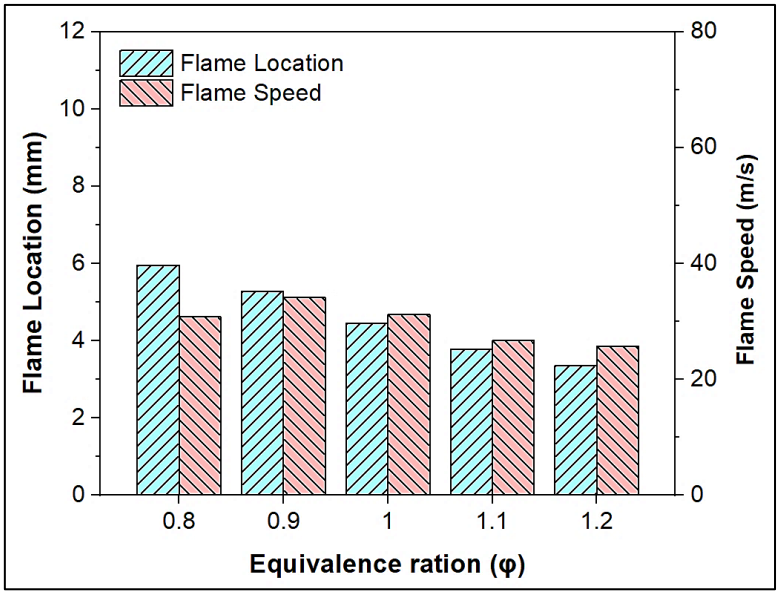

Figure IV.1.71. *Flame front location and flame speed for the different equivalent ratios: Effect of operating conditions*

As shown in **Figure IV.1.71,** the equivalence ratio plays a significant role in dictating the location and speed of the flame front in both lean and rich combustion conditions. In lean mixtures (lower equivalence

ratios), the flame front tends to be situated further downstream within the micro-combustor. This is primarily due to the limited availability of fuel (hydrogen) relative to the amount of oxidizer (air). The lower concentration of hydrogen delays the ignition and combustion processes, resulting in a flame front that penetrates deeper into the combustion chamber before achieving complete combustion. Conversely, in rich mixtures (higher equivalence ratios), the flame front is positioned closer to the micro-combustor entrance. This proximity is attributed to the surplus of fuel (excess hydrogen) compared to the available oxidizer. The higher concentration of hydrogen accelerates the ignition process, leading to a quicker formation and advancement of the flame front. As a result, the flame front is established closer to the entrance of the micro-combustor in rich conditions. The flame speed, which represents the rate at which the combustion front advances through the mixture, follows a similar trend. In lean mixtures, the flame speed is comparatively slower due to the limited fuel availability. The delayed ignition and combustion result in a more gradual progression of the flame front. On the other hand, in rich mixtures, the excess of fuel accelerates the combustion process, leading to a higher flame speed. The flame advances rapidly through the mixture, reaching its peak intensity earlier in the combustion chamber.

- ***Flame Efficiency***

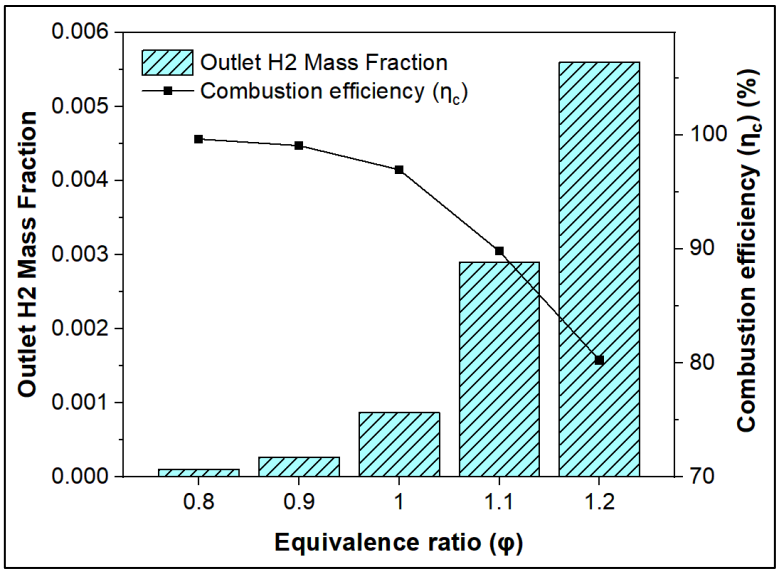

Figure IV.1.72. *Outlet H2 mass fraction and Combustion conversion efficiency for the different equivalent ratios: Effect of operating conditions*

The equivalence ratio plays a crucial role in determining the combustion conversion efficiency in micro-combustors. The combustion conversion efficiency is a measure of how effectively the fuel is converted into useful energy, such as heat, during the combustion process. As shown in **Figure IV.1.72**, it is influenced by the ratio of actual fuel-to-air mixture (equivalence ratio) compared to the stoichiometric ratio required for complete combustion. In lean mixtures (equivalence ratio below 1), where there is insufficient fuel relative to the available oxidizer, the combustion conversion efficiency tends to be lower. This is due to the incomplete combustion of the fuel, as some fuel molecules may not find sufficient oxygen for complete reaction. As a result, a portion of the fuel remains unburned, leading to a decrease in combustion efficiency. Conversely, in rich mixtures (equivalence ratio above 1), there is an excess of fuel compared to the available oxidizer. While this condition can lead to a more rapid and intense combustion, it may also result in incomplete combustion due to limited oxygen availability. In such cases, combustion conversion efficiency may be compromised, as not all the fuel can be efficiently converted into heat energy. The stoichiometric mixture, where the equivalence ratio is 1, represents the ideal condition for achieving maximum combustion efficiency. In this state, the fuel and oxidizer are present in the exact proportions required for complete combustion. Any deviation from this stoichiometric ratio can impact the efficiency of combustion process.

b. Thermal Characteristics

- ***Temperature Distribution***

In this section, the impact of the mixture equivalence ratio on the thermal performance of the proposed micro-combustor (MCRD1) is investigated. To achieve this, a set of numerical simulations was conducted under an inlet velocity of 6 m/s and four different mixture compositions: lean (0.8 and 0.9) and rich (1.1 and 1.2), and compared against the stoichiometric case. Therefore, the temperature distribution along the centerline and outer wall surface of the micro-combustor will be analyzed, along with an examination of the outer wall surface heat transfer mechanisms. Finally, the key parameters of the thermal performance will be compared.

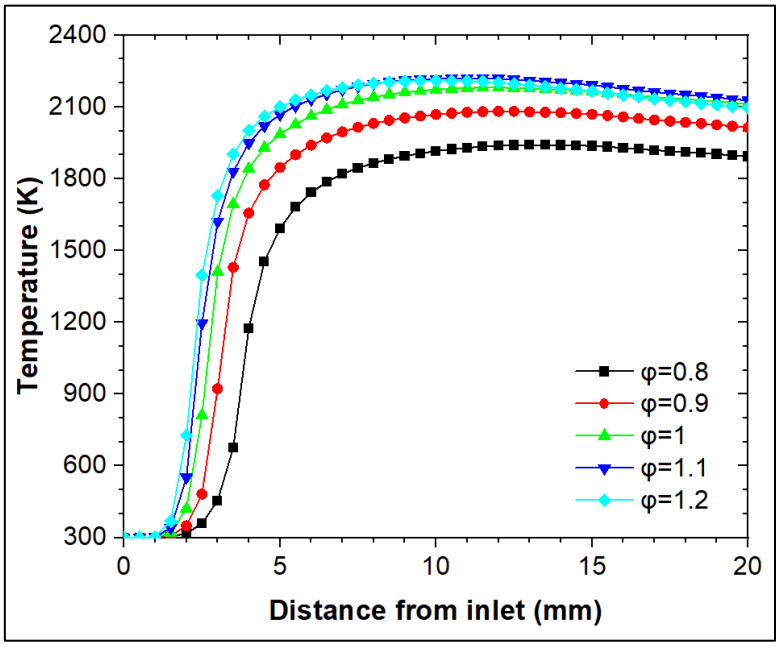

Figure IV.1.73. *Temperature distribution along the micro-combustor centerline for the different equivalence ratios: Effect of operating conditions*

Figure IV.1.73 presents the temperature distribution along the centerline of the micro-combustor for different lean and rich equivalence ratios, all compared to the stoichiometric mixture composition case. One can observe that the gaseous temperature increases from the inlet, reaches a peak constant level, and gradually decreases all along the chamber to the outlet. As shown, the temperature levels of both lean mixture compositions (φ=0.8, φ=0.9) are respectively below the temperature profile of the stoichiometric mixture composition. However, the results indicate that decreasing the concentration of hydrogen in the combustion mixture has a negative impact on the rate of micro-combustion reactions, ultimately leading to a lower heat release rate. It can also be noticed that the temperature level significantly decreases as the mixture composition shifts away from stoichiometric. Accordingly, the lean mixture with the equivalence ratio of φ=0.8 presents the lowest temperature level among the cases. Additionally, the lean mixture composition shows a more uniform temperature distribution within the micro combustor, which improve the stability of the flame. On the other hand, the temperature profiles of both rich mixture compositions (φ=1.1, φ=1.2) are slightly higher than the stoichiometric temperature profile, respectively. The increase in the fuel-to-air equivalence ratios drags the reaction zone back toward the micro-combustor entrance, which is reflected in the regression of the rich mixtures' temperature profiles towards the entrance. In return, the increase of the hydrogen ratio at the mixture composition shows a minimal increase in the micro-combustion reactions rate resulting in a higher heat release rate. Accordingly, the temperature level significantly decreases as the mixture composition shifts away from stoichiometric and the case with the equivalence ratio of φ=1.2 presents the highest temperature level among the cases.

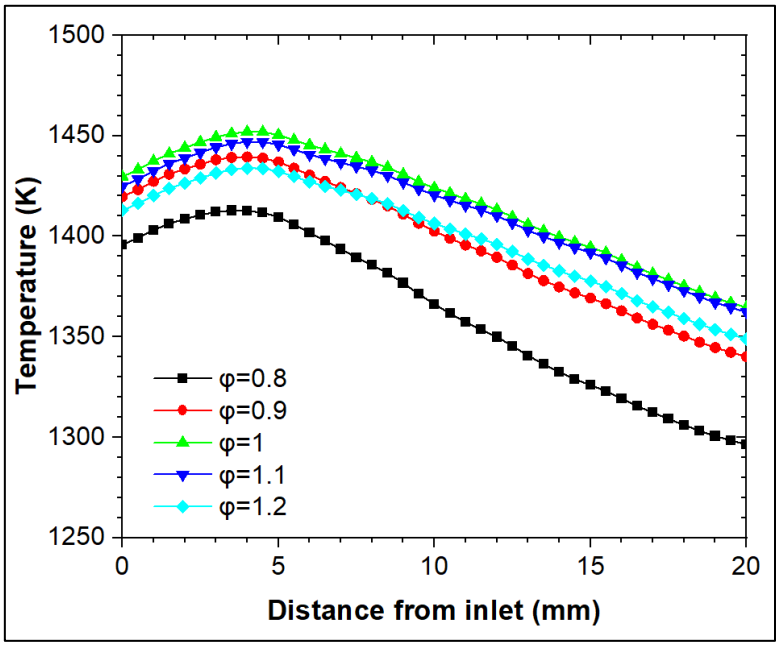

Figure IV.1.74. *Outer wall temperature distribution for the different equivalence ratios: Effect of operating conditions*

Figure IV.1.74 depicts the outer wall temperature profiles for different lean and rich equivalence ratios cases, all compared to the stoichiometric mixture composition case. The temperature profiles increase gradually from the inlet and reach a peak value around 4 mm from the micro-combustor entrance. Subsequently, the temperature profiles start decreasing gradually, but differently depending on the fuel-to-air equivalence ratio. As seen in Fig. 18, the temperature level significantly decreases as the mixture composition shifts away from stoichiometric. Consistent with the previous results, the lean mixture with φ=0.8 presents the lowest temperature level, followed by the lean mixture with the equivalence ratio of φ=0.9 and the rich mixture with the equivalence ratio of φ=1.2. Meanwhile, the outer wall temperature profile for the rich mixture with the equivalence ratio of φ=1.1 is the closest to the stoichiometric temperature profile. Based on the above results, it can be concluded that the slight increase in the temperature level of the combustion gases was not reflected in the micro-combustor's outer wall temperature.

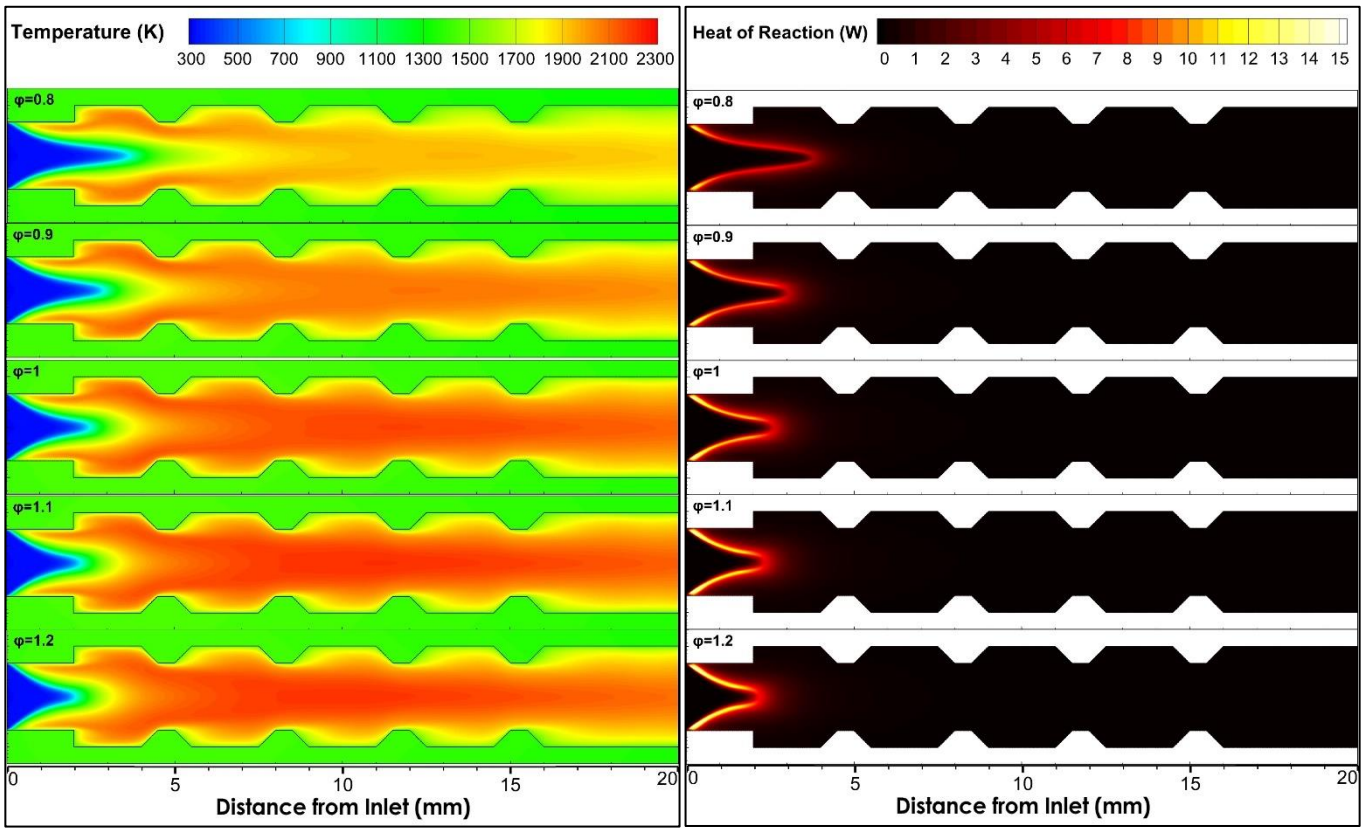

Figure IV.1.75. *(a) Temperature and (b) heat of reaction contours for the different equivalence ratios: Effect of operating conditions*

Figure IV.1.75 presents temperature contours for different lean and rich equivalence ratios cases, compared to the stoichiometric mixture composition case. The results are consistent with previous conclusions, indicating that the temperature level for lean mixture compositions with the equivalence ratios of φ=0.8 and φ=0.9 gradually decreases as the hydrogen to air equivalence ratio decreases. The temperature contours also show that reducing the hydrogen ratio leads to the reaction zone being displaced away from the micro-combustor entrance. Hence, the flame shapes are elongated, and the flame front penetrate downstream within the micro-combustor entrance. This is mainly due to the lower hydrogen concentration compared to the available oxygen in each of the lean cases resulting in a lower reaction rate. Therefore, it can be deduced that the combustion process under lean mixture composition is characterized by lower flame temperatures and slower reaction rates. On the other hand, the temperature contours for the rich mixture compositions with the equivalence ratios of φ=1.1 and φ=1.2 show a much higher temperature level than the lean mixture compositions, and a temperature level closer to the stoichiometric mixture composition. However, the temperature contours reveal that increased concentration of the hydrogen to air leading to the approximation of the ignition position from the micro-combustor entrance. Additionally, the flame shapes are diminished, and the flame front becomes closer to the micro-combustor entrance.

- ***Thermal Efficiency***

Figure IV.1.76 presents heat flux ratios transferred through the micro-combustor outer wall via different mechanisms for different lean and rich mixture compositions. The results show that the total heat flux decreases proportionally as the hydrogen to air equivalence ratio moves away from the stoichiometric mixture composition. Specifically, the total heat flux decreases for the lean mixture compositions from 1.66 10^5 (W/m^2) to 1.58 10^5 (W/m^2) and 1.43 10^5 (W/m^2) as the equivalence ratios decrease from φ=0.9 to φ=0.8. Meanwhile, the total heat flux for the rich mixture compositions cases ranges from 1.64 10^5 (W/m^2) to 1.58 10^5 (W/m^2), which is closer to the stoichiometric level, respectively for φ=1.1 and φ=1.2.

Additionally, the results show that the stoichiometric mixture composition produces the highest radiative heat flux compared to both the lean and rich mixture compositions. Furthermore, the results demonstrate that the radiative heat flux emitted under the rich mixture compositions is higher than that emitted by the lean mixture compositions. Specifically, the radiative heat flux decreases from 1.49 10^5 (W/m^2) to 1.4 10^5 (W/m^2) and 1.27 10^5 (W/m^2) for the lean mixture compositions with the equivalence ratios of φ=0.9 to φ=0.8, respectively. Meanwhile, the radiative heat flux for the rich mixture compositions of φ=1.1 and φ=1.2 ranges from 1.47 10^5 (W/m^2) to 1.42 10^5 (W/m^2), which is closer to the radiative heat flux of the stoichiometric case.

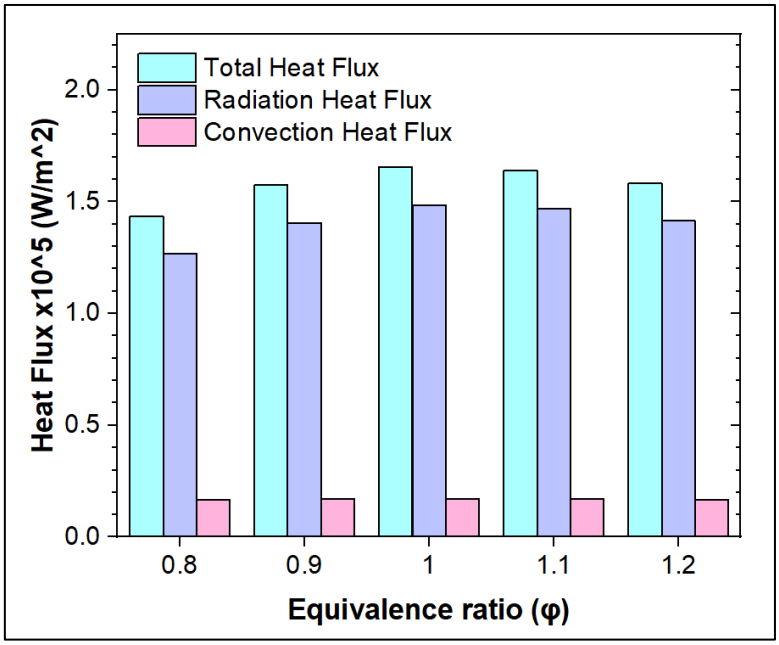

Figure IV.1.76. *The convective and radiative heat fluxes ratio to the total heat flux emitted via the outer wall for the different equivalence ratios: Effect of operating conditions*

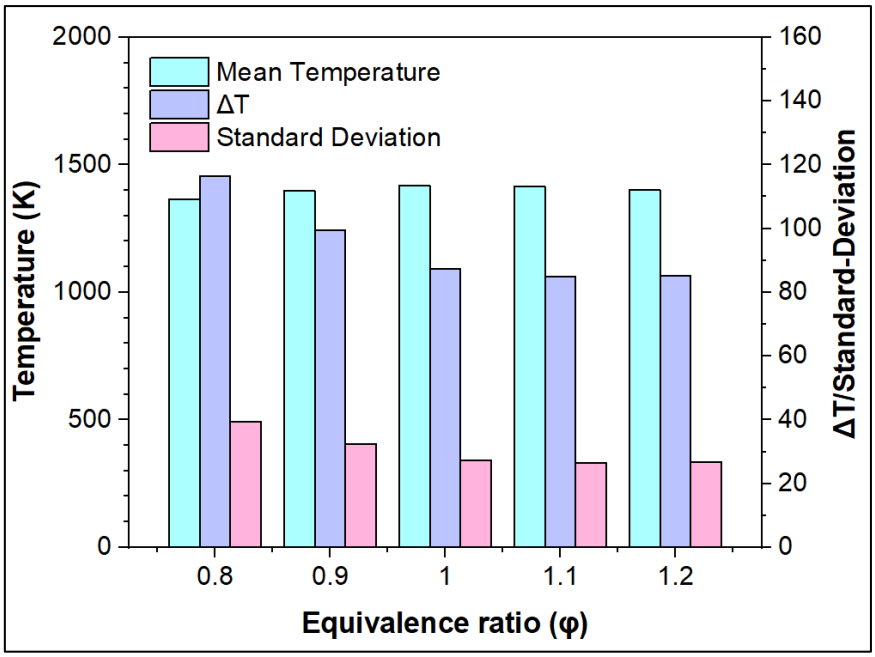

Figure IV.1.77. *The outer wall: Average temperature, temperature difference and Standard deviation for the different equivalence ratios: Effect of operating conditions*

Figure IV.1.77 presents a comparison of the thermal performance key quantities for the different lean and rich equivalence ratios. However, it can be seen that the mean temperature of the micro-combustor outer

wall does not show any significant change with the variation of the equivalence ratio, for either the lean or rich mixture compositions. Thus, the mean temperature decreases to 1398.33 K and 1363.05 K for the lean mixture compositions with the equivalence ratios of φ=0.9 to φ=0.8, respectively. On the other hand, the outer wall mean temperature for both of the rich mixture compositions (φ=1.1 and φ=1.2) decreases from the stoichiometric mean temperature level of 1417.706 K to 1414.06 K and 1400.43 K, respectively. The results indicate that the fuel-to-air equivalence ratio has a limited effect on the micro-combustor outer wall mean temperature. However, the outer wall temperature differences increase significantly for the lean mixture compositions of φ=0.9 and φ=0.8, respectively, to 99.37 K and 116.44 K compared to the temperature differences corresponding to the stoichiometric mixture composition of 87.5 K. In contrast, the temperature differences for the rich mixture compositions (φ=1.1 and φ=1.2) are 84.92 K and 85.07 K, respectively, which are slightly less than the temperature difference of the stoichiometric case. Lastly, the figure reveals that the outer wall non-uniformity increases to 32.41 and 39.52, respectively, for the lean mixture compositions of φ=0.9 to φ=0.8, compared to the non-uniformity level of the stoichiometric case of 27.41. Conversely, the rich mixture compositions with the equivalence ratios of φ=1.1 and φ=1.2 reveal an equivalent level of non-uniformity of 26.43 and 26.7, respectively, compared to the stoichiometric case.

Therefore, it can be deduced that these phenomena are related to the fact that using a lean equivalence ratio result in a more diluted hydrogen-to-air mixture compared to the stoichiometric case. Hence, the concentration of reactants available for combustion reduces, which slows down the reaction rates and reduces the heat release rate. This, in turn, result in a lower mean temperature on the micro combustor outer wall, as well as higher temperature differences. Additionally, the lean equivalence ratio led to a higher non-uniformity of the temperature distribution at the micro combustor outer wall. On the other hand, using a rich equivalence ratio result in a a more concentrated hydrogen-to-air mixture compared to the lean and stoichiometric cases. In contrast, the increased concentration of reactants slightly slows down the reaction rates and reduces the heat release rate with the increase of the equivalence ratio. Consequently, the mean temperature, as well as the temperature differences and the uniformity of the micro combustor outer wall temperature distribution are closer to the stoichiometric case. The results show that the rich mixture composition of φ=1.1 provides the closest thermal performance to the stoichiometric case, which widen the operating range for MTPV systems. Thus, the choice between a lean and rich mixture composition in micro combustion depends on the specific application and design requirements. However, the benefits of using a lean mixture composition in micro combustion include lower NOx emissions, longer combustion stability. On the other hand, the benefits of using a rich mixture composition in micro combustion include higher reaction rates resulting in a shorter combustion time, and improved combustion efficiencies. Moreover, using a rich mixture composition can also increase the risk of incomplete combustion as well as increase the formation and emissions of harmful pollutants such as nitrogen oxides (NOx). Therefore, the mixture composition in micro combustion should be carefully optimized to balance the competing demands of combustion efficiency, stability, and emissions, depending on the specific requirements of the MTPV systems application.

IV.2. 3D Numerical Simulation

This segment of our doctoral exploration extends the groundwork laid in our earlier 2D investigations, now delving into the tridimensional (3D) realm to scrutinize the impact of micro combustor cross sections on Micro-Thermophotovoltaic (MTPV) performance. This marks the application of our established numerical methodology in practical simulations, transitioning from theoretical underpinnings to real-world scenarios. The primary objective is to evaluate how the proposed trapezoidal-shaped rib enhancements influence the overall efficiency of MTPV systems within the context of three-dimensional geometrical configurations. Aligned with the central theme of our thesis, we embark on an in-depth numerical analysis of turbulent mixing within the micro combustor, exploring cylindrical and planar geometrical configurations. Rooted in the field of micro-combustion and its enhancement strategies, our numerical study carries the potential to impact diverse applications crucial to contemporary advancements, with a specific focus on MTPV systems.

IV.2.1. Effect of Geometry

- **Physical Model**

The primary focus of our investigation is to examine the influence of micro combustor cross-sectional shapes, specifically cylindrical and planar configurations, on various aspects of Micro-Thermophotovoltaic (MTPV) systems. A critical parameter under examination is the impact of the cross-sectional shape on the area of the external surface. This consideration is paramount as it directly affects the thermal radiation emissions from the micro combustor, a crucial aspect in the functioning of MTPV systems. The importance of cross-sectional shape exceeds the micro combustor itself, extending to the overall configuration and composition of the MTPV system and its constituent parts. The chosen shape significantly influences the design and layout of the Thermal Photovoltaic (TPV) cells, dictating how they will be installed within the system. This interdependence highlights the intricate relationship between the micro combustor's geometry and the subsequent design considerations for efficient energy conversion within the MTPV system. On the other hand, the shape of the micro combustor plays a pivotal role in determining the form and arrangement of MTPV system. This, in turn, impacts their installation and alignment, crucial factors in optimizing energy capture and conversion efficiency. The cross-sectional shape of the micro combustor emerges as a key factor in shaping the overall structure and performance of the MTPV system. Our study employs a set of numerical simulations conducted using our established methodology. These simulations form the basis of a comparative analysis, evaluating the performance of micro-combustors in terms of flow-field dynamics, combustion characteristics, and heat transfer attributes. Furthermore, a second phase of investigation involves calculating the overall efficiency and performance metrics for each shape, providing comprehensive insights into their respective contributions to the efficiency and effectiveness of the MTPV system. This multi-faceted exploration aims to unravel the intricate interplay between micro combustor cross-sectional shapes and the broader design and performance considerations within the realm of Micro-Thermophotovoltaic systems.

In the following, the dimensions of various geometrical configurations will be defined, encompassing the geometrical configuration to be used in the study of the effects of cross-section shape. As shown in **Figure IV.2.1.**, the micro-combustor with cylindrical configuration featured two tubes, with the first tube has a diameter of $d_1 = 2\ mm$ and a corresponding length of $L_2 = 2\ mm$. The second tube diameter is of $d_1 = 3\ mm$. Therefore, the backward-facing step and equidistant distributed ribs have a height of $s = 0.5\ mm$. The micro combustor has a total length of the of $L_1 = 20\ mm$ and a thickness of $t_1 = 0.5\ mm$. Furthermore, the micro-combustor with planar configuration featured two channels, with the first channel has a height of $h_1 = 2\ mm$ and a corresponding length of $L_2 = 2\ mm$. The second channel height is of

$h_2 = 3\,mm$. Moreover, the micro combustor has an external width of $W_{ext} = 9\,mm$, and an internal width of $W_{int} = 8\,mm$. Furthermore, the step and equidistant distributed ribs have a height of $s = 0.5\,mm$. The micro combustor has a total length of the of $L_1 = 20\,mm$ and a thickness of $t_1 = 0.5\,mm$.

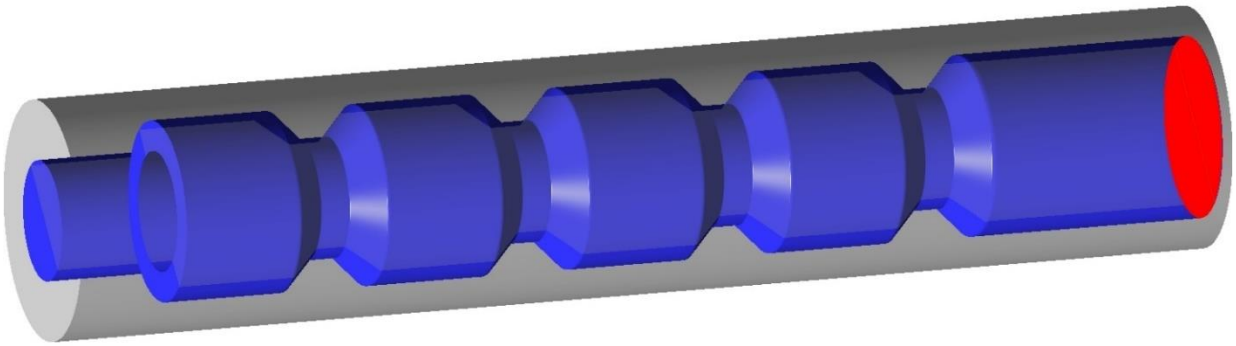

(a) Cylindrical micro combustor

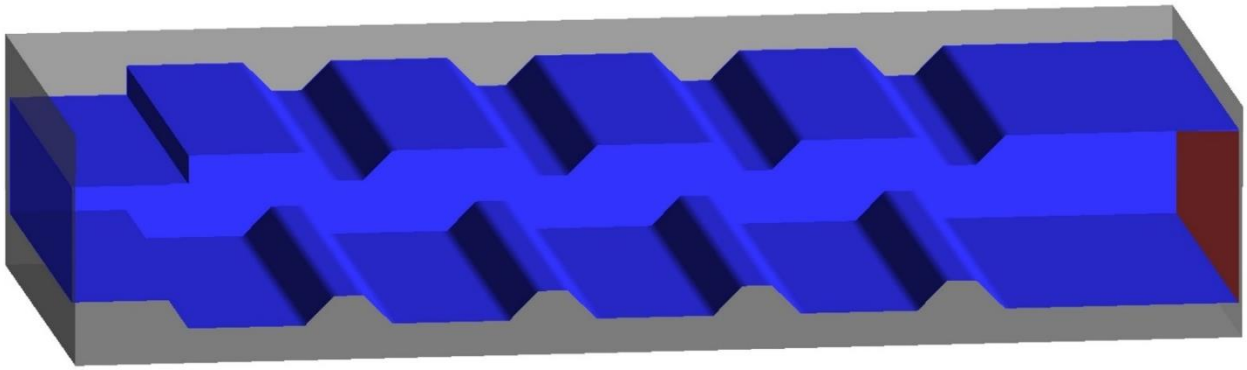

(b) Planar micro combustor

Figure IV.2.1. *Schematic diagram of the cylindrical and planar micro combustor configurations.*

- ## Computational Parameters: 3D Approach

In the realm of numerical simulations for micro combustors, it is crucial to establish well-defined boundary conditions to ensure accurate and consistent results. In the study of cross section effect, we maintain stringent control over two key parameters during each simulation: the equivalence ratio (ϕ) and the inlet velocity (U_{in}). The equivalence ratio represents the ratio of the actual fuel-to-air mixture compared to the stoichiometric ratio required for complete combustion, and we consistently set it at 1.0. This value is fundamental in determining the fuel-air mixture's composition and its influence on combustion characteristics. Additionally, we maintain the inlet velocity at a constant 6 m/s. The details of these boundary conditions are summarized in **Table IV.2.1** for quick reference.

Table IV.2.1. *Computational parameters for the effect of geometry: 3D Approach*

Boundary	Parameters	Values
Inlet	Velocity Inlet (m/s)	6
	Temperature (K)	300
	Gauge pressure (Pa)	0
	Hydraulic diameter (mm)	2
	Turbulent intensity (%)	5
	Equivalence ratio ϕ	1
Outlet	Gauge pressure (Pa)	0
	Hydraulic diameter (mm)	3
	Turbulent intensity (%)	5
Wall	Material	316 Stainless-steel
	Thermal condition	Mixed
	Natural convective heat transfer coefficient (W/(m^2.K))	15
	External & internal emissivity	0.65

- ## Results and Discussions: 3D Approach

a. Flow field characteristics

In the investigation of flow-field characteristics for cylindrical and planar micro combustor configurations, distinctive observations emerge, reflecting the nuanced impact of cross-sectional shape on fluid dynamics. The cylindrical configuration manifests a symmetrical and streamlined flow pattern, characterized by a well-defined axial flow along the combustion chamber's central axis. The circular symmetry of the cylindrical micro combustor promotes a more uniform distribution of flow velocities, fostering stable combustion conditions. Conversely, the planar configuration introduces a departure from radial symmetry, instigating complex flow structures, including vortices and recirculation zones. The planar shape induces asymmetry in the flow field, leading to variations in velocity profiles and turbulence intensity. The interaction between the planar geometry and the flow dynamics generates intricate flow patterns, potentially influencing combustion stability and heat transfer characteristics. This comparative analysis sheds light on the distinct flow-field behaviors associated with cylindrical and planar micro combustor configurations, providing valuable insights for optimizing the design and performance of MTPV systems.

- ***Stream Field***

In the non-reacting conditions, the **Figure IV.2.2** and **Figure IV.2.3** illustrates differences in velocity contours between the cylindrical and planar micro combustor configurations remain consistent with the inherent characteristics of their cross-sectional shapes under non reacting and reacting conditions, respectively. In the cylindrical configuration, the symmetrical velocity profile persists, indicating a uniform flow distribution along the central axis. The circular cross-section promotes a smooth and regular flow pattern, fostering stability in the non-reacting state. The planar configuration, on the other hand, maintains its asymmetry, with localized variations in velocity across the mid-plane. This asymmetry can be attributed to the planar shape, which introduces distinct flow dynamics near the corners and edges. When transitioning to reacting conditions, the impact of combustion on velocity contours becomes

evident. In the cylindrical micro combustor, combustion processes tend to maintain the symmetrical velocity distribution observed in the non-reacting state, with the flame propagating uniformly within the circular cross-section. The combustion-induced flow alterations are relatively minimal, and the cylindrical shape contributes to a stable combustion environment. Conversely, in the planar micro combustor under reacting conditions, the combustion process introduces additional complexities to the flow field. The asymmetry observed in non-reacting conditions persists, but combustion-related effects, such as flame propagation and heat release, lead to localized changes in velocity. The planar shape influences the interaction between combustion and flow, resulting in distinct regions of higher and lower velocities along the mid-plane. Scientifically, these observations underscore the intricate interplay between combustion and cross-sectional geometry. The differences in velocity contours under non-reacting and reacting conditions highlight the need for a comprehensive understanding of flow dynamics in both scenarios. This knowledge is essential for optimizing micro combustor designs to ensure stable and efficient combustion processes, particularly in the context of Micro-Thermophotovoltaic systems where precise control of combustion is paramount for energy conversion efficiency.

Non-reacting flow

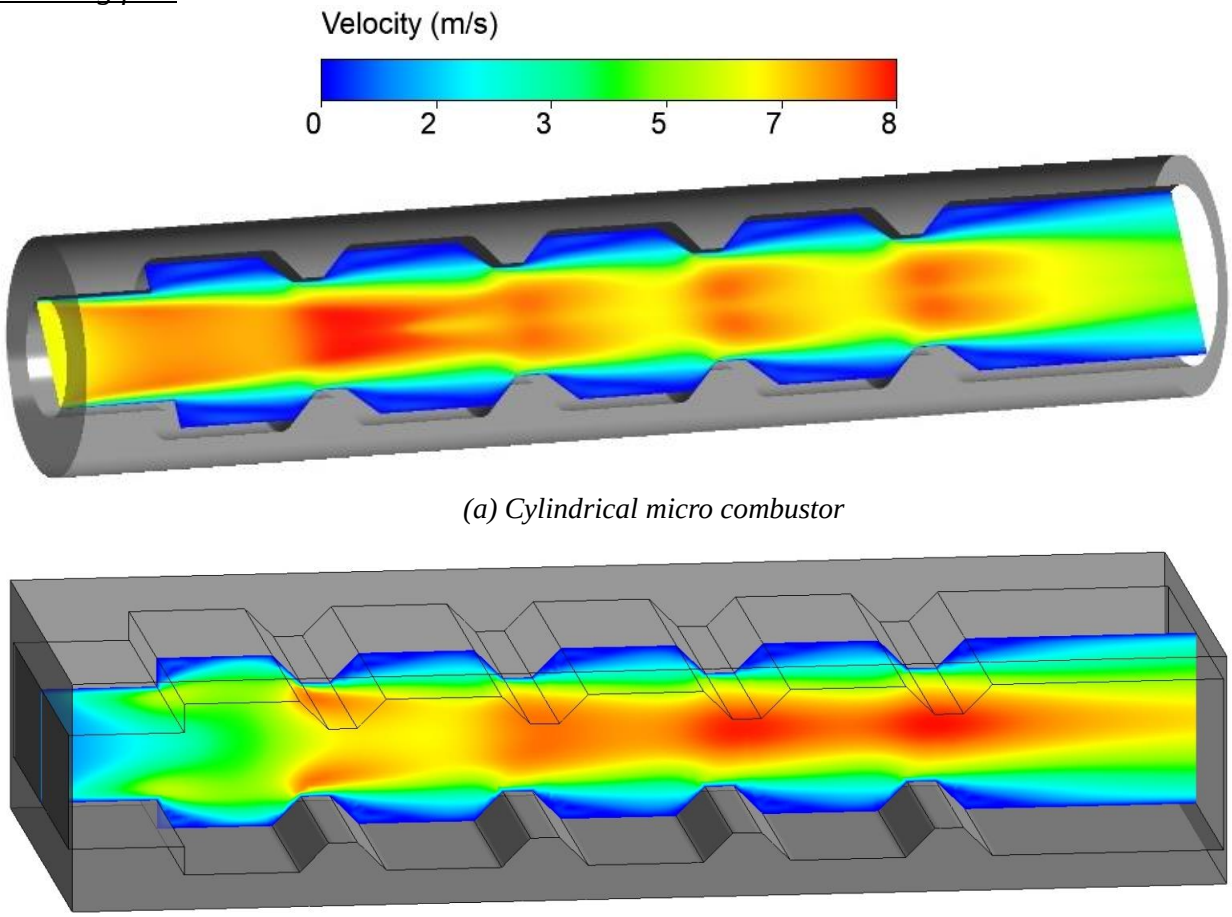

(a) Cylindrical micro combustor

(b) Planar micro combustor

Figure IV.2.2. *Non-reacting flow-field velocity contours for cylindrical and planar micro combustors: Effect of cross section.*

Reacting flow

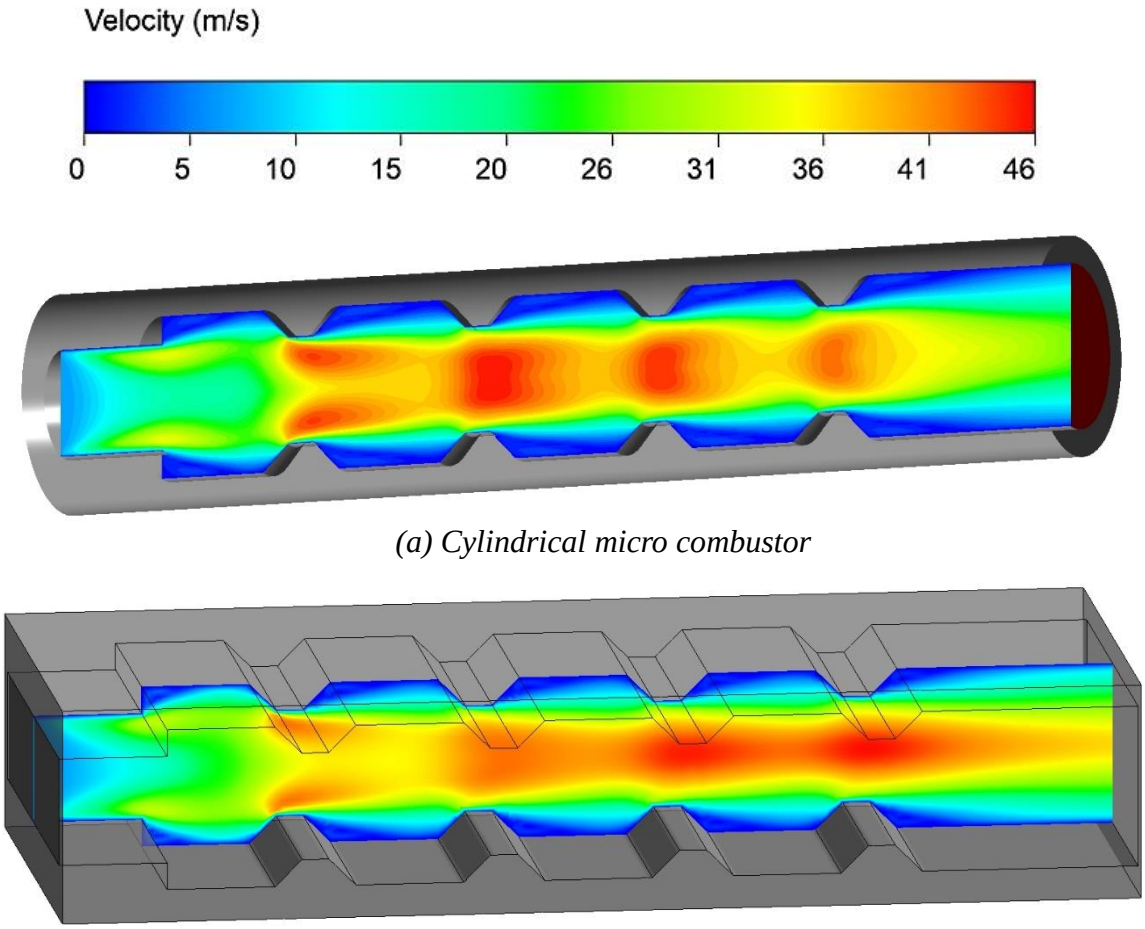

(a) Cylindrical micro combustor

(b) Planar micro combustor

Figure IV.2.3. *Reacting flow-field velocity contours for cylindrical and planar micro combustors: Effect of cross section.*

- ***Pressure Field***

Figure IV.2.4 and **Figure IV.2.5** illustrate the pressure field on the mid-plane of cylindrical and planar micro combustor configurations provides insights into the dynamic variations in pressure distribution. In the case of the cylindrical configuration, the pressure contours exhibit a symmetrical pattern, with a gradual decrease in pressure towards the outer edges. This symmetrical pressure profile corresponds to the circular cross-section, fostering a balanced pressure distribution along the central axis. On the other hand, the planar micro combustor displays a more complex pressure contour pattern on the mid-plane. The planar configuration introduces asymmetry in the pressure distribution, leading to localized pressure variations and gradients. The pressure contours on the mid-plane of the planar micro combustor underscore the impact of cross-sectional shape on the development of intricate pressure fields. Recognizing these pressure field differences is essential for optimizing combustion stability, heat transfer, and overall system efficiency in the context of Micro-Thermophotovoltaic applications. The observed differences in pressure field characteristics between cylindrical and planar micro combustor configurations are rooted in their distinct geometric features and their influence on fluid dynamics. In the case of the cylindrical micro combustor, the symmetrical pressure contours on the mid-plane are a result of the circular cross-section, which promotes a uniform distribution of pressure along the central axis. The cylindrical shape encourages a streamlined flow pattern, with the fluid moving symmetrically around the central axis, leading to a gradual decrease in pressure towards the outer edges. This configuration facilitates a more balanced pressure distribution, contributing to stable combustion conditions.

Non-reacting flow

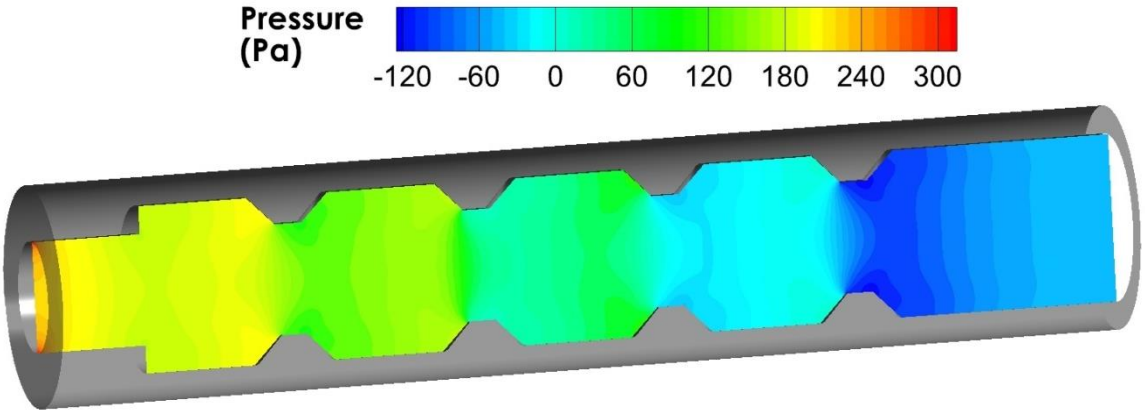

(a) Cylindrical micro combustor

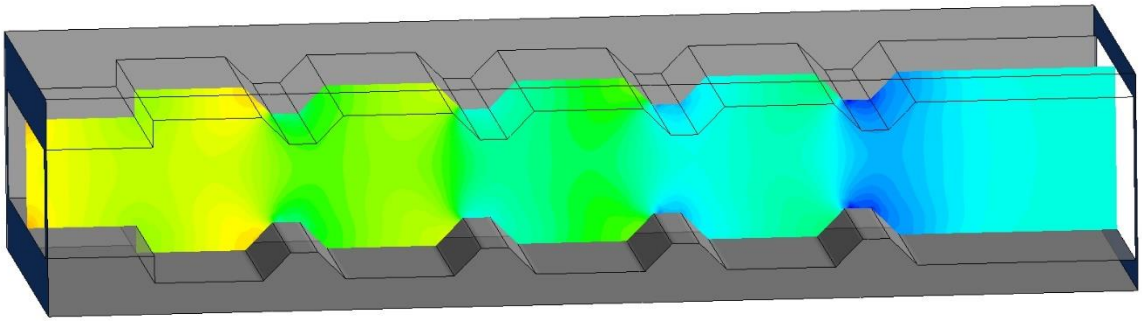

(b) Planar micro combustor

Figure IV.2.4. *Non-reacting flows static pressure contours for cylindrical and planar micro combustors: Effect of cross section.*

Reacting flow

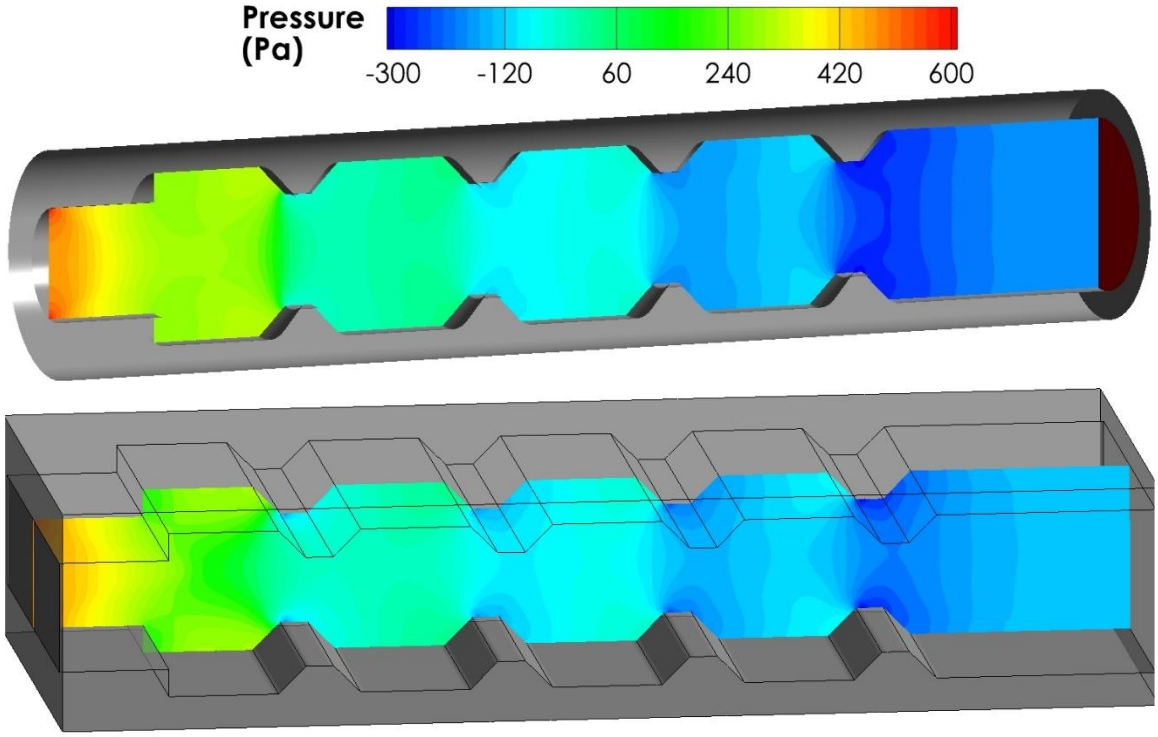

Figure IV.2.5. *Reacting flows static pressure contours for cylindrical and planar micro combustors: Effect of cross section.*

Conversely, the planar micro combustor introduces asymmetry to the pressure distribution on the mid-plane due to its flat and rectangular cross-sectional shape. The planar configuration disrupts the symmetry of the flow, resulting in localized pressure variations and gradients. The corners and edges of the planar shape create areas of higher pressure, leading to a more complex pressure contour pattern. This asymmetry can impact combustion stability and heat transfer characteristics within the micro combustor. From a scientific standpoint, these observations align with fundamental fluid dynamics principles. The shape of the cross-section significantly influences the development of boundary layers, vortices, and pressure gradients within the micro combustor. The differences in pressure field behaviors for cylindrical and planar configurations highlight the need for a nuanced understanding of how geometric variations impact flow dynamics. This understanding is crucial for optimizing micro combustion systems, especially in the context of Micro-Thermophotovoltaic applications, where efficient heat transfer and combustion stability are paramount for overall system performance.

- ***Turbulence Level***

Turbulence level of chemical reactions flow is known to play an important role in combustion performance and stability. Since the flow and chemical reactions are coupled processes, the chaotic dynamics of turbulent flow will cause the enhancement of mixing between the unburnt and burnt reactants. Thus, the turbulent environment increases the burning velocity of the cold reactants which then accelerates the reactions heat releasing. This reveals the mutual effect of turbulence present on both chemical and thermal processes of combustion. However, the introducing of ribs leads to direct increment of turbulence level. Hence, the turbulence level is characterized using: turbulent kinetic energy (k), turbulence intensity (I) and turbulent vorticity. Therefore, to isolate the effect of the combustion and to elicit the effect of the proposed geometry, a comparative study of the level of turbulence under non-reaction and reacting conditions between the cylindrical and planar micro combustors will take place.

- ***Turbulence Kinetic energy***

As shown in **Figure IV.2.6** and **Figure IV.2.7** The distinctions in turbulent kinetic energy (TKE) characteristics between cylindrical and planar micro combustor configurations stem from their respective cross-sectional shapes and the resulting impact on turbulent flow patterns. In the case of the cylindrical micro combustor, the symmetrical distribution of TKE on the mid-plane is influenced by the circular cross-section. The cylindrical shape promotes a more uniform velocity profile and turbulence distribution along the central axis. The rotational symmetry of the cylindrical configuration facilitates a smoother flow, reducing turbulent fluctuations and minimizing TKE near the centerline. Conversely, the planar micro combustor, with its flat and rectangular cross-section, introduces asymmetry to the TKE distribution on the mid-plane. The planar shape disrupts the symmetry of the flow, leading to variations in turbulence intensity across the cross-section. The corners and edges of the planar configuration create regions with higher TKE, resulting in an uneven TKE contour pattern. This asymmetry signifies increased turbulent fluctuations and more complex flow dynamics within the planar micro combustor. Scientifically, these observations align with turbulence theory, where the geometry of the flow domain plays a crucial role in shaping turbulence characteristics. The differences in turbulent kinetic energy behaviors for cylindrical and planar configurations underscore the importance of considering cross-sectional shape in micro combustion studies. This understanding is vital for optimizing combustion efficiency and turbulence control, especially in the context of Micro-Thermophotovoltaic applications, where stable and controlled combustion is essential for maximizing energy conversion efficiency.

Non-reacting flow

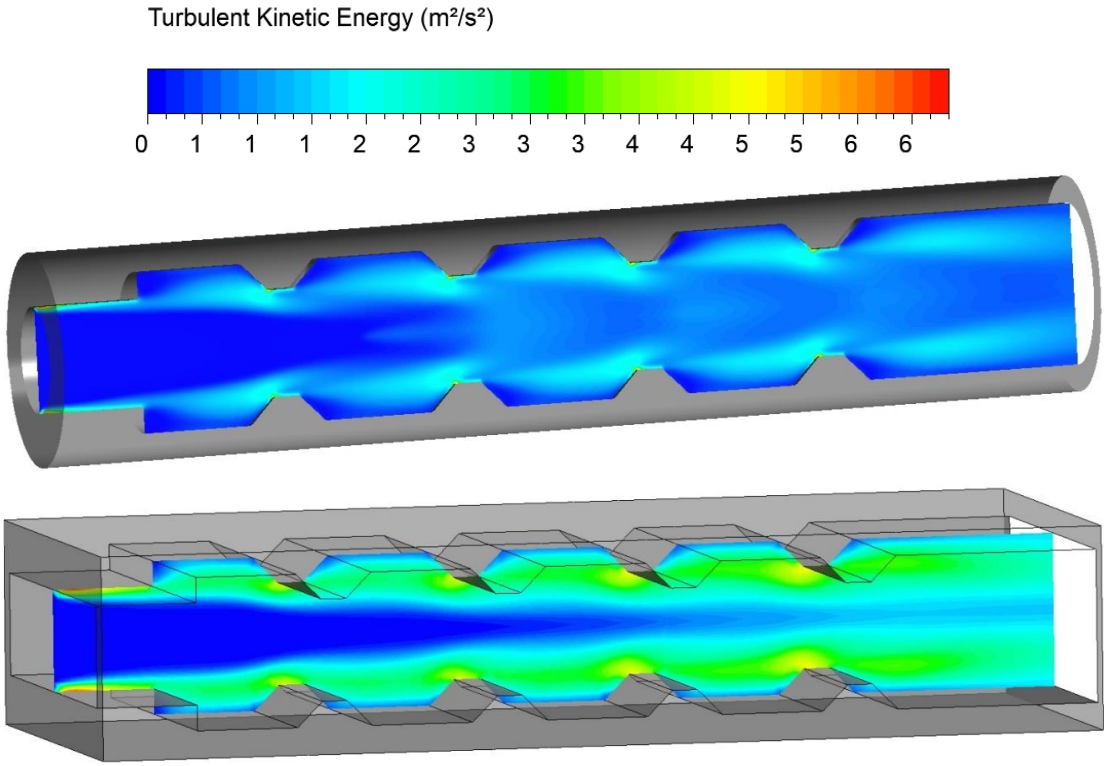

Figure IV.2.6. *Non-reacting flows turbulence level. Turbulent kinetic energy (TKE) contours for cylindrical and planar micro combustors: Effect of cross section.*

Reacting flow

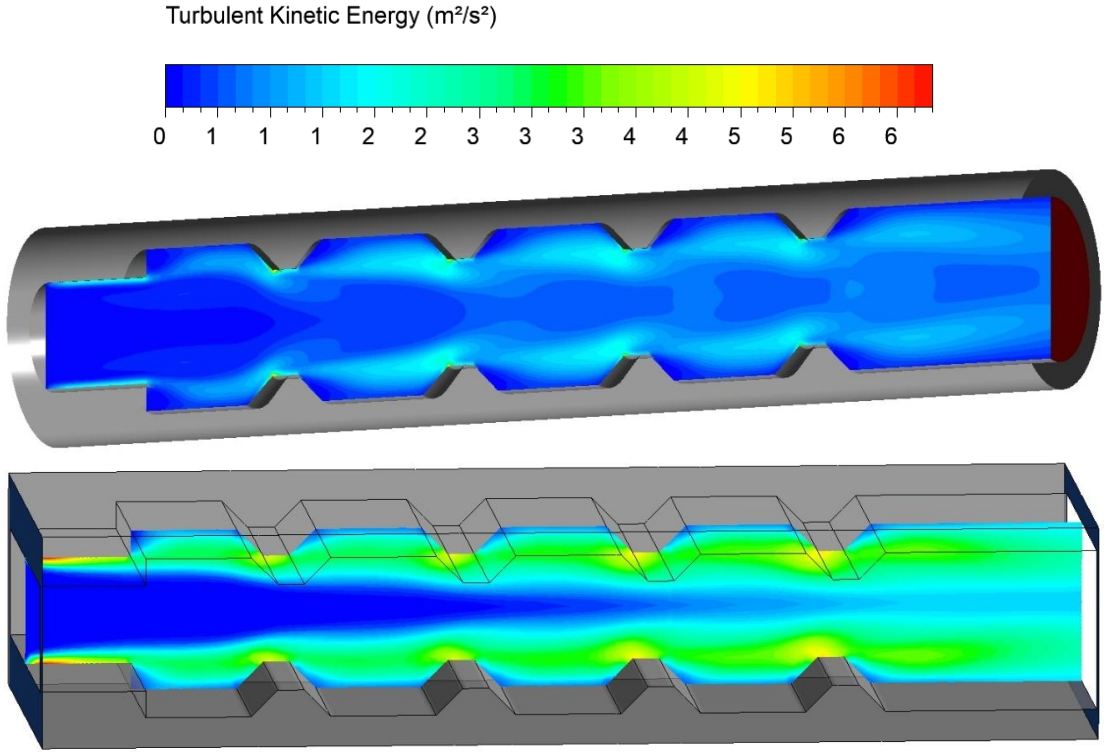

Figure IV.2.7. *Reacting flows turbulence level. Turbulent kinetic energy (TKE) contours for cylindrical and planar micro combustors: Effect of cross section.*

- ***Vorticity dynamics***

Vorticity is a key parameter in understanding the flow characteristics of micro combustors, and the Q criterion is a valuable tool for visualizing vortical structures. The Q criterion is based on the second invariant of the velocity gradient tensor and is often used to identify regions of vorticity in a flow field. In the context of micro combustors, vorticity plays a crucial role in combustion dynamics and heat transfer. Using the Q criterion, the vortical structures in both cylindrical and planar micro combustor configurations can be examined in **Figure IV.2.8** and **Figure IV.2.9**. In non-reacting conditions, vorticity is primarily influenced by the geometry of the micro combustor. For the cylindrical configuration, the Q criterion reveals well-defined vortices along the central axis, indicative of a stable and organized flow. The circular cross-section promotes the formation of coherent vortical structures. In contrast, the planar configuration exhibits more complex vorticity patterns, with distinct regions of vortices near corners and edges. Transitioning to reacting conditions, the Q criterion provides insights into how combustion interacts with vortical structures. In the cylindrical micro combustor, the combustion-induced vorticity tends to align with the existing flow patterns, contributing to a relatively ordered combustion process. The circular cross-section aids in maintaining coherent vortical structures even during combustion. In the planar micro combustor under reacting conditions, combustion introduces additional vortical complexities. The interaction between combustion and the planar geometry leads to the formation of intricate vortical structures, especially in regions where flame fronts and recirculation zones coincide. The Q criterion helps identify these areas of intensified vorticity. Scientifically, the analysis of vorticity using the Q criterion provides valuable insights into the coupling of combustion and flow dynamics in micro combustors. Understanding vortical structures is essential for optimizing combustion efficiency, heat transfer, and overall performance in Micro-Thermophotovoltaic systems. This knowledge contributes to the advancement of micro-combustion technology for enhanced energy conversion in future applications.

Non-reacting flow

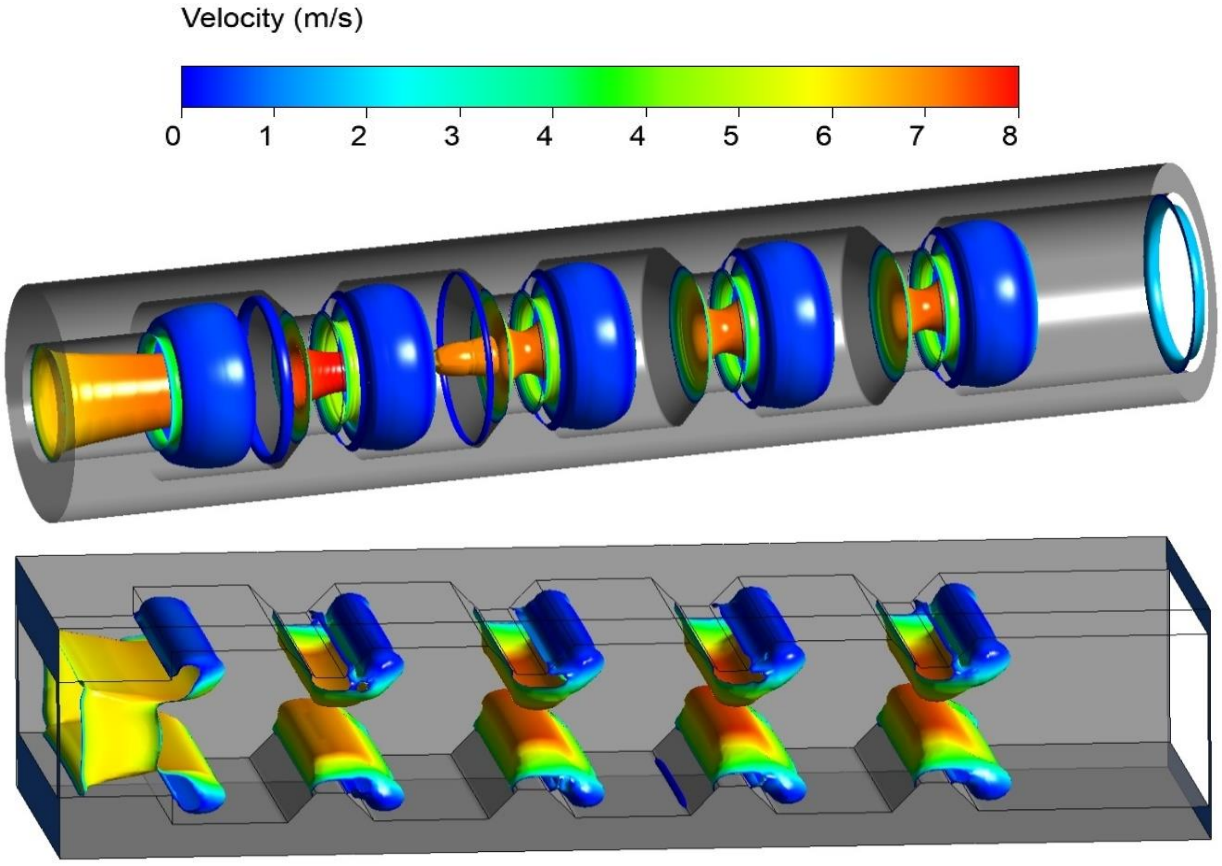

Figure IV.2.8. *Non-reacting flows turbulence level. Turbulence Vorticity contours for cylindrical and planar micro combustors: Effect of cross section.*

Reacting flow

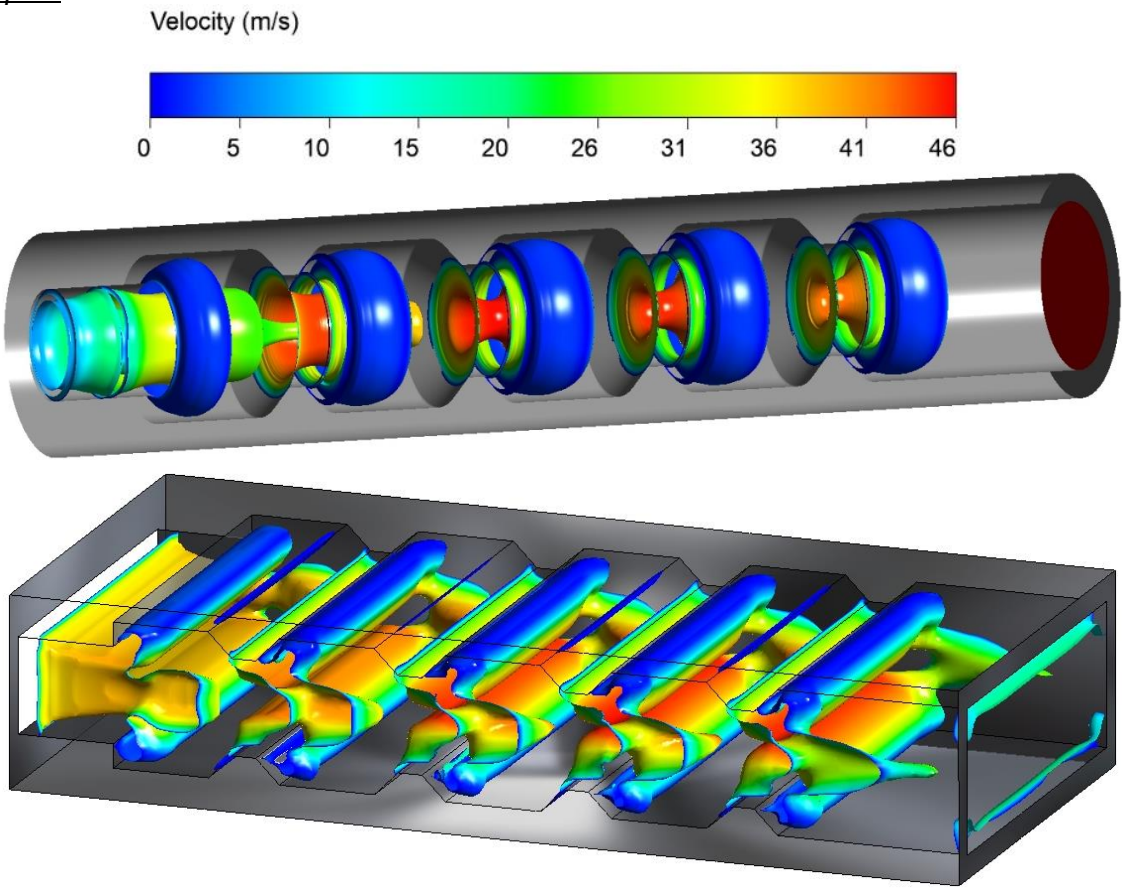

Figure IV.2.9. *Reacting flows turbulence level. Turbulence Vorticity contours for cylindrical and planar micro combustors: Effect of cross section.*

b. Combustion characteristics

In the realm of reacting flows, the utilization of H2 and OH isosurfaces emerges as a pivotal technique for unraveling the intricacies of the flame and reaction zones within 3D structures. As shown in **Figure IV.2.10** and **Figure IV.2.11,** this method provides a visual representation of the regions where hydrogen (H2) and hydroxyl (OH) radicals are present in significant concentrations, offering valuable insights into the spatial distribution of the combustion process. In the context of 3D cylindrical and planar micro combustor configurations, these isosurfaces become indispensable tools for discerning the dynamics of the flame and reaction zones. As the combustion reactions unfold, the H2 isosurfaces delineate the areas enriched with hydrogen, showcasing the flame front and regions where the fuel is actively participating in chemical reactions. Simultaneously, the OH isosurfaces provide a glimpse into the zones abundant in hydroxyl radicals, serving as indicators of the reaction intensity and aiding in identifying the specific locations of the reaction zones. In the 3D cylindrical configuration, the isosurfaces contribute to capturing the three-dimensional nature of the combustion process. The circular cross-section influences the shape and distribution of these isosurfaces, providing a unique perspective on the evolving flame structure. The isosurfaces become intricate visual representations of the coupling between combustion and vortical structures, contributing to a comprehensive understanding of the combustion dynamics. Similarly, in the planar micro combustor, the isosurfaces play a crucial role in revealing the flame and reaction zones within the distinct geometric features. The planar configuration introduces complexities in the flame patterns, and the isosurfaces act as powerful tools for elucidating the interplay between combustion and vortical structures in three-dimensional space. Scientifically, the application of H2 and OH isosurfaces in reacting flows enhances our ability to analyze and interpret the spatial characteristics of combustion. This visualization technique significantly contributes to the advancement of micro-combustion research, providing valuable data for optimizing combustion efficiency and heat transfer in complex 3D structures.

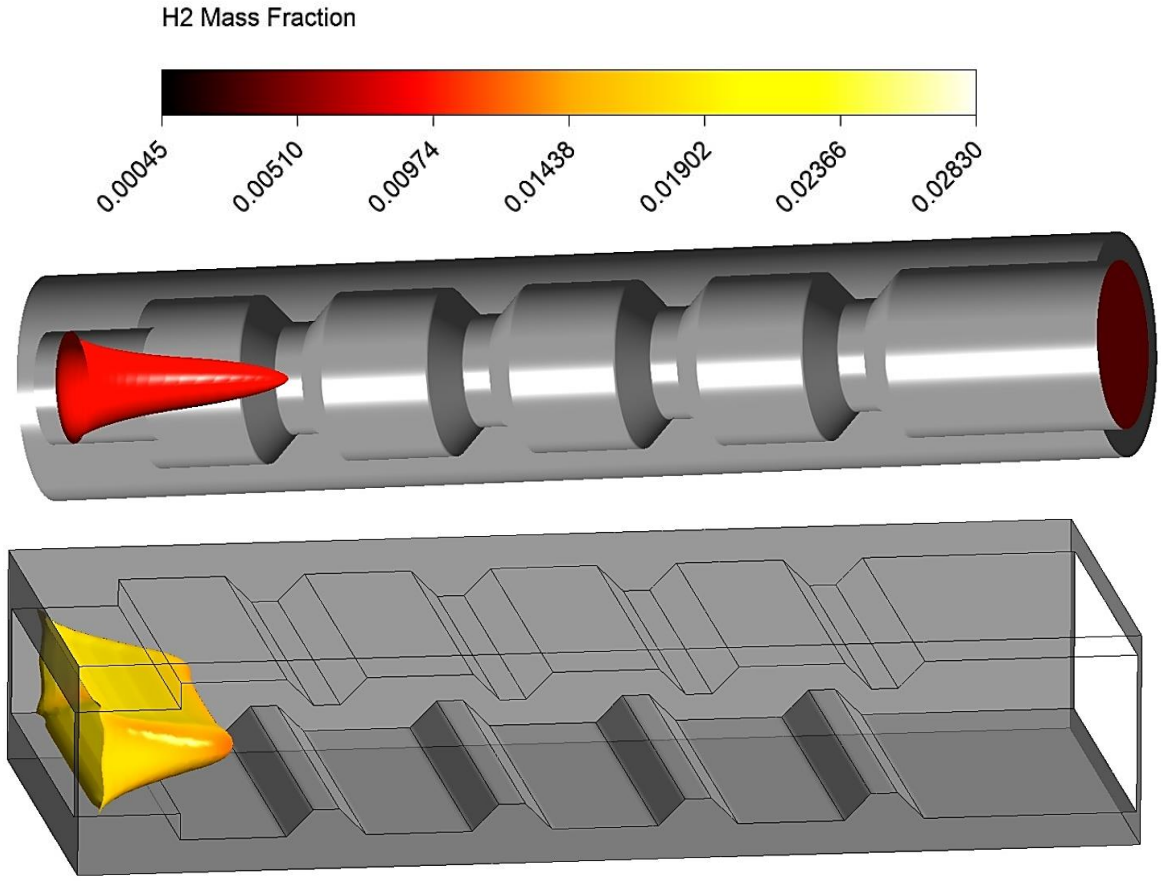

Figure IV.2.10. *Reaction zone shape (H_2 isosurfaces) for cylindrical and planar micro combustors: Effect of cross section.*

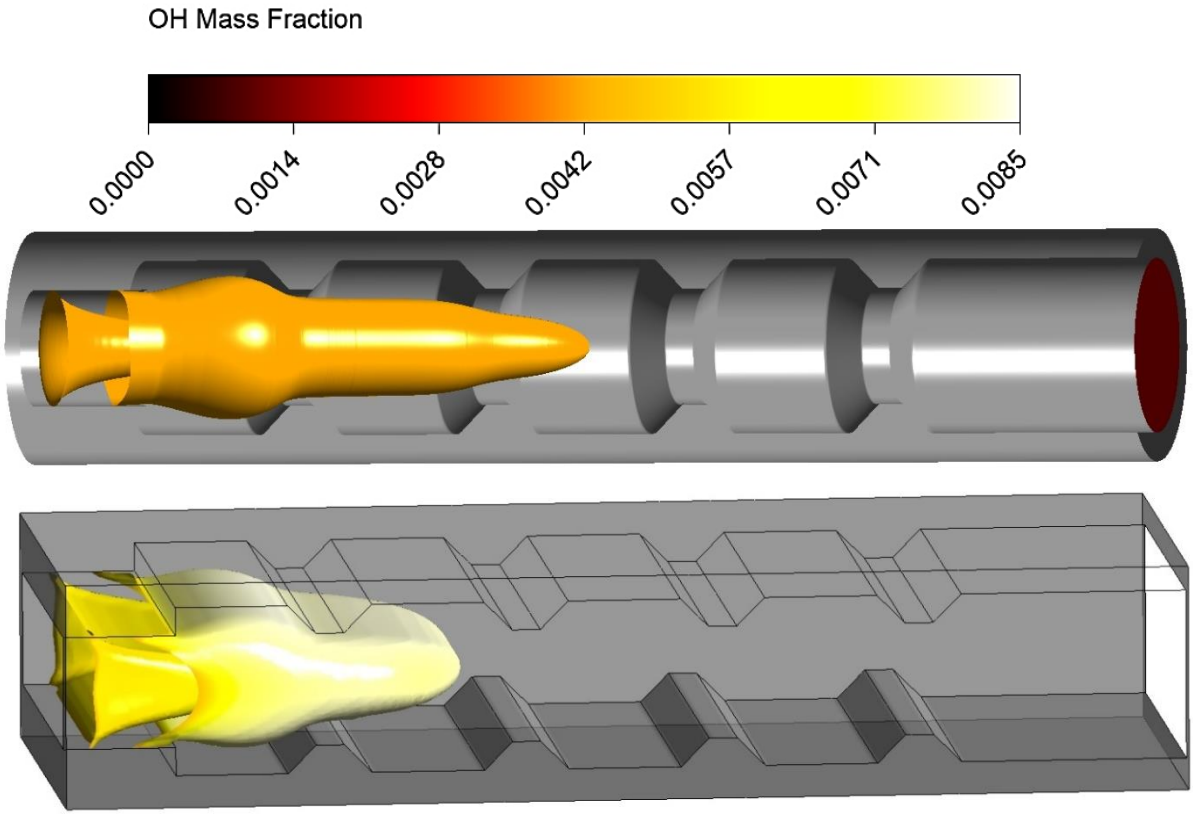

Figure IV.2.11. *Flame shape (OH isosurfaces) for cylindrical and planar micro combustors: Effect of cross section.*

c. Thermal Characteristics

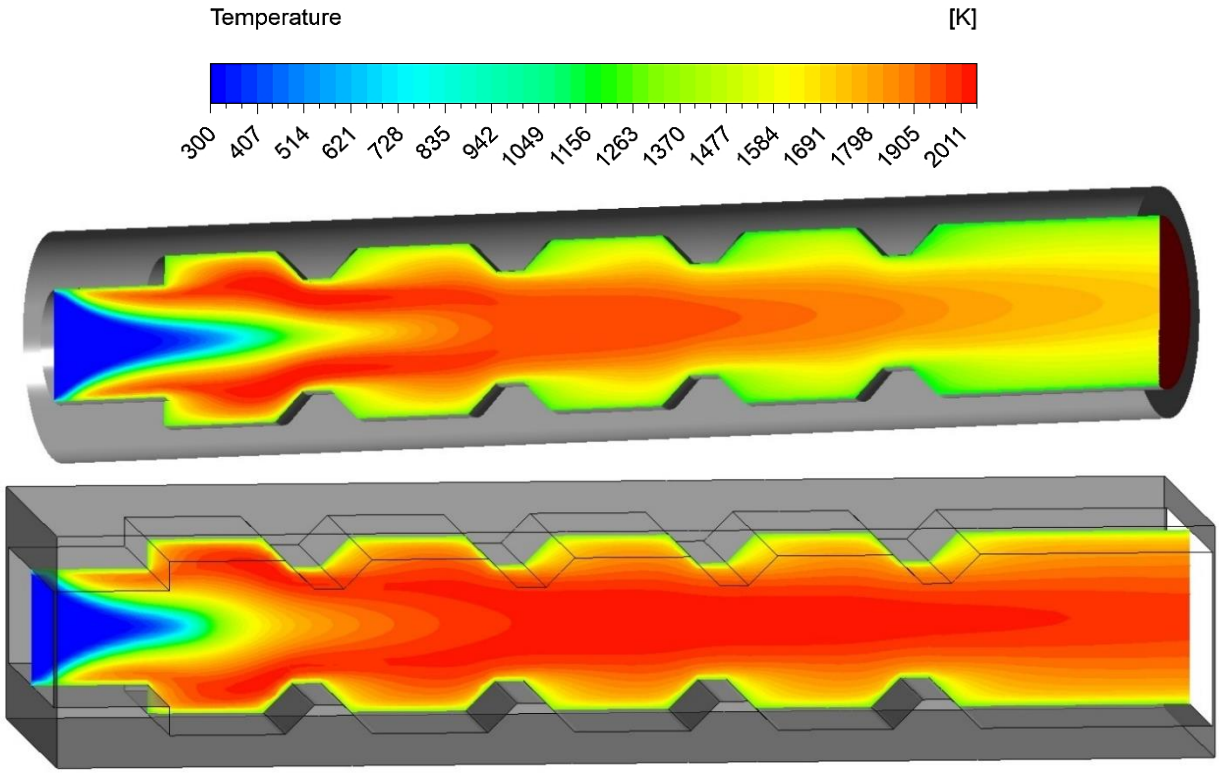

Figure IV.2.12. *Gas phase temperature distribution contours for cylindrical and planar micro combustors: Effect of cross section.*

In the context of reacting flows, the visualization of temperature contours in **Figure IV.2.12**, assumes paramount importance as it unravels the intricate thermal dynamics within 3D structures, offering valuable insights into temperature distribution and combustion behavior. This technique becomes especially crucial when comparing the temperature contours between 3D cylindrical and planar micro combustor configurations. The temperature contours within a cylindrical micro combustor exhibit distinctive characteristics, primarily influenced by the circular cross-section. In non-reacting conditions, the contours illustrate a well-defined temperature distribution, with elevated temperatures concentrated along the central axis. The circular symmetry promotes efficient heat transfer and combustion within the confined space, leading to a more ordered and coherent temperature profile. Transitioning to reacting conditions, the temperature contours in the cylindrical configuration dynamically respond to the combustion-induced thermal gradients. The circular cross-section aids in maintaining a relatively uniform temperature distribution, allowing for effective heat transfer and combustion. The isosurfaces of temperature contours provide a comprehensive view of the flame structure and reaction zones within the cylindrical geometry. In contrast, the planar micro combustor introduces a different set of temperature contour patterns due to its distinct geometry. The planar configuration inherently creates more complex temperature gradients, especially near corners and edges. In non-reacting conditions, the temperature contours showcase variations, with regions of elevated temperature corresponding to geometric features. Under reacting conditions, the interaction between combustion and the planar geometry contributes to intricate temperature contours. The planar structure introduces challenges such as flame bending and interaction with recirculation zones, resulting in non-uniform temperature distribution. The temperature contours in this configuration reveal the impact of the planar shape on combustion dynamics and heat transfer. The disparities in temperature contours between cylindrical and planar configurations stem from their respective geometric features. The circular symmetry of the cylindrical configuration promotes a more ordered and centralized temperature profile. In contrast, the planar geometry introduces complexities, leading to variations in temperature gradients and localized hotspots.

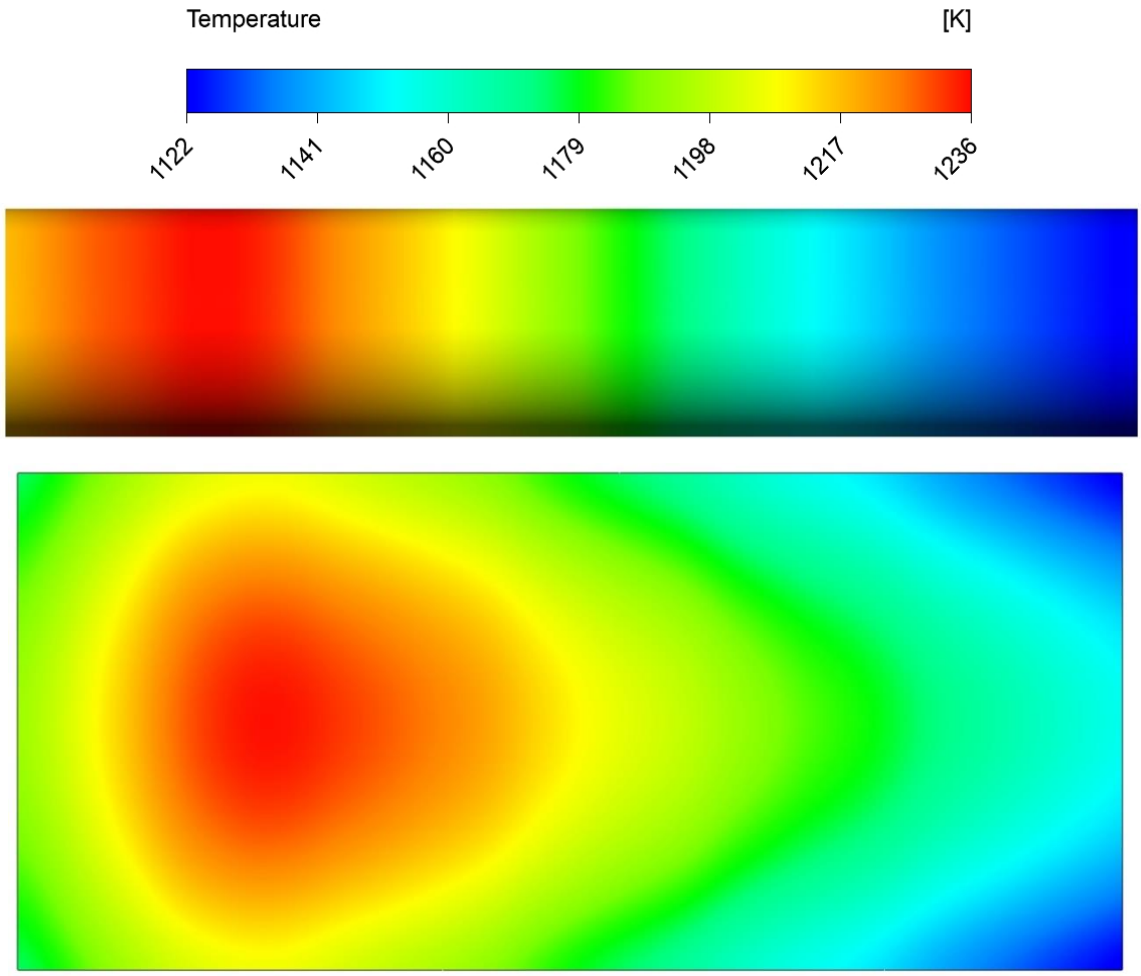

Figure IV.2.13. *Outer wall surface temperature distribution contours for cylindrical and planar micro combustors: Effect of cross section.*

Additionally, as shown in **Figure IV.2.13,** the outer wall temperature distribution in both configurations reflects the influence of geometric features on convective and conductive heat transfer. In the cylindrical micro combustor, the circular outer wall contributes to a more uniform temperature distribution. However, in the planar configuration, the outer wall temperature may exhibit non-uniformities due to the presence of corners and edges, influencing heat transfer processes. In essence, the difference in temperature contours between cylindrical and planar micro combustors underscores the importance of geometric considerations in optimizing combustion efficiency and heat transfer within these compact combustion systems. These insights contribute to advancing the understanding of thermal behavior in micro-scale combustion and MTPV applications.

IV.2.2. Overall Efficiency

The assessment of overall efficiency is a pivotal aspect of our study, delving into the performance disparities between cylindrical and planar micro combustor configurations. In our investigation, the overall efficiency is a comprehensive metric that considers the combined impact of flow-field characteristics, combustion dynamics, and heat transfer behaviors on the Micro-Thermophotovoltaic (MTPV) system. The cylindrical micro combustor, characterized by its circular cross-section, exhibits notable efficiency owing to the well-defined vortical structures observed in both non-reacting and reacting conditions. This stable and organized flow pattern contributes to efficient combustion processes, enhancing overall system performance. On the other hand, the planar micro combustor, with its rectangular cross-section, presents a distinctive set of challenges and advantages. The complex vorticity patterns observed in both non-reacting and reacting conditions contribute to increased turbulence and intricate flame structures. While this complexity introduces challenges in terms of combustion efficiency, it also offers opportunities for enhanced heat transfer and thermal performance. Our numerical simulations extend beyond merely quantifying the thermal efficiency of each configuration. They involve a meticulous examination of the interplay between geometric features, combustion characteristics, and overall system behavior. This holistic approach allows us to decipher the nuanced factors influencing the efficiency of Micro-Thermophotovoltaic systems with varying micro combustor shapes. The insights gained from this investigation into overall efficiency contribute significantly to the broader understanding of micro-combustion technology. By elucidating the intricate balance between geometric configurations and system efficiency, we pave the way for informed design decisions in future energy systems, particularly those relying on Micro-Thermophotovoltaic technology. This exploration not only advances the theoretical foundation but also holds practical implications for optimizing the performance of micro combustors in real-world applications.

Table IV.2.2 outlines the efficiency parameters for different micro combustor configurations, focusing on mass flow rate, input energy, radiative heat transfer efficiency, TPV type, TPV efficiency, and overall Micro-Thermophotovoltaic (MTPV) system efficiency. The data presented is derived from our comprehensive numerical simulations and represents a thorough evaluation of the cylindrical and planar micro combustor shapes. The results reveal that the cylindrical micro combustor configuration consistently exhibits higher mass flow rates across various input energy levels. This indicates a more robust flow dynamics within the cylindrical geometry, contributing to increased fuel consumption and combustion efficiency. However, the planar micro combustor, while featuring lower mass flow rates, demonstrates competitive radiative heat transfer efficiency, suggesting effective thermal performance despite reduced fuel consumption. In terms of TPV type and efficiency, both GaSb and InGaAs configurations showcase comparable efficiencies for both cylindrical and planar shapes. However, the InPAsSb TPV type exhibits slightly lower efficiency in the planar configuration, emphasizing the sensitivity of efficiency to the specific combination of materials and geometric design. The MTPV system efficiency results further underscore the intricate relationship between micro combustor configuration and overall system performance. While the cylindrical shape demonstrates higher MTPV system efficiency across TPV types, the planar shape exhibits commendable efficiency levels, especially with InGaAs and InPAsSb TPV types. In interpreting these results, it is crucial to consider the trade-offs between mass flow rate, radiative heat transfer efficiency, and TPV efficiency. The cylindrical micro combustor excels in fuel consumption and combustion dynamics, making it a favorable choice for higher mass flow rates. On the other hand, the planar micro combustor, with its efficient radiative heat transfer and competitive TPV efficiency, presents a compelling option for applications prioritizing thermal performance and overall system efficiency. This nuanced analysis guides the selection of micro combustor configurations based on specific performance criteria, contributing valuable insights to the optimization of Micro-Thermophotovoltaic systems.

***Table IV.2.2**. Overall energy conversion efficiency values for different combustor cross-sections.*

Micro Combustor Configuration	Mass Flow Rate (kg/s)	Input Energy (W)	Radiative Heat Transfer Efficiency (W)	TPV Type	TPV Efficiency (%)	MTPV System Efficiency (%)
Cylindrical	1.60437E-5	15.517	- 4.541	GaSb	15.4	4.507
	8.49E-06	23.362	- 5.495	InGaAs	20	3.622
	1.14E-05	31.304	- 6.643	InPAsSb	25	3.268
Planar	5.67E-06	15.602	- 3.885	GaSb	15.4	3.834
	8.53E-06	23.478	- 5.445	InGaAs	20	3.572
	1.14E-05	31.409	- 6.580	InPAsSb	25	3.226

General Conclusion

In this work, a novel micro-combustor configuration with four equidistant pair of angled ribs for the micro thermo-photovoltaic systems is proposed. Fundamental understanding of the flow dynamics, combustion behavior and thermal performance is presented. The effect of introducing the angled ribs and their heights on the premixed H_2-air combustion are characterized one at time using a set of 2D and 3D numerical simulations. Therefore, comparative studies with the characteristics on both non-reacting and reacting flows are conducted. The main concluded remarks of the present investigation can be summarized as follows:

(1) For non-reacting and reacting flows, it is observed that the introducing of ribs elongates the recirculation zone length. Moreover, the recirculation zones are relatively becoming larger with the increasing of the rib's number and height. Thus, we conclude that the flow residence time is considerably increased for the novel proposed combustor geometry MCRD against the MCSD. In addition, the variation of the rib's number and heights is proposed as a passive flow control technique.

(2) The pressure loss increases gradually by the introducing of ribs or the increase of its number and height and importantly in the presence of combustion in comparison to the non-reacting flows. In conclusion, high pumping power is required to achieve the reacting flow needed velocities.

(3) The visual observation of the turbulent level under non-reacting and reacting flows conditions, reveals that the introducing of ribs leads to direct increment of turbulence level. The increasing becomes more importantly with the increasing of the rib's number and height. Consequently, the turbulent environment increases the burning velocity and accelerating the heat releasing. The increasing becomes more importantly with the increasing of the rib's number and height.

(4) Based on the combustion characteristics results, it can be concluded that the novel proposed trapezoidal shaped ribs bring a favorable effect in terms of the flame sustainability and combustion intensity. Simultaneously, the introducing four ribs on the combustors walls with inter-rib spacing of 2 mm brings another unfavorable effect for the flame stabilization. On the other hand, the increment of the rib's height might be a negative effect too on the flame stability.

(5) Comparing to MCSD, the introducing of trapezoidal ribs shifted slightly the flame front location forward in the micro combustor. Moreover, the increase of the rib number and height slips the flame location more from the inlet. In addition, the tendency of the flame speed level can be explained by the increment of turbulence level which increases in return the amount of products trapped behind the pair of steps and ribs cavities. The recirculation's of the reaction's products had a favorable effect by increasing the preheating of the cold reactants which in return speeds the reactions. Hence, this reveals that the novel proposed geometry is helpful in terms of activating the combustion process and increasing the flame location and speed. Hence, the ribs number and height can also be used as passive control techniques to adjust the flame shape, location and speed.

(6) The gas phase temperature is found stable for the different proposed geometries which reveals the smallness of the convective heat transfer unfavorable effects on the flame stability.

(7) The effect of introducing the angled ribs on the outer-wall temperature level and uniformity is clearly shown and reflects the favorable effect of the novel proposed designs. It is clearly shown that approximately 90% of the heat is losses by radiation and only 10% by convection. Quantitatively, the mean temperature of the outer wall temperature profile has increases from

1371.25 K for MCSD to 1450.71 K for certain configurations. Besides, the mean temperature increases to 1452.54 K, respectively.

(8) The introduced ribs and rise of their number and heights tend to reduce the outer wall temperature differences significantly, which represents a beneficial factor for the MTPV systems. In addition, the uniformity of the temperature profile increases, as expected, with the introducing of the ribs, and it continues to increase with the increment of the rib's height.

(9) Our study compares the efficiency of cylindrical and planar micro combustor configurations in MTPV systems, finding that while cylindrical shapes excel in combustion dynamics, planar shapes offer competitive thermal performance and overall system efficiency, guiding design decisions for future energy systems.

To evaluate the effectiveness of the novel proposed geometrical configuration, a comparison is made with several literature results using different geometrical techniques such as backward facing step, flame holder, ribs, and wall shape. Therefore, we have provided a thorough explanation of the underlying physical mechanisms and phenomena to support our findings, and have referenced the most relevant and closely related studies to support our claims. The results of this comparison are presented in the following Table of key insights and contributions and emphasize the importance of geometrical configurations on thermal performance quantified by the mean temperature parameter. The purpose of this cross-referencing is to evaluate the effectiveness of the proposed configuration and to identify its potential for further optimization in micro combustor design. This will provide valuable insights for researchers and engineers in the field of micro-combustors and assist in the development of more efficient and reliable designs. The present work exhibits the higher outer wall mean temperature among all geometries considered. Moreover, the use of different operating conditions including the inlet velocity and the equivalence ratio in present study resulted in higher outer wall mean temperature values among all geometries considered. These findings indicate that the present work's proposed geometry is a promising alternative to the traditional geometries in micro combustors for achieving better thermal performance. However, to fully harness the capabilities of our doctoral research, we have to delve into comparative analysis of the different enhancement techniques aimed at improving combustion efficiency and thermal performance. This comparative study seeks to consolidate and critically evaluate the existing literature on enhancement techniques, focusing on mean temperature as a key performance indicator. By examining the mean temperature achieved in various micro-combustor configurations and operating conditions, this review sheds light on the strengths and limitations of each approach.

Authors (Year)	Geometrical Configuration	Materials	Operating Conditions and Geometric Parameters	Mean Temperature (K)
Abdelbasset Lachraf and Mohamed Si Ameur (2023) [73]	Micro-combustor with trapezoidal ribs 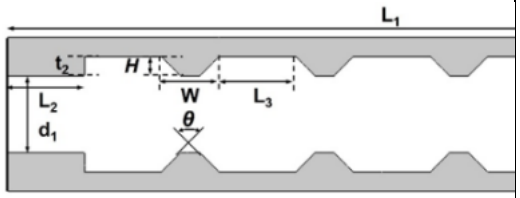	• Stainless steel 316 • Hydrogen-air	• Vin = 6 m/s • φ = 1 • L_3 = 2 mm • H = 0.5 mm – 0.7 mm	• MCSD: 1313 • MCRD1: 1417.71 • MCRD2: 1436.31 • MCRD3: 1452.54
			• Vin = 8 m/s – 14 m/s • φ = 1 • L_3 = 2 mm • H = 0.5 mm	• Vin = 8 m/s: 1466.95 • Vin = 10 m/s: 1503.48 • Vin = 12 m/s: 1530.34 • Vin = 14 m/s: 1549.78
			• Vin = 6 m/s • φ = 0.8 – 1.2 • L_3 = 2 mm • H = 0.5 mm	• φ = 0.8: 1363.05 • φ = 0.9: 1398.33 • φ = 1.0: 1417.71 • φ = 1.1: 1414.06 • φ = 1.2: 1400.43
Jiaqiang et al. (2018) [12]	Two-step micro combustor 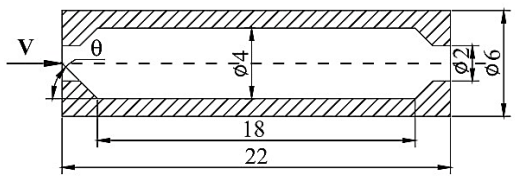	• Steel • Methane-air	• Vin = 6 m/s – 10 m/s • φ = 1	Vin = 6 m/s: 1161.32 Vin = 8 m/s: 1203.52 Vin = 10 m/s: 1235.00

Tang et al. (2015) [26]	Micro planar combustor with parallel separating plates 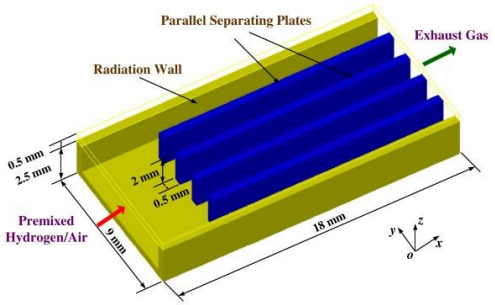	• Stainless steel 316 • Hydrogen-air	• Vin = 6 m/s • φ = 1	• Single passage: 1329.64 • Multi-passages: 1431.09 • 2 passages: 1348.51 • 4 passages: 1402.98 • 6 passages: 1460.35 • 8 passages: 1502.22
Ni et al. (2019) [17]	Micro-combustors with (a) rectangular ribs; (b) outer ring ribs; (c) Inner ring ribs	• Stainless steel 316 • Hydrogen-air	• Vin = 5 m/s – 12.5 m/s • φ = 1 • L_3 = 6 mm • H = 0.8 mm	Rectangular rib • Vin = 5 m/s: 1232.66 • Vin = 7.5 m/s: 1313.18 • Vin = 10 m/s: 1355.11 • Vin = 12.5 m/s: 1373.08
			• Vin = 7.5 m/s • φ = 1 • L_3 = 4 mm – 8 mm • H = 0.5 mm - 0.8 mm	H = 0.5 mm • L_3 = 4 mm: 1314.39 • L_3 = 6 mm: 1313.44 • L_3 = 8 mm: 1305.42 L_3 = 0.5 mm • H = 0.5 mm: 1294.73 • H = 0.65 mm: 1304.03 • H = 0.8 mm: 1313.33

	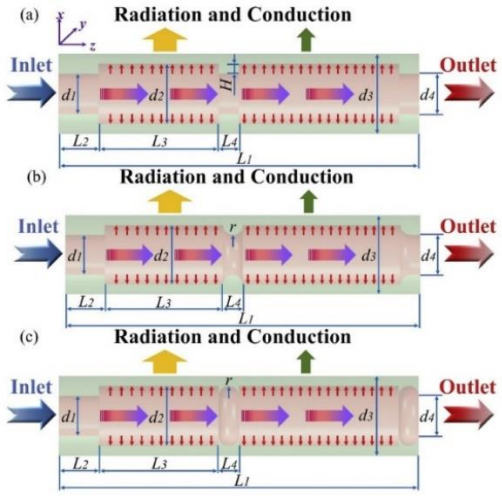		• Vin = 7.5 m/s • φ = 1 • L_3 = 6 mm • H = 0.5 mm	• Rectangular rib: 1294.73 • Outer ring rib: 1305.70 • Inner ring rib: 1312.67
			• Vin = 7.5 m/s • φ = 0.8 – 1.2 • L_3 = 6 mm • H = 0.8 mm	Double rib • φ = 0.8: 1249.51 • φ = 0.9: 1288.73 • φ = 1.0: 1313.33 • φ = 1.1: 1294.72 • φ = 1.2: 1286.15

Yang et al. (2018) [37]	Converging-diverging micro combustor 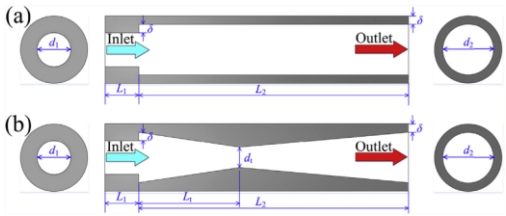	• Steel • Hydrogen-air	• Vin = 5 m/s – 11 m/s • φ = 1	Cylindrical channel • Vin = 5 m/s: 1174.01 • Vin = 7 m/s: 1235.34 • Vin = 9 m/s: 1277.16 • Vin = 11 m/s: 1306.77 Converging-diverging channel • Vin = 5 m/s: 1190.68 • Vin = 7 m/s: 1256.04 • Vin = 9 m/s: 1299.39 • Vin = 11 m/s: 1329.87

Perspectives

Moving forward, our perspectives extend from the geometrical configurations explored within the scope of this doctoral work, towards broader horizons, encompassing multifaceted avenues for future exploration and innovation in the realm of micro-combustion-based power generation. While our research has diligently scrutinized the intricate interplay between geometric parameters and combustion performance, our endeavors pave the way for a more expansive understanding of micro-combustion dynamics and its implications for Micro-Thermophotovoltaic (MTPV) systems. Beyond the confines of our current investigations, our perspectives advocate for a holistic approach towards micro-combustion research, encompassing diverse facets ranging from fundamental principles to practical applications. Embracing the complexities inherent in micro-scale combustion phenomena, our future trajectory envisages an integrative exploration of fluid dynamics, combustion kinetics, and thermal management strategies. By elucidating the underlying mechanisms governing heat and mass transfer within micro-combustors, we aspire to unlock new frontiers in energy conversion efficiency and MTPV systems optimization.

Moreover, our perspectives emphasize the imperative of addressing emerging challenges in micro-combustion technology, such as combustion instabilities, pollutant emissions, and material compatibility. Through interdisciplinary collaborations and synergistic endeavors, we aim to devise innovative solutions that reconcile performance objectives with sustainability imperatives. By harnessing the collective expertise across diverse domains, we envisage a paradigm shift towards environmentally conscious micro-combustion systems that uphold efficiency, reliability, and environmental stewardship. Furthermore, our perspectives underscore the pivotal role of numerical modeling and experimental prototyping in advancing micro-combustion research. By synergistically integrating computational simulations with empirical investigations, we aspire to refine predictive capabilities and enhance the fidelity of experimental prototypes. Through meticulous validation against experimental data, we seek to instill confidence in computational tools as indispensable assets for elucidating complex combustion phenomena and guiding design optimizations. In essence, our perspectives transcend the boundaries of conventional research paradigms, advocating for a comprehensive and forward-thinking approach towards micro-combustion innovation. By embracing the inherent challenges as catalysts for innovation and collaboration, we aspire to chart a transformative course towards sustainable, efficient, and resilient micro-combustion technologies that pave the way towards a greener, more energy-abundant future.

References

[1] N. S. Kaisare and D. G. Vlachos, “A review on microcombustion: Fundamentals, devices and applications,” *Progress in Energy and Combustion Science*, vol. 38, no. 3. pp. 321–359, 2012. doi: 10.1016/j.pecs.2012.01.001.

[2] L. C. Chia and B. Feng, “The development of a micropower (micro-thermophotovoltaic) device,” *J. Power Sources*, vol. 165, no. 1, pp. 455–480, 2007, doi: 10.1016/j.jpowsour.2006.12.006.

[3] D. C. Walther and J. Ahn, “Advances and challenges in the development of power-generation systems at small scales,” *Progress in Energy and Combustion Science*, vol. 37, no. 5. pp. 583–610, 2011. doi: 10.1016/j.pecs.2010.12.002.

[4] B. Aravind, B. Khandelwal, and S. %J A. energy Kumar, “Experimental investigations on a new high intensity dual microcombustor based thermoelectric micropower generator,” vol. 228, pp. 1173–1181, 2018.

[5] A. H. Epstein, “MILLIMETER-SCALE, MEMS GAS TURBINE ENGINES,” in *Proceedings of ASME Turbo Expo 2003 Power for Land, Sea, and Air*, 2003, pp. 1–10.

[6] S. E. Hosseini, “Micro-power generation using micro-turbine (moving) and thermophotovoltaic (non-moving) systems,” *Proceedings of the Institution of Mechanical Engineers, Part A: Journal of Power and Energy*, vol. 233, no. 8. pp. 1085–1101, 2019. doi: 10.1177/0957650919841958.

[7] W. H. Kim and T. S. Park, “Effects of blade angle on combustion characteristics in a micro combustor with a swirler of micro fan type,” *JMST Adv.*, vol. 1, no. 1–2, pp. 65–71, Jun. 2019, doi: 10.1007/s42791-019-0002-4.

[8] T. C. Narayan *et al.*, “Platform for Accurate Efficiency Quantification of > 35% Efficient Thermophotovoltaic Cells,” in *2021 IEEE 48th Photovoltaic Specialists Conference (PVSC)*, Jun. 2021, pp. 1352–1354. doi: 10.1109/PVSC43889.2021.9518588.

[9] K. Qiu, A. C. S. Hayden, M. G. Mauk, and O. V. Sulima, “Generation of electricity using InGaAsSb and GaSb TPV cells in combustion-driven radiant sources,” *Sol. Energy Mater. Sol. Cells*, vol. 90, no. 1, pp. 68–81, 2006, doi: 10.1016/j.solmat.2005.02.002.

[10] L. Fu, Z. Feng, and G. Li, “Experimental investigation on overall performance of a millimeter-scale radial turbine for micro gas turbine,” *Energy*, vol. 134, pp. 1–9, 2017, doi: 10.1016/j.energy.2017.06.006.

[11] Z. He, Y. Yan, T. Zhao, Z. Zhang, and H. Mikulčić, “Parametric study of inserting internal spiral fins on the micro combustor performance for thermophotovoltaic systems,” *Renew. Sustain. Energy Rev.*, vol. 165, no. May, p. 112595, Sep. 2022, doi: 10.1016/j.rser.2022.112595.

[12] R. E. Nelson, “A brief history of thermophotovoltaic development,” *Semicond. Sci. Technol.*, vol. 18, no. 5, 2003, doi: 10.1088/0268-1242/18/5/301.

[13] A. LaPotin *et al.*, “Thermophotovoltaic efficiency of 40%,” *Nature*, vol. 604, no. 7905, pp. 287–291, Apr. 2022, doi: 10.1038/s41586-022-04473-y.

[14] A. C. Zuppero, B. Krawetz, C. R. Barklund, and G. D. Seifert, “Portable thermo-photovoltaic power source.” Google Patents, 1997.

[15] W. M. Yang, S. K. Chou, C. Shu, Z. W. Li, and H. Xue, “Development of microthermophotovoltaic system,” *Appl. Phys. Lett.*, vol. 81, no. 27, pp. 5255–5257, Dec. 2002, doi: 10.1063/1.1533847.

[16] W. . Yang, S. . Chou, C. Shu, Z. . Li, and H. Xue, “Combustion in micro-cylindrical combustors

with and without a backward facing step," *Appl. Therm. Eng.*, vol. 22, no. 16, pp. 1777–1787, Nov. 2002, doi: 10.1016/S1359-4311(02)00113-8.

[17] Y. Wenming, C. Siawkiang, S. Chang, X. Hong, and L. Zhiwang, "Research on micro-thermophotovoltaic power generators with different emitting materials," *J. Micromechanics Microengineering*, vol. 15, no. 9, pp. S239–S242, Sep. 2005, doi: 10.1088/0960-1317/15/9/S11.

[18] J. F. Pan, J. Huang, D. T. Li, W. M. Yang, W. X. Tang, and H. Xue, "Effects of major parameters on micro-combustion for thermophotovoltaic energy conversion," *Appl. Therm. Eng.*, vol. 27, no. 5–6, pp. 1089–1095, Apr. 2007, doi: 10.1016/j.applthermaleng.2006.07.038.

[19] J. F. Pan *et al.*, "Micro combustion in sub-millimeter channels for novel modular thermophotovoltaic power generators," *J. Micromechanics Microengineering*, vol. 20, no. 12, p. 125021, Dec. 2010, doi: 10.1088/0960-1317/20/12/125021.

[20] K. F. Mustafa, S. Abdullah, M. Z. Abdullah, and K. Sopian, "A review of combustion-driven thermoelectric (TE) and thermophotovoltaic (TPV) power systems," *Renew. Sustain. Energy Rev.*, vol. 71, no. January, pp. 572–584, May 2017, doi: 10.1016/j.rser.2016.12.085.

[21] J. Wan and A. Fan, "Recent progress in flame stabilization technologies for combustion-based micro energy and power systems," *Fuel*, vol. 286. 2021. doi: 10.1016/j.fuel.2020.119391.

[22] J. E *et al.*, "A comprehensive review on performance improvement of micro energy mechanical system: Heat transfer, micro combustion and energy conversion," *Energy*, vol. 239, p. 122509, 2022, doi: https://doi.org/10.1016/j.energy.2021.122509.

[23] J. E, Y. Mei, C. Feng, J. Ding, L. Cai, and B. Luo, "A review of enhancing micro combustion to improve energy conversion performance in micro power system," *Int. J. Hydrogen Energy*, vol. 47, no. 53, pp. 22574–22601, 2022, doi: https://doi.org/10.1016/j.ijhydene.2022.05.042.

[24] P. Qian and M. Liu, "Influencing factors of wall temperature and flame stability of micro-combustors in micro-thermophotovoltaic and micro-thermoelectric systems," *Fuel*, vol. 310, no. October, p. 122436, 2022, doi: 10.1016/j.fuel.2021.122436.

[25] L. Cai, J. E, J. Li, J. Ding, and B. Luo, "A comprehensive review on combustion stabilization technologies of micro/meso-scale combustors for micro thermophotovoltaic systems: Thermal, emission, and energy conversion," *Fuel*, vol. 335, p. 126660, Mar. 2023, doi: 10.1016/j.fuel.2022.126660.

[26] Z. Kang *et al.*, "A Review of Micro Power System and Micro Combustion: Present Situation, Techniques and Prospects," *Energies*, vol. 16, no. 7, pp. 1–28, 2023, doi: 10.3390/en16073201.

[27] K. Maruta, "Micro and mesoscale combustion," *Proc. Combust. Inst.*, vol. 33, no. 1, pp. 125–150, 2011, doi: 10.1016/j.proci.2010.09.005.

[28] S. K. Chou, W. M. Yang, K. J. Chua, J. Li, and K. L. Zhang, "Development of micro power generators - A review," *Applied Energy*, vol. 88, no. 1. pp. 1–16, 2011. doi: 10.1016/j.apenergy.2010.07.010.

[29] G. P. S. Sahota, B. Khandelwal, and S. Kumar, "Experimental investigations on a new active swirl based microcombustor for an integrated micro-reformer system," *Energy Convers. Manag.*, vol. 52, no. 10, pp. 3206–3213, 2011, doi: 10.1016/j.enconman.2011.05.007.

[30] B. Khandelwal, A. A. Deshpande, and S. Kumar, "Experimental studies on flame stabilization in a three step rearward facing configuration based micro channel combustor," *Appl. Therm. Eng.*, vol. 58, no. 1–2, pp. 363–368, Sep. 2013, doi: 10.1016/j.applthermaleng.2013.04.058.

[31] S. Akhtar, J. C. Kurnia, and T. Shamim, "A three-dimensional computational model of H2–air premixed combustion in non-circular micro-channels for a thermo-photovoltaic (TPV)

application," *Appl. Energy*, vol. 152, pp. 47–57, Aug. 2015, doi: 10.1016/j.apenergy.2015.04.068.

[32] J. E, W. Zuo, X. Liu, Q. Peng, Y. Deng, and H. Zhu, "Effects of inlet pressure on wall temperature and exergy efficiency of the micro-cylindrical combustor with a step," *Appl. Energy*, vol. 175, pp. 337–345, 2016, doi: 10.1016/j.apenergy.2016.05.039.

[33] E. Jiaqiang *et al.*, "Investigation on the combustion performance enhancement of the premixed methane/air in a two-step micro combustor," *Appl. Therm. Eng.*, vol. 141, pp. 114–125, 2018, doi: 10.1016/j.applthermaleng.2018.05.101.

[34] Q. Peng, Y. Wu, J. E, W. Yang, H. Xu, and Z. Li, "Combustion characteristics and thermal performance of premixed hydrogen-air in a two-rearward-step micro tube," *Appl. Energy*, vol. 242, pp. 424–438, 2019, doi: 10.1016/j.apenergy.2019.03.137.

[35] W. Zuo, E. Jiaqiang, H. Liu, Q. Peng, X. Zhao, and Z. Zhang, "Numerical investigations on an improved micro-cylindrical combustor with rectangular rib for enhancing heat transfer," *Appl. Energy*, vol. 184, pp. 77–87, 2016, doi: 10.1016/j.apenergy.2016.10.009.

[36] H. Chen and W. qiang Liu, "Numerical Investigation of the Combustion in an Improved Microcombustion Chamber with Rib," *J. Chem.*, vol. 2019, 2019, doi: 10.1155/2019/8354541.

[37] S. Ni, D. Zhao, Y. Sun, and J. E, "Numerical and entropy studies of hydrogen-fuelled micro-combustors with different geometric shaped ribs," *Int. J. Hydrogen Energy*, vol. 44, no. 14, pp. 7692–7705, 2019, doi: 10.1016/j.ijhydene.2019.01.136.

[38] A. Qamareen, S. S. Alam, and M. A. Ansari, "Performance Evaluation of H2/Air Premixed Combustion in a Suddenly Expanded Microcombustor with Wall Fin," *Energy Technol.*, vol. 9, no. 10, 2021, doi: 10.1002/ente.202100294.

[39] J. Wan *et al.*, "A numerical investigation on combustion characteristics of H 2/air mixture in a micro-combustor with wall cavities," *Int. J. Hydrogen Energy*, vol. 39, no. 15, pp. 8138–8146, 2014, doi: 10.1016/j.ijhydene.2014.03.116.

[40] J. Wan and A. Fan, "Effect of channel gap distance on the flame blow-off limit in mesoscale channels with cavities for premixed CH4/air flames," *Chem. Eng. Sci.*, vol. 132, pp. 99–107, 2015, doi: 10.1016/j.ces.2015.04.010.

[41] Y. Su *et al.*, "Numerical investigation of a novel micro combustor with double-cavity for micro-thermophotovoltaic system," *Energy Convers. Manag.*, vol. 106, pp. 173–180, 2015, doi: 10.1016/j.enconman.2015.09.043.

[42] Q. Peng, J. E, Z. Zhang, W. Hu, and X. Zhao, "Investigation on the effects of front-cavity on flame location and thermal performance of a cylindrical micro combustor," *Appl. Therm. Eng.*, vol. 130, pp. 541–551, Feb. 2018, doi: 10.1016/j.applthermaleng.2017.11.016.

[43] L. Li, W. Yang, and A. Fan, "Effect of the cavity aft ramp angle on combustion efficiency of lean hydrogen/air flames in a micro cavity-combustor," *Int. J. Hydrogen Energy*, vol. 44, no. 11, pp. 5623–5632, 2019, doi: 10.1016/j.ijhydene.2018.07.162.

[44] W. Zuo, Y. Zhang, Q. Li, J. Li, and Z. He, "Numerical investigations on hydrogen-fueled micro-cylindrical combustors with cavity for micro-thermophotovoltaic applications," *Energy*, vol. 223, p. 120098, May 2021, doi: 10.1016/j.energy.2021.120098.

[45] W. Gao, Y. Yan, K. Shen, L. Huang, T. Zhao, and B. Gao, "Combustion characteristic of premixed H2/air in the micro cavity combustor with guide vanes," *Energy*, vol. 239, no. September, p. 121975, Jan. 2022, doi: 10.1016/j.energy.2021.121975.

[46] A. Tang, J. Pan, W. Yang, Y. Xu, and Z. Hou, "Numerical study of premixed hydrogen/air combustion in a micro planar combustor with parallel separating plates," *Int. J. Hydrogen Energy*,

vol. 40, no. 5, pp. 2396–2403, 2015, doi: 10.1016/j.ijhydene.2014.12.018.

[47] Y. Wenming, J. Dongyue, C. K. Y. Kenny, Z. Dan, and P. Jianfeng, “Combustion process and entropy generation in a novel microcombustor with a block insert,” *Chem. Eng. J.*, vol. 274, pp. 231–237, 2015, doi: 10.1016/j.cej.2015.04.034.

[48] A. Tang, J. Deng, Y. Xu, J. Pan, and T. Cai, “Experimental and numerical study of premixed propane/air combustion in the micro-planar combustor with a cross-plate insert,” *Appl. Therm. Eng.*, vol. 136, pp. 177–184, 2018, doi: 10.1016/j.applthermaleng.2018.03.001.

[49] J. Wan, C. Shang, and H. Zhao, “Dynamics of methane/air premixed flame in a mesoscale diverging combustor with/without a cylindrical flame holder,” *Fuel*, vol. 232, pp. 659–665, 2018, doi: 10.1016/j.fuel.2018.06.026.

[50] J. Wan, C. Shang, and H. Zhao, “Anchoring mechanisms of methane/air premixed flame in a mesoscale diverging combustor with cylindrical flame holder,” *Fuel*, vol. 232, pp. 591–599, 2018, doi: 10.1016/j.fuel.2018.06.027.

[51] J. Wan and X. Cheng, “Numerical investigation of the local extinction and re-ignition mechanisms of premixed flame in a micro combustor with a flame holder and preheating channels,” *Fuel*, vol. 264, p. 116837, Mar. 2020, doi: 10.1016/j.fuel.2019.116837.

[52] J. Wan, A. Fan, K. Maruta, H. Yao, and W. Liu, “Experimental and numerical investigation on combustion characteristics of premixed hydrogen/air flame in a micro-combustor with a bluff body,” *Int. J. Hydrogen Energy*, vol. 37, no. 24, pp. 19190–19197, Dec. 2012, doi: 10.1016/j.ijhydene.2012.09.154.

[53] A. Fan *et al.*, “The effect of the blockage ratio on the blow-off limit of a hydrogen/air flame in a planar micro-combustor with a bluff body,” *Int. J. Hydrogen Energy*, vol. 38, no. 26, pp. 11438–11445, 2013, doi: 10.1016/j.ijhydene.2013.06.100.

[54] A. Fan, J. Wan, Y. Liu, B. Pi, H. Yao, and W. Liu, “Effect of bluff body shape on the blow-off limit of hydrogen/air flame in a planar micro-combustor,” *Appl. Therm. Eng.*, vol. 62, no. 1, pp. 13–19, 2014, doi: 10.1016/j.applthermaleng.2013.09.010.

[55] J. Niu, J. Ran, L. Li, X. Du, R. Wang, and M. Ran, “Effects of trapezoidal bluff bodies on blow out limit of methane/air combustion in a micro-channel,” *Appl. Therm. Eng.*, vol. 95, pp. 454–461, 2016, doi: 10.1016/j.applthermaleng.2015.11.061.

[56] Y. Yan, H. Yan, L. Zhang, L. Li, J. Zhu, and Z. Zhang, “Numerical investigation on combustion characteristics of methane/air in a micro-combustor with a regular triangular pyramid bluff body,” *Int. J. Hydrogen Energy*, vol. 43, no. 15, pp. 7581–7590, 2018, doi: 10.1016/j.ijhydene.2018.02.168.

[57] X. Yang, Z. He, S. Dong, and H. Tan, “Enhancement of thermal performance by converging-diverging channel in a micro tube combustor fueled by premixed hydrogen/air,” *Int. J. Hydrogen Energy*, vol. 44, no. 2, pp. 1213–1226, Jan. 2019, doi: 10.1016/j.ijhydene.2018.10.239.

[58] L. Han, J. Li, D. Zhao, Y. Xi, X. Gu, and N. Wang, “Effect analysis on energy conversion enhancement and NOx emission reduction of ammonia/hydrogen fuelled wavy micro-combustor for micro-thermophotovoltaic application,” *Fuel*, vol. 289, no. x, 2021, doi: 10.1016/j.fuel.2020.119755.

[59] P. L. Reza Ghodsi, *Multi-Wafer Rotating MEMS Machines*. Boston, MA: Springer US, 2010. doi: 10.1007/978-0-387-77747-4.

[60] Y. Ju and K. Maruta, “Microscale combustion: Technology development and fundamental research,” *Progress in Energy and Combustion Science*, vol. 37, no. 6. pp. 669–715, 2011. doi: 10.1016/j.pecs.2011.03.001.

[61] C. Spadaccini and I. Waitz, *3.15 – Micro-Combustion*. 2008. doi: 10.1016/b978-044452190-3.00049-5.

[62] A. C. Fernandez-Pello, "Micropower generation using combustion: Issues and approaches," *Proc. Combust. Inst.*, vol. 29, no. 1, pp. 883–899, 2002, doi: 10.1016/s1540-7489(02)80113-4.

[63] J. E, J. Ding, J. Chen, G. Liao, F. Zhang, and B. Luo, "Process in micro-combustion and energy conversion of micro power system: A review," *Energy Conversion and Management*, vol. 246. 2021. doi: 10.1016/j.enconman.2021.114664.

[64] J. Li, S. K. Chou, W. M. Yang, and Z. W. Li, "Experimental and numerical study of the wall temperature of cylindrical micro combustors," *J. Micromechanics Microengineering*, vol. 19, no. 1, p. 015019, Jan. 2009, doi: 10.1088/0960-1317/19/1/015019.

[65] D. Pashchenko, "Comparative analysis of hydrogen/air combustion CFD-modeling for 3D and 2D computational domain of micro-cylindrical combustor," *Int. J. Hydrogen Energy*, vol. 42, no. 49, pp. 29545–29556, 2017, doi: 10.1016/j.ijhydene.2017.10.070.

[66] C. H. Kuo and P. D. Ronney, "Numerical modeling of non-adiabatic heat-recirculating combustors," *Proc. Combust. Inst.*, vol. 31 II, no. 2, 2007, doi: 10.1016/j.proci.2006.08.082.

[67] J. Li, S. K. Chou, Z. W. Li, and W. M. Yang, "Characterization of wall temperature and radiation power through cylindrical dump micro-combustors," *Combust. Flame*, vol. 156, no. 8, pp. 1587–1593, 2009, doi: 10.1016/j.combustflame.2009.05.003.

[68] A. Tang, Y. Xu, C. Shan, J. Pan, and Y. Liu, "A comparative study on combustion characteristics of methane, propane and hydrogen fuels in a micro-combustor," *Int. J. Hydrogen Energy*, vol. 40, no. 46, pp. 16587–16596, Dec. 2015, doi: 10.1016/j.ijhydene.2015.09.101.

[69] Q. Lu, J. Pan, W. Yang, A. Tang, S. Bani, and X. Shao, "Interaction between heterogeneous and homogeneous reaction of premixed hydrogen–air mixture in a planar catalytic micro-combustor," *Int. J. Hydrogen Energy*, vol. 42, no. 8, pp. 5390–5399, 2017, doi: 10.1016/j.ijhydene.2016.12.039.

[70] J. Li, Q. Li, Y. Wang, Z. Guo, and X. Liu, "Fundamental flame characteristics of premixed H2-air combustion in a planar porous micro-combustor," *Chem. Eng. J.*, vol. 283, 2016, doi: 10.1016/j.cej.2015.08.056.

[71] S. Chattopadhyay and G. Veser, "Heterogeneous–homogeneous interactions in catalytic microchannel reactors," *AIChE J.*, vol. 52, no. 6, pp. 2217–2229, Jun. 2006, doi: 10.1002/AIC.10825.

[72] K. Yamamoto, M. Ozeki, N. Hayashi, and H. Yamashita, "Burning velocity and OH concentration in premixed combustion," *Proc. Combust. Inst.*, vol. 32 I, no. 1, 2009, doi: 10.1016/j.proci.2008.06.077.

[73] A. Lachraf and M. Si Ameur, "Numerical investigation of thermal performance of hydrogen fueled micro-combustor with trapezoidal ribs," *Int. J. Hydrogen Energy*, vol. 48, no. 99, pp. 39570–39585, Dec. 2023, doi: 10.1016/j.ijhydene.2023.05.264.

Note

In the course of our bibliographic analysis, we meticulously examined 220 references. However, due to constraints related to the prescribed page limit, we have regrettably restricted our citation selection to a subset of 73 references. This curation was undertaken with the objective of presenting a focused and representative selection that aligns with the scope and depth of our research, while still encompassing the most pertinent and influential works in the field. In addition, in order to maintain effective reference management, a proprietary VBA application have developed.

Achievements

List of Publications

Paper I

Article Title:

Numerical investigation of thermal performance of hydrogen fueled micro-combustor with trapezoidal ribs

Journal Title: International Journal of Hydrogen Energy (IJHE)

Online Publication Date: June 10th, 2023

Publication Date: December 25th, 2023

Volume: 48

Issue: 99

Pages: 39570-39585

Journal Impact Factor: 7.2

Abstract:

This paper presents a new micro combustor design based on four trapezoidal ribs equidistant distributed on its inner wall. The aim is to highlight its promising thermal performance improvements, using numerical simulations as a tool of investigation, compared to other micro combustors. The achieved improvement reflected the favorable effect of the trapezoidal ribs through quantitative computation of mean temperature, temperature difference, and standard deviation. The hydrodynamic study shows that the ribs shape and height elongate the equidistant distributed recirculation zones, resulting in a significant increase in the flow residence time. Furthermore, the outer wall temperature level increases significantly from 1371.25 K to 1417.71 K and the non-uniformity zone is reduced compared to the simple backward facing step micro combustor. A better understanding of the mechanisms involved in heat transfer and their respective contributions to the overall thermal performance of the different micro combustors are explicitly analyzed. Moreover, the results highlight the favorable effect of the inlet velocity of 10 m/s to obtain the optimal outer wall temperature level and uniformity. The rich mixture composition provides the closest thermal performance to the stochiometric case, which widens the operating range for MTPV systems and improves their efficiency and reliability.

Citation:

A. Lachraf and M. Si Ameur, “Numerical investigation of thermal performance of hydrogen fueled micro-combustor with trapezoidal ribs,” *Int. J. Hydrogen Energy*, vol. 48, no. 99, pp. 39570–39585, Dec. 2023, doi: 10.1016/j.ijhydene.2023.05.264.

DOI: 10.1016/j.ijhydene.2023.05.264.

Paper II

Article Title:

Numerical investigation of H2/Air fueled micro combustion characteristics with trapezoidal ribs for micro thermophotovoltaic applications: Effect of rib height

Journal Title: Proceedings of the Institution of Mechanical Engineers, Part A: Journal of Power and Energy

Online Publication Date: July 14th, 2023

Publication Date: February, 2024

Volume: 238

Issue: 1

Pages: 111-122

Journal Impact Factor: 1.7

Abstract:

In this numerical study, the impact of equidistant trapezoidal ribs on the characteristics of premixed H2-air micro-combustion was investigated, with a specific focus on the rib height. The study comprehensively examined flame structure, flame front position, flame speed, and combustion efficiency. A comparative analysis was performed between a backward-facing step micro combustor (MCSD) and micro combustors with varying rib heights: MCRD1 (0.5 mm), MCRD2 (0.6 mm), and MCRD3 (0.7 mm). The incorporation of trapezoidal ribs resulted in the creation of elongated and evenly distributed recirculation zones, significantly enhancing mixing and promoting flame stability, particularly at higher rib heights. The recirculation zones played a critical role in influencing the chemical reaction rate and the species distribution, leading to higher flame speed and greater combustion intensity. The findings highlight the outcomes of incorporating ribs in terms of combustion efficiency. The combustion efficiency values for MCRD1, MCRD2, and MCRD3 were recorded as 96.95%, 96.75%, and 96.61%, respectively, while the MCSD had a combustion efficiency of 97.14%. Hence, the recommended range of rib height is considered advantageous in ensuring an optimal balance between improved flame stabilization and maintaining a satisfactory level of combustion efficiency. The findings provide valuable insights for optimizing micro-thermophotovoltaic systems.

Citation:

Lachraf A, Si Ameur M. Numerical investigation of H2/Air fueled micro combustion characteristics with trapezoidal ribs for micro thermophotovoltaic applications: Effect of rib height. Proceedings of the Institution of Mechanical Engineers, Part A: Journal of Power and Energy. 2024;238(1):111-122. doi:10.1177/09576509231189774

DOI: 10.1177/09576509231189774.

ملخص

في السنوات الأخيرة، حفزت حركة التصغير على تطوير مولدات الطاقة القائمة على الاحتراق الدقيق. من بين هذه المولدات، ظهر نظام الخلايا الكهروضوئية الدقيقة (MTPV) كتقنية واعدة، لتحويل الحرارة الإشعاعية من مولدات الاحتراق الصغيرة إلى كهرباء باستخدام الخلايا الكهروضوئية. يعد تعزيز أداء مولدات الاحتراق الصغيرة أمر بالغ الأهمية لتحقيق كفاءة الاحتراق، الاستقرار وتقليل الهدر. تتناول أبحاث الدكتوراه الحالية الحاجة إلى حلول مبتكرة لتعزيز أداء مولدات الاحتراق الصغيرة. تركز أبحاث الدكتوراه الحالية على الدراسة العددية لتصميم جديد لمولد الاحتراق الصغير يتميز بوجود أربعة أزواج من الأضلاع المائلة المتباعدة بالتساوي على الجدار الداخلي للقناة الثانية للمولد. تستكشف الدراسة حَرَكِيَّات (ديناميكيات = dynamics) التدفق، وسلوك الاحتراق، والأداء الحراري لهذا التكوين الجديد. تكشف النتائج عن تحسينات كبيرة في مستويات درجة حرارة الجدار الخارجي عند إدخال الأضلاع المائلة. علاوة على ذلك، عزز كل من زيادة عدد وارتفاع الأضلاع وكذلك شكل القطع الجانبي للمولد من الأداء الحراري بشكل كبير. يبرز التكوين المقترح لمولد الاحتراق الصغير خصائص حرارية متفوقة، مما يسهم في تطوير تكنولوجيا توليد الطاقة الأكثر كفاءة واستدامة. تهدف الدراسة إلى سد الفجوات وتقديم رؤى قيمة للابتكارات المستقبلية في توليد الطاقة المستدامة.

Résumé

Ces dernières années, la tendance à la miniaturisation a conduit au développement de générateurs de puissance basés sur la micro-combustion, le système Micro-Thermophotovoltaic (MTPV) émergeant comme une technologie prometteuse. Cette recherche doctorale vise à améliorer les performances des micro-combusteurs grâce à des solutions innovantes. Elle explore un nouveau design de micro-combusteur comprenant des nervures angulaires équidistantes sur la paroi interne du canal aval. L'étude examine la dynamique des écoulements, le comportement de la combustion et les performances thermiques, révélant des améliorations significatives des niveaux de température des parois et de l'efficacité thermique avec l'introduction des nervures angulaires. L'augmentation du nombre et de la hauteur des nervures avec la section transversale du micro-combusteur améliore encore les performances thermiques en facilitant l'allumage et en maintenant des flammes stables. La configuration proposée du micro-combusteur démontre des caractéristiques thermiques supérieures, contribuant au développement de technologies de génération d'énergie plus efficaces et durables. En comblant les lacunes de recherche existantes, en particulier dans les géométries de nervures, l'étude met en avant l'importance d'une approche d'analyse intégrative. En comblant ces lacunes, elle vise à faire progresser le domaine de la micro-combustion et à fournir des perspectives précieuses pour les futures innovations dans la génération d'énergie durable.

Abstract

In recent years, the trend towards miniaturization has driven the advancement of micro-combustion-based power generators, with the Micro-Thermophotovoltaic (MTPV) system emerging as a promising technology. This doctoral research aims to enhance micro-combustor performance through innovative solutions. It investigates a novel micro-combustor design featuring equidistant angled ribs on the inner wall of the downstream channel. The study explores flow dynamics, combustion behavior, and thermal performance, revealing significant improvements in wall temperature levels and thermal efficiency with the introduction of angled ribs. Increasing rib number and heights further with the micro-combustor cross section enhances thermal performance by facilitating ignition and sustaining stable flames. The proposed micro-combustor configuration demonstrates superior thermal characteristics, contributing to the development of more efficient and sustainable energy generation technologies. Addressing existing research gaps, particularly in rib geometries, the study emphasizes the importance of an integrative analysis approach. By bridging the gaps, it aims to advance the field of micro-combustion and provide valuable insights for future innovations in sustainable power generation.